(12) STANDARD PATENT (11) Application No. **AU 2018255346 B2**
(19) AUSTRALIAN PATENT OFFICE

(54) Title
Methods and compositions for treating skeletal muscular dystrophy

(51) International Patent Classification(s)
A61K 31/713 (2006.01) ***C12N 15/113*** (2010.01)
A61K 35/34 (2015.01)

(21) Application No: **2018255346** (22) Date of Filing: **2018.04.18**

(87) WIPO No: **WO18/195210**

(30) Priority Data

(31) Number	(32) Date	(33) Country
62/614,753	**2018.01.08**	**US**
62/535,672	**2017.07.21**	**US**
62/569,440	**2017.10.06**	**US**
62/487,402	**2017.04.19**	**US**
62/487,408	**2017.04.19**	**US**
62/487,393	**2017.04.19**	**US**

(43) Publication Date: **2018.10.25**
(44) Accepted Journal Date: **2024.05.02**

(71) Applicant(s)
Cedars-Sinai Medical Center;Capricor, Inc.

(72) Inventor(s)
Marbán, Eduardo;Aminzadeh, Mark A.;Rogers, Russell;Moseley, Jennifer;Rodriguez-Borlado, Luis;Kanagavelu, Saravana;Sakoda, Christopher Stewart

(74) Agent / Attorney
FB Rice Pty Ltd, L 33 477 Collins Street, Melbourne, VIC, 3000, AU

(56) Related Art
AMINZADEH M A ET AL: "Mitigation of Skeletal Myopathy After Intramyocardial Injection of Cardiosphere-derived Cells in the Mdx Mouse Model of Duchenne Muscular Dystrophy", CIRCULATION RESEARCH, vol. 117, no. 12, 22919, (2015), pages E125,
WO 2016/054591 A1

(12) INTERNATIONAL APPLICATION PUBLISHED UNDER THE PATENT COOPERATION TREATY (PCT)

(19) World Intellectual Property Organization
International Bureau

(43) International Publication Date
25 October 2018 (25.10.2018)

WIPO | PCT

(10) International Publication Number
WO 2018/195210 A1

(51) International Patent Classification:
A61K 31/713 (2006.01) *C12N 15/113* (2010.01)
A61K 35/34 (2015.01)

(21) International Application Number:
PCT/US2018/028184

(22) International Filing Date:
18 April 2018 (18.04.2018)

(25) Filing Language: English

(26) Publication Language: English

(30) Priority Data:

62/487,393	19 April 2017 (19.04.2017)	US
62/487,402	19 April 2017 (19.04.2017)	US
62/487,408	19 April 2017 (19.04.2017)	US
62/535,672	21 July 2017 (21.07.2017)	US
62/569,440	06 October 2017 (06.10.2017)	US
62/614,753	08 January 2018 (08.01.2018)	US

(71) Applicants: **CEDARS-SINAI MEDICAL CENTER** [US/US]; 8700 Beverly Boulevard, Suite TSB-290, Los Angeles, California 90048 (US). **CAPRICOR, INC.** [US/US]; 8840 Wilshire Blvd., 2nd Floor, Beverly Hills, California 90211 (US).

(72) Inventors: **MARBÁN, Eduardo**; 8700 Beverly Boulevard, Suite TSB-290, Los Angeles, California 90048 (US). **AMINZADEH, Mark, A.**; 8700 Beverly Boulevard, Suite TSB-290, Los Angeles, California 90048 (US). **ROGERS, Russell**; 8700 Beverly Boulevard, Suite TSB-290, Los Angeles, California 90211 (US). **MOSELEY, Jennifer**; 8840 Wilshire Blvd., 2nd Floor, Beverly Hills, California 90211 (US). **RODRIGUEZ-BORLADO, Luis**; 8840 Wilshire Blvd., 2nd Floor, Beverly Hills, California 90211 (US). **KANAGAVELU, Saravana**; 8840 Wilshire Blvd., 2nd Floor, Beverly Hills, California 90211 (US). **SAKODA,**

(54) Title: METHODS AND COMPOSITIONS FOR TREATING SKELETAL MUSCULAR DYSTROPHY

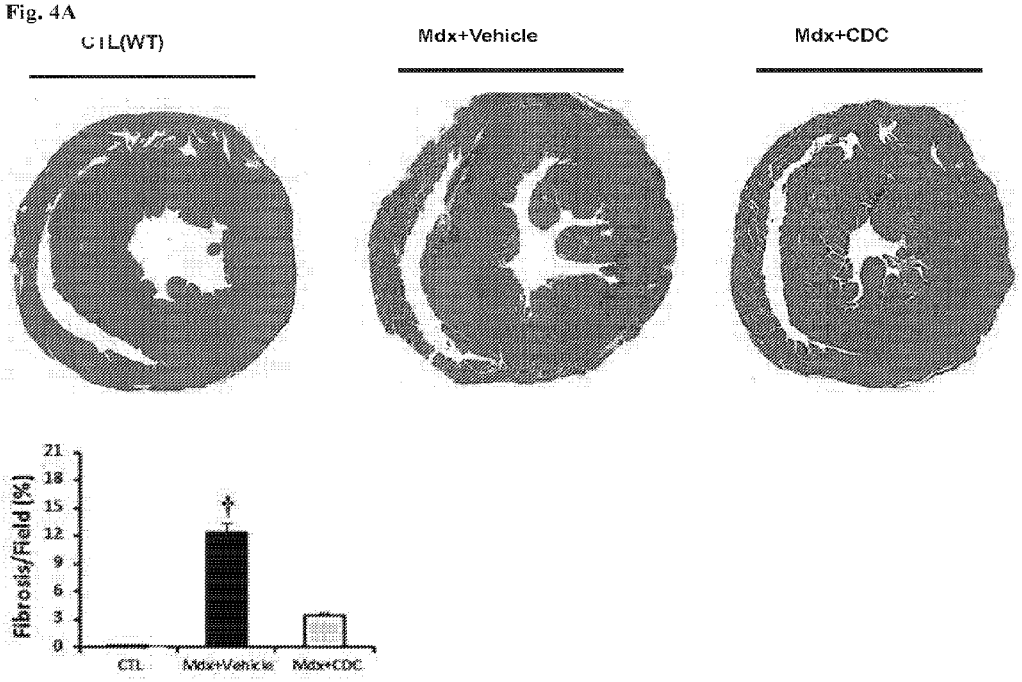

(57) Abstract: Some embodiments provide a method of treating skeletal muscular myopathy, e.g., Duchenne muscular dystrophy (DMD), with cardiosphere-derived cells (CDCs), wherein a therapeutically effective amount of CDCs is delivered to a targeted dystrophic skeletal muscle. Some embodiment enable delivery of a therapeutically effective amount of CDCs via intramuscular injection directly at a skeletal muscle or systemic administration, e.g., intravenous injection, in a single dose or multiple doses, to treat a targeted dystrophic skeletal muscle. Some embodiments provide a method for improving exercise capabilities in DMD patients. Additional embodiments relate to exosome mediated transfer of noncoding RNAs ameliorates Duchenne muscular dystrophy by restoring dystrophin in heart and skeletal muscle. Delivery of noncoding RNA species found in CDC-derived exosomes mimics the ability of CDCs and CDC-derived exosomes to increase dystrophin protein levels.

WO 2018/195210 A1

[Continued on next page]

Christopher, Steward; 8840 Wilshire Blvd., 2nd Floor, Beverly Hills, California 90211 (US).

(74) **Agent: ALTMAN, Daniel, E.**; KNOBBE, MARTENS, OLSON & BEAR, LLP , 2040 Main Street , 14th Floor, Irvine, California 92614 (US).

(81) **Designated States** *(unless otherwise indicated, for every kind of national protection available)*: AE, AG, AL, AM, AO, AT, AU, AZ, BA, BB, BG, BH, BN, BR, BW, BY, BZ, CA, CH, CL, CN, CO, CR, CU, CZ, DE, DJ, DK, DM, DO, DZ, EC, EE, EG, ES, FI, GB, GD, GE, GH, GM, GT, HN, HR, HU, ID, IL, IN, IR, IS, JO, JP, KE, KG, KH, KN, KP, KR, KW, KZ, LA, LC, LK, LR, LS, LU, LY, MA, MD, ME, MG, MK, MN, MW, MX, MY, MZ, NA, NG, NI, NO, NZ, OM, PA, PE, PG, PH, PL, PT, QA, RO, RS, RU, RW, SA, SC, SD, SE, SG, SK, SL, SM, ST, SV, SY, TH, TJ, TM, TN, TR, TT, TZ, UA, UG, US, UZ, VC, VN, ZA, ZM, ZW.

(84) **Designated States** *(unless otherwise indicated, for every kind of regional protection available)*: ARIPO (BW, GH, GM, KE, LR, LS, MW, MZ, NA, RW, SD, SL, ST, SZ, TZ, UG, ZM, ZW), Eurasian (AM, AZ, BY, KG, KZ, RU, TJ, TM), European (AL, AT, BE, BG, CH, CY, CZ, DE, DK, EE, ES, FI, FR, GB, GR, HR, HU, IE, IS, IT, LT, LU, LV, MC, MK, MT, NL, NO, PL, PT, RO, RS, SE, SI, SK, SM, TR), OAPI (BF, BJ, CF, CG, CI, CM, GA, GN, GQ, GW, KM, ML, MR, NE, SN, TD, TG).

Published:

— *with international search report (Art. 21(3))*
— *before the expiration of the time limit for amending the claims and to be republished in the event of receipt of amendments (Rule 48.2(h))*
— *with sequence listing part of description (Rule 5.2(a))*

METHODS AND COMPOSITIONS FOR TREATING SKELETAL MUSCULAR DYSTROPHY

CROSS-REFERENCE TO RELATED APPLICATIONS

[0001] This application claims priority to U.S. Provisional Application No. 62/487393, filed April 19, 2017, U.S. Provisional Application No. 62/487402, filed April 19, 2017, and U.S. Provisional Application No. 62/487408, filed April 19, 2017, and U.S. Provisional Application No. 62/535672, filed July 21, 2017. This application also claims priority to U.S. Provisional Application No. 62/569,440, filed October 6, 2017 and 62/614,753, filed January 8, 2018. All of the foregoing applications are hereby incorporated by reference in their entireties.

STATEMENT REGARDING FEDERALLY-SPONSORED RESEARCH

[0002] This invention was made with government support under Grant No. HL124074 awarded by the National Institutes of Health. The government has certain rights in the invention.

BACKGROUND

Field

[0003] Some embodiments relate to the use of cardiosphere-derived cells and extracellular vesicles derived therefrom (e.g., exosomes, etc.), as well as the isolated molecular cargo thereof (e.g., nucleic acids, short non-coding RNAs, microRNAs, and/or mutants and synthetic analogs thereof), for treating dystrophinopathy (muscular dystrophy, Duchenne muscular dystrophy and Becker muscular dystrophy), and symptoms or disease states associated therewith (including skeletal muscle myopathy associated with Duchenne muscular dystrophy).

Background

[0004] Duchenne muscular dystrophy (DMD) afflicts ~20,000 boys and young men in the USA. The central cause is a genetic abnormality in the dystrophin complex, with secondary damage to skeletal muscle and heart tissue. Dystrophin is a large, rod-shaped, sarcolemmal protein that provides a physical link between the intracellular cytoskeleton and the extracellular matrix. With dystrophin deficiency, the sarcolemma is destabilized and the muscle fibers are susceptible to physical damage with repeated contraction. This devastating X-linked muscle wasting disease has no specific treatment. Affecting 1 in 3500 male births, DMD accounts for 80% of all cases of

muscular dystrophy. Dystrophic muscle undergoes myopathy (cell membrane damage in muscle fiber), leading to loss of ambulation at a very early age, with subsequent respiratory muscle weakness and cardiac failure. In pediatric subjects, skeletal muscle weakness starts 3-5 years from onset, progressive weakness occurs, with wheelchair dependency at approximately 13 years from onset. Importantly, cardiomyopathy is observed to take hold in 1/3 of patients from less than 13 years from onset, increasing to 1/2 of patients less than 18 years from onset, and in all patients after 18 years. Heart failure resulting from and/or secondary to DMD (HF-DMD), particularly at later stages, presents significant exclusionary comorbidities, wherein cell, tissue, heart or mechanical transplantation may not be an option for late stage heart failure with over symptomatic or advanced heart failure (HF). Patients may further suffer from smooth muscle myopathy including vascular dysfunction, further including gastrointestinal and urinary tract systems involvement. Common prognosis is death from respiratory insufficiency or cardiomyopathy.

[0005] Underlying these clinical features is a dystrophin gene mutation (deletion) wherein loss of dystrophin results in cellular membrane damage and leakage of extracellular Ca^{2+} into the cell. Elevated intracellular calcium levels ultimately result in increased oxidative and/or nitrosative stress and inflammation, and activation of calpain. The combination of these effects results in muscle proteolysis and apoptosis, leading to the degradative features described above. Current treatment is limited to the use of corticosteroids, and cardioprotective medications to ease the effects of the disease, but does not treat or slow down the progression of the disease itself. Accordingly, there still exists a great need in the art for treatments, including pediatric subjects where early intervention would ward off emergence of late stage comorbidities.

SUMMARY

[0006] Described herein are methods of treating a dystrophinopathy and/or one or more disease states associated therewith, by administering a therapeutically effective amount of cardiosphere-derived cells (CDCs), exosomes derived from CDCs (CDC-XOs), and/or combinations thereof to a patient suffering from a dystrophinopathy and/or a disease state associated therewith. In some embodiments, the dystrophinopathy is one or more of Duchenne's muscular dystrophy (DMD) and/or Becker muscular dystrophy. In some embodiments, the disease state that is treated is a skeletal myopathy (e.g., skeletal DMD or skeletal Becker muscular dystrophy). In some embodiments, administration of CDCs and/or CDC-XOs delays the onset of muscular dysfunction (including in skeletal muscle dysfunction) and/or maintains, improves,

and/or restores muscular function and integrity (including in skeletal muscles) in the subject having a dystrophinopathy. In some embodiments, dystrophic skeletal muscles of the patient that are treated include one or more of the diaphragm, the limb muscles (e.g., in the arms and/or legs), and/or torso muscles.

[0007] For brevity, several embodiments are disclosed with reference to CDC-XOs and CDCs specifically. It should be understood, however, that one or more of the treatments disclosed herein can be achieved with extracellular vesicles derived from CDCs (referred to herein as CDC-EVs, which may include CDC-derived microvesicles (CDC-MVs)), the isolated molecular cargo of CDC-XOs or CDC-EVs, and combinations thereof. Thus, in some embodiments, the methods of treatment described herein can be performed using one or more of CDC-XOs, CDCs, CDC-EVs, isolated and/or purified molecular cargo of CDC-XOs, isolated and/or purified molecular cargo of CDC-EVs, and/or combinations thereof.

[0008] In some embodiments, the methods of treatment comprise administering to the subject (e.g., a patient suffering from dystrophinopathy or a disease state associated therewith) a therapeutically effective amount of CDCs, CDC-XOs, and/or CDC-EVs. In some embodiments, the CDCs, CDC-XOs, and/or CDC-EVs are autologous or allogeneic to the subject (e.g., derived from their own tissue, from another subject's tissue, and/or from the tissue of another animal species). In some embodiments, the methods of treatment comprise administering to the subject a therapeutically effective amount of molecular cargo from CDC-XOs and/or CDC-EVs (including CDC-derived microvesicles (CDC-MVs)). In some embodiments, molecular cargo of CDC-XOs or CDC-EVs is isolated and/or synthesized and that molecular cargo (e.g., particular molecules and/or combinations of different molecules, including RNA polynucleotides and/or short non-coding RNAs) is administered to the subject in need thereof (e.g., a subject having a dystrophinopathy and/or a disease state thereof). In some embodiments, the method of treatment comprises administering to the subject a therapeutically effective amount of an isolated RNA polynucleotide or a vector encoding (and/or containing) a RNA polynucleotide found in CDC-XOs and/or CDC-EVs.

[0009] In some embodiments, the CDCs, CDC-EVs, and/or CDC-XOs are delivered to the subject systemically. In some embodiments, the CDCs, CDC-EVs, and/or CDC-XOs are delivered to the subject systemically and locally. In some embodiments, the CDCs, CDC-EVs, and/or CDC-XOs are delivered to the subject systemically but not locally. In some embodiments,

the CDCs, CDC-EVs, and/or CDC-XOs are delivered to the subject systemically locally. In some embodiments, the CDCs, CDC-EVs, and/or CDC-XOs are delivered to the subject locally but not systemically. In some embodiments, non-limiting examples of a methods to administer a therapeutically effective amount of CDCs, CDC-EVs, and/or CDC-XOs include systemic administration (*e.g.*, intravenous, intra-arterial, intraventricular, intra-aortic, and/or intraperitoneal injection and/or infusion). In some embodiments, the CDCs, CDC-EVs, and/or CDC-XOs are injected or infused intravenously. In some embodiments, a therapeutically effective amount of CDCs, CDC-EVs, and/or CDC-XOs is administered to a patient by intramuscular injection and/or infusion. In some embodiments, a therapeutically effective amount of CDCs, CDC-EVs, and/or CDC-XOs is administered to a patient by infusion directly at a local site (e.g., into or near a dystrophic skeletal muscle and/or a target site where treatment is desired). In some embodiments, an effective amount of CDCs, CDC-EVs, and/or CDC-XOs is delivered systemically via injection and/or infusion at an area of the body that is not in the heart. In some embodiments, the intravenous administration of CDCs, CDC-EVs, and/or CDC-XOs includes jugular and/or femoral vein injection and/or infusion.

[0010] In some embodiments, the administration of CDCs, CDC-EVs, and/or CDC-XOs to a subject in need thereof includes a single dose and/or multiple doses (e.g., 2, 4, 6, 8, 10, or more doses). In some embodiments, where multiple doses are used, the administration of CDCs, CDC-EVs, and/or CDC-XOs is performed daily, weekly, biweekly, every three weeks, monthly, every six months, or every year. In some embodiments, the dosing schedule is performed over a period of, for example, 2 weeks, 1 month, 2 months, 3 months, 5 months, 6 months, a year, 5 years, or ranges including and/or spanning the aforementioned values. For illustration, in some embodiments, the interval includes the administration of 2-10 doses at intervals of 1-5 months. In some embodiments, the dosing schedule is 3 doses with about 3 months between each dose. In some embodiments, the dosing schedule is 5 doses with about 1 week separating each dose. In some embodiments, the dosing schedule is 3 administrations (e.g., 3 single doses at different times) at weeks 0, 6 and 9. In some embodiments, an interval schedule is used, where there are periods of dosing and periods of rest between dosing periods (e.g., weekly doses for a month followed by a rest period of 5 months, followed by weekly doses for a month and so on). In some embodiments, a single dose comprises a therapeutically effective amount of CDCs, CDC-XOs, and/or CDC-EVs. In some embodiments, the dosing periods and/or interval schedule is performed throughout the life

of the patient. In some embodiments, multiple administrations of each single dose are provided to the subject. In various embodiments, as disclosed elsewhere herein, the administration can be in repeated doses, such as two, three, four, four or more sequentially-applied doses.

[0011] In some embodiments, a therapeutically effective amount of CDCs includes at least about 75 x 10^6 to 500 x 10^6 CDCs. In some embodiments, a therapeutically effective amount of CDCs includes greater than or equal to about: 75 x 10^6 CDCs, 150 x 10^6 CDCs, 300 x 10^6 CDCs, 400 x 10^6 CDCs, 500 x 10^6 CDCs, or ranges including and/or spanning the aforementioned values. In some embodiments, a therapeutically effective amount of CDCs includes less than or equal to about: 75 x 10^6 CDCs, 150 x 10^6 CDCs, 300 x 10^6 CDCs, 400 x 10^6 CDCs, 500 x 10^6 CDCs, or ranges including and/or spanning the aforementioned values.

[0012] In some embodiments, the number of CDC-EVs or CDC-XOs administered in each dose (where a single or multiple doses are used) and/or over the course of a treatment regimen is equal to or at least about: 1 x 10^6, 1 x 10^7, 1 x 10^8, 1 x 10^9, 1 x 10^{10}, 1 x 10^{11}, 1 x 10^{12}, or ranges including and/or spanning the aforementioned values. In some embodiments, the quantities of CDC-EVs or CDC-XOs administered in each dose (where a single or multiple doses are used) and/or over the course of a treatment regimen ranges from 1 x 10^6 to 1 x 10^7, 1 x 10^7 to 1 x 10^8, 1 x 10^8 to 1 x 10^9, 1 x 10^9 to 1 x 10^{10}, 1 x 10^{10} to 1 x 10^{11}, 1 x 10^{11} to 1 x 10^{12}, 1 x 10^{12} or more.

[0013] In some embodiments, the number of CDC-XOs (or CDC-EVs) delivered to the subject in a dose (or dosing regimen) is determined based on the number of CDCs that would be used in a clinically effective dose in a cell-based therapy method. For example, in some embodiments, where 75-500 x 10^6 CDCs is an effective dose for therapeutic treatment of skeletal myopathy, using the equivalent amount of CDC-XOs or CDC-MVs that would be released by those CDCs in vivo would be administered to a patient in a "cell-free" method of treatment. In other words, CDC equivalent doses of CDC-XOs and/or CDC-MVs can be used. As an illustration, in some embodiments, 3 mL / 3 x 10^8 CDCs, is capable of providing therapeutic benefit. Therefore, a plurality of CDC-XOs as would be derived from that number of CDCs over the time course of those CDCs' residence in the body is used. In some embodiments, the amount of CDC-XOs or CDC-EVs delivered to the patient is the amount of CDC-XOs or CDC-EVs that would be released via an injection of equal to or at least about: 75 x 10^6 CDCs, 150 x 10^6 CDCs, 300 x 10^6 CDCs, 400 x 10^6 CDCs, 500 x 10^6 CDCs, or ranges including and/or spanning the aforementioned values. In some embodiments, the number of CDCs administered in any single dose is 1 x 10^5, 1 x 10^6, 1

x 10^7, 1 x 10^8, 1 x 10^9, 1 x 10^{10}, 1 x 10^{11}, 1 x 10^{12} (or ranges including and/or spanning the aforementioned values). In some embodiments, the amount of CDC-XOs or CDC-EVs delivered to the patient is the amount of CDC-XOs or CDC-EVs that would be released via an injection of equal to or at least about: 1 x 10^5 CDCs, 1 x 10^6 CDCs, 1 x 10^7 CDCs, 1 x 10^8 CDCs, 1 x 10^9 CDCs, 1 x 10^{10} CDCs, 1 x 10^{11} CDCs, 1 x 10^{12} CDCs, or ranges including and/or spanning the aforementioned values. In some embodiments, a dose of CDCs ranges between about 10 and 90 million CDCs, including about 10 to about 20 million, about 20 to about 30 million, about 30 to about 50 million, about 50 to about 60 million, about 60 to about 70 million, about 70 to about 75 million, about 75 million to about 80 million, about 80 million to about 90 million, and ranges including and/or spanning the aforementioned values. Some such does are particularly favorable for coronary delivery. In several embodiments, the dose of CDCs ranges from about 30 million to about 1.5 billion CDCs, including about 30 million to about 45 million, about 40 million to about 50 million, about 50 million to about 50 million, about 60 to about 75 million, about 75 to about 1 billion, about 90 million to about 1.1 billion, about 1 billion to 1.25 billion, about 1.25 billion to about 1.5 billion, and ranges including and/or spanning the aforementioned values. Without being bound to a particular theory, when injected, it is believed that CDCs are transient residents in the subject. Depending on the embodiment, the degree of CDC retention varies. For example, in several embodiments, the retention rate is between about 0.01% and 10%, including about 0.01% to about 0.05%, about 0.05% to about 0.1%, about 0.1% to about 0.5%, about 0.5% to about 1.0%, about 1.0% to about 2.5%, about 2.5% to about 5%, about 5% to about 10%, and ranges including and/or spanning the aforementioned values. Thus, in some embodiments, the equivalent amount of CDC-XOs or CDC-EVs delivered to the patient is calculated as the amount of CDC-XOs or CDC-EVs that would be released via an administration (e.g., injection or infusion) of the disclosed amounts CDCs over a given time of CDC residence in the body of about 1 week, about 2 weeks, about 3 weeks, or more. In certain instances, the dosage may be prorated to body weight (range 100,000-1M CDCs/kg body weight total CDC dose). In some embodiments, for injection into the heart, the number of administered CDCs includes 25 million CDCs per coronary artery (i.e., 75 million CDCs total) as another baseline for XO or EV dosage quantity.

[0014] In some embodiments, the CDC, CDC-XO, and/or CDC-EV quantity delivered to the patient (e.g., the dose) may be measured by weight (in mg) of CDCs, CDC-XOs, and/or CDC-EVs (e.g., where the solution and/or milieu surrounding the CDCs, CDC-XOs, and/or CDC-

EVs has been removed or substantially removed). For instance, in some embodiments, a dose of CDCs, CDC-XOs, and/or CDC-EVs may comprise equal to or at least about the following weights in mg: about 0.001 to about 0.005, about 0.005 to about 0.01, about 0.01 to about 0.05, about 0.05 to about 0.1, about 0.1 to about 0.5, about 0.5 to about 1, about 1 to about 10, about 10 to about 25, about 25 to about 50, about 50 to about 75, about 75 to about 100, or ranges including and/or spanning the aforementioned values. As discussed in additional detail herein, those masses are representative, of the number of CDCs, CDC-XOs or CDC-EVs that are dosed to a subject, depending on the embodiment. For example, in several embodiments, the number of CDCs in a dose can range from about 5×10^4 to about 2×10^9, including about 5×10^4 to about 1×10^5, about 1×10^5 to about 2.5×10^5, about 2.5×10^5 to about 1×10^6, about 1×10^6 to about 1×10^7, about 1×10^7 to about 1×10^8, about 1×10^8 to about 1×10^9, about 1×10^9 to about 2×10^9, about 2×10^9 to about 5×10^9, and ranges including and/or spanning the aforementioned values. Likewise, depending on the embodiment, the number of exosomes or particles (e.g., vesicles) dosed to a subject can range from about 1×10^9 to about 2×10^{14}, including about 1×10^9 to about 2×10^9, about 2×10^9 to about 4×10^9, about 4×10^9 to about 1×10^{10}, about 1×10^{10} to about 1×10^{11}, about 1×10^{11} to about 1×10^{12}, about 1×10^{12} to about 2×10^{12}, about 2×10^{12} to about 2×10^{13}, about 2×10^{13} to about 1×10^{14}, about 1×10^{14} to about 2×10^{14}, and ranges including and/or spanning the aforementioned values. In some embodiments, the CDC, CDC-XO, and/or CDC-EV quantity delivered to the patient may be measured by protein weight (in mg) and/or by total cell or vesicle weight (e.g., where water has been removed from the area outside the cells or vesicles). In some embodiments, the CDC, CDC-XO, and/or CDC-EV quantity delivered to the patient is equal to 1-10, 10-25, 25-50, 50-75, 75-100, or 100 or more mg protein. In some embodiments, administering a therapeutically effective amount of a composition includes about 1 to about 100 mg XO and/or EV protein in a single dose.

[0015] In some embodiments, a formulation or a composition comprising CDCs, CDC-EVs, and/or CDC-XOs is provided. In some embodiments, the formulation and/or composition includes a pharmaceutically acceptable carrier. In some embodiments, the carrier is water at physiologic pH and/or isotonicity. In some embodiments, the formulation or composition is used in the treatment of dystrophinopathy (e.g., skeletal muscular dystrophy, dystrophic cardiomyopathy, etc.) according to the aforementioned methods. In some embodiments, the formulation or composition is used to effectively and/or safely treat dystrophinopathy in a subject

in need thereof wherein a formulation and/or composition comprising a therapeutically effective amount of CDCs, CDC-EVs, and/or CDC-XOs is delivered to a targeted dystrophic skeletal muscle.

[0016] In some embodiments, as disclosed elsewhere herein, method of treatment is for a subject (e.g., patient) afflicted with myopathy. In some embodiments, the muscle myopathy includes one or more of cell membrane degradation, interstitial inflammation, fatty replacement, and fibrosis, one or more of which is treated and/or substantially alleviated during the treatment as disclosed herein.

[0017] In some embodiments, as disclosed elsewhere herein, method of treatment is for a subject (e.g., patient) afflicted with cardiomyopathy. In some embodiments, the subject is afflicted with cardiomyopathy, but not heart failure. In some embodiments, the subject is diagnosed with cardiomyopathy. In some embodiments, the subject is diagnosed with cardiomyopathy, but not heart failure. In some embodiments, the cardiomyopathy includes one or more of left ventricle posterobasal fibrosis, conduction abnormalities that are intra-atrial, including SVT with abnormal AV nodal conduction, one or more of which is treated and/or substantially alleviated by the treatment as disclosed herein. In various embodiments, cardiomyopathy includes advanced stages of ventricle enlargement, dyspnea, peripheral edema and liver enlargement, one or more of which is treated and/or substantially alleviated by the treatment as disclosed herein. In various embodiments, heart failure (HF) includes asymptomatic abnormalities in cardiac structure and function wherein heart function is depressed (stage B), overt symptomatic HF (stage C), to advanced HF (stage D), one or more of which is treated and/or substantially alleviated by the treatment as disclosed herein.

[0018] In various embodiments, subject is afflicted with skeletal muscle myopathy, smooth muscle myopathy including vascular dysfunction, further including GI and urinary tract systems involvement. In some embodiments, one or more of these disease states is treated and/or substantially alleviated by the methods as disclosed elsewhere herein. In some embodiments, the myopathy includes one or more of cell membrane degradation, interstitial inflammation, fatty replacement, and fibrosis, one or more of which is treated and/or substantially alleviated by the treatment as disclosed herein.

[0019] In some embodiments, treatment of the subject further includes assessing functional improvement in the subject, including functional improvement in skeletal muscle tissue.

In some embodiments, the methods disclose herein result in functional improvement of muscle tissue. In some embodiments, the methods disclose herein result in functional improvement in, for example, voluntary muscle contraction. In some embodiments, the functional improvement includes one or more of increased contractile strength, improved ability to walk, improved ability to stand from a seated position, improved ability to sit from a recumbent or supine position, and improved manual dexterity such as pointing and/or clicking a mouse. In some embodiments, treatment of the subject further includes assessing cognition in response to treatment of neural damage, blood-oxygen transfer in response to treatment of lung damage, and immune function in response to treatment of damaged immunological-related tissues.

[0020] In some embodiments, said subject in need of treatment for dystrophinopathy is a human subject. In some embodiments, the human subject is a pediatric subject at the age of less than or equal to about: 3, 8, 11, 12, 15, 18, or ranges including and/or spanning the aforementioned values. In some embodiments, the human subject is a pediatric subject at the age, for example, about 3 to about 11 years old, or about 12 to about 18 years old. In some embodiments, the subject is categorized by one or more of the above characteristics, such as one of the recited age groups, and/or is afflicted and/or diagnosed with one or more of the above disease states (e.g., myopathy, cardiomyopathy and/or heart failure). In some embodiments, the patient suffers from one or more of the disease states disclosed above, but not others. For example, a subject that is 3-11 years old, afflicted with and/or diagnosed with cardiomyopathy, but not heart failure. As another illustration, the subject may be 8-15 years old and afflicted with skeletal muscle myopathy but not cardiomyopathy or heart failure.

[0021] In some embodiments, as disclosed elsewhere herein, infusion can be intra-arterial or intravenous. The arteries and veins can include those in a limb, in the torso (e.g., at or around the lung), the neck, etc. In some embodiments, infusion delivers a therapeutically effective dose of CDC-XOs, CDC-EVs, and/or CDCs to one or more locations in the body (e.g., locations at the infusion site or away from the infusion site). In some embodiments, infusion delivers a therapeutically effective dosage of exosomes to smooth or skeletal muscle tissue. In some embodiments, administering a therapeutically effective amount of a composition includes injection. In some embodiments, the injection includes injection into the heart, including intramyocardial injection, cavities and chambers of the heart, vessels associated thereof. In some embodiments, injection into the heart, cavities and chambers of the heart, vessels associated

thereof, is capable of delivering a therapeutically effective dosage of exosomes to smooth or skeletal muscle tissue. In some embodiments, injection results in and/or is performed to achieve systemic delivery. In some embodiments, injection delivers a therapeutically effective dose of CDC-XOs, CDC-EVs, and/or CDCs to one or more targeted locations in the body (e.g., locations that may be at the injection site or away from the injection site). In some embodiments, the injection includes skeletal muscle injection (into the skeletal muscle). In some embodiments, the injection includes intraperitoneal injection. In some embodiments, the injection includes percutaneous injection.

[0022] According to several embodiments, there are provided herein methods of treating muscular dystrophy (e.g., a dystrophinopathy) in a subject in need thereof, the method comprising administrating to the subject a therapeutically effective amount of cardiosphere-derived cells (CDCs). In several embodiments, there are also provided methods of treating cardiomyopathy in a subject in need thereof, the method comprising systemically administering to the subject a therapeutically effective amount of CDCs. In several embodiments, the cardiomyopathy is dystrophic cardiomyopathy, with some embodiments, wherein the dystrophic cardiomyopathy is heart failure secondary to a chronic muscular dystrophy. In several embodiments, the methods employ exosomes derived from CDCs, in place of, or in addition to CDCs themselves. In several embodiments, methods of treating a dystrophinopathy are provided, the methods, comprising administering a therapeutically effective amount of exosomes to a pediatric subject afflicted with a dystrophinopathy, thereby treating the subject. In several embodiments, the plurality of the exosomes is isolated from cardiosphere-derived cells (CDCs) grown in serum-free media. In several embodiments, there are provided methods of treating a dystrophic skeletal muscle, comprising administering cardiosphere-derived cells (CDCs) and/or CDC-derived exosomes (CDC-XOs) to a subject afflicted with a dystrophinopathy, thereby treating the dystrophic skeletal muscle, wherein the CDCs and/or CDC-XOs are administered to the subject at a site that is not the heart and wherein the dystrophic skeletal muscle is a targeted dystrophic skeletal muscle and wherein the targeted dystrophic skeletal muscle receives a therapeutically effective amount of CDCs and/or CDC-XOs. In one embodiment, there is provided a method of treating skeletal muscular dystrophy in a subject in need thereof, the method comprising administering to the subject a first dose of a composition comprising a therapeutically effective amount of cardiosphere-derived cells (CDCs), wherein the therapeutically effective

amount of the first dose ranges from about 1 x 10^7 to about 1 x 10^9 CDCs, waiting a first period of time after administration of said first dose, wherein said first period of time is between about 1 and 6 months, administering to the subject a second dose of a composition comprising a therapeutically effective amount of CDCs, wherein the therapeutically effective amount of the second dose ranges from about 1 x 10^7 to about 1 x 10^9 CDCs, waiting a second period of time after administration of said second dose, wherein said second period of time is between about 1 and 6 months, administering to the subject at least one additional dose of a composition comprising a therapeutically effective amount of CDCs, wherein the therapeutically effective amount of the at least one additional dose ranges from about 1 x 10^7 to about 1 x 10^9 CDCs, waiting at least one additional period of time after administration of said at least one additional dose, wherein said second period of time is between about 1 and 6 months, wherein said administrations result in an improvement in exercise capacity or muscle function, wherein said CDCs are allogeneic with respect to said subject, wherein said administrations do not induce a significant immune response in the subject, and wherein said administrations comprise systemic administration. In several embodiments, the administration of CDCs (one or more times) alters expression of one or more markers of T cell activation or proliferation, the markers comprising CD69 and/or HLA-DR.

[0023] In several embodiments, the therapeutically effective amount of CDCs is sufficient to treat a dystrophic skeletal muscle of the subject, which according to some embodiments, is afflicted by Duchenne muscular dystrophy (DMD) or Becker muscular dystrophy, each involving dystrophinopathy of a skeletal muscle. Any skeletal muscle may be affected, however, according to several embodiments, the dystrophic skeletal muscle is a skeletal muscle of the diaphragm, the arm, or the leg.

[0024] Administration routes can vary, depending on the embodiment. For example, in several embodiments, the CDCs are administered to the subject via intramuscular injection at a dystrophic skeletal muscle (e.g., a local administration). In several embodiments, the CDCs are administered to the subject systemically, of which several routes are optional. For example, in several embodiments, systemic administration is via intravenous injection or infusion. In several embodiments, systemic administration via injection into the right ventricle, whereas in additional embodiments, systemic administration is via injection into the left ventricle.

[0025] In some embodiments, administration of the CDCs is via a single dose, while in some embodiments, two or more doses are administered. In several embodiments, with multiple

doses, the doses are given at intervals of about 3 weeks to about three months, for example, about 3-4 weeks, 4-5 weeks, 5-6 weeks, 6-8 weeks, 8-12 weeks, or any time there between, including endpoints. In several embodiments, the subsequent doses are given at 6 and 12 weeks after an initial CDC dose is administered. Depending on the embodiment, the number of CDCs and/or the location of administration can vary over the repeated doses. Alternatively, the dosing regimen can use constant CDC numbers and locations across a regimen.

[0026] By way of example, the methods disclosed herein can employ dose (e.g., a therapeutically effective amount of CDCs) of at least, about 75 x 10^6 CDCs. More specifically, in several embodiments, the dose is at least about 150 x 10^6 CDCs, at least about 300 x 10^6 CDCs, at least about 350 x 10^6 CDCs, at least about 400 x 10^6 CDCs, at least about 450 x 10^6 CDCs, at least about 500 x 10^6 CDCs, at least about 550 x 10^6 CDCs, at least about 600 x 10^6 CDCs, or any number there between. In those embodiments employing exosomes, some embodiments, comprise a dose of about 1 to about 100 mg exosome protein in a single dose.

[0027] In several embodiments the CDCs or exosomes are allogeneic with respect to the subject receiving the CDCs.

[0028] In several embodiments, the administration of CDCs or exosomes results in increased dystrophin expression (e.g., increased over 'normal' dystrophin expression, for example a control population or an earlier time point in a disease). In several embodiments, the increase in dystrophin is detectable in for example, the skeletal muscle and/or the diaphragm.

[0029] In several embodiments, the methods further comprise administering (e.g., separately or co-administering) a steroid with the CDCs.

[0030] In several embodiments, the methods, uses and compositions disclosed herein result in an improvement in muscle function, or a decrease in muscle fibrosis or tissue damage. In several embodiments, the improvements are with respect to skeletal muscle. In some embodiments, improvements are with respect to cardiac muscle.

[0031] Also provided herein is the use of a composition comprising CDCs and/or CDC-exosomes, wherein the composition is suitable for systemic administration to a subject having a muscular dystrophy, and wherein the administration of the composition treats said muscular dystrophy (e.g., skeletal muscle is treated).

[0032] Further provided, in several embodiments, is a composition comprising an isolated RNA polynucleotide derived from a CDC, a CDC-XO, or a CDC-derived extracellular

vesicle (CDC-EV) or a vector encoding the RNA polynucleotide, wherein the RNA polynucleotide comprises a short non-coding RNA. In several embodiments, the RNA polynucleotide sequence comprises at least about 80%, 85%, 90%, 95%, 96%, 97%, 98%, or 99% percentage identity to short non-coding RNA from DMD (srDMD). In several embodiments, the short non-coding RNA comprises srDMD. In several embodiments, the short non-coding RNA comprises a microRNA. Depending on the embodiment, the microRNA may comprise GCG on the 5' end or 3' end. In several embodiments, the RNA polynucleotide comprises at least about 80%, 85%, 90%, 95%, 96%, 97%, 98%, 99% percentage identity to miR-148a. In one embodiment, the microRNA comprises miR-148a. In several embodiments, the vector is a virus (e.g., a parvovirus, a retrovirus, lentivirus, etc.). In one embodiment, the adenovirus or adeno-associated virus.

[0033] In some embodiments, the methods disclosed herein achieve one or more desired patient outcomes. In some embodiments, the treatment of a subject results in an increase in dystrophin expression. In some embodiments, increase in dystrophin expression occurs in skeletal muscle. In some embodiments, the increase in dystrophin expression in the skeletal muscles includes skeletal muscle in limbs (e.g., the arms or legs), such as a soleus muscle. In some embodiments, the increase in dystrophin expression occurs in the diaphragm. In some embodiments, treatment of the subject results in decreased fibrosis, decreased inflammation, and/or increased mitochondrial function. In some embodiments, decreased fibrosis includes a reduction in collagen accumulation. In some embodiments, collagen includes collagen I and/or collagen III. In some embodiments, decreased inflammation includes an increase in cytoplasmic nuclear factor (erythroid-derived 2)-like 2 (Nrf2), reduction in fatty acid peroxidation end products, reduced numbers of inflammatory cells, and/or upregulated expression of antioxidants. In some embodiments, upregulated antioxidants include one or more of heme oxygenase-1 (HO-1), catalase, superoxide dismutase-2 (SOD-2), and glutamate-cystein ligase catalytic (GCLC) subunit. In some embodiments, down regulated inflammatory cells include CD68+ macrophages and CD3+ T-cells. In some embodiments, increased mitochondrial function includes increased mitochondrial ultrastructure and/or increased mitochondrial biogenesis. In some embodiments, increased mitochondrial function includes increased nuclear PPAR-γ co-activator-1 (PGC-1) expression.

[0034] In some embodiments, as disclosed elsewhere herein, therapeutic compositions comprising one or more isolated components of the molecular cargo of CDC-XOs are used in the

methods disclosed herein. In some embodiments, the therapeutic compositions comprise CDC-XO RNAs. In some embodiments, the RNAs can be isolated from CDCs, CDC-XOs, and/or CDC-MVs and re-combined (e.g., mixed and matched) to provide therapeutic mixtures for use in methods of treatment as disclosed elsewhere herein. In some embodiments, a therapeutic mixture of RNA can include a single RNA or multiple RNAs (e.g., 2, 3, 4, 5, 6, 7, 8, 9, 10 or more RNAs), including non-coding RNAs. In some embodiments, the non-coding RNAs include tRNAs, Y RNAs, rTNAs, mirRNAs, lncRNAs, piRNAs, snRNAs, snoRNAs, further including fragments thereof, among others. In some embodiments, the therapeutic mixture includes one or more microRNAs selected from the group consisting of: microRNAs miR-146a, miR-148a, miR-22, miR-24, miR-210, miR-150, miR-140-3p, miR-19a, miR-27b, miR-19b, miR-27a, miR-376c, miR-128, miR-320a, miR-143, miR-21, miR-130a, miR-9, miR-185, miR-23a, miR-215, miR-33a, miR 204, miR-376c, miR4532, miR-4742, miR-582, miR-629, miR-223, miR-3125, miR-3677, miR-376b, miR-4449, miR-4773, miR-4787, miR-491, miR-495, miR-500a, miR-548ah, miR-550, miR-548ah, miR-550a, miR-551n, miR-5581, miR-616, or any other microRNAs depicted as enriched in Figure 29, and/or a polynucleotide having at least about 80%, 85%, 90%, 95%, 96%, 97%, 98%, or 99% percentage identity to any of the foregoing. In some embodiments, the therapeutic mixture can include one or more of miR-148a, miR-148-5p, miR-148-39, srDMD, and/or a polynucleotide having at least about 80%, 85%, 90%, 95%, 96%, 97%, 98%, or 99% percentage identity to any of the foregoing. In some embodiments, the therapeutic mixture microRNA includes miR-148a-3p, and/or a polynucleotide having at least about 80%, 85%, 90%, 95%, 96%, 97%, 98%, or 99% percentage identity to any of the foregoing. In some embodiments, the microRNA includes miR-148a-3p, and/or a polynucleotide having at least about 80%, 85%, 90%, 95%, 96%, 97%, 98%, or 99% percentage identity to any of the foregoing. In various embodiments, the exosomes include a small non-coding RNA from DMD, srDMD, and/or a polynucleotide having at least about 80%, 85%, 90%, 95%, 96%, 97%, 98%, or 99% percentage identity to any of the foregoing.

[0035] In some embodiments, the methods as disclosed elsewhere herein, can be accomplished using non-coding RNAs isolated from CDC-XOs. Without being bound to a particular theory, it is believed that non-coding RNAs appear to be well-suited for regulatory roles that require highly specific nucleic acid recognition, including short non-coding RNA genes have been identified and designated as microRNAs. In some embodiments, the isolated RNA

polynucleotide is selected from one or more of miR-148a, miR-148-5p, miR-148-39, srDMD, and/or a polynucleotide having at least about 80%, 85%, 90%, 95%, 96%, 97%, 98%, or 99% percentage identity to miR-148a, miR-148-5p, miR-148-39, or srDMD. In some embodiments, the nucleotide sequence of miR-148a is:

5'GAGGCAAAGUUCUGAGACACUCCGACUCUGAGUAUGAUAGAAGUCAGUG CACUACAGAACUUUGUCUC3' (SEQ ID NO: 1);

the nucleotide sequence of miR-148-5p is:

5'AAAGUUCUGAGACACUCCGACU3' (SEQ ID NO: 2);

the nucleotide sequence of miR-148-3p is:

5'UCAGUGCACUACAGAACUUUGU3' (SEQ ID NO: 3); and

the nucleotide sequence of srDMD is:

5'UGUACACAGAGGCUGAUCGAUUCUCCCUGAACAGCCUAUUACGGAGGCA CUGCAGAUCAAGCCCGCCUGGAGAGGUGGAGUUUCAAGAGUCCCUUCCUGGUUCA CCGUCUCCUUU3' (SEQ ID NO: 4).

[0036] In some embodiments, the one or more isolated components of the molecular cargo of CDCs, CDC-XOs, and/or CDC-MVs are delivered to the cell using viral or non-viral vectors. In some embodiments, the vector is a virus. In various embodiments, the virus is adenovirus or adeno-associated virus.

[0037] In some embodiments, a formulation or a composition comprising miR-148a, miR-148-5p, miR-148-39, srDMD, and/or a polynucleotide having at least about 80%, 85%, 90%, 95%, 96%, 97%, 98%, or 99% percentage identity to miR-148a, miR-148-5p, miR-148-39, or srDMD, for use in the treatment of skeletal muscular dystrophy and/or dystrophic cardiomyopathy according to the aforementioned method of effectively and/or safely treating dystrophinopathy in a subject in need thereof. In some embodiments, a use of the aforementioned formulation and/or composition for treating skeletal muscular dystrophy and/or dystrophic cardiomyopathy according to the aforementioned methods of effectively and/or safely treating dystrophinopathy in a subject in need thereof are provided.

[0038] In some embodiments, the CDCs are generated from a biopsy sample cultured into an explant, further cultured into an explant derived cell, additionally cultured as cardiosphere forming cells, thereafter cultured as cardiospheres, and subsequently cultured as CDCs from which XOs and EVs are isolated. In some embodiments, the CDCs are human. In various embodiments,

the CDCs are generated from a biopsy sample obtained the subject afflicted with dystrophinopathy. In some embodiments, the CDCs are cultured under hypoxic conditions (e.g., 2% O_2) for a period of about 24 hours. In some embodiments, the CDCs are cultured under serum-free conditions.

[0038a] In some embodiments, as disclosed elsewhere herein, a method of improving skeletal muscle isometric force production in a skeletal muscle of a subject with muscular dystrophy in need of treatment for skeletal muscle myopathy, the method comprising: administering to the subject a first dose of a composition comprising a therapeutically effective amount of cardiosphere-derived cells (CDCs), wherein the therapeutically effective amount of the first dose ranges from about 1 x 10^7 to about 1 x 10^9 CDCs; waiting a first period of time after administration of said first dose, wherein said first period of time is between about 1 and 6 months; administering to the subject a second dose of a composition comprising a therapeutically effective amount of cardiosphere-derived cells (CDCs), wherein the therapeutically effective amount of the second dose ranges from about 1 x 10^7 to about 1 x 10^9 CDCs; waiting a second period of time after administration of said second dose, wherein said second period of time is between about 1 and 6 months; administering to the subject at least one additional dose of a composition comprising a therapeutically effective amount of cardiosphere-derived cells (CDCs), wherein the therapeutically effective amount of the at least one additional dose ranges from about 1 x 10^7 to about 1 x 10^9 CDCs; waiting at least one additional period of time after administration of said at least one additional dose, wherein said at least one additional period of time is between about 1 and 6 months; wherein said administrations result in an improvement in exercise capacity or muscle function, wherein said CDCs are allogeneic with respect to said subject, wherein said administrations do not induce a significant immune response in the subject, and wherein said administrations comprise systemic administration.

[0038b] Throughout this specification the word "comprise", or variations such as "comprises" or "comprising", will be understood to imply the inclusion of a stated element, integer or step, or group of elements, integers or steps, but not the exclusion of any other element, integer or step, or group of elements, integers or steps.

[0038c] Any discussion of documents, acts, materials, devices, articles or the like which has been included in the present specification is not to be taken as an admission that any or all of these matters form part of the prior art base or were common general knowledge in the field

relevant to the present disclosure as it existed before the priority date of each of the appended claims.

BRIEF DESCRIPTION OF THE DRAWINGS

[0039] Figures 1A-J. CDC transplantation into *mdx* hearts. Function, survival, antioxidant pathways, inflammation, mitochondrial dysfunction and dystrophin expression improved by CDC transplantation into *mdx* mice. Fig. 1A: Ejection fraction (EF) in CDC-injected *mdx* mice (Mdx+CDC) and vehicle-injected *mdx* mice (Mdx+Vehicle) in response to injections atbaseline (10 months of age) and 3 months later (CTL: n=7; Mdx+Vehicle & Mdx+CDC: n=12 each). Fig. 1B: Exercise capacity in mice subjected to weekly high-intensity treadmill exercise, starting 3 weeks after single-dose CDC or vehicle administration (CTL: n=7; Mdx+Vehicle & Mdx+CDC: n=11 each). Cardiac and treadmill experiments were performed separately on different groups of experimental mice. Fig. 1C: Kaplan-Meier analysis of survival in the same animals as Fig. 1C shows lower survival in vehicle-treated *mdx* mice than in CDC-treated *mdx* mice or wild-type controls ($p<0.001$, log rank test); the latter two groups, however, were statistically comparable. Fig. 1D: Immunohistochemical images of Nrf2 in *mdx* mouse hearts 3 weeks after administration of vehicle or CDCs. Age-matched wild-type mice (CTL) served as control. The hearts are stained for inflammatory cell markers CD68, CD20, and CD3. Black arrows point to $CD68^+$ (upper row), $CD20^+$ (middle row), and $CD3^+$ (lower row) cells. Fig. 1E: Malondialdehyde protein adducts in *mdx* mouse hearts 3 weeks after administration of vehicle or CDCs (WT, n = 4; Mdx + vehicle, n=6; and Mdx + CDC, n = 6). Fig. 1F: Western blots and pooled data for protein abundance of phospho-Akt (Akt-p^{T308}, Akt-p^{S473}), cytoplasmic phospho-Nrf2 (Nrf2-p^{S40}), and nuclear Nrf2. Fig. 1G: Western blots and pooled data for protein abundance of nuclear p65, p-IκB (NF-κB pathway) in *mdx* mouse hearts. Fig. 1H: Western blots and pooled data for protein abundance of Nrf2 downstream gene product, heme oxygenase-1 (HO-1). Fig. 1I: Western blots, pooled data, and bar graph representing protein abundance of MCP1 (monocyte chemoattractant protein1) and average number of indicated inflammatory cells and in *mdx* mouse hearts. Fig. 1J: Immunohistochemical images of Nrf2 in *mdx* mouse hearts 3 weeks after administration of vehicle or CDCs. Pooled data are means ± SEM; CM: cardiomyocytes; *$p<0.05$; #$p<0.005$; †$p<0.05$; ‡$p<0.002$; scale bars: 10 μm.

[0040] Figures 2A-B. Restoration of mitochondrial integrity. Fig. 2A: Transmission electron microscopy (TEM) images from *mdx* mouse hearts 3 weeks after administration of vehicle or CDCs. Age-matched WT mice served as control. Scale bars: 5 μm. Mitochondrial structures displayed a clear restoration of organized structure. Fig. 2B: Western blots and pooled data for mitochondrial respiratory chain subunits in WT and vehicle/CDC *mdx* heart tissues and oxygen consumption rate (OCR) of mitochondria isolated from the hearts of WT and CDC- or vehicle-treated *mdx* mice 3 weeks after treatment (WT, n = 3; Mdx + vehicle and Mdx + CDC, n = 8 each). Substrates (pyruvate, malate, and ADP), a selective uncoupler (FCCP) and blockers (oligomycin; antimycin and rotenone) of oxidative phosphorylation were applied when indicated.

[0041] Figures 3A-B. Repopulation with stable competent mitochondria. Fig. 3A: Initial turnover of damaged mitochondria was followed by repopulation with healthy mitochondria. Fig. 3B: Numbers of mitochondria from TEM images, wherein the same mitochondrial number between groups existed, and mitochondrial DNA copy numbers per nuclear genome in *mdx* heart tissue.

[0042] Figures 4A-B. Reduced cardiac collagen content and fibrosis. Fig. 4A: Diminished cardiac fibrosis. Representative Masson trichrome images of a wild-type heart, an *mdx* heart that had been vehicle-injected and an *mdx* heart that had been CDC-injected, and pooled data for morphometric analysis. Fig. 4B: Western blots and pooled data for myocardial cardiac collagen IA1 and IIIA 1, 3 weeks after CDC injection in *mdx* hearts. Data are means ± SEM; †$p<0.05$; #$p<0.05$.

[0043] Figures 5A-B. Cardiomyogenesis. Enhanced cardiomyogenesis 3 weeks after CDC injection in *mdx* mice is evident from representative immunohistochemical images and pooled data. Fig. 5A: Immunohistochemical images (wild type, vehicle-treated and CDC-treated *mdx* mouse hearts stained for Ki67 and Aurora B; n=4-6 per group). Arrows point to $Ki67^+$ (upper row) and Aurora B^+ (lower row) cardiomyocytes. Fig. 5B: Pooled data for morphometric analysis of Aurora B^+ and $ki67^+$ staining. Data are means ± SEM; †$p<0.05$; scale bars: 10 μm.

[0044] Figure 6. Depiction of the various mechanisms unpinning muscular dystrophy pathogenesis involving myocyte loss, fibrosis, oxidative stress, inflammation, mitochondrial inefficiency/loss, apoptosis, fibrosis, etc.

[0045] Figures 7A-B. Restoration of dystrophin expression. Fig. 7A: Immunohistochemical images, western blots, and pooled data for protein abundance of dystrophin

isoforms: dp427, dp260, dp140, dp116, dp71, dp40 in *mdx* mouse hearts 3 weeks after administration of vehicle or CDCs. CDC injection in *mdx* hearts resulted in restoration of dystrophin expression across all measured isoforms. Fig. 7B: Additional representative depiction.

[0046] Figure 8. Schematic of pathophysiological mechanisms operative in muscular dystrophy and the cellular mechanisms recruited by CDCs and CDC-XOs involving myocyte loss, fibrosis, oxidative stress, inflammation, mitochondrial inefficiency/loss, apoptosis, fibrosis, etc.

[0047] Figures 9A-D. CDC-XOs recap effects of CDCs. Intramyocardial injection of CDC-XOs reduces collagen to nearly the same levels as wild-type. Fig. 9A: Western blots and pooled data for cardiac collagen IA and IIIA. WGA (wheat germ agglutinin) was applied for staining and delineation of cell membrane. Fig. 9B: Immunohistochemical images and pooled data (wild type, n = 4; vehicle-treated and CDC-XO-treated, n = 6 each) from *mdx* mouse hearts stained for Ki67 and Aurora B. Arrows point to $Ki67^+$ (upper row) and Aurora B^+ (lower row) cardiomyocytes. Fig. 9C: Western blots and pooled data for protein abundance of dystrophin isoforms: dp427, dp260, dp140, dp116, dp71, dp40 in *mdx* mouse hearts 3 weeks after administration of vehicle, CDCs or CDC-XOs (n=4-6). Fig. 9D: Injection of CDC-XOs into *mdx* hearts retarded progressive decrease in ejection fraction (n=11). Data are means ± SEM; *$p<0.05$; †$p<0.02$; ‡$p<0.01$. Scale bar: 10 μm.

[0048] Figures 10A-B. Disproportional increase in cardiac function and exercise capacity in CDC-treated mdx mice. This could be due to CDCs themselves, secreted mediators (exosomes, EVs, proteins, etc.) from engrafted CDCs, modulated cardiac secretome, and/or improved systemic hemodynamics. Fig. 10A: Disproportional increase in cardiac function and Fig. 10B: exercise capacity in CDC-treated *mdx* mice.

[0049] Figures 11A-N. Intraventricular injection of CDC-XOs. Administration of CDC-XOs demonstrated similar beneficial results. Fig. 11A: Systemic biodistribution of CDC-XOs after intraventricular injection in *mdx* mice. CDC-XOs were stained with fluorescent lipid dye and tracked 6 hours later using bioluminescence imaging. Fig. 11B: CDC-XOs modulated gene expression in a manner mirroring CDCs. Fig. 11C: Dimensional hierarchical clustering using genes from hearts of non-treated *mdx* mice and of *mdx* mice treated intramyocardially with CDCs or intraventricularly with CDC-XOs. Genes with at least 2-fold differences with corresponding transcripts in non-treated *mdx* mice were included. Fig. 11D: Ejection fraction improved with intraventricular injection of CDC-XOs. Fig. 11E: Exercise capacity improved with intraventricular

injection of CDC-XOs. Fig. 11F: Correlation of fold changes in expression of the same genes in the diaphragm 3 weeks after intramyocardial CDC injection or intraventricular CDC-XO injection. Fig. 11G: 2-Dimensional hierarchical clustering using genes from the diaphragm of non-treated *mdx* mice and of *mdx* mice treated intramyocardially with CDCs or intraventricularly with CDC-XOs. Genes with at least 2-fold differences with corresponding genes in nontreated *mdx* mice were included. Fig. 11H: Diaphragm contractile properties 3 weeks after intraventricular CDC-XO injection. Both twitch and specific force improved with intraventricular CDC-XO injection. Fig. 11I: These results were further observed in the soleus, as shown for gene expression results. Fig. 11J: Dimensional hierarchical clustering. Fig. 11K: Contractile properties from the soleus 3 weeks after intraventricular CDC-XO injection. Both twitch and specific force improved with intraventricular CDC-XO injection. Dystropin levels shown for Fig. 11L: heart, Fig. 11M: diaphragm, Fig. 11N: soleus. Data are means ± SEM; *$p<0.05$; †$P<0.05$.

[0050] Figure 12. Biodistribution after intraventricular CDC-XO injection. Figure 12 shows distribution of CDC-XOs stained with fluorescent lipid dye in *mdx* mice.

[0051] Figures 13A-J. Intramuscular injection of CDC-XOs resulted in muscle growth and reversal of pathophysiological abnormalities of muscular dystrophy. Fig. 13A: H&E and immunohistochemical images of the soleus stained for MyoD (wild type, vehicle-treated and CDC-XO-treated *mdx* mouse soleus). Arrows in H&E images point to the linearly arranged nuclei (left column) and myofibers (right column). In the immunohistochemistry, linearly arranged nuclei were positive for MyoD (middle column). Figs. 13B & 13C: Frequency distribution of myofiber sizes and number of myoblasts ($MyoD^+$) 3 weeks after vehicle and CDC-XO injection in *mdx* soleus (n=59). Figs. 13D-13F: Western blots and pooled data for protein abundance of Fig. 13D: MyoD and myogenin, Fig. 13E: IGF1 receptor, and Fig. 13F: cytoplasmic p-p65 in *mdx* soleus 3 weeks after intrasoleus vehicle and CDC-XO injection (n=4-6). Fig. 13G: CDC-XO microRNA reads as a measure of myogenesis. Fig. 13H: Representative Masson trichrome images and morphometric analysis in *mdx* soleus 3 weeks after administration of vehicle and CDC-XOs into *mdx* soleus (n=5-9). Fig. 13I: Immunohistochemical images of dystrophin in *mdx* mouse soleus 3 weeks after intrasoleus injection of vehicle and CDC-XOs (n=4-6). Age-matched wild-type mice served as control. Western blots and pooled data for protein abundance of dystrophin isoform dp427 in *mdx* mouse soleus 3 weeks after administration of vehicle and CDC-XOs (n=4-6). Fig. 13J: *Ex vivo* measurement of soleus contractile properties: twitch force and absolute force 3 weeks

after vehicle and CDC-XO injection into *mdx* soleus. Pooled data are means ± SEM; *p<0.05; †p<0.05; ‡p<0.002; scale bars: 5 μm (Fig. 13A, right column), 10 μm (Fig. 13A, middle column), 50 μm (Fig. 13A, left column), 200 μm (Fig. 13H), 20 μm (Fig. 13I).

[0052] Figures 14A-C. Fig. 14A: CDC-XO injection was capable of modulating transcriptome of diaphragm. Fig. 14B: Western blots and pooled data for protein abundance of dystrophin isoforms in human Duchenne cardiomyocytes (DMD CM) one week after priming with CDC-XOs. Calcium transients from normal and DMD CM measured during 1Hz burst pacing. Duchenne cardiomyocytes were primed with vehicle or CDC-XOs 1 week before assessment. Bar graphs are of calcium transient alternans (variation in beat-to-beat calcium transient amplitude) and time to peak. Western blots and pooled data for protein abundance of dystrophin isoforms: dp427, dp260, dp140, dp116, dp71, dp40 in *mdx* mouse hearts after 3 weeks. Fig. 14C: Oxygen consumption rate (OCR) in DMD CM primed with CDC-XOs or EVs derived from normal human dermal fibroblasts (NHDF-XOs) 1 week before OCR measurement. Normal and non-treated DMD CM were studied in parallel.

[0053] Figure 15. Left ventricular end-diastolic (LV EDV) and end-systolic (LV ESV) volumes after CDC administration. CDC transplantations resulted in a sustained improvement of LV EDV and LV ESV for 3 months after both first and second (3 months interval) injections in *mdx* mice, relative to placebo. Data are means ± SEM; n=12 in each group; #p<0.05.

[0054] Figure 16. Percentage engraftment of CDCs in the heart 1, 2 and 3 weeks after transplantation. Percentage engraftment of CDCs at 1 week was ~8% and <1% at 2 weeks. By 3 weeks, no surviving CDCs could be detected. n=3 at each time point.

[0055] Figures 17A-D. Changes in *mdx* heart transcriptome 3 weeks after CDC treatment. Fig. 17A: 2-Dimensional hierarchical clustering using 560 genes with at least 2-fold differences between vehicle-treated and CDC-treated *mdx* hearts. Each column represents an *mdx* heart and each row a gene. Probe set signal values were normalized to the mean across *mdx* hearts. The relative level of gene expression is depicted from the lowest (green) to the highest (red), according to the scale shown on the top. Examples of fold changes of transcripts for genes involved in the various pathways of interest are plotted here, including Fig. 17B: mitochondrial integrity, Fig. 17C: oxidative stress, and Fig. 17D: inflammation.

[0056] Figure 18. Western blots and pooled data for protein abundance. Measurements including catalase, superoxide dismutase-2 (SOD-2), and catalytic subunit of glutamate-cysteine ligase (GCLC) in *mdx* mouse hearts 3 weeks after administration of vehicle or CDCs.

[0057] Figure 19. IPA analysis of differentially expressed genes. Depicted are genes involved in inflammation in CDC-treated and vehicle-treated *mdx* hearts, denoting inhibition of inflammatory response concomitantly with reduced migration of inflammatory cells in *mdx* hearts 3 weeks after CDC treatment. The blue color represents inhibition of function/response and the red and green colors represent up and downregulation, respectively.

[0058] Figures 20A-C. Immunohistochemical images. Depicted are *mdx* hearts stained for inflammatory cell marker CD3 with blowups of the boxed areas, including Fig. 20A: vehicle-treated *mdx* heart, Fig. 20B: CDC-treated *mdx* heart, and Fig. 20C: wild type heart as control.

[0059] Figures 21A-B. Mitochondria. Fig. 21A: Numbers of mitochondria from TEM images. Fig. 21B: Mitochondrial DNA copy numbers per nuclear genome in the heart tissue 3 weeks after treatment.

[0060] Figure 22. XO analysis. Isolated XOs obtained by ultracentrifugation were analyzed by nanoparticle tracking, using the NanoSight NS300 system (NanoSight Ltd, UK). Videos were collected and analyzed using NTA-software (version 2.3), with the minimal expected particle size, minimum track length, and blur setting all set to automatic. Camera shutter speed was fixed at 30.01 ms and camera gain was set to 500. Camera sensitivity and detection threshold were set close to maximum (15 or 16) and minimum (3 or 4), respectively, to reveal small particles. Ambient temperature was recorded manually, ranging from 24°C to 27°C. For each sample, five videos of 60 seconds duration were recorded, with a 10-second delay between recordings, generating five replicate histograms that were averaged. Representative five replicate histograms depicting size/concentration. Standard error of the mean concentration, calculated from 5 replicates, is shown in red.

[0061] Figure 23. LV end-diastolic (LV EDV) and end-systolic (LV ESV) volumes after CDC-XO administration. CDC-XO transplantation resulted in a sustained improvement of LV EDV and LV ESV for 3 months after both first and second (3 months interval) injections in *mdx* mice, relative to placebo. Data are means ± SEM; n=11 in each group; #$p<0.05$.

[0062] Figure 24. Immunoglobin serum level. IgG serum levels 6 months after the first injection and 3 months after repeat injection of mouse CDCs, human CDC-XOs, and vehicle in *mdx* mice. Circulating anti-donor IgG antibodies were screened by flow cytometry.

[0063] Figure 25. Clathrin-dependent myocardial uptake of XOs. Distribution of intramyocardially injected CDC-XOs in the *mdx* mouse heart with and without chlorpromazine (CPZ) pretreatment. CPZ is an inhibitor of clathrin-dependent endocytosis. Fluorescent-labeled XOs (XenoLight DiR, 5μM, overnight incubation; Caliper Life Sciences, Hopkinton, MA) were injected intramyocardially into the apex of *mdx* mouse hearts; 6 hours later, the hearts were harvested, fixed and sectioned for evaluation of XO distribution. The average number of labelled XOs in the interior of cardiomyocytes (verified by co-staining for sarcomeric α-actinin [green] and DAPI [blue]) was calculated by counting intracardiomyocyte XOs in 10 fields from each of 10 sections selected randomly from the apical (3 sections; 50μm interval), middle (4 sections; 50μm interval) and basal (3 sections; 50μm interval) regions of each heart. The presence of fluorescently labeled XOs in the interior of the cardiomyocytes is a measure of endocytic uptake; pretreatment with CPZ (50μg/g, i.p., single dose, 1 hour before XO injection), resulted in marked reduction in intracellular presence of XOs, indicating participation of clathrin-mediated uptake in internalization of CDC-XOs in *mdx* cardiomyocytes, among others. Bar graph depicts the number of labeled XOs (purple) in the interior of cardiomyocytes with and without CPZ administration, expressed as the number of intracardiomyocyte labelled XOs divided by the total number of cardiomyocytes per high-power field (HPF). Arrows point to fluorescent-labeled exosomes. Pooled data are means ± SEM; †$p<0.001$.

[0064] Figure 26. Contractile properties. Depicted are extensor digitorum longus (EDL) contractile properties after intramyocardial CDC injection: *In situ* measurement of EDL contractile properties, absolute twitch and maximum tetanic force, 3 weeks after CDC/vehicle treatment of *mdx* hearts.

[0065] Figure 27. IPA analysis of differentially expressed genes. Depicted are genes involved in inflammation in the liver of *mdx* mice treated intramyocardially with CDC or vehicle, denoting inhibition of the NF-κB inflammatory pathway in *mdx* livers 3 weeks after intramyocardial CDC injection. The blue color represents inhibition of function/response and the red and green colors represent up and downregulation, respectively.

[0066] Figure 28. Fold change of mitochondrial-related microRNAs in XOs from hypoxically-cultured CDCs relative to XOs from CDCs grown under normoxia. Depicted is 2-dimensional hierarchical clustering using microRNAs with -6 to 6 times log2 fold change (230 microRNAs). The relative log2 fold change of microRNAs is represented from the lowest (red (bottom), -6) to the highest (green (top), +6), according to the scale shown at the top. Each column represents an XO preparation and each row a microRNA species. Among 389 detected microRNAs in hypoxic XOs, 248 were previously reported to be mitochondria-related microRNAs.

[0067] Figure 29. Fold changes of microRNAs under different culturing conditions. Depicted are properties of CDC-XOs isolated from hypoxic conditioned media (2% O_2) compared to CDC-XOs isolated from normoxic conditioned media; fold change >10 and <-20 were included. NEBNext Small RNA Library Prep kit (New England BioLabs, Ipswich, MA) was used for miRNA-seq library preparation of extracted small RNAs from the XOs. RNAs were extracted from XOs using miRNeasy Serum/Plasma Kit (QIAGEN, Germantown, MD).

[0068] Figures 30A-B. Physiological properties following CDC-XO and miR-148 administration. Fig. 30A: LV ejection fraction at baseline and 3 weeks after intramyocardial injection of CDC-XOs and NHDF-XOs in *mdx* mice. Fig. 30B: LV ejection fraction at baseline and 3 weeks after intramyocardial injection of miR-148 and microRNA mimic control in *mdx* mice. Data are means ± SEM; n=5 per group.

[0069] Figures 31A-B. Age-related changes in dystrophin expression in *mdx* hearts. Fig. 31A: Dystrophin expression in young (8 weeks) and old (10 months) *mdx* hearts. Fig. 31B: Western blot of dystrophin protein in wild-type control mouse heart and *mdx* mouse hearts 3 weeks and 3 months after first intramyocardial CDC injection and 3 months after second (repeat) CDC injection into myocardium. All hearts were from mice 10 months old at baseline. CS: citrate synthase.

[0070] Figures 32A-D. Non-cardiac manifestations CDC or CDC-XO injections. Fig. 32A: Ingenuity pathway analysis of differentially expressed genes involved in inflammation in the liver of *mdx* mice injected intramyocardially with CDCs or vehicle, showing inhibition of the NF-κB inflammatory pathway in *mdx* livers 3 weeks after intramyocardial CDC injection. The blue color represents inhibition of function/response and the red and green colors represent up and downregulation, respectively. Fig. 32B: Bioluminescence imaging of *mdx* mouse organs after systemic injection of dyed human CDC-XOs. 6 hours after injection of XOs systemically into the

mdx mouse left ventricular cavity, the indicated organs were dissected and imaged using IVIS molecular imaging systems (Caliper Life Sciences, Hopkinton, MA, USA). Fig. 32C: Western blot of dystrophin protein in wild type mouse heart and *mdx* mouse hearts 1 week, 3 weeks and 3 months after first intraventricular CDC-XO injection and 3 months after second (repeat) CDC-XO injection. Fig. 32D: Western blot showing protein content of dystrophin in wild type control and in *mdx* mouse heart, hypothalamus, diaphragm, soleus, tibialis anterior, and extensor digitorum longus, 3 weeks after systemic CDC-XO delivery by intraventricular injection. CS: citrate synthase loading control. Although no dystrophin expression is evident in the EDL, contractile force was increased in EDL after intramyocardial CDC injection, suggesting that dystrophin re-expression may not be the sole mechanism of benefit in skeletal muscle.

[0071] Figure 33. Dystrophin expression and its consequences. Absence of dystrophin in XOs. Wild type heart lysate was used as a positive control for probing dystrophin.

[0072] Figures 34A-D. Verification that the bioactivity of the XOs studied here are attributable to exosomes characterized. Exosomes were floated on a linear iodixanol density gradient, which demonstrated vesicles by transmission electron microscopy (TEM) and the presence of membrane proteins, and showed that the biological effect is vesicle associated. Fig. 34A: TEM images of sequentially-centrifuged exosomes with (Exo1, left) and without (Exo2, right) purification with linear iodixanol density gradient show vesicles in both conditions. The vesicles are variable in size and morphology, consistent with previous work. Fig. 34B: Western blot on lysed exosomes for key proteins characteristic of exosomes: CD63, CD81 and TSG. Fig. 34C, Fig. 34D: Biological activity of Exo1 and Exo2 were compared by injection into *mdx* soleus and evaluation of *mdx* soleus transcriptome 3 weeks after injection. Fig. 34C: Changes in *mdx* soleus transcriptome 3 weeks after Exo1 and Exo2 injection. 2-Dimensional hierarchical clustering using 332 genes with at least 2-fold differences between vehicle/Exo1 and vehicle/Exo2 in *mdx* soleus. Fig. 34D: Correlation of fold changes in expression of the same genes 3 weeks after Exo1 and Exo2 injection in *mdx* soleus. The similarity of the effects of Exo1 and Exo2 support the notion that the bioactivity of the vesicles isolated by the default protocol is genuinely due to exosomes, and not to other types of vesicles that might have been co-purified by ultracentrifugation. Scale bars: 50 μm (Exo1); 100 nm (Exo2).

[0073] Figures 35A-C. miR-148a-3p and srDMD transplantation into *mdx* heart. Fig. 35A: Differential expression of miR-148a-3p and srDMD in CDC-XOs isolated from hypoxic

conditioned media (2% O_2) compared to CDC-XOs isolated from normoxic conditioned media (n=2), along with depiction of apparent secondary structure of srDMD. Fig. 35B: Western blots and pooled data for protein abundance of dystrophin isoforms: dp427, dp260, dp140, dp116, dp71, dp40 in *mdx* mouse hearts 3 weeks after intramyocardial injection of vehicle, CDCs, CDC-XOs (n=4-6), miR-148a-3p, or srDMD. Fig 35C: Western blots and pooled data for protein abundance of dystrophin isoforms: dp427, dp260, dp140, dp116, dp71, dp40 in *mdx* mouse hearts 3 weeks after intramyocardial injection of vehicle, CDCs, CDC-XOs (n=4-6), miR-148a-3p, and srDMD.

[0074] Figures 36A-B. Exon skipping/alternative splicing excluded. Fig. 36A: miR-148a results in decreases in both NFκB p65 and phospho-Akt levels. Fig. 36B: RT-PCR using primers that flank the exon 23 of dystrophin. It was used to assess exon 23 inclusion in expressed dystrophin in *mdx* hearts from vehicle, miR-148a-3p, and srDMD-treated mice (n=4-6). Sashimi plots of RNA-seq data for dystrophin from vehicle, miR-148a-3p, or srDMD-treated *mdx* hearts depict no junction read that span exon 23. All data are means ± SEM; ǂp<0.03.

[0075] Figures 37A-B. Western blot detection of dystrophin. Fig. 37A: Western blot depicting protein content of dystrophin in wild type mouse hearts and srDMD-treated *mdx* mouse hearts 3 weeks after intramyocardial injection of srDMD. Fig. 37B: Percentage increase relative to vehicle (PBS) in dystrophin/eGFP expression after treatment with CDC-XOs, miR-148a-3p, or srDMD in transfected HEK293 NT cells with dual reporter constructs harboring a point mutation in exon 23 of dystrophin gene or deletion of exon 50 of dystrophin gene.

[0076] Figures 38A-B. Dystrophin expression and its consequences. Fig. 38A: Ejection fraction at baseline and 3 weeks after intramyocardial injection of miR-148a-3p or microRNA mimic control in *mdx* mice. Wild type EF values also shown for reference; n=5 per group. Fig. 38B: Western blot depicting protein content of dystrophin in wild type mouse hearts and in vehicle-, mutant srDMD, or srDMD-injected mdx mouse hearts 3 weeks after intramyocardial injection.

[0077] Figures 39A-B. Fig. 39A: Plasmid map of synthetic DNA constructs cloned into mammalian expression vectors. Full length human dystrophin was cloned into the ORF, either as wild-type or as one of two mutants: UAA premature termination codon in exon 23 (PTC), or exon 50 deletion (Exon 50 Δ). The construct creates a fusion protein of full-length dystrophin in frame with eGFP, such that green fluorescence can be taken as a reporter of dystrophin expression. Constitutive luciferase expression (driven independently by an SV40 promoter) was used to normalize for transfection efficiency. Fig. 39B: Dystrophin/eGFP expression in HEK-293NT cells

transfected with full-length (WT), PTC or Exon 50 Δ constructs. Fluorescence and luminescence of total cell lysates were quantified on a well-by-well basis in a 96-well spectrophotometer; fluorescence in each well was also quantified with nontransfected cells at an equivalent seeding density and lysis volume.

[0078] Figures 40A-D. Ten-to-twelve month old *mdx* mice were treated with the following: a single dose of vehicle (*mdx*), 2.5 x 10^5 syngeneic CDCs, or 2.0 x 10^9 human CDC-exosomes (CDC-XOs) via intravenous injection into the femoral vein. Fig. 40A shows maximal exercise capacity (n=8-10 per group) and Fig. 40B *in vivo* cardiac ejection fraction (n=6-8 per group) before (baseline) and 3 weeks following treatment. Fig. 40C shows Masson's trichrome micrographs of hearts from vehicle- (top panel), CDC- (middle panel), or XO- (bottom panel) treated *mdx* mice. Fig. 40D shows pooled data analyzing area of blue staining (collagen) relative to red staining (cytoplasm) as a marker of cardiac fibrosis (n=5-6 per group). Data are represented as mean ± SEM. * indicates statistically different from vehicle treatment. Statistical significance was set to $P<0.05$.

[0079] Figures 41A-D. Animals were treated as described in Figure 40, Fig. 41A shows whole transcriptome analysis of hearts from RNA-sequencing data. Transcripts with a 2-fold or higher change with $P<0.05$ were considered differentially expressed and represented in the heatmap in panel A. The *mdx* column was compared to an age-matched wild-type mouse heart, while the CDCs and XOs columns were each compared to *mdx* mouse hearts. Fig. 41B shows representative Western blot and pooled data probing for phosphorylated NFκB protein levels (n=5-6 per group) in the hearts from wild-type (WT), vehicle (*mdx*), CDC, or XO treated mice. Fig. 41C shows pooled data from CD68 immunofluorescent images (n=3 per group) Fig. 41D from *mdx*, CDC, or XO treated hearts. Data are represented as mean ± SEM. * indicates statistically different from vehicle treatment. Statistical significance was set to $P<0.05$.

[0080] Figures 42A-D. Animals were treated as described in Fig. 40. Fig. 42A. Pooled data from Western blot analysis of mitochondrial electron transport chain complexes (n=6 per group) from WT, *mdx*, CDC, or XO treated hearts. Fig. 42B. Protein-carbonyl adduct formation (n=8-10 per group) in WT, *mdx*, CDC, or XO treated hearts. Fig. 42C. Pooled data from Ki-67 immunofluorescent images (n=3 per group). Fig. 42D from *mdx*, CDC, or XO treated hearts. Data are represented as mean ± SEM. * indicates statistically different from vehicle treatment. Statistical significance was set to $P<0.05$.

[0081] Figures 43A-F. Animals were treated as described in Fig. 40. Fig. 43A. Force-frequency relationship of solei (n=5-8 per group) from WT (circle), *mdx* (square), CDCs (upward triangle), or XOs (downward triangle). Fig. 43B Twitch and Fig. 43C tetanic force developed by solei from WT, *mdx*, CDCs, or XO treated mice. Fig. 43D Force-frequency relationship of diaphragms (n=5-6 per group) from WT (circle), *mdx* (square), CDCs (upward triangle), or CDC-XOs (downward triangle). Fig. 43E Twitch and Fig. 43F tetanic force developed by diaphragms from WT, *mdx*, CDCs, or CDC-XO treated mice. Fig. 43G Masson's trichrome micrographs from *mdx* (left panel), CDC- (middle panel), or CDC-XO- (right panel) treated mice. Fig. 43H Pooled data analyzing area of blue staining (collagen) relative to red staining (cytoplasm) as a marker of skeletal muscle fibrosis in the soleus (n=5-6 per group). Fig. 43I Quantification of the number of myofibers per whole muscle section of the soleus (n=5-6 per group). Data are represented as mean ± SEM. * indicates statistically different from vehicle treatment. Statistical significance was set to $P<0.05$.

[0082] Figures 44A-D. Animals were treated as described in Fig. 40. Fig. 44A. Whole transcriptome analysis of hearts from RNA-sequencing data. Transcripts with a 2-fold or higher change with $P<0.05$ were considered differentially expressed and represented in the heatmap in panel A. The *mdx* column was compared to an age-matched wild-type mouse soleus, while the CDCs and CDC-XOs columns were each compared to *mdx* mouse solei. Fig. 44B. Kyoto Encyclopedia of Genes and Genomes analysis of a CDC-XO treated soleus. Pathways listed are considered *up*regulated relative to *mdx* soleus – many are involved in inflammation. Fold change in genes known to be involved in Fig. 44C TNF and Fig. 44D NFκB signaling altered in the soleus by CDC and CDC-XO treatment.

[0083] Figures 45A-C. Animals were treated as described in Fig. 40. Fig. 45A Representative Western blot and pooled data probing for phosphorylated NFκB protein levels (n=3 per group) in the soleus from wild-type (WT), vehicle (*mdx*), CDC, or CDC-XO treated mice. Fig. 45B Pooled data from CD68 immunofluorescent images (n=3 per group). Fig. 45C from *mdx*, CDC, or CDC-XO treated hearts. Data are represented as mean ± SEM. * indicates statistically different from vehicle treatment. Statistical significance was set to $P<0.05$.

[0084] Figures 46A-B. Animals were treated as described in Fig. 40. Western blot probing for full-length (427 kDa) dystrophin in the soleus Fig. 46A and diaphragm Fig. 46B from

vehicle (*mdx*), CDC, GW4869 treated CDCs, and CDC-XO treated mice. The left 2 columns represent a relative level of WT dystrophin (e.g., 5% and 1%).

[0085] Fig. 47 depicts a schematic protocol that was used for evaluating the efficacy of escalating doses of intravenous administration of CDCs to improve exercise capacity using a mouse model of DMD (*mdx* mice), wherein *mdx* mice received treatment or control vehicle in Week 0, exercised every week, and were sacrificed in Week 6.

[0086] Figs. 48A-48B graphically show effects of intravenous (IV) administration of CDCs on the exercise capacity of *mdx* mice injected with 75,000, 150,000, or 250,000 (referred to as "75K," "150K," and "250K," in the figure) CDCs versus phosphate buffered saline (PBS) control.

[0087] Fig. 49 graphically shows the effects of jugular IV administration of CDCs on the diaphragm muscle function of mice injected with 75K-250K CDCs versus PBS control.

[0088] Figs. 50A and 50B graphically show the effects of jugular IV administration of CDCs on the body weight of *mdx* mice injected with 37K-150K CDCs versus PBS control.

[0089] Fig. 51 shows that CDCs administered in accordance with several embodiments disclosed herein reduce fibrosis in the hearts of *mdx* mice (shown is collagen staining, an indicator of fibrosis).

[0090] Fig. 52A depicts a schematic protocol that was used for evaluating effects of CDC treatment on cardiac ejection fraction using echocardiography.

[0091] Fig. 52B graphically shows the effects of jugular IV administration of CDCs on the cardiac ejection fraction of *mdx* mice injected with 150K CDCs versus PBS control.

[0092] Fig. 53 depicts histology data of Masson's trichrome staining of heart tissue sections of *mdx* mice injected with 150K CDCs via jugular IV injection, or 250K CDCs via femoral IV injection, versus PBS control.

[0093] Fig. 54 graphically shows the effects of IV administration on the cardiac (left ventricular) ejection fraction in a mouse model of myocardial infarction with 300K CDCs via systemic injection (femoral IV injection or 100K CDCs via injection into the right ventricle) versus 100K CDCs via intramyocardial injection versus PBS control.

[0094] Fig. 55A graphically shows that qPCR performed on purified human CDC DNA was validated.

[0095] Fig. 55B graphically shows standard curves of human CDC DNA spiked into mouse tissue DNA prepared for each tissue to be tested.

[0096] Fig. 56A depicts a schematic protocol for determining the biodistribution of human CDCs in wild type (WT) mice after jugular vein administration by a human Alu sequence qPCR method.

[0097] Fig. 56B graphically shows human CDC biodistribution in WT mice 10 minutes and 24 hours after jugular vein injection, in the lung, liver, blood, heart, soleus, diaphragm, and spleen tissues.

[0098] Fig. 57A depicts a schematic protocol for determining the biodistribution and clearance of human CDCs in severe combined immunodeficiency (SCID) mice after jugular vein administration by human Alu sequence qPCR method.

[0099] Fig. 57B graphically shows human CDC biodistribution in SCID mice 24 hours, 1 week, and 3 weeks after jugular vein injection, in the lung tissue.

[0100] Fig. 57C graphically shows human CDC biodistribution in SCID mice 24 hours, 1 week, and 3 weeks after jugular vein injection, in the liver, blood, heart, soleus, diaphragm, spleen, and testes tissue.

[0101] Fig. 58 schematically illustrates lung tissue sample collection for histopathological analysis to evaluate safety of high dose of CDCs in a porcine model of acute myocardial infarction.

[0102] Fig. 59 graphically shows changes in serum troponin I (TnI) levels in pigs treated with 50, 100 or 200 million ("50M," "100M," or "200M," respectively) CDCs.

[0103] Fig. 60 graphically shows average area at risk (AAR) in pigs treated with 50, 100 or 200 million CDCs.

[0104] Fig. 61 graphically shows average ratio between no reflow (unstained) and area at risk, indicating myovascular obstruction (MVO) in pigs treated with 50, 100 or 200 million CDCs.

[0105] Fig. 62 graphically shows average ratio of triphenyl tetrazolium chloride (TTC) stain and area at risk, indicating scar size, in pigs treated with 50, 100 or 200 million CDCs.

[0106] Fig. 63 graphically shows ΔEF calculated for treated and untreated animals, in pigs treated with 50, 100 or 200 million CDCs.

[0107] Fig. 64 graphically shows the expression of immune molecules involved in T and natural killer (NK) immune response by steady state CDCs. The percentage of positive cells and geometric mean fluorescence intensity are indicated.

[0108] Fig. 65 shows representative images of tailored-MLR cultures.

[0109] Fig. 66 graphically shows the activation of T cells by CDC. Expression of CD69 (left panel) and HLA-DR (right panel) by CD4+ (black) and CD8+ T (white) cells by three different PBMC (Donor A, C, and D). Results are mean values ± SD of triplicates. *$p<0.05$; **$p<0.01$; ***$p<0.001$; ****$p<0.0001$.

[0110] Figs. 67A-67C graphically show the proliferation of T cells from unfractionated PBMC in response to CDCs; Fig. 67A shows the representative dot plots (from Donor A); Fig. 67B shows the proliferation of T cells from three different PBMC donors; Fig. 67C shows the proliferation of T cells from 3 different donors. For Fig. 67B, results are mean values ± SD from triplicates. For Fig. 67C, results are mean values ± SD obtained from three different donors each in triplicates.

[0111] Fig. 68 graphically shows the purified T cells activation and proliferation in response to CDCs. Results are mean values ± SD obtained from responses (duplicates) for each donor (upper and middle panels) and as mean values ± SEM obtained from both donors each in duplicate (lower panel).

[0112] Fig. 69 graphically shows the immune modulation of phytohemagglutinin (PHA)-induced T cells proliferation by CDCs. Representative cultures and histograms (upper panel) and results presented as mean percentage values ± SD from 3 different donors each done in triplicates.

[0113] Fig. 70 graphically shows the modulation of PHA-induced CD69 and HLA-DR expression and PHA-induced T cells proliferation by CDCs. Results for each donor are presented as mean values ± SD obtained from triplicates. Lower panel presents mean values ± SD of the percentages of decrease (CD69) or increase (HLA-DR) in expression of activation markers (left and middle panels) and percentage of proliferation inhibition obtained from both donors each done in triplicates.

[0114] Fig. 71 is a western blot showing CDC-EVs' contents of recognized exosomes markers.

[0115] Fig. 72 graphically shows the expression of immune molecules involved in T and natural killer (NK) immune response on CDC-EVs.

[0116] Figs. 73A-73B show the activation of T cells by CDCs and CDC-EVs; Fig. 73A shows the representative images of tailored-MLR cultures; Fig. 73B shows the expression of CD69 and HLADR by $CD4^+$ and $CD8^+$ T cells.

[0117] Figs. 74A-74B graphically show T cells proliferation in response to CDC and EVs; Fig. 74A shows the representative dot plots; Fig. 74B shows the proliferation of T cells from 3 different donors presented as mean values ± SD from triplicates.

[0118] Fig. 75 graphically shows the purified T cells activation and proliferation in response to CDCs and CDC-EVs. Results are presented as mean values ± SD obtained from responses (duplicates) from 2 different donors.

[0119] Fig. 76 shows the IDC cultures in the presence and absence of EVs (upper panel) and expression of relevant immune molecules (lower panel).

[0120] Fig. 77 graphically shows the purified T cells activation and proliferation by CDC-EVs presented by iDC. Results are presented as mean values ± from triplicates.

[0121] Fig. 78 shows the mDC cultures in the presence and absence of EVs (upper panel) and expression of relevant immune molecules (lower panel).

[0122] Fig. 79 graphically shows the purified T cells activation and proliferation by mDC and mDC-EVs. Results are presented as mean values ± from triplicates.

[0123] Fig. 80 shows the immune modulation of PHA-induced T cells proliferation by CDCs and CDC-EVs. Results are mean percentage values ± SEM from 3 different donors each done in triplicates.

[0124] Fig. 81 graphically shows the down-regulation of PHA-induced CD69 and/or HLA-DR expression by CDCs and CDC-EVs. Results are mean percentage values ± SD obtained from triplicates.

[0125] Fig. 82 graphically shows that CDCs and CDC-EVs down regulate PHA-induced T cells proliferation. Results are mean values ± SD obtained from triplicates.

[0126] Fig. 83 graphically shows that Immune modulation of PHA-induced $CD4^+$ and $CD8^+$ T cells proliferation by CDC and CDC-EVs. Results are mean percentage values ± SEM from 2 different donors each done in triplicates.

[0127] Fig. 84A is a graphical depiction of changes from baseline in exercise capacity with multiple administrations of syngeneic CDCs (from C57BL/10 mice) or a PBS control. 84B is a graphical depiction of changes from baseline in exercise capacity after multiple administrations of allogeneic CDCs (from C3H mice) or a PBS control. Fig. 84C is a combination of Figs. 84A and 84B into a single graph.

[0128] Fig. 85A is a graphical depiction of changes from baseline in exercise capacity with two administrations of allogeneic CDCs (from C3H mice), a steroid, and/or PBS vehicle. Fig. 85B is a graph of the percent of cells positive for various genetic markers. Fig. 85C is a graph indicating the amount of IgG antibodies.

[0129] Fig. 86 shows data related to evaluation of antibody production in response to administration of CDCs (as compared to PBS).

DETAILED DESCRIPTION

[0130] Some embodiments disclosed herein pertain to methods of treating disease, disease states, and/or symptoms of disease using CDCs, CDC-XOs, CDC-EVs, the isolated molecular cargo of CDCs (e.g., individual molecules or combinations of molecules derived from CDCs, CDC-XOs, and/or CDC-EVs), and/or combinations of the forgoing. In some embodiments, the disease is a dystrophinopathy. In some embodiments, the disease state is a dystrophic disorder. In some embodiments, the dystrophinopathy includes one or more of Duchenne muscular dystrophy (DMD) and/or Becker muscular dystrophy. In some embodiments, the disease state is a myopathy. In some embodiments, the myopathy is a skeletal muscle myopathy. In some embodiments, the method includes administering a therapeutically effective amount of CDCs, CDC-XOs, CDC-EVs, the molecular cargo of CDC-XOs or CDC-EVs, and/or combinations of the forgoing to a subject (e.g., a patient) suffering from the disease, thereby treating the disease and/or its symptoms. Some embodiments of the methods and compositions provided herein are based on the surprising discovery that, *inter alia*, despite the finding that intravenous administration of CDCs to *mdx* mice resulted in accumulation of the at least a portion of administered CDCs in their lungs, functional improvements at dystrophic skeletal muscles were achieved as demonstrated by the various data presented herein, thereby enabling an effective treatment of a human subject suffering from skeletal muscular dystrophy, e.g., Duchenne muscular

dystrophy (DMD), by administering a therapeutically effective amount of CDCs to a human subject suffering from skeletal muscular dystrophy.

[0131] As used herein, "and/or" refers to and encompasses any and all possible combinations of one or more of the associated listed items, as well as the lack of combinations when interpreted in the alternative ("or").

[0132] "Treat" or "treating" or "treatment" refers to any type of action that imparts a modulating effect, which, for example, can be a beneficial effect, to a subject afflicted with a disorder, disease or illness, including preventing the manifestation of disease states associated with the condition, improvement in the condition of the subject (e.g., in one or more symptoms or in the disease), delay or reduction in the progression of the condition, and/or change in clinical parameters, disease or illness, curing the illness, etc.

[0133] The term "therapeutically effective amount," as used herein, refers to an amount of the therapeutic (e.g., CDC-XOs, CDC-EVs, CDCs, molecular cargo of XOs and EVs, or combinations thereof) that imparts a modulating effect, which, for example, can be a beneficial effect, to a subject afflicted with a disorder, disease or illness, including improvement in the condition of the subject (e.g., modulating one or more symptoms), delay or reduction in the progression of the condition, prevention or delay of the onset of the disorder, and/or change in clinical parameters, disease or illness, etc. For example, in some embodiments, an effective amount can refer to the amount of a composition, compound, or agent that improves a condition in a subject by at least 5%, e.g., at least 10%, at least 15%, at least 20%, at least 25%, at least 30%, at least 35%, at least 40%, at least 45%, at least 50%, at least 55%, at least 60%, at least 65%, at least 70%, at least 75%, at least 80%, at least 85%, at least 90%, at least 95%, or at least 100%. Actual dosage levels of active ingredients and agents in an active composition of the disclosed subject matter can be varied so as to administer an amount of the active agent(s) that is effective to achieve the desired response for a particular subject and/or application. The selected dosage level will depend upon a variety of factors including, but not limited to, the activity of the composition, formulation, route of administration, combination with other drugs or treatments, severity of the condition being treated, and the physical condition and prior medical history of the subject being treated. Determination and adjustment of an effective dose, as well as evaluation of when and how to make such adjustments, are contemplated herein. The term "a therapeutically effective amount" can mean an amount of CDC-XOs, CDC-EVs, CDCs, and/or molecular cargo XOs and EVs sufficient

to reverse dystrophinopathy through dystrophin re-expression and/or to durably (e.g., substantially irreversibly) restore skeletal muscle function at a targeted dystrophic skeletal muscle.

[0134] The term "a targeted dystrophic skeletal muscle" as used herein is the delivery of an amount of CDC-XOs, CDC-EVs, CDCs, a molecular cargo CDC-XOs and CDC-EVs, and/or combinations thereof at the site of a dystrophic skeletal muscle. In some embodiments, targeted delivery does not include incidental, accidental, or inadvertent delivery CDC-XOs, CDC-EVs, CDCs, and/or molecular cargo CDC-XOs and CDC-EVs to a target site. In some embodiments, targeted delivery does not include systemic delivery. In some embodiments, targeted delivery does not include incidental, accidental, or inadvertent delivery CDC-XOs, CDC-EVs, CDCs, and/or molecular cargo of CDC-XOs and CDC-EVs in an amount that would be insufficient to treat dystrophinopathy at the site of a dystrophic skeletal muscle.

[0135] The term "dystrophic" as used herein is a lack of or deficiency of dystrophin (e.g., in skeletal and/or heart muscles).

[0136] Cells release into the extracellular environment diverse types of extracellular vesicles (EVs) of endosomal and plasma membrane origin called exosomes (XOs) and microvesicles (MVs). EVs represent an important mode of intercellular communication and serve as vehicles for the transfer of molecular cargo (e.g., one or more of cytosolic proteins, lipids, and RNA) between cells and through cell membranes. XOs, secreted lipid vesicles containing a rich milieu of biological factors, provide powerful paracrine signals by which stem cells potentiate their biological effects to neighboring cells, including diseased or injured cells. Through the encapsulation and transfer of proteins, bio-active lipid and nucleic acid cargo, these natural delivery devices can induce significant phenotypic and functional changes in recipient cells that lead to activation of regenerative programs. Administration of XOs has been demonstrated to treat heart failure in mdx mice in WO2016/05491, which is herein incorporated by reference in its entirety.

[0137] Some embodiments disclosed herein pertain to the use of CDCs and CDC-XOs in methods of therapeutic use. In some embodiments, described herein are methods of treating a dystrophic disorder, including a step of administering a therapeutically effective amount of CDCs and/or CDC-XOs to a subject afflicted or having dystrophinopathy, thereby treating the subject. In some embodiments, the subject is a pediatric subject afflicted with a dystrophinopathy. In some embodiments, the XOs are isolated from CDCs. In some embodiments, the CDCs are grown in

serum-free media. In some embodiments, the dystrophinopathy is Duchenne muscular dystrophy. In other embodiments, the dystrophinopathy is Becker muscular dystrophy. In some embodiments, CDC-XOs, CDC-EVs, molecular cargo of CDC-XOs or CDC-EVs, CDCs producing XOs and EVs, and/or combinations of the forgoing are used in a method for achieving dystrophin re-expression. In some embodiments, the CDC-XOs, CDC-EVs, molecular cargo of CDC-XOs or CDC-EVs, CDCs producing XOs and EVs, and/or combinations upon systemic intraventricular injection of CDC-EVs, as well as upon direct intramuscular injection of CDC-EVs into skeletal muscles of *mdx* mice, whereby the present inventors conceived of the novel treatment method as described for the first time herein, *e.g.*, a method of treating skeletal DMD by administering a therapeutically effective amount of CDCs and/or CDC-EVS in a single or multiple systemic administrations. In some embodiments, the disease is muscular dystrophy.

[0138] The data and experiments disclosed herein demonstrate an unexpected advantage of CDCs, CDC-XOs, and/or CDC-EVs in inducing dystrophin expression. As shown elsewhere herein, injection of CDCs into the hearts of *mdx* mice boosts full-length dystrophin protein levels in both heart and skeletal muscle, dramatically and durably improving cardiac function, ambulatory capacity and survival. Similar results are demonstrated with human Duchenne cardiomyocytes. Positive factors appear to exist in cellular XO's produced by CDCs, which are the lipid bilayer nanovesicles secreted by cells when multivesicular endosomes fuse with the plasma membrane.

[0139] In some embodiments, XOs (and EVs) secreted by human CDCs are demonstrated to reproduce the benefits of CDCs in *mdx* mice and in human Duchenne cardiomyocytes. In some embodiments, the delivery of noncoding RNA species found in CDC-XOs (*e.g.*, miR-148a) mimics the ability of CDCs, CDC-XOs, and/or CDC-EVs to increase dystrophin protein levels, without affecting transcript length or exon/intron junctions. In some embodiments, CDC-XO mediated transfer of noncoding RNAs ameliorates DMD by restoring dystrophin in heart and skeletal muscle.

[0140] In some embodiments, the results described herein demonstrate CDCs and their XOs (and/or EVs) as a therapeutic option for dystrophinopathy. CDCs and their secreted XOs (and/or EVs) robustly increase dystrophin levels in heart and skeletal muscle. In some embodiments, the increasing dystrophin levels in the heart and skeletal muscle leads to major durable systemic benefits after injection of CDCs, CDC-XOs, and/or CDC-EVs into the body (e.g.,

systemically or locally, including locally into the skeletal muscle). In some embodiments, as disclosed herein, CDCs, CDC-XOs, and/or CDC-EVs are not only regenerative, but also anti-inflammatory and anti-fibrotic. CDCs secrete diffusible factors that promote angiogenesis, recruit endogenous progenitor cells, and coax surviving heart cells to proliferate; transplanted CDCs also suppress maladaptive remodeling, and apoptosis. In some embodiments, CDCs operate through indirect pathways (via CDC-XOs and/or CDC-EVs); they work indirectly via the secretion of CDC-XOs and/or CDC-EVs laden with noncoding RNA including microRNAs (constituents of the molecular cargo). In some embodiments, while allogeneic CDCs are cleared completely within several weeks, but their functional and structural benefits persist at least 6 months. These diverse mechanisms are mediated via the secretion of CDC-XOs and/or CDC-EVs laden with noncoding RNA including microRNAs.

[0141] Without being bound to a particular theory, the above mechanisms afford CDCs, CDC-EVs, or CDC-XOs the capacity to treat DMD, with application to similar muscular dystrophies such as Becker muscular dystrophy. In some embodiments, CDCs, CDC-XOs, and/or CDC-EVs replace dystrophin, and offset the pathophysiological consequences of dystrophin deletion, by recruiting regenerating cells, reversing fibrosis and targeting inflammation. In some embodiments, reversing the central deficits of DMD in pediatric patients, the methods herein are capable of forestalling or preventing progression of the disease, allowing those patients to avoid comorbidities which may otherwise significantly limit options for therapeutic intervention.

[0142] While the disclosed methods herein include those involving the delivery of CDCs to a patient, in some embodiments, using CDC-EVs (e.g., CDC-XOs) secreted by CDCs, and not cells, may provide advantages when compared to transplant and delivery of cells themselves. In some embodiments, CDC-EVs and CDC-XOs, including those produced by CDCs, can provide a potent and rich source for developing "cell-free" therapies. CDC-XO-based, "cell-free" therapies, in contrast to cell therapy, provide one or more of the following advantages in regenerative medicine. In some embodiments, as non-viable entities, with reduced or non-existent immunogenic or tumorigenic potential, these features significantly obviate certain safety issues. In some embodiments, stem cell-derived exosomes (and/or CDC-XOs) can be less immunogenic than parental cells, as a result of a lower content of membrane-bound proteins, including MHC complex molecules. In some embodiments, CDC-XO encapsulation of bioactive components in lipid vesicles allows protection of contents from degradation *in vivo*, thereby potentially negating

obstacles often associated with delivery of soluble molecules such as cytokines, growth factors, transcription factors and RNAs. In some embodiments, the ease of administration (and/or storage) for CDC-XOs and/or CDC-EVs can ultimately allow for repeated and sustained delivery to patients, thereby maximizing the potential for regeneration and repair of diseased and/or dysfunctional tissue.

[0143] In some embodiments, CDCs and/or CDC-XOs can be used to stimulate numerous cellular, tissue and physiological processes, including immune modulating processes, angiogenesis, and migration of endothelial cells. As disclosed herein, based on the pathophysiology of DMD patients, including an environment of increased oxidative and/or nitrosative stress, elevated inflammation, pro-apoptotic and remodeling states, therapeutic approaches involving CDCs and/or CDC-XOs secreted by cells, provide significant benefits in reversing the course of the disease (and one or more of the aforementioned disease states and/or manifestations). In some embodiments, CDCs, CDC-XOs, and/or CDC-EVs promote anti-oxidative, anti-inflammatory, anti-apoptotic, anti-remodeling effects. In some embodiments, CDCs, CDC-XOs, and/or CDC-EVs enhance regenerative capacity of diseased cells and tissues. In some embodiments, CDC, CDC-XO, and/or CDC-EV administration is beneficial in retarding and/or reversing DMD, and exosome populations derived from CDCs allow for these benefits to be delivered. Early therapeutic intervention in pediatric subjects provides durable and systemic benefits that will prevent or ward off comorbidities in late stage disease, such as heart failure. In some embodiments, durable benefits are those lasting equal to or at least about: 3 months, 6 months, 12 months, or ranges including and/or spanning the aforementioned values.

[0144] **Some Embodiments of Exosomes.** XOs are lipid bilayer vesicles that are enriched in a variety of biological factors, including cytokines, growth factors, transcription factors, lipids, and coding and non-coding nucleic acids. XOs are found in blood, urine, amniotic fluid, interstitial and extracellular spaces. These exocytosed vesicles of endosomal origin can range in size between 30-200 nm, including sizes of 40-100 nm, and possess a cup-shaped morphology, as revealed by electron microscopy. Their initial formation begins with inward budding of the cell membrane to form endosomes, which is followed by invagination of the limiting membrane of late endosomes to form multivesicular bodies (MVB). Fusion of the MVB with the plasma membrane results in the release of the internal vesicles to the extracellular space, through the formation of vesicles thereafter known as exosomes. In some embodiments, XOs as described herein are those

extracellular vesicles that are exocytosed and/or are of endosomal origin. In some embodiments, XO as described herein can have diameters of less than or equal to about: 30 nm, 50 nm, 100 nm, 150 nm, 200 nm, or ranges including and/or spanning the aforementioned values.

[0145] As described herein, the "cargo" contents of XOs reflect their parental cellular origin, as containing distinct subsets of biological factors in connection with their parent cellular origin, including the cell regulatory state of the parental cells when formed. The rich biological milieu of different proteins, including cytokines and growth factors, lipids, coding and noncoding RNA molecules, within exosomes are all necessarily derived from their parental cells. In addition to containing a rich array of cytosolic derivatives, exosomes further express the extracellular domain of membrane-bound receptors at the surface of the membrane.

[0146] In some embodiments, the described encapsulation and formation processes create heterogeneity in XO compositions based on parental cellular origin and regulatory state at time of formation. Nevertheless, in some embodiments, generic budding formation and release mechanisms establish a common set of features as a consequence of their origin, such as endosome-associated proteins (e.g., Rab GTPase, SNAREs, Annexins, and flotillin), proteins that are known to cluster into microdomains at the plasma membrane or at endosomes (four transmembrane domain tetraspanins, e.g., CD63, CD81, CD82, CD53, and CD37), lipid raft associated proteins (e.g., glycosylphosphatidylinositol- anchored proteins and flotillin), cholesterol, sphingomyelin, and hexosylceramides.

[0147] In some embodiments, in addition to components reflecting their vesicle origin, XOs contain both mRNA and microRNA associated with signaling processes, with both cargo mRNA being capable of translation in recipient cells, or microRNA functionally degrading target mRNA in recipient cells. In some embodiments, other noncoding RNAs, capable for influencing gene expression, may also be present in XOs. While the processes governing the selective incorporation of mRNA or microRNA populations into XOs is not entirely understood and without being bound to any particular theory, it is believed that RNA molecules are selectively, not randomly incorporated into XOs, as demonstrated by the enrichment of XOs cargo RNAs when compared to the RNA profiles of other exosomes and their originating cells. In some embodiments, in view of RNA molecules potential a role in disease pathogenesis and regenerative processes, without being bound by a theory, the presence of RNA molecules in XOs and apparent potency in

affecting target recipient cells allow XOs and their molecular cargo therapeutically effective as disclosed elsewhere herein.

[0148] In some embodiments, the natural bilayer membrane encapsulation of exosomes also provides a protected and controlled internal microenvironment that allows cargo contents to persist or migrate in the bloodstream or within tissues without degradation. In some embodiments, the later release of this cargo into the extracellular environment allows for interaction with recipient cells via adhesion to the cell surface mediated by lipid-ligand receptor interactions, internalization via endocytic uptake, or by direct fusion of the vesicles and cell membrane. These processes lead to the release of exosome cargo content into the target cell.

[0149] In some embodiments, XO-cell interactions can modulate genetic pathways in the target recipient cell, as induced through any of several different mechanisms including antigen presentation, the transfer of transcription factors, cytokines, growth factors, nucleic acid such as mRNA and microRNAs.

[0150] **Isolation and Preparation of Exosomes.** In some embodiments, XO isolation can be accomplished using their generic biochemical and biophysical features for separation and analysis. In some embodiments, differential ultracentrifugation can be used as a technique wherein secreted XOs are isolated from the supernatants of cultured cells. In some embodiments, this approach allows for separation of XOs from nonmembranous particles, by exploiting their relatively low buoyant density. In some embodiments, size exclusion allows for their separation from biochemically similar, but biophysically different MVs, which possess larger diameters of up to 1,000 nm. In some embodiments, MVs are also included in therapeutic mixtures with XOs (where EVs encompass both XOs and MVs) and/or MVs are not removed from XOs. In other embodiments, XOs can be isolated from MVs so that the XOs are enriched and/or substantially free of MVs. In some embodiments, differences in flotation velocity further allows for separation of differentially sized exosomes. In some embodiments, XOs sizes will possess a diameter ranging from 30-200 nm, including sizes of 40-100 nm. In some embodiments, the disclosed MVs and EVs have sizes (in nm) of greater than or equal to about: 1000, 750, 500, 400, 300, 250, 200, or ranges including and/or spanning the aforementioned values.

[0151] In some embodiments, further purification of XOs may be performed based on specific properties of the particular exosomes of interest. This includes, for example, use of

immunoadsorption with a protein of interest to select specific vesicles with exoplasmic or outward orientations.

[0152] In some embodiments, while any one of differential centrifugation, discontinuous density gradients, immunoaffinity, ultrafiltration and high performance liquid chromatography (HPLC) may be used to isolate XOs (and/or MVs), differential ultracentrifugation is used. In some embodiments, this technique utilizes increasing centrifugal force from 2000xg to 10,000xg to separate the medium- and larger-sized particles and cell debris from the exosome pellet at 100,000xg. While centrifugation alone allows for significant separation/collection of XOs from a conditioned medium, in some embodiments, ultracentrifugation may also remove various protein aggregates, genetic materials, particulates from media and cell debris that are common contaminants. In some embodiments, enhanced specificity of exosome purification may deploy sequential centrifugation in combination with ultrafiltration, or equilibrium density gradient centrifugation in a sucrose density gradient, to provide for the greater purity of the exosome preparation (flotation density 1.1-1.2g/ml) or application of a discrete sugar cushion in preparation.

[0153] In some embodiments, ultrafiltration can be used to purify exosomes without compromising their biological activity. In some embodiments, membranes with different pore sizes - such as molecular weight cut-off (MWCO) less than or equal to about: 200 kDa, 100 kDa, 75 kDa, 50 kDa, or ranges including and/or spanning the aforementioned values. In some embodiments, gel filtration can alternatively or also be used to eliminate smaller particles. In some embodiments, membrane (e.g., dialysis, ultrafiltration, etc.) and/or gel filtration is performed using a substantially physiological pH and/or at substantially physiological salt concentrations (e.g., avoiding the use of a nonneutral pH or non-physiological salt concentration). In some embodiments, tangential flow filtration (TFF) systems used. In some embodiments, TFF systems are scalable (to >10,000L), allowing one to not only purify, but concentrate the XO fractions. In some embodiments, such approaches are advantageously less time consuming than differential centrifugation. In some embodiments, HPLC is used to purify the XOs. In some embodiments, HPLC can also be used to purify exosomes to homogeneously sized particles and preserve their biological activity as the preparation is maintained at a physiological pH and salt concentration.

[0154] In some embodiments, chemical methods are used to isolate XOs. In some embodiments, these chemical methods include separation by differential solubility in precipitation techniques. In some embodiments, a precipitation reagent is added to a solution of XOs to purify

the XOs. In some embodiments, these chemical methods include separation by addition to volume-excluding polymers (e.g., polyethylene glycols (PEGs), etc.). In some embodiments, these chemical methods can be combined with additional rounds of centrifugation or filtration, etc. In some embodiments, for example, a precipitation reagent, ExoQuick®, is added to a conditioned cell media to quickly and rapidly precipitate a population of exosomes. In some embodiments, flow field-flow fractionation (FlFFF) is an elution-based technique that is used to separate and characterize macromolecules (e.g., proteins) and nano- to micro-sized particles (e.g., organelles and cells) and which is successfully applied to fractionate exosomes from culture media.

[0155] In some embodiments, beyond the techniques disclosed elsewhere herein, relying on biochemical and biophysical features of the XOs, focused techniques may be applied to isolated specific exosomes of interest. In some embodiments, antibody immunoaffinity is used to recognize XO-associated antigens. In some embodiments, XOs express the extracellular domain of membrane-bound receptors at the surface of the membrane of the parent cells. In some embodiments, this expression allows isolating and segregating XOs in connections with their parental cellular origin, based on a shared antigenic profile. In some embodiments, conjugation to magnetic beads, chromatography matrices, plates or microfluidic devices, and/or combinations of such techniques with other techniques disclosed herein allows isolating of specific XO or MV populations of interest (e.g., as may be related to their production from a parent cell of interest or associated cellular regulatory state). Other affinity-capture methods use lectins which bind to specific saccharide residues on the XO surface.

[0156] **Exosome-Based Therapies.** In some embodiments, as disclosed elsewhere herein, XO-based therapy advantageously allows potential "cell-free" therapies (e.g., where CDCs etc. are separated from CDC-XOs, etc.). The use of a "cell-free" therapy holds potential benefits of cellular therapeutics with reduced risks and/or can be used in scenarios in which cell therapy would be unavailable (and/or impossible). In some embodiments, as described elsewhere herein, the therapeutic benefits of cell-based therapies such as CDCs may occur through indirect mechanisms involving regenerated tissue arising from endogenous origin. In some embodiments, cellular XOs produced by CDCs may allow for production and delivery of growth factors, transcription factors, cytokines and nucleic acids for new therapeutic approaches in a manner that not only ameliorates progression of the disease, but repairs and regenerates disease and/or dysfunctional tissue. In this regard, CDC-derived exosomes can effectively address a major unmet

medical need, by recruiting synergistic mechanisms to attract endogenous stem cells to sites of myocardial injury, promote cellular differentiation, reversing chronic disease pathophysiology, such as Duchenne muscular dystrophy. In some embodiments, CDCs can be used as XO (and/or EV) factories, advantageously providing a lasting source of XOs throughout the time of residence of the CDC in the patient.

[0157] In some embodiments, particularly for chronic conditions, such as DMD, repeated and sustained delivery to patients of CDC-XOs or CDCs that produce XOs may enhance the potential for regeneration and repair of diseased and/or dysfunctional tissue, in a manner that would be easier and potentially safer than when using a cell-based therapy. Dosing regimens and schedules are disclosed in additional detail elsewhere herein.

[0158] In some embodiments, as disclosed elsewhere herein, the administration methods and amounts of XOs and/or CDCs provided to a patient can be provided in a variety of ways to deliver a therapeutic dose. In some embodiments, for example, administering a composition and/or solution for administration of XOs includes about 1 to about 100 mg CDC-XO protein in a single dose. In some embodiments, a dose of CDC-EVs (e.g., CDC-XOs) may comprise a weight of EVs or XOs (in mg) of equal to or at least about: 1, 10, 25, 50, 75, 100, 200, or ranges including and/or spanning the aforementioned values. In some embodiments, the administration method includes multiple administrations of each single dose to the subject. In some embodiments, administering a composition (e.g., a composition including CDC-XOs, CDC-EVs, CDCs, or combinations thereof) includes injection. In some embodiments, injection includes skeletal muscle injection. In some embodiments, injection includes intraperitoneal injection. In some embodiments, administering a composition includes intra-arterial or intravenous infusion. In some embodiments, treatment of the subject (e.g., by delivery of a dose or doses of CDC-XOs and/or CDCs that release CDC-XOs) results in increased dystrophin expression. In some embodiments, increased dystrophin expression occurs in skeletal muscle in a limb (e.g., one or more of an arm or leg). In some embodiments, increased dystrophin expression occurs in the diaphragm. In some embodiments, patient undergoing therapy as disclosed elsewhere herein is a pediatric subject afflicted with cardiomyopathy. In some embodiments, the pediatric subject is diagnosed with cardiomyopathy. In some embodiments, the pediatric subject is afflicted with cardiomyopathy, but not heart failure. In some embodiments, the pediatric subject is 3-11 years old. In other embodiments, the pediatric subject is 12-18 years old. In some embodiments, the

human subject is a pediatric subject at the age of less than or equal to about: 3, 6, 11, 12, 15, 18, or ranges including and/or spanning the aforementioned values.

[0159] In some embodiments, as disclosed elsewhere herein, administering a composition (e.g., one including CDCs, CDC-XOs, or CDC-EVs) includes injection. In some embodiments, the injection includes skeletal muscle injection. In some embodiments, the injection includes intraperitoneal injection. In some embodiments, administering a composition includes intra-arterial or intravenous infusion. In some embodiments, treatment of the subject results in increased dystrophin expression. In some embodiments, increased dystrophin expression occurs in skeletal muscle in a limb. In other embodiments, the increased dystrophin expression occurs in the diaphragm. In other embodiments, the subject is afflicted with cardiomyopathy. In other embodiments, the subject is diagnosed with cardiomyopathy. In other embodiments, the subject is afflicted with cardiomyopathy, but not heart failure. In other embodiments, the subject is 3-11 years old. In other embodiments, the subject is 12-18 years old.

[0160] Described herein are compositions and methods providing significant benefits in the repair or regeneration of damaged or diseased tissues via CDCs and CDC-XOs. Certain supporting techniques are described in, for example, U.S. App. No. 11/666,685, 12/622,143, 12/622,106, 14/421,355, PCT App. No. PCT/US2013/054732, PCT/US2015/053853, PCT/US2015/054301 and PCT/US2016/035561, which are fully incorporated by reference herein.

[0161] In some embodiments, described herein is a method of treating a skeletal myopathy disease including administering a therapeutically effective amount of CDCs and/or CDC-XOs to a subject, thereby treating the subject. Further described herein is a method of treating a skeletal myopathy disease including administering a therapeutically effective amount of a composition including CDCs and/or CDC-XOs to a subject, thereby treating the subject. In other embodiments, the composition includes a pharmaceutically acceptable carrier. Further described herein is a method of treating a chronic muscular disease including administering a therapeutically effective amount of a composition including a plurality of CDCs and/or CDC-XOs to a subject, thereby treating the subject. In various embodiments, the plurality of the CDCs and/or CDC-XOs are isolated from CDCs grown in serum-free media. In various embodiments, the exosomes have a diameter of about 90 nm to about 200 nm and are CD81+, CD63+, or both. In other embodiments, the chronic muscular disease includes a dystrophinopathy. In various embodiments, the dystrophinopathy includes Duchenne muscular dystrophy. In various embodiments, the

dystrophinopathy includes Becker muscular dystrophy. In various embodiments, the subject is a pediatric patient of less than 18 years old. In various embodiments, the subject is a prepubescent patient of less than 13 years old. In various embodiments, the subject is a prepubescent patient of less than 12 years old. In various embodiments, the subject is a prepubescent patient of less than 11 years old. In various embodiments, the subject is a prepubescent patient of less than 10 years old. In various embodiments, the subject is 3-11 years old. In various embodiments, the subject is 12-18 years old.

[0162] In some embodiments herein is a method of treating a skeletal myopathy disease including administering a therapeutically effective amount of CDC-XOs, CDC-EVs, and/or XO-releasing CDCs to a subject, thereby treating the subject. Some embodiments, pertain to a method of treating a skeletal myopathy disease including administering a therapeutically effective amount of a composition including CDC-XOs, CDC-EVs, and/or XO-releasing CDCs to a subject, thereby treating the subject. In some embodiments, the composition includes a pharmaceutically acceptable carrier. Further described herein is a method of treating a chronic muscular disease including administering a therapeutically effective amount of a composition including CDC-XOs, CDC-EVs, and/or XO-releasing CDCs to a subject, thereby treating the subject. In some embodiments, the chronic muscular disease includes a dystrophinopathy. In other embodiments, the dystrophinopathy is Duchenne muscular dystrophy. In some embodiments, the dystrophinopathy includes Becker muscular dystrophy. In various embodiments, the subject is a pediatric patient of less than 18 years old. In various embodiments, the subject is a prepubescent patient of less than 13 years old. In various embodiments, the subject is a prepubescent patient of less than 12 years old. In various embodiments, the subject is a prepubescent patient of less than 11 years old. In various embodiments, the subject is a prepubescent patient of less than 10 years old. In various embodiments, the subject is 3-11 years old. In various embodiments, the subject is 12-18 years old.

[0163] In various embodiments, the subject is afflicted with cardiomyopathy. In various embodiments, the subject is afflicted with cardiomyopathy, but not heart failure. In various embodiments, the subject is diagnosed with cardiomyopathy. In various embodiments, the subject is diagnosed with cardiomyopathy, but not heart failure.

[0164] In various embodiments, the cardiomyopathy includes one or more of cell membrane degradation, interstitial inflammation, fatty replacement and fibrosis. In various

embodiments, cardiomyopathy includes left ventricle posterobasal fibrosis; conduction abnormalities that are intra-atrial, including SVT with abnormal AV nodal conduction. In various embodiments, cardiomyopathy includes advanced stages of ventricle enlargement, dyspnea, peripheral edema and liver enlargement. In various embodiments, heart failure (HF) includes asymptomatic abnormalities in cardiac structure and function wherein heart function is depressed (stage B), overt symptomatic HF (stage C), to advanced HF (stage D). In various embodiments, subject is afflicted with smooth muscle myopathy including vascular dysfunction, further including GI and urinary tract systems involvement.

[0165] In some embodiments, the subject is one or more of the above, such as one of the recited age groups, afflicted and/or diagnosed with cardiomyopathy and/or heart failure. This includes for example, a subject that is 3-11 years old, afflicted with and/or diagnosed with cardiomyopathy, but not heart failure.

[0166] In other embodiments, administering a therapeutically effective amount of a composition includes about 1 x 10^5 to about 1 x 10^8 or more CDCs in a single dose. In another example, the number of administered CDCs includes 25 million CDCs per coronary artery (i.e., 75 million CDCs total) as another baseline for exosome dosage quantity. In various embodiments, the numbers of CDCs includes 1 x 10^5, 1 x 10^6, 1 x 10^7, 1 x 10^8, 1 x 10^9 CDCs in a single dose as another baseline for exosome dosage quantity. In certain instances, this may be prorated to body weight (range 100,000-1M CDCs/kg body weight total CDC dose). In various embodiments, the administration can be in repeated doses, such as two, three, four, four or more sequentially-applied doses.

[0167] In other embodiments, administering a therapeutically effective amount of a composition includes infusion, including intra-arterial and intravenous infusion. In other embodiments, infusion results in systemic delivery. In other embodiments, infusion is capable of delivering therapeutically effective dosages of exosomes to one or more locations in the body. In other embodiments, infusion is capable of delivering a therapeutically effective dosage of exosomes to smooth or skeletal muscle tissue. In other embodiments, administering a therapeutically effective amount of a composition includes injection. In other embodiments, the injection includes injection into the heart, including intramyocardial injection, cavities and chambers of the heart, and vessels associated thereof. In other embodiments, injection into the heart, cavities and chambers of the heart, vessels associated thereof, is capable of delivering a

therapeutically effective dosage of exosomes to smooth or skeletal muscle tissue. In other embodiments, the injection includes skeletal muscle injection. In other embodiments, the injection includes intraperitoneal injection. In other embodiments, the injection includes percutaneous injection.

[0168] In other embodiments, treatment of the subject results in an increase in dystrophin expression. In other embodiments, increase in dystrophin expression occurs in skeletal muscle. This includes skeletal muscle in limbs, such as a soleus muscle. In other embodiments, increase in dystrophin expression occurs in the diaphragm. In other embodiments, treatment of the subject results in decreased fibrosis, decreased inflammation, and/or increased mitochondrial function. In other embodiments, decreased fibrosis includes a reduction in collagen accumulation. In other embodiments, collagen includes collagen I and/or collagen III. In other embodiments, decreased inflammation includes an increase in cytoplasmic nuclear factor (erythroid-derived 2)-like 2 (Nrf2), reduction in fatty acid peroxidation end products, reduced numbers of inflammatory cells, and/or upregulated expression of antioxidants. In other embodiments, antioxidants include heme oxygenase-1 (HO-1), catalase, superoxide dismutase-2 (SOD-2), and glutamate-cystein ligase catalytic (GCLC) subunit. In other embodiments, inflammatory cells include CD68+ macrophages and CD3+ T-cells. In other embodiments, increased mitochondrial function includes increased mitochondrial ultrastructure and/or increased mitochondrial biogenesis. In other embodiments, increased mitochondrial function includes increased nuclear PPAR-γ co-activator-1 (PGC-1) expression.

[0169] In various embodiments, the CDCs are generated from a biopsy sample cultured into an explant, further cultured into an explant derived cell, additionally cultured as cardiosphere forming cells, thereafter cultured as cardiospheres, and subsequently cultured as. In other embodiments, the CDCs are human. In various embodiments, the CDCs are generated from a biopsy sample obtained the subject afflicted with a dystrophinopathy.

[0170] In other embodiments, treatment of the subject further includes assessing functional improvement in the subject, including functional improvement in skeletal muscle tissue. In various embodiments, functional improvement includes one or more of increased contractile strength, improved ability to walk, improved ability to stand from a seated position, improved ability to sit from a recumbent or supine position, and improved manual dexterity such as pointing and/or clicking a mouse. In other embodiments, treatment of the subject further includes assessing

cognition in response to treatment of neural damage, blood-oxygen transfer in response to treatment of lung damage, and immune function in response to treatment of damaged immunological-related tissues.

[0171] In some embodiments, described herein is a method including isolating a biopsy specimen from a subject, culturing the biopsy specimen as an explant, generating explant derived cells (EDCs), culturing the EDCs into cardiospheres, and inducing formation of cardiosphere-derived cells (CDCs). In other embodiments, the method includes administering CDCs to a subject. In other embodiments, the method includes isolating exosomes from the CDCs and administering CDC-derived exosomes to a subject. In various embodiments, culturing the biopsy specimen as an explant includes mincing the biopsy specimen and culturing on a fibronectin coated vessel. In various embodiments, generating EDCs includes isolating cells from the explant. In various embodiments, isolated cells from the explant include loosely adherent cells and/or stromal-like cells. In various embodiments, culturing the EDCs into cardiospheres includes culturing of EDCs on poly-D-lysine dishes. In various embodiments, formation of CDCs includes culturing detached cardiospheres on a fibronectin coated vessel. Further examples and embodiments for CDC generation are described in U.S. Pat. Pub. No. 2008/0267921, which is fully incorporated by reference herein. In various embodiments, isolating CDC-derived exosomes includes use of any of the techniques described herein. In various embodiments, administering CDCs to a subject includes use of any of the techniques described herein. In various embodiments, administering CDCs or CDC-derived exosomes to a subject includes use of any of the techniques described herein. In various embodiments, the biopsy specimen is isolated from the same subject that is administered the CDCs or CDC-derived exosomes. In various embodiments, biopsy specimen is isolated from a different subject that the subject that is administered the CDC-derived exosomes. In various embodiments, the subject is afflicted with a chronic muscular disease. In other embodiments, the chronic muscular disease includes dystrophinopathy. In other embodiments, the dystrophinopathy is Duchenne muscular dystrophy. In other embodiments, the dystrophinopathy includes Becker muscular dystrophy. In various embodiments, the subject afflicted with a chronic muscular disease is a pediatric subject less than 18 years old. In various embodiments, the subject is a prepubescent subject less than 12 years old.

[0172] In some embodiments, delivery of noncoding RNA species found in CDC-derived exosomes (e.g., miR-148a-3p, or srDMD, a small 115-nucleotide RNA of previously

unknown function) mimics the ability of CDCs and CDC-derived exosomes to increase dystrophin protein levels, without affecting transcript length or exon/intron junctions. In some embodiments, these noncoding RNAs ameliorate Duchenne muscular dystrophy by restoring dystrophin in heart and skeletal muscle. In some embodiments, disclosed herein are factors capable of replacing dystrophin, and offsetting the pathophysiological consequences of dystrophin deletion. In some embodiments, the factors include one or more of miR-148a-3p and srDMD that, transferred into recipient cells to influence dystrophin expression, establishing for the first time, nucleic acids as a therapeutic option for DMD.

[0173] In some embodiments, a RNA polynucleotide is whose sequence is at least 80%, 85%, 90%, 95%, 96%, 97%, 98%, 99% or 100% identical to any of the microRNAs or short non-coding RNAs mentioned elsewhere herein are used. As used herein, the term "identical" (i.e., "sequence identity") means that two polynucleotide sequences are the same (i.e., on a nucleotide-by-nucleotide basis) over a window of comparison. When referring a percentage of sequence identity, (i.e., sequences that are "X% identical", "percent identity"), the percentage of "identical" is calculated by comparing two aligned sequences, including optimally aligned sequences, over a window of comparison, determining the number of positions at which the identical nucleic acid base (e.g., A, T, C, G, U, or I) occurs in both sequences to yield the number of matched positions, dividing the number of matched positions by the total number of positions in the window of comparison (i.e., the window size), and multiplying the result by 100 to yield the percentage of sequence identity. In some embodiments, a comparison window of at least 15 nucleotide positions, frequently over a window of at least 15-50, 50-100, or 100 or more nucleotides, wherein the percentage of sequence identity is calculated by comparing a reference sequence to a polynucleotide sequence of interest. In some embodiments, one or more comparison windows between reference and polynucleotide sequence of interest, including discontiguous segments in the polynucleotide sequence of interest, may be added together to calculate percentage of sequence identity to account for translocations. In some embodiments, the polynucleotide sequence of interest may include deletions or additions which total 20 percent or less of the reference sequence over the window of comparison. In some embodiments, microRNA of the invention may include additional nucleotides at the 5′, 3′, or both 5′ and 3′ ends of at least, at most or about 1, 2, 3, 4, 5, 6, 7, 8, 9, 10 or more nucleotides. This includes, for example, addition of GCG-modified miR-148a with GCG added on the 5' end or on the 3' end.

[0174] In some embodiments, the one or more polynucleotides is encoded in one or more vectors as disclosed elsewhere herein. In some embodiments, the one or more vectors is introduced into the cell via a gene delivery vehicle. In some embodiments, the delivery vehicle includes a viral vector such as an adenoviral vector and (e.g., an adeno-associated virus vector). In some embodiments, the delivery vehicle includes expression vectors and delivery vehicles. In some embodiments, polynucleotides are capable of acting on release factors or on the ribosome itself. In some embodiments, the one or more polynucleotides is capable of enhancing read-through of dystrophin transcript.

[0175] While in some embodiments, the therapeutic compositions can include CDCs, CDC-XOs, and/or CDC-EVs, in other embodiments, a therapeutic composition can lack CDCs and/or vesicles and instead includes a composition with an effective amount of RNA polynucleotide or vector encoding RNA polynucleotide. In some embodiments, an effective amount of an RNA therapeutic ranges between 0.1 and 20 mg/kg, 0.5 and 10 mg/kg. In some embodiments, the therapeutically effective amount is a single unit dose. In some embodiments, an effective amount includes concentration at a range between 0.1 nM and 10M. In some embodiments, the concentration ranges between 0.3 to 400 nM, and/or between 1 to 200 nM. In some embodiments, an effective amount includes an amount capable of increasing dystrophin expression in one or more tissues, including for example, cardiac and skeletal muscle tissue. In some embodiments, the short non-coding RNA and microRNA include length of an RNA polynucleotide that is at least, at most, or about 6, 7, 8, 9, 10, 11, 12, 13, 14, 15, 16, 17, 18, 19, 20, 21, 22, 23, 24, 25, 50, 100, 150 or 200 nucleotides, including all integers or ranges derivable there between, and ranges including and/or spanning the aforementioned values. In some embodiments, as with any administration disclosed herein, administration of the therapeutically effective amount in a dosage regime depends on the subject to be treated and can be extrapolated based on patient size (increased for larger patients, decreased for smaller patients, extrapolated from mouse models (such as multiplying a mouse dose by a factor of equal to or at least about: 1500, 2000 2500, 3000, and/or ranges including and/or spanning the aforementioned values, etc.). In some embodiments, administration in a dosage regime may be a single dose, or multiple administrations of dosages over a period of time spanning 10, 20, 30, 40, 50, 60 minutes, and/or 1, 2, 3, 4, 5, 6, 7, 8, 9, 10, 11, 12, 13, 14, 15, 16, 17, 18, 19, 20, 21, 22, 23, 24 or more hours, and/or 1, 2, 3, 4, 5, 6, 7, days or

more. In some embodiments, administration may be through a time release or sustained release mechanism, implemented by formulation and/or mode of administration.

[0176] In some embodiments, the one or more RNA polynucleotides possess biological activity. In some embodiments, biological activity can include enhanced translation readthrough of a peptide or protein of interest. This includes for example, assessment of biological activity using peptide or protein expression in a heterologous expression system. In some embodiments, using a heterologous expression fusion protein system, such as dystrophin-eGFP, wild-type or mutant protein can be transfected into cells as a measure of enhanced translation readthrough to assess biological activity. In some embodiments, biological activity can be assessed as a percentage of fluorescence normalized against vehicle only, when compared to wild-type or mutant proteins. In some embodiments, G418 can serve as a positive control. In some embodiments, percentage of fluorescence to assess biological activity includes an increase of about 10-25%, 25-50%, 50-75%, 75-100% or 100% more increase in fluorescence signal compare to a mutant. In some embodiments, percentage of fluorescence to assess biological activity includes a 0-25%, 25-50%, 50-75%, 75-100% or 100% of fluorescence of wild-type peptide or protein expression, or G418 positive control.

[0177] In some embodiments, administering an RNA polynucleotide composition includes infusion, including intra-arterial, intravenous, and myocardial infusion. In some embodiments, administering a composition includes injection. In some embodiments, the injection includes injection into the heart, including intramyocardial injection, cavities and chambers of the heart, vessels associated thereof. In some embodiments, the injection includes skeletal muscle injection. In some embodiments, the injection includes intraperitoneal injection. In some embodiments, the injection includes percutaneous injection. In some embodiments, administering a composition includes inhalation.

[0178] In some embodiments, treatment of the subject with an RNA polynucleotide composition results in an increase in dystrophin expression. In some embodiments, the increase in dystrophin expression occurs in skeletal muscle. In some embodiments, this includes skeletal muscle in limbs, such as a soleus muscle. In some embodiments, the increase in dystrophin expression occurs in the diaphragm. In some embodiments, treatment of the subject results in decreased fibrosis, decreased inflammation, and/or increased mitochondrial function. In some embodiments, decreased fibrosis includes a reduction in collagen accumulation. In some

embodiments, collagen includes collagen I and/or collagen III. In some embodiments, decreased inflammation includes an increase in cytoplasmic nuclear factor (erythroid-derived 2)-like 2 (Nrf2), reduction in fatty acid peroxidation end products, reduced numbers of inflammatory cells, and/or upregulated expression of antioxidants. In some embodiments, antioxidants include heme oxygenase-1 (HO-1), catalase, superoxide dismutase-2 (SOD-2), and glutamate-cysteine ligase catalytic (GCLC) subunit. In some embodiments, inflammatory cells include CD68+ macrophages and CD3+ T-cells. In some embodiments, increased mitochondrial function includes increased mitochondrial ultrastructure and/or increased mitochondrial biogenesis. In some embodiments, increased mitochondrial function includes increased nuclear PPAR-γ co-activator-1 (PGC-1) expression.

[0179] In some embodiments, treatment of the subject with an RNA polynucleotide further includes functional improvement in the subject, including functional improvement in skeletal muscle tissue. In some embodiments, functional improvement includes one or more of increased contractile strength, improved ability to walk, improved ability to stand from a seated position, improved ability to sit from a recumbent or supine position, and improved manual dexterity such as pointing and/or clicking a mouse. In some embodiments, treatment of the subject further includes improved cognition in response to treatment of neural damage, blood-oxygen transfer in response to treatment of lung damage, and immune function in response to treatment of damaged immunological-related tissues.

[0180] In some embodiments, as disclosed elsewhere herein, described herein is an RNA polynucleotide composition including one or more RNA polynucleotides, such as 2, 3, 4, 5, 6, 7, 8, 9, 10 or more RNA polynucleotides. In some embodiments, the composition includes one or more RNA polynucleotides such as 2, 3, 4, 5, 6, 7, 8, 9, 10 or more RNA polynucleotides. In some embodiments, the RNAs include non-coding RNAs. In some embodiments, the non-coding RNAs include tRNAs, yRNAs, rTNAs, mirRNAs, lncRNAs, piRNAs, snRNAs, snoRNAs, further including fragments thereof, among others. In some embodiments, the one or more RNA polynucleotides are microRNAs. In some embodiments, the microRNAs are selected from the group consisting of miR-148a, miR-215, miR-33a, miR 204, miR-376c, miR4532, miR-4742, miR-582, miR-629, miR-223, miR-3125, miR-3677, miR-376b, miR-4449, miR-4773, miR-4787, miR-491, miR-495, miR-500a, miR-548ah, miR-550, miR-548ah, miR-550a, miR-551n, miR-5581, miR-616, or any other microRNAs depicted as enriched in Figure 29. In some embodiments,

the microRNAs are selected from the group consisting of: microRNAs miR-146a, miR148a, miR-22, miR-24, miR-210, miR-150, miR-140-3p, miR-19a, miR-27b, miR-19b, miR-27a, miR-376c, miR-128, miR-320a, miR-143, miR-21, miR-130a, miR-9, miR-185, and miR-23a. In some embodiments, the microRNA includes miR-148a-3p. In some embodiments, the exosomes include a small non-coding RNA from DMD, srDMD. In some embodiments, the one or more polynucleotides are capable of increasing dystrophin expression in a subject. In some embodiments, the one or more polynucleotides or a vector including one or more polynucleotides can be incorporated into a pharmaceutically active mixture or composition by adding a pharmaceutically acceptable carrier. In some embodiments, the pharmaceutical composition includes one or more polynucleotides and/or a viral-based vector encoding the one or more polynucleotides and a pharmaceutically acceptable carrier. In some embodiments, the pharmaceutical composition including the one or more polynucleotides and/or a vector encoding the one or more polynucleotides, and a pharmaceutical acceptable carrier or excipient, includes excipients capable of forming complexes, vesicles and/or liposomes that deliver the one or more polynucleotides, and/or an oligonucleotide complexed or trapped in a vesicle or liposome through a cell membrane. In some embodiments, excipients can include one or more of polyethylenimine and derivatives, or similar cationic polymers, including polypropyleneimine or polyethylenimine copolymers (PECs) and derivatives, synthetic amphiphils, Lipofectin™, DOTAP and/or viral capsid proteins that are capable of self-assembly into particles that can deliver such one or more polynucleotides

[0181] In some embodiments, concentration of the one or more polynucleotides ranges between 0.1 nM and 10M. In various embodiments, the concentration ranges between 0.3 to 400 nM, even more and/or between 1 to 200 nM. In some embodiments, the one or more polynucleotides may be used at a dose which is ranged between 0.1 and 20 mg/kg, and/or 0.5 and 10 mg/kg. In some embodiments, the one or more polynucleotides include concentrations that refer to the total concentration of polynucleotides or the concentration of each polynucleotides added.

[0182] In some embodiments, as described elsewhere herein, the RNA polynucleotide is a microRNA (and/or combination of microRNAs). In some embodiments, the microRNA includes miR-148a. In some embodiments, the miR-148a microRNA has the following sequence 5'GAGGCAAAGUUCUGAGACACUCCGACUCUGAGUAUGAUAGAAGUCAGUGCACU ACAGAACUUUGUCUC3' [SEQ ID NO: 1]. In some embodiments, a microRNA can be

designated by a suffix "5P" or "3P", with "5P" indicating that the mature microRNA derives from the 5' end of the precursor and a corresponding "3P" indicates that it derives from the 3' end of the precursor. In some embodiments, the microRNA comprises miR-148-5p, whose sequence is 5'AAAGUUCUGAGACACUCCGACU3' [SEQ ID NO: 2]. In some embodiments, the microRNA comprises miR-148a-3p, whose sequence is 5'UCAGUGCACUACAGAACUUUGU3' [SEQ ID NO: 3]. In various embodiments, the microRNA includes an RNA polynucleotide whose sequence is at least 80%, 85%, 90%, 95%, 96%, 97%, 98%, 99% or 100% identical to miR-148a, miR-148-5p, and/or miR-148a-3p and/or fragments of any of the foregoing. In some embodiments, for example, a comparison window of at least 15 nucleotide positions, frequently over a window of at least 15-50, 50-100, or 100 or more nucleotides, wherein the percentage of sequence identity is calculated by comparing a reference sequence to a polynucleotide sequence of interest. In some embodiments, one or more comparison windows between reference and polynucleotide sequence of interest, including discontiguous segments in the polynucleotide sequence of interest, may be added together to calculate percentage of sequence identity to account for translocations. In some embodiments, the polynucleotide sequence of interest may include deletions or additions which total 20 percent or less of the reference sequence over the window of comparison. In some embodiments, microRNA of the invention may include additional nucleotides at the 5′, 3′, or both 5′ and 3′ ends of at least, at most or about 1, 2, 3, 4, 5, 6, 7, 8, 9, 10 or more nucleotides. This includes, for example, addition of GCG-modified miR-148a with GCG added on the 5' end or on the 3' end.

[0183] In some embodiments, the RNA polynucleotide is a short non-coding RNA from Duchenne muscular dysrophy (DMD), srDMD, whose sequence is 5'UGUACACAGAGGCUGAUCGAUUCUCCCUGAACAGCCUAUUACGGAGGCACUGC AGAUCAAGCCCGCCUGGAGAGGUGGAGUUUCAAGAGUCCCUUCCUGGUUCACCGU CUCCUUU3' [SEQ ID NO: 4]. In some embodiments, the short non-coding RNA includes an RNA polynucleotide whose sequence is at least 80%, 85%, 90%, 95%, 96%, 97%, 98%, 99% or 100% identical to srDMD and/or fragments thereof. This includes, for example, a 113-nucleotide length variant of srDMD (srDMD variant) whose sequence is 5'UGUACACGGUGGAGUUUCAAGAGUCCCUUCCUGGUUCACCGUCUCCUUUAGAG GCUGAUCGAUUCUCCCUGAACAGCCUAUUACGGAGGCACUGCAGAUCAAGCCCGC CUGGA3' [SEQ ID NO: 5]. Another example includes a srDMD mutant whose sequence is

5'UCCCCACAGAGGCUGAUCGAUUCUCCCUGAACAGCCUCCUCCGGAGGCACUGCA GAUCAAGCCCGCCUGGAGAGGUGGAGUUUCAAGAGUCCCUUCCUGGUUCACCGUC UCCUUU3' [SEQ ID NO: 6].

[0184] In some embodiments, the short non-coding RNA, including microRNAs, include lengths that are, are at least, or are at most 12, 13, 14, 15, 16, 17, 18, 19, 20, 21, 22, 23, 24, 25, 26, 27, 28, 29, 30, 31, 32,33, 34,35, 36, 37, 38, 39, 40, 41, 42,43, 44, 45,46, 47, 48,49, 50, 51, 52, 53, 54, 55, 56, 57, 58, 59, 60, 61, 62, 63, 64, 65,66, 67,68, 69, 70, 71,72, 73,74, 75, 76, 77,78, 79,80, 81, 82.83, 84,85, 86, 87, 88, 89, 90,91, 92,93, 94, 95, 96, 97,98, 99, 100, 101, 102, 103, 104, 105, 106, 107, 108, 109, 110, 111, 112, 113, 114, 115, 116, 117, 118, 119, 120, 121, 122, 123, 124, 125, 126, 127, 128, 129, 130, 140, 145, 150, 160, 170, 180, 190, 200 or more residues in length, including any integer or any range there between. In some embodiments, short non-coding RNAs, including microRNAs, refers to a length of an RNA polynucleotide that is at least, at most, or about 6, 7, 8, 9, 10, 11, 12, 13, 14, 15, 16, 17, 18, 19, 20, 21, 22, 23, 24, 25, 50, 100, 150 or 200 nucleotides, including all integers or ranges derivable there between.

[0185] In some embodiments, the RNA polynucleotide possesses biological activity. In some embodiments, biological activity can include enhanced translation readthrough of a peptide or protein of interest. This includes for example, assessment of biological activity using peptide or protein expression in a heterologous expression system. For example, using a heterologous expression fusion protein system, such as dystrophin-eGFP, wild-type or mutant protein can be transfected into cells as a measure of enhanced translation readthrough to assess biological activity. In various embodiments, biological activity can be assessed as a percentage of fluorescence normalized against vehicle only, when compared to wild-type or mutant proteins. In various embodiments, G418 can serve as a positive control. In various embodiments, percentage of fluorescence to assess biological activity includes an increase of about 10-25%, 25-50%, 50-75%, 75-100% or 100% more increase in fluorescence signal compare to a mutant. In various embodiments, percentage of fluorescence to assess biological activity includes a 0-25%, 25-50%, 50-75%, 75-100% or 100% of fluorescence of wild-type peptide or protein expression, or G418 positive control.

[0186] In some embodiments, the RNA polynucleotide is synthetic. For example, nucleic acids can be synthesized by phosphotriester, phosphite, or phosphoramidite chemistry and solid phase techniques. In various embodiments, the RNA polynucleotide is produced in a

recombinant method. For example, this includes the use of vectors (viral and non-viral), plasmids, cosmids, and other vehicles for delivering a nucleic acid to a cell, such as a host cell (to produce large quantities of the desired RNA molecule).

[0187] In some embodiments, the vector encoding an RNA polynucleotide is a viral vector such as an adenoviral vector (e.g., an adeno-associated virus vector). In various embodiments, the vector is a non-viral expression vector.

[0188] In some embodiments, an effective amount of RNA ranges between 0.1 and 20 mg/kg, and/or 0.5 and 10 mg/kg. In some embodiments, the therapeutically effective amount is a single unit dose. In some embodiments, an effective amount of RNA includes concentration at a range between 0.1 nM and 10M. In some embodiments, the concentration of RNA ranges between 0.3 to 400 nM, or between 1 to 200 nM. In some embodiments, the RNA polynucleotide or vector includes concentrations that refer to the total concentration of RNA polynucleotide or vector added. In some embodiments, an amount of a RNA polynucleotide or vector is provided to a cell or organism is an effective amount for a particular result, which refers to an amount needed to achieve a desired goal, such as inducing a particular cellular characteristic(s). In various embodiments, an effective amount of RNA polynucleotide includes an amount capable of increasing dystrophin expression in one or more tissues, including for example, cardiac and skeletal muscle tissue.

[0189] In some embodiments, the RNA polynucleotide or a vector encoding the RNA polynucleotide are incorporated into a pharmaceutically active mixture or composition by adding a pharmaceutically acceptable carrier or excipients. In some embodiments, the pharmaceutical composition includes the RNA polynucleotide and/or a viral-based vector encoding the RNA polynucleotides and a pharmaceutically acceptable carrier or excipient. In some embodiments, the pharmaceutical composition including the RNA polynucleotide and/or a vector encoding the RNA polynucleotide, and a pharmaceutical acceptable carrier or excipient, includes excipients capable of forming complexes, vesicles and/or liposomes that deliver the RNA polynucleotide, and/or an oligonucleotide complexed or trapped in a vesicle or liposome through a cell membrane. Many of these excipients are known to one of skill in the art, including polyethylenimine and derivatives, or similar cationic polymers, including polypropyleneimine or polyethylenimine copolymers (PECs) and derivatives, synthetic amphiphils, Lipofectin™, DOTAP and/or viral capsid proteins that are capable of self-assembly into particles that can deliver such RNA polynucleotide. In other

embodiments, the RNA polynucleotide is contained within an exosome. In some embodiments, the RNA polynucleotide contained within an exosome is enriched compared to the RNA polynucleotide within an exosome derived from a cell. In some embodiments, enrichment can include 10-100%, 100-200%, 200-400, 400-1000% greater levels of the RNA polynucleotide when compared to that RNA polynucleotide within an exosome derived from a cell.

[0190] In some embodiments, a method of treating a chronic muscular disease including administering an RNA polynucleotide or vector encoding a RNA polynucleotide is provided. In some embodiments, the administration of the composition treats a chronic muscular disease in the subject. In some embodiments, the chronic muscular disease is a dystrophinopathy. In some embodiments, the dystrophinopathy is Duchenne muscular dystrophy. In some embodiments, the dystrophinopathy is Becker muscular dystrophy. In some embodiments, the RNA polynucleotide is a microRNA. In various embodiments, the microRNA includes miR-148a [SEQ ID NO: 1]. In some embodiments, the microRNA includes miR-148-5p [SEQ ID NO: 2], and/or miR-148a-3p [SEQ ID NO:3]. In some embodiments, the microRNA includes an RNA polynucleotide whose sequence is at least 80%, 85%, 90%, 95%, 96%, 97%, 98%, 99% or 100% identical (i.e., percentage identity) to miR-148a [SEQ ID NO:1] and/or fragments thereof (e.g., [SEQ ID NO:2], [SEQ ID NO:3]. In some embodiments, microRNA may include additional nucleotides at the 5′, 3′, or both 5′ and 3′ ends of at least, at most or about 1, 2, 3, 4, 5, 6, 7, 8, 9, 10 or more nucleotides. This includes, for example, addition of GCG-modified miR-148a with GCG added on the 5' end or 3' end. In some embodiments, the RNA polynucleotide is a short non-coding RNA from Duchenne muscular dysrophy (DMD), srDMD. In some embodiments, the short non-coding RNA includes an RNA polynucleotide whose sequence is at least 80%, 85%, 90%, 95%, 96%, 97%, 98%, 99% or 100% identical to srDMD [SEQ ID NO: 4] and/or fragments thereof. In some embodiments, the short non-coding RNA includes srDMD variant [SEQ ID NO:5] and/or srDMD mutant [SEQ ID NO:6].

[0191] In some embodiments, administering the composition includes a composition with an effective amount of RNA polynucleotide or vector encoding RNA polynucleotide. In some embodiments, an effective amount of RNA polynucleotide or vector encoding RNA polynucleotide ranges between 0.1 and 20 mg/kg, and/or 0.5 and 10 mg/kg. In some embodiments, the therapeutically effective amount is a single unit dose. In some embodiments, an effective amount includes concentration at a range between 0.1 nM and 10M. In some embodiments, the

concentration ranges between 0.3 to 400 nM, and/or between 1 to 200 nM. In some embodiments, an effective amount includes an amount capable of increasing dystrophin expression in one or more tissues, including for example, cardiac and skeletal muscle tissue. In some embodiments, the short non-coding RNA and microRNA include length of an RNA polynucleotide that is at least, at most, or about 6, 7, 8, 9, 10, 11, 12, 13, 14, 15, 16, 17, 18, 19, 20, 21, 22, 23, 24, 25, 50, 100, 150 or 200 nucleotides, including all integers or ranges derivable there between.

[0192] In some embodiments, administration of the therapeutically effective amount in a dosage regime depends on the subject to be treated. In some embodiments, administration in a dosage regime may be a single dose, or multiple administrations of dosages over a period of time spanning 10, 20, 30, 40, 50, 60 minutes, and/or 1, 2, 3, 4, 5, 6, 7, 8, 9, 10, 11, 12, 13, 14, 15, 16, 17, 18, 19, 20, 21, 22, 23, 24 or more hours, and/or 1, 2, 3, 4, 5, 6, 7, days or more. Moreover, administration may be through a time release or sustained release mechanism, implemented by formulation and/or mode of administration.

[0193] In some embodiments, administering a composition includes infusion, including intra-arterial, intravenous, and myocardial infusion. In some embodiments, administering a composition includes injection. In some embodiments, the injection includes injection into the heart, including intramyocardial injection, cavities and chambers of the heart, vessels associated thereof. In some embodiments, the injection includes skeletal muscle injection. In some embodiments, the injection includes intraperitoneal injection. In some embodiments, the injection includes percutaneous injection. In some embodiments, administering a composition includes inhalation.

[0194] In some embodiments, treatment of the subject results in an increase in dystrophin expression. In some embodiments, increase in dystrophin expression occurs in skeletal muscle. In some embodiments, this includes skeletal muscle in limbs, such as a soleus muscle. In other embodiments, increase in dystrophin expression occurs in the diaphragm. In some embodiments, treatment of the subject results in enhanced readthrough translation of a protein, including for example, dystrophin. In some embodiments, treatment of the subject further includes assessing functional improvement in the subject, including functional improvement in skeletal muscle tissue. In some embodiments, functional improvement includes one or more of increased contractile strength, improved ability to walk, improved ability to stand from a seated position, improved ability to sit from a recumbent or supine position, and improved manual dexterity such

as pointing and/or clicking a mouse. In some embodiments, treatment of the subject further includes assessing cognition in response to treatment of neural damage, blood-oxygen transfer in response to treatment of lung damage, and immune function in response to treatment of damaged immunological-related tissues.

EXAMPLES

[0195] Embodiments herein demonstrate that CDCs and CDC-derived XOs can be used to reverse key pathophysiological hallmarks of Duchenne muscular dystrophy in *mdx* mice. Exosomes secreted by human CDCs reproduce the benefits of CDCs in *mdx* mice, and reverse abnormalities of calcium cycling and mitochondrial respiration in human Duchenne cardiomyocytes. Both CDCs and their exosomes improve heart function in *mdx* mice; a single injection of CDCs suffices to increase maximal exercise capacity and improve survival. Delivery of noncoding RNA species found in CDC-derived exosomes (e.g. miR-148a) mimics the ability of CDCs and CDC-derived exosomes to increase dystrophin protein levels, without affecting transcript length or exon/intron junctions. Thus, CDCs and CDC-derived exosomes ameliorate features of Duchenne muscular dystrophy via exosome-mediated transfer of signaling molecules.

Example 1

Animal study

[0196] The Inventors studied *mdx* mouse model of DMD (C57BL/10ScSn-Dmdmdx/J) and wild-type strain matched mouse (C57BL/10ScSnJ wild type mouse heart) (Jackson Laboratory, USA) from 10 months of age. To optimize the process of CDC transplantation, preliminary dose-response experiments were performed, which identified $1x10^5$ cells in first injection and $1x10^4$ cells in second injection (3 months after first injection) as effective doses, consistent with prior dose ranging experiments in ischemic and non-ischemic mouse models. A total of $1x10^5$ cells/40μL phosphate-buffered saline (PBS; first injection) or $1x10^4$ cells/40μL PBS (second injection) or PBS alone were injected into left ventricular (LV) myocardium divided equally among 4 sites as described. The LV was visually divided into three zones: basal, middle, and apical, with one injection in the basal, two in the middle and one in the apical zone. Ten-month old CDC/*mdx* and vehicle/*mdx* mice were injected with CDCs (Mdx+CDC, n=12) or vehicle [placebo: Mdx+Vehicle (PBS), n=12] twice (3 months interval), respectively. Injections were during open-chest thoracotomy via a 28½ gauge-needle. All surgical procedures were carried out

while the animals were under general anesthesia (Dexmedetomidine (0.5mg/kg)/Ketamine (75mg/kg); IP; once before surgery). Similar protocols were used for injection of CDC-derived exosomes, NHDF-derived exosomes (as control), miR-148a-3p (Sigma-Aldrich Catalog No. HMI0237), microRNA mimic control (Sigma-Aldrich Catalog No. HMC0002), srDMD, and mutant srDMD. Intraventricular single injection of CDC-derived exosomes [(10.32±3.28) $x10^9$/150 µL PBS] or PBS alone into LV cavity were performed during open-chest thoracotomy via a 28½ gauge-needle. Intraaortic injections of CDCs ($1x10^4$ cells/40µL PBS) or PBS were conducted using PE-10 catheter (ALZET; Cupertino, CA) via neck carotid artery. Intramuscular injection of exosomes into soleus (SOL) muscles were performed at a single site at the lower 1/3 of the muscle using a 25 µl Hamilton syringe (with 0.5 µl marks) with a 31 gauge needle. The needle was advanced up to the upper 1/3 of the muscle and then slowly retracted through the belly as exosomes [(20.64±2.12)$x10^7$/3 µL] were injected.

Example 2

CDC, CDC-derived exosome, NHDF-derived exosome, miR-148a-3p, miR mimic control, srDMD and mutant srDMD

[0197] Mouse CDCs were expanded from wild-type strain-matched mouse hearts (C57BL/10ScSnJ wild type mouse heart) as described. Briefly, ventricular tissues were minced into ~1 mm explants, partially digested enzymatically and plated on adherent (fibronectin coated) culture dishes. These explants spontaneously yield outgrowth cells (explant-derived cells) which were harvested once confluent and plated in suspension culture (10^5 cells/mL on poly-D-lysine–coated dishes) to enable self-assembly of three-dimensional cardiospheres. Subsequent replating of cardiospheres on adherent culture dishes yielded CDCs which were used in all experiments at passage one. CDC-derived exosome: Exosomes were isolated from serum-free media conditioned overnight (24 hr) by cultured human CDCs. (CDC-derived exosome) [or normal human dermal fibroblasts (NHDF) as a control] in hypoxia (2% O_2; default condition) or normoxia (20% O_2, solely for studies comparing RNA content of exosomes). Ultracentrifugation (100,000*g* for 1 hr) was used to isolate exosomes from conditioned media after sequential centrifugations at 300*g* (10min) and 10,000*g* (30min) and filtration with 0.22 micron filters. Isolated exosomes were re-suspended in PBS (for *in vivo* and *in vitro* experiments) and the ratio of exosome to protein was measured using Nanosight particle counter and Micro BCA Protein Assay Kit (Life technologies, Grand Island, NY), respectively. Preliminary dose-response studies identified [(2.24±1.34)$x10^7$]

and [6.19±3.68 x10^8] exosomes from hypoxic CDCs as effective doses for *in vitro* and *in vivo* (intramyocardial CDC-derived exosome injection) experiments, respectively.

[0198] A miR-148a-3p mimic and miR mimic control (hsa-miR-148a-3p & miRNA negative control 1; 2μg each; Sigma-Aldrich, St. Louis, MO), short non-coding RNA, srDMD, or srDMD mutant (12μg each; GE Dharmacon, Lafayette, CO) mixed with RNAiMAX transfection reagent (life technologies, Grand Island, NY) for 30 min at room temperature at a total volume of 40 μl were injected into 4 points per heart as described above.

[0199] The nucleotide sequence of srDMD mutant is 5'UCCCCACAGAGGCUGAUCGAUUCUCCCUGAACAGCCUCCUCCGGAGGCACUGCA GAUCAAGCCCGCCUGGAGAGGUGGAGUUUCAAGAGUCCCUUCCUGGUUCACCGUC UCCUUU3' (SEQ ID NO: 6).

Example 3

Echocardiography

[0200] Echocardiographic studies were performed two days before (Baseline) and 3 weeks, 2 and 3 months after first CDC/CDC-derived exosome or vehicle injection and 3 weeks, 2 and 3 months after second CDC/CDC-derived exosome or vehicle injection (when applicable) using the Vevo 770 Imaging System (VisualSonics, Toronto, Canada). The same imaging system was used to perform echocardiographic studies at baseline (2 days before) and 3 weeks after selected RNA (or control) injection. After induction of light general anesthesia, the heart was imaged at the level of the greatest LV diameter. LV ejection fraction (LVEF) was measured with VisualSonics version 1.3.8 software from 2-dimensional long-axis views.

[0201] Changes in left ventricular (LV) end diastolic and systolic volumes after CDC injection. First and second CDC transplantation resulted in a sustained improvement of LV end-diastolic (LV EDV) and end-systolic (LV ESV) volumes in *mdx* mice, relative to placebo, for at least 6 months.

Example 4

Treadmill exercise testing and survival analysis

[0202] Exercise capacity was assessed weekly with Exer-3/6 open treadmill (Columbus Instruments, Columbus, OH), beginning 1 week pre-operatively and 3 weeks after CDC/vehicle injection (exercise capacity measured in a subset of *mdx* mice 1 week pre-operatively was equivalent to that measured 3 weeks post-operatively in the Mdx+Vehicle group). After an

acclimation period (10 m/min for 20 min), stepwise increases in average speed (1 m/min) were applied every two minutes during treadmill exercise until the mouse became exhausted (spending >10 seconds on shocker; continuous nudging was used during treadmill to help mice stay on the track). Subsequently, the mouse was returned to the cage and the total distance recorded. The treadmill protocol conformed to guidelines from the American Physiological Society. After 3 months of weekly exercise, CDC/vehicle *mdx* mice along with wild-type age-matched mice were followed for assessment of mortality (Fig. 1C).

Example 5

In vitro isometric contractile properties of skeletal muscle

[0203] Mice were deeply anesthetized with Ketamine/Xylazine (80 mg/kg and 10 mg/kg body weight IP), the soleus (SOL) and/or extensor digitorum longus (EDL) and/or diaphragm (DIA) muscles were rapidly excised, and the animal was euthanized. Briefly, following a lateral midline skin incision of the lower leg the SOL and/or EDL muscle was dissected and isolated and its tendons of origin and insertion were tightened with silk suture (3-0) and rapidly excised. The SOL or EDL muscle was vertically mounted in a tissue bath containing a mammalian Ringer's solution of the following composition: (in mM) 137 NaCl, 5 KCl, 2 $CaCl_2$, 1 $MgSO_4$, 1 NaH_2PO_4, 24 $NaHCO_3$, 11 glucose. The solution was constantly aerated with 95% O_2 and 5% CO_2 with pH maintained at 7.35 and temperature kept at 24°C. For studies of the diaphragm, following a left costal margin skin and muscle incision, a section of the midcostal hemidiaphragm was transferred to a preparatory Sylgar-lined dish containing cold Ringer's and a narrow 3-4 mm wide strip of diaphragm was isolated maintaining fiber attachments to the rib and central tendon intact which were tighten with silk suture and mounted vertically in the tissue bath. One end of the SOL, EDL or DIA was secured to a clamp at the bottom of the dish and one end was attached to a calibrated force transducer (Cambridge Technology Model 300B, Watertown, MA). A micromanipulator linked to the system was used to adjust muscle length. Platinum plate electrodes placed on each side of the muscle were used for direct muscle stimulation (Grass Model S88 stimulator; Quincy, MA) using 0.2 msec duration monophasic rectangular pulses of constant current delivered at supramaximal intensity. Muscle length was adjusted until maximum isometric twitch force responses were obtained. Isometric contractile properties were determined at optimal length (Lo). Peak twitch force (Pt) was determined from a series of single pulses. Force/frequency relationships were measured at stimulus frequencies ranging from 5-150 pulses per second (pps).

The stimuli were presented in trains of 1 sec duration with an interval of at least 1 min intervening between each stimulus train. Muscle forces generated, including Pt and maximum tetanic force (Po), were normalized for the estimated physiological cross-sectional areas (CSA) of the muscle segment (CSA = muscle weight/1.056 x Lo; where 1.056 g/cm^3 represents the density of muscle) and expressed in Newtons (N)/cm^2. For the SOL and EDL muscle Lo was also normalized for muscle fiber length (0.71 and 0.44 of Lo, respectively) in estimating muscle specific force. Absolute muscle forces generated by the SOL and EDL are also reported (mN).

Example 6

iPSC derived cardiomyocytes

[0204] Urine-derived cells were seeded onto Matrigel (BD, San Jose, California) coated 12 well plates at 50,000 cells/well and allowed to attach overnight (day 0). On day two, cells were transduced with high-titer OSKM viral supernatants in the presence of 8 μg/ml polybrene for three hours. Viral supernatants were replaced with fresh USC medium and after three days, replaced with mTeSR1 medium (StemCell Technology, Vancouver, BC) and changed daily. As iPSC-like colonies appeared over time, they were picked using glass Pasteur pipettes under a stereo dissection microscope (Leica M205C, Buffalo Grove, IL) and transferred to new Matrigel-coated plates for further expansion. Urine-derived iPSCs were differentiated to cardiomyocytes following an established protocol with modifications. Briefly, iPSC colonies were detached by 10 minute incubation with Versene (Life technologies, Carlsbad, CA), triturated to a single-cell suspension and seeded onto Matrigel-coated plastic dishes at a density of 250,000cells/cm^2 in mTeSR1 medium and cultured for 4 more days. Differentiation was then initiated by switching the medium to RPMI-1640 medium supplemented with 2% insulin reduced B27 (Life Technologies) and fresh L-glutamine.

Example 7

Histology

[0205] Mice were sacrificed 3 weeks (CTL: n=4; Mdx+Vehicle: n=6; Mdx+CDC/Mdx+CDC-derived exosome: n=6 each) or 3 months (CTL: n=4; Mdx+Vehicle: n=6; Mdx+CDC/Mdx+CDC-derived exosome: n=6) after first CDC/CDC-derived exosome injections and 3 weeks after miR-148 injection (n=6). Paraffin-embedded sections from apical, middle and basal parts of each heart were used for histology. Masson's trichrome staining (HT15 Trichrome Stain [Masson] Kit; Sigma-Aldrich, St. Louis, MO) was performed for evaluation of fibrosis. T

cells, B cells and macrophages were assessed by immunostaining with antibodies against mouse CD3, CD20 and CD68, respectively, and the average number of cells was calculated by counting cells in 10 fields from each of 10 sections selected randomly from the apical (3 sections; 50μm interval), middle (4 sections; 50μm interval) and basal (3 sections; 50μm interval) regions of each heart. The data were presented as number of cells/mm^2 field. Actively-cycling ($Ki67^+$) and proliferating (Aurora B^+) cardiomyocytes and the cardiomyocytes positive for dystrophin were counted in the same manner, and the cycling and proliferating fractions and the dystrophin positive cardiomyocytes were expressed as the number of $Ki67^+$, Aurora B^+ and $dystrophin^+$ cardiomyocytes divided by the total number of cardiomyocytes per high-power field (HPF), respectively, as described. Measurements were averaged for each heart.

[0206] Immunofluorescence staining: Heat-induced epitope retrieval in low or high pH buffer (DAKO, Carpinteria, CA) was followed by 2 hours permeabilization/blocking with Protein Block Solution (DAKO, Carpinteria, CA) containing 1% saponin (Sigma, St. Louis, MO; Protein Block Solution contained 3% saponin was applied for immunofluorescence staining of Ki67). Subsequently, primary antibodies in Protein Block Solution were applied overnight in 4 C° for immunofluorescence staining of 5-μm sections from apical, middle and basal parts of each heart. After 3x wash with PBS, each 10 minutes, Alexa Fluor secondary antibodies (Life Technologies, Grand Island, NY) were used for detection. Images were taken by a Leica TCS SP5 X confocal microscopy system. Immunofluorescence staining was conducted using antibodies against mouse dystrophin (1μg/ml; Thermo Fisher Scientific, Fremont, CA), Ki-67 (SP6; 1:50; Thermo Fisher Scientific, Fremont, CA), WGA (Wheat germ agglutinin; 1:200; Life Technologies, Grand Island, NY), Nrf2 (C20; 1:50; Santa Cruz Biotechnology, Santa Cruz, CA), aurora B (1:250; BD Biosciences, San Jose, CA).

[0207] Immunoperoxidase staining: Immunohistochemical detection of CD3, CD20 and CD68 was performed on 5-μm sections using prediluted rabbit monoclonal antibodies from Ventana Medical System (Tuscon, AZ; CD68) and Cell Marque (Rocklin, CA; CD3, CD20). Staining was conducted on the Leica Bond-Max Ventana automated slide stainer (Chicago, IL) using onboard heat-induced epitope retrieval method in high pH ER2 buffer (Leica Biosystems, Buffalo Grove, IL). Staining was visualized using the Dako $Envision^+$ rabbit detection System and Dako DAB (Carpinteria, CA). The slides were subsequently counterstained with Mayer's hematoxylin for 1 minute and coverslipped.

[0208] Electron microscopy: Apical (1 cube), middle (3 cubes from right, middle and left subparts) and basal (3 cubes from right, middle and left subparts) parts of posterior wall from each heart (CTL: n=3; Mdx+Vehicle: n=3; Mdx+CDC: n=3) were fixed by immersion of $1mm^3$ cubes in 2% glutaraldehyde, postfixed in osmium, and embedded in epon. Sections were cut at silver thickness, stained with uranyl acetate and lead citrate, and viewed with JEOL 1010 equipped with AMT digital camera system.

Example 8

Western blots

[0209] Western blot analysis was performed to compare myocardial abundance of dystrophin and target proteins contributing to Nrf2 signaling [Nrf2, phospho-Nrf2 (Nrf2-p^{s40}) and Nrf2 downstream gene products: heme oxygenase-1 (HO-1), catalase, superoxide dismutase-2 (SOD-2), and catalytic subunit of glutamate-cysteine ligase (GCLC)], Nrf2 phosphorylation [phosphoAkt(Akt-p^{308})], oxidative phosphorylation [CI (NDUFB8 subunit), CII (SDHB subunit), CIV (MTCO1 subunit), CIII (UQCRC2 subunit) and CV (ATPSA subunit)], mitochondrial biogenesis (PGC-1), mitophagy (PINK1), inflammation (NF-κB and MCP-1) and fibrosis (Collagen IA1 and collagen IIIA1). Myocardial density of malondialdehyde protein adducts, a marker of oxidative stress, was also measured by Western blotting (WB). Samples from apical, middle and basal parts of each heart (each 1 mm-thick transverse section) were mixed and homogenized, and nuclear and cytoplasmic fractions were extracted per manufacturer's instructions (CelLytic NuCLEAR Extraction Kit, Sigma-Aldrich, St. Louis, MO). Mitochondria were extracted from fresh whole hearts (CTL: n=3; Mdx+Vehicle: n=8; Mdx+CDC: n=8) as described in respirometry section. Cytoplasmic, nuclear and mitochondrial extracts for WB analysis were stored at −80C°. The protein concentrations in extracts were determined by the Micro BCA Protein Assay Kit (Life technologies, Grand Island, NY). Target proteins in the cytoplasmic, nuclear and mitochondrial fractions were measured by Western blot analysis using the following antibodies: antibodies against mouse Nrf2, HO-1, catalase, SOD-2, GCLC, collagen IA1, and collagen IIIA1, and PGC-1 were purchased from Santa Cruz Biotechnology (Santa Cruz, CA), phospho-Nrf2 (Nrf2-p^{s40}; Biorbyt, San Francisco, CA), respiratory chain subunits (Total OXPHOS Rodent WB Antibody Cocktail antibody), malondialdehyde, citrate synthase and TBP (Abcam, Cambridge, MA), Akt and Akt-p^{T308} , IκB-α, p-IκB-α, (Cell Signaling Technology, Denver, CO), PINK1, MCP-1 and NF-κB p65 (Sigma-Aldrich, St. Louis, MO) antibodies were

purchased from the cited sources. Antibodies to TBP (TATA binding protein) and citrate synthase were used for measurements of the housekeeping proteins for nuclear (TBP), cytosolic and mitochondrial (citrate synthase) target proteins.

[0210] Western blot methods: Briefly, aliquots containing 20 μg proteins were fractionated on 8, 10 and 4-12% Bis-Tris gel (Life technologies, Grand Island, NY) at 120 V for 2 h and transferred to a PVDF membrane (Life technologies, Grand Island, NY). The membrane was incubated for 1 h in blocking buffer (1× TBS, 0.05% Tween-20 and 5% nonfat milk) and then overnight in the same buffer containing the given antibodies at optimal dilutions. The membrane was washed 3 times for 5 min in 1× TBS, 0.05% Tween-20 before a 2-h incubation in a buffer (1× TBS, 0.05% Tween-20 and 3% nonfat milk) containing horseradish peroxidase-linked anti-rabbit IgG, anti-mouse IgG (Cell Signaling Technology, Denver, CO) and anti-goat IgG (Sigma-Aldrich, St. Louis, MO) at 1:1000-3000 dilution. The membrane was washed 3 times for 5 min in 1× TBS, 0.05% Tween20 and developed by autoluminography using the ECL chemiluminescent agents (Super Signal West Pico Chemiluminescent Substrate; Life Technologies, Grand Island, NY). Citrate synthase and TBP were used as housekeeping proteins against which expressions of the proteins of interest were normalized. Phosphorylated Akt, Nrf2 and IκB-α were normalized to total Akt, Nrf2 and IκB-α. Western blot analyses of collagen I and collagen III were conducted under nonreducing, non-denaturing conditions.

Example 9

Statistical analysis

[0211] All pooled data are presented as mean±SEM, except results for alternate data which are presented as mean ±SD. Normality and equality of variances of data sets were first tested using Kolmogorov-Smirnov and Levene's tests, respectively. If both were confirmed, t-test or analysis of variance followed by Bonferroni's post hoc test were used for determination of statistical significance; if either normality or equality of variances was not assured, nonparametric tests (Wilcoxon test or Kruskal-Wallis test followed by Dunn's post-test) were applied (SPSS II, SPSS Inc., Chicago, Illinois). No preliminary data were available for a power analysis. Results from a pilot project allowed us to power subsequent studies. The study followed preclinical reporting standards, as described. Age-matched mice were randomly allocated to experimental groups using computer generated randomization schedules. Conduct of experiments and analysis of results and outcomes were performed in a blinded manner (allocation concealment and blinded

assessment of outcome). There was no post-hoc exclusion of mice or data after the analysis before unblinding.

[0212] Ejection Fraction Data: Preliminary data were collected from a pilot study of 5 animals per group measuring ejection fraction at baseline, and again 3 weeks after treatment with cells or vehicle control in *mdx* and corresponding wild-type mice (C57BL/10ScSnJ). The measured treatment effect was approximately 4 units, with a time effect of approximately 1 unit, with group standard deviations of 3.5 units. The Inventors anticipated larger differences between groups over later time points with possible increase in measured variance. Therefore, with 12 animals per treatment group in the each of the *mdx* groups, and 7 wild-type control animals, the study had at least 80% power to detect a difference of 4.5 units or greater in treatment effect and 1.4 units or greater in time effect in a study design with 6 measurements per animal over time assuming a compound symmetry covariance structure, a correlation of 0.7 between measurements within animals over time, and a two-sided alpha of 0.05. (Power computed via PASS v. 11.0.)

[0213] Treadmill Data: Preliminary data were collected from a pilot study of 5 animals per group measuring treadmill distance (i.e., the distance ambulated before exhaustion, as described below) at baseline, and again 3 weeks after treatment with cells or vehicle control in *mdx* animals and corresponding wild-type animals. The measured treatment effect was approximately 150 meters, with limited differences observed over time in untreated groups. Group standard deviations were approximately 75 meters, with more variation observed after treatment. The Inventors anticipated larger differences between groups over later time points with possible increase in measured variance. Therefore, with 11 animals per treatment group in the each of the transgenic groups, and 7 wild-type control animals, the study had at least 80% power to detect a difference of 100 meters or greater in treatment effect and changes of at least 30 meters over time in a study design with 12 measurements per animal over time assuming a compound symmetry covariance structure, a correlation of 0.7 between measurements within animals over time, and a two-sided alpha of 0.05. (Power computed via PASS v. 11.0.).

Example 10

Assessment of CDC engraftment by real-time polymerase chain reaction

[0214] Quantitative polymerase chain reaction (PCR) was performed 1, 2 and 3 weeks after CDC injection to assess cell engraftment. Male CDCs were injected into female *mdx* mice to enable detection of the SRY gene located on the Y chromosome as a marker of engraftment using

the TaqMan assay (Applied Biosystems, Foster City, CA). The whole mouse heart was harvested, weighed, and homogenized. A standard curve was generated with multiple dilutions of genomic DNA isolated from the injected CDCs. All samples were spiked with equal amounts of genomic DNA from non-injected mouse hearts as a control. For each reaction, 50 ng of genomic DNA was used. Real-time PCR was performed in triplicate.

[0215] Engraftment was quantified from the standard curve. Percentage engraftment of CDCs at 1 week was ~8% and <1% at 2 weeks. By 3 weeks, no surviving CDCs could be detected.

Example 11

Respirometry

[0216] Mice were sacrificed via cervical dislocation after isofluorane anesthesia. Hearts were immediately excised, rinsed in PBS and homogenized via polytron in 1mL ice cold HES buffer (250mM sucrose, 1mM EDTA, 10mM HEPES, pH 7.4). Lysates were spun down at 1000*g* for 5min at 4°C to remove unbroken cells and large debris. Supernatant was then spun down at 7000*g* for 10min at 4°C to separate mitochondria-enriched fraction from crude cytosol. Pellet was resuspended in 1mL HES buffer (A subportion in lysis buffer for WB). Protein quantification was performed and adjustment with HES buffer to obtain sample containing 10µg protein in 50µL buffer which was loaded into a 24-well Seahorse cell culture plate, which was spun down at 2000*g* for 20min at 4°C to allow mitochondria to adhere to the plate surface. 450µL MAS buffer (70mM sucrose, 220mM mannitol, 5mM KH2PO4, 5mM MgCl2, 1mM EGTA, 0.2% fatty acid-free BSA, pH 7.4) was then added prior to Seahorse XF24 mitochondria stress test. 5mM/5mM pyruvate/malate and 0.25mM ADP was used to stimulate mitochondrial oxidative phosphorylation followed by 1µM oligomycin, 1µM FCCP, and a mixture of 1µM antimycin, 500nM rotenone. Citrate synthase activity was measured in sample lysates to normalize for actual amount of mitochondria loaded for test. Seahorse respirometry on normal and Duchenne iPSC cell-derived cardiomyocytes was performed using Seahorse™ XF96 Extracellular Flux analyzer as described.

Example 12

Bioluminescence imaging of mdx mouse organs after systemic injection of fluorescently-labeled CDC-derived exosomes

[0217] 6 hours after injection of fluorescently-labeled CDC-derived exosomes systemically into the *mdx* mouse left ventricular cavity, the mice sacrificed and the organs

dissected and imaged using IVIS molecular imaging systems (Caliper Life Sciences, Hopkinton, MA, USA).

[0218] Intracellular Ca^{2+} recordings: iPSC-derived cardiomyocytes were loaded for 30 min with 5 μM of the fluorogenic calcium-sensitive dye, Cal-520 (AAT Bioquest, Sunnyvale, CA) and paced via field stimulation at a frequency of 1 Hz using an Ion-Optix Myopacer (IonOptix Corp) delivering 0.2 ms square voltage pulses with an amplitude of 20 V via two platinum wires placed on each side of the chamber base (~1 cm separation). The Inventors used the xyt mode (2D) of a Leica TCS-SP5-II (Leica Microsystems Inc.; Wetzlar, Germany) to image intracellular Ca^{2+}. Cal 520 was excited with a 488 nm laser and its emission (>505 nm) was collected with a 10X objective (Leica: N PLAN 10x/0.25) at scan speeds ranging from 36 to 7 ms per frame depending on the field size. The fluorescence intensity (F) proportional to Ca^{2+} concentration was normalized to baseline fluorescence, F0 (F/F0). Time to peak and Ca^{2+} transient amplitude (F/F0) were analyzed with the software Clampfit (ver. 10.2, Molecular Devices, Inc.). Beat-to-beat alternans in each group calculated over the 5-10 sec interval of pacing at 1 Hz. The amplitude of each transient from each cell (n=10 cells in each group) was measured during pacing and mean and standard deviation were calculated and compared among groups.

[0219] RNA sequencing and 2-Dimensional hierarchical clustering: Nugen Ovation RNA-Seq System V2 kit was used to generate the double-stranded cDNA using a mixture of random and poly (T) priming. Kapa LTP library kit (Kapa Biosystems, Wilmington MA) was used to make the sequencing library. The workflow consists of fragmentation of double stranded cDNA, end repair to generate blunt ends, A-tailing, adaptor ligation and PCR amplification. Different adaptors were used for multiplexing samples in one lane. Sequencing was performed on Illumina HiSeq 2500 for a pair read 100 run. Data quality check was done on Illumina SAV. Demultiplexing was performed with Illumina CASAVA 1.8.2. The reads were first mapped to the latest UCSC transcript set using Bowtie2 version 2.1.0 and the gene expression level was estimated using RSEM v1.2.15. TMM (trimmed mean of M-values) was used to normalize the gene expression. Differentially expressed genes were identified using the edgeR program. Genes showing altered expression with $p<0.05$ and more than 2 fold changes were considered differentially expressed. The pathway and network analyses were performed using Ingenuity (IPA). IPA computes a score for each network according to the fit of the set of supplied focus genes. These scores indicate the likelihood of focus genes to belong to a network versus those obtained by chance. A score > 2

indicates ~99% confidence that a focus gene network was not generated by chance alone. The canonical pathways generated by IPA are the most significant for the uploaded data set. Fischer's exact test with FDR option was used to calculate the significance of the canonical pathway. 2-Dimensional hierarchical clustering used genes with at least 2 times fold change difference (log_2) between vehicle/CDC or vehicle/CDC-derived exosome (intraventricular injection) *mdx* hearts, diaphragms, soleus and EDL muscles. Each column represents an *mdx* analyzed tissue and each row a gene. Probe set signal values were normalized to the mean across *mdx* analyzed tissues. The relative level of gene expression is depicted from the lowest (green) to the highest (red), according to the scale shown; examples of fold changes of transcripts for genes involved in the various pathways of interest are plotted.

[0220] Cardiac mitochondria after intramyocardial CDC injection: TEM images of sections from apical, middle and basal parts of each heart were used for calculating the average numbers of mitochondria in CTL (wild type) and CDC/vehicle *mdx* mouse hearts. Extracted DNAs (QIAamp DNA Mini Kit, QIAGEN, Germantown, MD) from whole heart tissue were used to measure mitochondrial to nuclear DNA ratio using PCR format per manufacturer's instructions (NovaQUANT™ Mouse Mitochondrial to Nuclear Ratio kit, EMD Millipore, Billerica, MA).

Example 13

CDC transplantation in mdx hearts

[0221] Following intramyocardial injections of CDCs, improvements were observed in cardiac function as shown in Fig. 1A, increased exercise capacity, as shown in Fig. 1B, and increased survival rate as shown in Fig. 1C. Oxidative stress & inflammation were also confirmed as major players in DMD. CDC administration resulted in decreased inflammatory cell infiltration, as shown in Figure 1D, and reduction in oxidative stress as shown in Fig. 1E, Fig. 1F, and Fig. 1G.

[0222] These results further included restoration of mitochondrial integrity. Mitochondrial structures displayed a clear restoration of organized structure as shown in Fig. 2A and confirmed by subunit measurements as shown in Fig. 2B. Repopulation with stable competent mitochondria was further observed. Initial turnover of damaged mitochondria was followed by repopulation with healthy mitochondria, as shown in Fig. 3A. The same mitochondrial number between groups existed as shown in Fig. 3B.

[0223] In addition, reductions in cardiac collagen content and fibrosis was observed as shown in microscopic imaging as shown in Fig. 4A, and confirmed in collagen protein detection as shown in Fig. 4B. Further improvements in cardiomyogenesis were observed, as shown in Fig. 5A and via AuroraB+ and ki67+ staining in Fig. 5B.

[0224] In this aspect, CDCs are shown as effective in improving key features of DMD, including skeletal myopathy, cardiomyopathy resulting in myocyte loss, fibrosis, oxidative stress, inflammation, mitochondrial inefficiency/loss, apoptosis and fibrosis.

[0225] More specifically, intramyocardial injection of first and second (lower) doses of CDCs into the hearts of *mdx* mice improved left ventricular function (as manifested by ejection fraction [EF]) and volumes, relative to placebo, for at least 6 months. The CDC-induced improvement in EF persisted beyond the point at which no surviving CDCs were detectable in *mdx* hearts (3 weeks after CDC delivery). In addition to improving EF, CDC injection enhanced ambulatory function. Ten-month-old wild-type mice (CTL) and *mdx* mice (distinct from the *mdx* mice studied in other experiments) were subjected to weekly high-intensity treadmill exercise, starting 3 weeks after single-dose CDC or vehicle administration. CDC-treated *mdx* mice showed a substantial increase in maximal exercise capacity, relative to vehicle-treated *mdx* mice, over the 3 mos that exercise capacity was measured; survival also differed in the two groups. By ~23 mos of age, all vehicle-treated *mdx* mice had died, whereas >50% of CDC-treated *mdx* mice remained alive. In investigating mechanism, the Inventors first studied the anti-oxidative, anti-inflammatory, anti-fibrotic, and cardiomyogenic effects of CDCs. Injection of CDCs led to major changes in the expression of genes related to oxidative stress, inflammation and mitochondrial integrity. The Nrf2 anti-oxidant pathway was activated in CDC-treated *mdx* heart. Nrf2 is normally repressed by Keap1, but oxidative stress (as well as Nrf2 phosphorylation by protein kinases such as Akt) causes dissociation of the Nrf2-Keap1 complex, culminating in nuclear translocation of Nrf2 and transcriptional activation of antioxidant enzymes. In *mdx* hearts, levels of phosphorylated Akt, total Nrf2 and nuclear Nrf2 were high (as expected in response to oxidative stress); CDC treatment further increased their protein levels and those of downstream gene products (heme oxygenase-1 [HO-1], catalase, superoxide dismutase-2 [SOD-2], and the catalytic subunit of glutamate-cysteine ligase [GCLC]). Concomitantly, oxidative stress was attenuated, as evidenced by a profound reduction of malondialdehyde adducts. Histological analysis revealed extensive fibrosis in vehicle-treated *mdx* hearts, but much less in CDC-treated *mdx* hearts (comparable to an age-matched wild-

type [WT] control. Likewise, CDC treatment largely reversed the accumulation of collagens I and III in *mdx* heart tissue 3 weeks after treatment. CDCs inhibited the inflammation and mitochondrial dysfunction characteristic of *mdx* cardiomyopathy. NFκB, the master regulator of pro-inflammatory cytokines and chemokines, was activated in vehicle *mdx* hearts. Increases in phosphorylated IκB and nuclear p65 were accompanied by upregulation of MCP1 (monocyte chemoattractant protein1) and accumulation of $CD68^+$ macrophages and $CD3^+$ T cells. CDC treatment reversed activation of NFκB and decreased the number of inflammatory cells in *mdx* hearts 3 weeks after CDC injection. Mitochondrial structure and function are abnormal in muscular dystrophy-associated heart failure. Whole-transcriptome analysis revealed major changes in the expression of genes related to mitochondrial integrity in *mdx* hearts. Consistent with this finding, CDCs restored mitochondrial ultrastructure, increased mitochondrial DNA copy numbers (but not mitochondrial number), augmented levels of respiratory chain subunits and normalized the deficient respiratory capacity of isolated *mdx* mitochondria. Of note, the improved mitochondrial integrity and decreased mitochondrial turnover observed 3 weeks after CDC treatment in *mdx* mouse hearts were associated with upregulation of antioxidant enzymes and reductions of oxidative stress and inflammation. The Inventors also probed the effects of CDCs on cardiomyogenesis. Vehicle-treated *mdx* hearts exhibited a modest increase in the numbers of cycling ($Ki67^+$) and proliferating (aurora B^+) cardiomyocytes, presumably as a compensation for ongoing cardiomyocyte loss. CDCs are known to increase endogenous cardiomyogenesis in ischemic and non-ischemic models. Similar effects were seen in the *mdx* heart: CDC treatment promoted cardiomyocyte cycling and proliferation, as evidenced by a marked increase in $Ki67^+$ and aurora B^+ cardiomyocytes.

[0226] Interestingly, the Inventors found, appreciable dystrophin staining by immunohistochemistry (IHC) in CDC-treated *mdx* hearts (19.8±2.7% dystrophin positive cardiomyocytes). Western blotting (using an antibody against the C-terminal of dystrophin) further revealed a virtual absence of dystrophin in vehicle-treated *mdx* hearts, but much higher levels after CDC injection. All of the naturally-occurring isoforms of dystrophin were augmented by CDCs; the physiologically-relevant full-length isoform was restored, on average, to 20.1±0.8 % of control levels by western blot densitometry. The values for dystrophin restoration, measured either by IHC or the more quantitatively reliable immunoblots, are notable, as CRISPR/Cas 9-mediated restoration of dystrophin expression in this range and even lower suffices to produce substantial

functional benefit. Intramyocardial CDC injection (LV 4 injection sites), resulted in an increase in expression of dystrophin as shown in Fig. 7A, including across all measured isoforms as shown in Fig. 7B.

Example 14

CDC-derived exosome transplantation in mdx hearts

[0227] Consistent with reports related to CDC mediating their therapeutic effects via secreted vesicle exosomes, a depiction of role of CDCs and CDC-derived exosomes in retarding or reversing Duchenne muscular dystrophy is shown in Figure 8. CDCs prevent myocyte loss, reduce apoptosis, fibrosis, and inflammation as mediated via CDC-derived exosomes. Interestingly, intramyocardial exosomes recap effects of CDCs. Intramyocardial CDC-derived exosome injection reduces collagen, to nearly the same levels as wild-type as shown in Fig. 9A. Moreover, intramyocardial exosomes recap effects of CDCs as shown in Fig. 9B and Fig. 9C. Injection of exosomes was able to retard progressive decrease in ejection fraction as shown in Fig. 9D.

[0228] A disproportional increase in cardiac function and exercise capacity in CDC-treated mdx mice. This could be due to CDCs themselves, secreted mediators (exosomes, ECV, proteins, etc.) from engrafted CDCs, modulated cardiac secretome, and/or improved systemic hemodynamics. Disproportional increase in cardiac function as shown in Fig. 10A and exercise capacity as shown in Fig. 10B in CDC-treated *mdx* mice.

[0229] Exosomes secreted by CDCs (i.e., CDC-derived exosomes) mimic the functional and structural benefits of CDCs in a murine model of myocardial infarction. In *mdx* mice, likewise, the benefits of CDCs were reproduced by exosomes isolated from media conditioned by hypoxic CDCs (~30-200 nm in diameter). Two repeat doses of human CDC-derived exosomes (separated by 3 months) led to sustained improvement in EF, relative to vehicle injection, with a minimal but detectable humoral response in the non-immunosuppressed *mdx* mice. Collagen I and III levels decreased while the numbers of cycling ($Ki67^+$) and proliferating (aurora B^+) cardiomyocytes increased in CDC-derived exosome-injected *mdx* hearts. The effects of CDC-derived exosomes were mediated at least in part via clathrin-mediated endocytosis by the surrounding myocardium. As with the parent CDCs, intramyocardial CDC-derived exosome injection increased dystrophin expression in *mdx* hearts. The extent of dystrophin protein upregulation was comparable after treatment with CDCs or CDC-derived exosomes.

Example 15

Systemic CDC-derived exosome injection

[0230] To further evaluate the potential of exosomes to mediate systemic benefits, the Inventors injected CDC-derived exosomes into the left ventricular cavity of *mdx* hearts.

[0231] Intraventricular injection of CDC-derived exosomes demonstrated similar beneficial results in the heart as shown in Fig. 11A. CDC-derived exosomes were capable of modulating gene expression in a manner mirroring CDCs themselves as shown in Fig. 11B, and with a high degree of correlation as shown in Fig. 11C. Moreover, both ejection fraction and distance improved with CDC-derived exosome injection, as shown in Fig. 11D and Fig. 11E, respectively. These results were further observed in diaphragm, as shown for gene expression results in Fig. 11F and Fig. 11G. Both twitch and specific force improved with CDC-derived exosome injection as shown in Fig. 11H. These results were further observed in soleus, as shown for gene expression results in Fig. 11I and Fig. 11J. Both twitch and specific force improved with CDC-derived exosome injection as shown in Fig. 11K. Biodistribution after intraventricular CDC-derived exosome injection showed wide distribution across many tissue types.

[0232] Six hours post-injection, fluorescently- labeled CDC-derived exosomes were evident not only in the heart and skeletal muscle, but also in brain, liver, lung, spleen, gut and kidneys. Changes in *mdx* heart, diaphragm and soleus 3 weeks after intraventricular CDC-derived exosome injection mimicked the modifications seen in these organs after intramyocardial CDC injection. In the *mdx* heart 3 weeks after injection of CDC-derived exosomes, the Inventors found major transcriptomic changes which mirrored the changes seen after intramyocardial CDC injection. Meanwhile, cardiac dystrophin levels increased, EF improved and exercise capacity was augmented. diaphragm similarly showed extensive transcriptomic changes which correlated well with those seen in *mdx* diaphragm after intramyocardial CDC injection, as well as increased dystrophin levels. The function of diaphragm was virtually normalized 3 weeks after intraventricular CDC-derived exosome injection. Likewise, the soleus exhibited characteristic changes in gene expression, robust restoration of dystrophin, and enhanced muscle function. The results collectively implicate CDC-derived exosomes as mediators of intramyocardial CDC injection.

Example 16

CDC-derived exosome injection into mdx skeletal muscle

[0233] To investigate primary effects on skeletal muscle, the Inventors injected CDC-derived exosomes directly into the soleus in *mdx* mice. The above results indicated that the observed effects in skeletal tissue effect is mediated at least in part via CDC-derived exosomes. Results of Direct CDC-derived exosome injection into soleus is shown in Fig. 13A, Fig. 13B, and Fig. 13C. Further improvements in MyoD and Myogenin levels are shown in Fig. 13D. Levels of IGF1R and p-p65 reaching nearly the same as wild-type levels in Fig. 13F and Fig. 13G. Visible improvements were observed in soleus mass as shown in Fig. 13H, and dystrophin expression and distribution as shown in Fig. 13I. These improvements were further measured in improvements in twitch and absolute force as shown in Fig. 13J.

[0234] In an intra-aortic arch injection of CDCs in mdx mice. CDC-derived exosome injection was capable of modulating transcriptome of diaphragm as shown in Fig. 14A. When evaluating Human Duchenne cardiomyocytes derived from iPSC cells, similar improvements in dystrophin protein expression was observed, as shown in Fig. 14B and Fig. 14C.

[0235] Histological analysis revealed a paucity of surviving myofibers in vehicle injected *mdx* soleus relative to wild-type controls, and those that remained were hypertrophic. CDC-derived exosomes markedly increased the total number of myofibers and shifted the size distribution to smaller diameters, indicative of myofiber proliferation 3 weeks after injection. Consistent with this interpretation, the number of $MyoD^+$ cells was augmented after CDC-derived exosome injection, with increased tissue levels of MyoD and myogenin, the major transcription factors orchestrating myoblast and myofiber differentiation. In physiological muscle growth, IGF-1 is commonly implicated as an upstream signal, but the effects of CDC-derived exosomes on *mdx* soleus muscle were independent of IGF-1 receptors. Along with enhanced muscle regeneration, intrasoleus CDC-derived exosome injection decreased inflammation and fibrosis while increasing expression of dystrophin protein in *mdx* soleus muscle (evident by both immunohistochemistry and western blotting). The net effect was complete restoration of contractile force in the soleus muscles that had been injected with CDC-derived exosomes.

Example 17

CDC-derived exosomes in human Duchenne cardiomyocytes derived from iPSC cells

[0236] Demonstration of efficacy in multiple models of DMD would bolster the notion that CDC-derived exosomes may be viable therapeutic candidates. Duchenne human induced pluripotent stem cell (iPSC)-derived cardiomyocytes (DMD CMs) exhibit a number of phenotypic deficits characteristic of DMD, including decreased oxygen consumption rate (OCR) reminiscent of that observed in *mdx* heart mitochondria, and abnormal calcium cycling. Priming DMD CMs with CDC-derived exosomes one week earlier increased dystrophin expression (here to 27.2± 1.1% of control levels, even greater than in *mdx* hearts), suppressed beat-to-beat calcium transient alternans during 1Hz burst pacing (a measure of arrhythmogenicity) and normalized OCR. The congruence of experimental findings in the two DMD models is noteworthy: the *mdx* mouse has a missense mutation in exon 23 of the murine dystrophin gene, while the DMD patient whose iPSC cells were studied here has a fundamentally different genetic lesion in the dystrophin gene (exon 50 deletion with frame shift). Thus, the active principle of CDC-derived exosomes is not specific for a single dystrophin mutation or for a single class of dystrophin mutations.

Example 18

CDC-derived exosomes prepared under serum-free hypoxic conditions

[0237] As shown in Fig. 28, microRNAs in exosomes from hypoxically-cultured CDCs are enriched relative to exosomes from CDCs grown under normoxia. Depicted is 2-Dimensional hierarchical clustering using microRNAs with -6 to 6 times log2 fold change (230 microRNAs. Among 389 detected microRNAs in hypoxic exosomes (derived from CDCs cultured for 24 hours in serum-free hypoxic medium), 248 were previously reported to be mitochondria-related microRNAs. Further depiction of exosomes of interest are shown in Fig. 29. In this aspect, culturing of CDCs under serum-free hypoxic exosomes may heighten potency and improve salutary benefits for exosomes derived therefrom when compared to alternative culturing conditions, such as normoxic conditions.

Example 19

Heterologous expression system

[0238] HEK-293NT cells were grown with 10% FBS in DMEM (without sodium pyruvate) supplemented with MEM-NEAA and 10mM L-glutamine. Cells were harvested and plated at passage 3 at a density of 3.5 x 105 cells per well of a 6-well tissue culture-treated plate.

The cells were allowed to adhere overnight, then the following day they were transfected using the Roche HP DNA Transfection Reagent according to the manufacturer's protocol. Briefly, all reagents were brought to room temperature. Then, for each well, 1μg of plasmid DNA was suspended in 100μL of Opti-MEM, and 4μL of transfection reagent was added to the solution. This reaction was allowed to incubate at room temperature for 30 minutes and then 100μL was added to each well in a dropwise fashion. The cells were incubated with the transfection solution for 24 hours at 30°C to stimulate protein translation, and then experimental treatments were added directly to each well. Treatments consisted of: 1mg G418 sulfate (Gibco), 125ng miR-148a mimic or 1.25μg srDMD reconstituted in UltraPure Distilled Water (DNase and RNase free). Vehicle treatments consisted of equivalent volumes of PBS corresponding to the volume used for each treatment listed above. Following a 24-hour treatment period, the cells were harvested for GFP fluorescence and luciferase activity analysis. Briefly, the 6-well plate was placed on ice and each well was washed twice with ice-cold PBS. Next, 1mL of ice-cold non-denaturing lysis buffer (20mM Tris HCl pH 8, 137mM NaCl, and 1% Triton X-100 in PBS) was added to each well and incubated on ice for 15 minutes. Cell lysates were then transferred to microcentrifuge tubes using cell scrapers and centrifuged at 12,000 RPM for 1 minute at 4°C. Supernatants were transferred to new, pre-chilled microcentrifuge tubes and kept on ice. For each sample, 200μL of cell lysate was transferred to one well of a black/clear-bottom 96-well plate. This plate was used to measure GFP fluorescence on a SpectraMax M5 plate reader. Then, 20μL of cell lysate was taken from each of those wells and transferred to a new black/clear bottom 96-well plate. Room temperature-equilibrated luciferase substrate (Sigma-Aldrich: LUC-1) was added to each well according to the manufacturer's protocol and luminescence was measured on the SpectraMax M5 plate reader (top read, 1s integration time). The luciferase measurements were done in shifts to ensure that no more than 20 seconds elapsed between adding the luciferase substrate and measuring luminescence. For each experiment, the raw GFP fluorescence measurements (in RFUs) for non-transfected controls were subtracted from the fluorescence measurements for all of the transfected samples. These corrected values were then divided by the corresponding luciferase activity measurements (in RLUs). Finally, the normalized values were transformed using the exponential function.

[0239] Raw GFP fluorescence measurements were corrected by corresponding luciferase activity and then transformed using the exponential function (Equation 1). On the Y axis, 1 is the fluorescence level of an untransfected well. Raw GFP fluorescence measurements were corrected by corresponding luciferase activity and then transformed using the exponential function (Equation 1). On the Y axis, 1 is the fluorescence level of an untransfected well.

$$\text{Normalized GFP} = e^{\left(\frac{GFP}{LUC} x\ 1000\right)}$$

The nonlinear relationship between basal levels of PTC and Exon 50 Δ expression versus WT was best described by a saturating function, consistent with the presumption that degradation of the full-length fusion protein increases with increasing expression (e.g., due to endoplasmic reticulum stress)3. PTC: vehicle (n = 15), G418 (n = 7), miR-148a-3p (n = 4), and srDMD (n = 4); Exon 50 Δ: vehicle (n = 8), G418 (n = 3), miR-148a-3p (n = 4), and srDMD (n = 3); * P<0.05 vs vehicle. Wild type: human DMD variant Dp427m [BC111587.2] in mammalian expression vector with CMV promoter + C-eGFP tag + SV40-firefly luc (no neomycin and no stop codon before C-eGFP) PTC: human DMD variant Dp427m [BC111587.2, G to U mutation at pos. 6863 based on transcript sequence to introduce UAA stop codon] in mammalian expression vector with CMV promoter + C-eGFP tag + SV40-firefly luc (no neomycin and no stop codon before C-eGFP) Exon 50 Δ: human DMD variant Dp427m [BC111587.2, del exon 50] in mammalian expression vector with CMV promoter + C-eGFP tag + SV40-firefly luc (no neomycin and no stop codon before C-eGFP)

Example 20

miR-148a-3p and srDMD transplantation into mdx heart

[0240] In Fig. 35A, differential expression of miR-148a-3p and srDMD in CDC-derived exosomes isolated from hypoxic conditioned media (2% O_2) was observed when compared to CDC-derived exosomes isolated from normoxic conditioned media, along with depiction of apparent secondary structure of srDMD. Further results of changes under culturing conditions as shown in Figures 28 and 29. As shown in Fig. 35B, western blots and pooled data for protein abundance of dystrophin isoforms: dp427, dp260, dp140, dp116, dp71, dp40 in *mdx* mouse hearts 3 weeks after intramyocardial injection of vehicle, or mimics of miR-148a-3p or srDMD. Further, in Fig 35C, western blots and pooled data for protein abundance of dystrophin isoforms: dp427,

dp260, dp140, dp116, dp71, dp40 in *mdx* mouse hearts 3 weeks after intramyocardial injection of vehicle, mimics of miR-148a-3p or srDMD and levels of dystrophin expression.

Example 21

Exon skipping/alternative splicing excluded

[0241] In Fig. 36A, miR-148a-3p results in decreases in both NFκB p65 and phospho-Akt levels. NFκB and Akt are known targets of miR-148a-3p. In Fig. 36B, RT-PCR using primers that flank the exon 23 of dystrophin. It was used to assess exon 23 inclusion in expressed dystrophin in *mdx* hearts from vehicle, miR-148a-3p or srDMD-treated mice (n=4-6). Sashimi plots of RNA-Seq data for dystrophin from vehicle, miR-148a-3p or srDMD-treated *mdx* hearts depict no junction read that span exon 23. All data are means ± SEM. ‡P<0.002 vs. miR-148a-3p and srDMD; ǂ P<0.03 vs. miR-148a-3p and CTL (Wild type).

[0242] In Fig. 37B, percentage increase [relative to vehicle (PBS)] in dystrophin/eGFP expression after treatment with miR-148a-3p or srDMD in transfected HEK293 NT cells with dual reporter constructs harboring a point mutation in exon 23 of dystrophin gene (PTC) or deletion of exon 50 of dystrophin gene (Exon 50 Δ).

Example 22

Dystrophin expression and its consequences

[0243] In Fig. 38A, ejection fraction (EF) at baseline and 3 weeks after intramyocardial injection of miR-148a-3p or microRNA mimic control [miRMimic(CTL)] in mdx mice. Wild type (WT) EF values also shown for reference, n=5 per group. In Fig. 38B, western blot depicting protein content of dystrophin in wild type (WT) mouse hearts and in vehicle- (Veh.), mutant srDMD- and srDMD-injected (srDMD) mdx mouse hearts 3 wks after intramyocardial injection.

Example 23

Mechanistic study using heterologous expression

[0244] As shown in Fig. 39A, full length human dystrophin was cloned into the ORF, either as wild-type or as one of two mutants: UAA premature termination codon in exon 23 (PTC), or exon 50 deletion (Exon 50 Δ). The construct creates a fusion protein of full-length dystrophin in frame with eGFP, such that green fluorescence can be taken as a reporter of dystrophin expression. Constitutive luciferase expression (driven independently by an SV40 promoter) was used to normalize for transfection efficiency.

[0245] As shown in Fig. 39B, dystrophin/eGFP expression in HEK-293NT cells transfected with full-length (WT), PTC or Exon 50 Δ constructs. Fluorescence and luminescence of total cell lysates were quantified on a well-by-well basis in a 96-well spectrophotometer; fluorescence in each well was also quantified with nontransfected cells at an equivalent seeding density and lysis volume. The responses mimic those to the aminoglycoside G418, and are qualitatively similar for both mutations. Without being bound by any particular theory, these findings support the idea that short non-coding RNAs act on release factors or on the ribosome itself.

Example 24

miR-148a-3p and srDMD as effectors of dystrophin re-expression

[0246] The Inventors utilized heterologous expression of novel dual-reporter constructs (wild-type and mutant dystrophins fused in-frame to eGFP, and independently-expressed luciferase) to explore mechanism. The responses mimic those to the aminoglycoside G418, and are qualitatively similar for both mutations. Given the efficacy on both types of mutations, short non-coding RNAs are most likely increase dystrophin expression indirectly, by acting on release factors or on the ribosome itself to enhance recoding.

[0247] More specifically, read-through of PTCs and ribosomal frameshifting are natural "recoding" processes which increase translational efficacy in certain genetic errors; both are enhanced by aminoglycoside antibiotics (albeit at concentrations that can be toxic in vivo). To quantify translation, The Inventors created dual-reporter plasmids expressing full-length human dystrophin fused in-frame with eGFP, and luciferase independently coexpressed to assay transfection efficiency. The Inventors compared green fluorescence, seen only when dystrophin-eGFP was translated, in HEK-293NT cells transfected with plasmids encoding wild-type dystrophin or each of two mutants: a point mutation in exon 23 introducing a PTC to mimic the mdx mutation, and another with deletion of exon 50, reproducing the human DMD mutation. Normalized fluorescence, expressed as percent enhancement over vehicle only, showed appropriate increases with the aminoglycoside G418 as a positive control in both mutants. Application of miR-148a-3p mimic or srDMD likewise enhanced dystrophin eGFP expression in both mutants.

[0248] There is firm evidence that the effects of exosomes are attributable to their RNA payloads. Dystrophin transcripts were absent by RNA-seq and undetectable by quantitative PCR

in CDC-derived exosomes, so dystrophin restoration is not due to cell-cell transfer of its mRNA. Nevertheless, regulatory RNA may act directly or indirectly to increase dystrophin expression, by splicing to remove defective exons or by readthrough of premature stop codons. RNA-seq of CDC-derived exosomes grown under the Inventors' conditions (24 hours of serum-free hypoxic medium) revealed major differences, including 144- and 337-fold augmentation, respectively, of miR-148a-3p and a small RNA from DMD (srDMD) samples of unknown function as compared to normoxic CDC-derived exosomes. Among sequenced small RNAs (25-200 bp) in the exosomes, miR-148a-3p seemed worthy of investigation given its enrichment. In addition to this consideration, srDMD caught the Inventors' attention as it had cognate sequences with UAA (the premature stop codon in exon 23 of dystrophin in the *mdx* mice), suggesting that it might function as a nonsense suppressor RNA to promote readthrough. Intramyocardial injection of miR-148a-3p or srDMD restored expression of dystrophin in *mdx* hearts 3 weeks after administration. The unexpected bioactivity of miR-148a-3p on dystrophin protein levels occurred in parallel to known effects of miR-148a-3p (decreases in both NFκB p65 and phosphoAkt levels). The effects of srDMD were striking insofar as this short RNA has no known function. Mutation of srDMD to alter the cognate UAA site rendered srDMD ineffective. While consistent with nonsense suppressor activity, these findings do not suffice to prove that mechanism. The Inventors did, however, exclude exon skipping as a contributory factor: junction read analysis of sequenced dystrophin mRNAs from miR-148a-3p or srDMD-injected *mdx* hearts revealed no read spanning exon 23. The evidence against alternative splicing leaves, by exclusion, enhanced readthrough as a likely mechanism underlying the increased dystrophin expression seen with miR-148a-3p or srDMD administration. Figures 28 and 29 list a variety of other RNA polynucleotides enriched under hypoxic conditions and possible candidates for therapeutic agents.

[0249] To compare possible exosome contents responsible for the aforementioned effects, miR-148a-3p was measured as compared to srDMD oligomer, both of which displayed similar levels of activity, and levels of dystrophin expression.

[0250] The Inventors utilized heterologous expression of novel dual-reporter constructs (wild-type and mutant dystrophins fused in-frame to eGFP, and independently-expressed luciferase) to explore mechanism. The data support the idea that exosomes increase translation of dystrophin mutants, as do their individual constituents miR-148a-3p and srDMD. The responses mimic those to the aminoglycoside G418, and are qualitatively similar for both

mutations. Given the efficacy on both types of mutations, CDC exosomes and their contents most likely increase dystrophin expression indirectly, by acting on release factors or on the ribosome itself to enhance recoding.

[0251] More specifically, read-through of PTCs and ribosomal frameshifting are natural "recoding" processes which increase translational efficacy in certain genetic errors; both are enhanced by aminoglycoside antibiotics (albeit at concentrations that can be toxic in vivo). To quantify translation, we created dual-reporter plasmids expressing full-length human dystrophin fused in-frame with eGFP, and luciferase independently coexpressed to assay transfection efficiency. We compared green fluorescence, seen only when dystrophin-eGFP was translated, in HEK-293NT cells transfected with plasmids encoding wild-type dystrophin or each of two mutants: a point mutation in exon 23 introducing a PTC to mimic the mdx mutation, and another with deletion of exon 50, reproducing the human DMD mutation. Normalized fluorescence, expressed as percent enhancement over vehicle only, showed appropriate increases with the aminoglycoside G418 as a positive control in both mutants. Application of CDC-exosomes (XO), miR-148a-3p mimic or srDMD likewise enhanced dystrophin eGFP expression in both mutants. Given the efficacy on both types of mutations, CDC exosomes and their contents most likely increase dystrophin expression indirectly, by acting on release factors or on the ribosome itself. In contrast, the observed augmentation of dystrophin-eGFP translation in non-dystrophic HEK-293NT cells argues against translational derepression by relief of oxidative stress. The expression vectors here used an open reading frame for dystrophin containing no introns, further excluding splicing as a mechanism of benefit. The data support the idea that exosomes themselves increase translational efficacy in dystrophin mutants, as do their constituents miR-148a-3p and srDMD.

Example 25

Identification of further short non-coding RNAs of interest, validation platform

[0252] The creation of a dual-reporter system using eGFP and luciferase provides a robust platform for identifying additional short non-coding RNAs that may possess bioactivity enhancing translation efficiency. In this aspect, RNA profiling of cells possessing therapeutic activity can be compared against inert cells to identify enriched RNAs. Alternatively, the same cells with therapeutic activity can be compared against variable culture conditions enhancing or diminishing therapeutic activity, again to identify enriched RNAs. Short non-coding RNAs identified by these approaches can then be validated by contact with cells expressing the dual-

report system. Specifically, by measuring green fluorescence, seen when a fused in-frame protein (e.g., dystrophin-eGFP) is translated. By further comparison to aminoglycoside as control, bioactivity of short non-coding RNAs that enhance translation can be identified.

Example 26

Remote effects of CDC transplantation in mdx heart

[0253] Intramyocardial injection of CDCs and their exosomes improved Duchenne cardiomyopathy by increasing dystrophin and reversing key pathophysiological processes in the *mdx* mouse heart. These changes were associated with a substantial increase in exercise capacity which seemed disproportionate to the CDC-related improvement in cardiac function: EF increased by <10%, while ambulatory capacity doubled. To further evaluate the mechanism of enhanced exercise capacity in CDC-treated *mdx* mice, the Inventors isolated and examined three distinct skeletal muscles: the diaphragm (DIA, a key respiratory muscle), and two limb muscles (soleus and extensor digitorum longus [EDL], representative of slow and fast twitch muscles, respectively) 3 weeks after intramyocardial injection of CDCs or vehicle.

[0254] To understand the contribution of CDC-derived exosomes in the above effects, the Inventors assessed skeletal muscles, diaphragm and soleus, 3 weeks after intramyocardial CDC injection. Secondary effect on diaphragm gene expression after intramyocardial CDC injection demonstrated differences in $Ca2^{+}$. Additional results were observed in inflammatory pathway and response. Intramyocardial CDC-derived exosome injection resulted in decrease of oxidative stress marker, MDA to nearly the same levels as wild-type as shown. Further decreases in inflammatory markers p65 and lkB were observed. Reduction in fibrosis was observed as well as a reduction in inflammatory cells. Improvements in diaphragm force production and soleus muscle was observed. Similarly, soleus and EDL showed notable improvements at both transcriptomic and functional levels; soleus contractile force was fully normalized. Changes in gene expression were significantly correlated in diaphragm and soleus.

[0255] To further evaluate the potential of exosomes to mediate systemic benefits, the Inventors injected CDC-derived exosomes into the left ventricular cavity of *mdx* hearts. Intraventricular injection of CDC-derived exosomes demonstrated similar beneficial results in the heart as shown in. CDC-derived exosomes were capable of modulating gene expression in a manner mirroring CDCs themselves. Moreover, both ejection fraction and distance improved with CDC-derived exosome injection. These results were further observed in diaphragm and both twitch

and specific force improved with CDC-derived exosome injection. These results were further observed in soleus, as shown for gene expression and again both twitch and specific force improved with CDC-derived exosome injection.

Example 27

Animals and Injections

[0256] All animal procedures were approved by the Cedars-Sinai Medical Center Institutional Animal Care and Use Committee. Ten – twelve-month-old *mdx* (C57BL10/ScSn-DMD^{mdx}/J) and wild-type strain-matched (C57BL10/ScSn/J) animals were used in this study. Mice were housed under pathogen-free conditions in a temperature controlled room with a 12-hour photoperiod. Baseline measurements of maximal exercise capacity and *in vivo* cardiac function were recorded prior to injection. CDCs ($2.5x10^5$) and CDC-exos ($2x10^9$) were suspended in 100 µL of DPBS and injected into the femoral vein of *mdx* mice. Vehicle-treated *mdx* mice received an equal volume of DPBS injected into the femoral vein. Mice were reassessed for maximal exercise capacity and *in vivo* cardiac function 3 weeks post-injection, then tissues were harvested and processed for muscle physiology experiments, histology and immunohistochemistry, or frozen in liquid nitrogen and stored at -80°C.

Cardiosphere-Derived Cell Culture and Exosome Purification

[0257] Mouse CDCs were expanded from an 8-week-old strain-matched wild-type donor. The ventricles were cut into fragments <1mm^3, washed, and partially digested with trypsin (0.05%; Gibco). These fragments were individually seeded onto fibronectin (Corning) coated culture dishes and cultured in growth media [Iscove's Modified Dulbecco's Medium (GIBCO), 20% fetal bovine serum (Atlas Biologicals), 1% penicillin/streptomycin (GIBCO), and 1X 2-mercaptoethanol (GIBCO)]. After a variable period of growth, a monolayer of cells emerged from the explants, which phase bright cells proliferated. The loosely adherent cells surrounding the explants (termed explant derived cells) were harvested using mild enzymatic digestion (TrypLE; GIBCO) and plated on poly-D-lysine coated culture flasks (ultra-low adherent) for three days. In suspension culture, explant-derived cells spontaneously form three-dimensional clusters termed cardiospheres, which were harvested and plated in fibronectin coated culture flasks. In adherent culture, as disclosed elsewhere herein, cardiospheres form a monolayer of cells termed CDCs. CDCs were expanded to passage 3-5, which were used for all experiments. To block exosome biosynthesis, confluent CDCs were washed with DPBS and the media was supplanted with serum-

free media. CDCs to be used for *in vivo* experiments were washed, enzymatically dissociated from the adherent culture dishes, counted, and suspended in DPBS. To generate exosomes, human CDCs were cultured until confluency at passage 5. The cells were washed with DPBS, and the media was supplanted to serum-free media. CDCs were then cultured in physiologically low oxygen (2% O_2) for 24 hours. The conditioned media was then collected, sterile filtered using a 0.45 μm filter, and frozen for later use. Later, the conditioned media was thawed and the exosomes were purified and concentrated by ultrafiltration via centrifugation using 3 kDa centrifugal filters (EMD Millipore). Exosome concentration of the filtrate was measured by nanoparticle tracking analysis (NanoSight NS300). Exosomes were then aliquoted in ready-to-use tubes, frozen, and stored at -80°C until later use.

Treadmill Exercise Testing

[0258] Mice were placed inside an Exer-3/6 rodent treadmill (Columbus Instruments) equipped with a shock plate. During the acclimatization period, the belt speed was set to 10 m/min with the shock plate inactivated, and mice were undisturbed for 20 minutes to acclimate to the environment. After the acclimatization period, the exercise protocol engaged (shock plate activated at 0.15 mA at a frequency of 1 shock/sec). The protocol is intended to induce volitional exhaustion by accelerating the belt speed by 1 m/min per minute. Mice that rest on the shock plate for >10 sec with nudging are considered to have reached their maximal exercise capacity (their accumulated distance traveled is recorded) and the exercise test is terminated.

In vitro Isolated Skeletal Muscle Physiology

[0259] Mice were deeply anesthetized with isoflurane inhalation and the soleus or diaphragm muscles were rapidly excised. Briefly, following a lateral midline skin incision of the lower leg the soleus was dissected and isolated and its tendons of origin and insertion were tightened with silk suture (3-0) and rapidly excised. The soleus muscle was vertically mounted in a tissue bath containing a mammalian Ringer's of the following composition: (in mM) 137 NaCl, 5 KCl, 2 $CaCl_2$, 1 $MgSO_4$, 1 NaH_2PO_4, 24 $NaHCO_3$, 11 glucose. The solution was constantly aerated with 95% O_2 and 5% CO_2 with pH maintained at 7.35 and temperature kept at 24°C. Following a left costal margin skin and muscle incision a section of the midcostal hemidiaphragm was transferred to a preparatory Sylgar-lined dish containing the aerated cold Ringer's and a narrow 3-4 mm wide strip of diaphragm was isolated maintaining fiber attachments to the rib and central tendon intact which were tighten with silk suture and mounted vertically in the tissue bath.

One end of the soleus or diaphragm was secured to a clamp at the bottom of the dish and one was attached to a calibrated force transducer (Cambridge Technology Model 300B, Watertown, MA). A micromanipulator linked to the system was used to adjust muscle length. Platinum wire electrodes placed on each side of the muscle were used for direct muscle stimulation (Grass Model S88 stimulator; Quincy, MA) using 0.2 msec duration monophasic rectangular pulses of constant current (Mayo Engineering, Rochester, MN) delivered at supramaximal intensity. Muscle preload was incrementally adjusted until the optimal muscle length for maximum isometric twitch force (Lo) was reached. Lo was measured at 0.1 mm accuracy using a digital caliper (Mitutoyo, Japan). Isometric contractile properties were then determined at this Lo. Peak twitch force (Pt), contraction time (i.e., time to Pt) and half-relaxation time (i.e., time for Pt to fall one-half maximum) were determined from a series of single pulses. Force-frequency relationships were measured at stimulus frequencies ranging from 5 to 180 pulses per second. The stimuli were presented in trains of 1 sec duration with an interval of at least 1 min intervening between each stimulus train. Muscle forces generated, including Pt and maximum tetanic force (Po), were normalized for the estimated physiological cross-sectional area(CSA) of the muscle segment (CSA = muscle weight/1.056 x Lo; where 1.056 g/cm^3 represents the density of muscle) and expressed in Newtons (N)/cm^2. For the soleus muscle, Lo was also normalized for muscle fiber length (0.71 of Lo) in estimating muscle specific force. Absolute muscle maximum forces generating are also reported (mN).

[0260] Figure 40 demonstrates functional improvements to the cardiorespiratory system by a single intravenous dose of syngeneic cardiosphere-derived cells (CDCs) and human CDC-derived exosomes (CDC-XOs) in *mdx* mice. Ten-twelve-month-old wild-type (WT) and *mdx* mice were subjected to baseline assessment of maximal exercise capacity and *in vivo* cardiac function by echocardiography. At this age, *mdx* mice have a markedly reduced ability to tolerate exercise concomitant with impaired left ventricular ejection fraction (Fig. 40A). A single intravenous dose of CDCs or CDC-XOs dramatically improved the maximal exercise capacity of *mdx* mice 3 weeks after treatment. In addition to improving exercise capacity, CDC and CDC-XO treatment boosted left ventricular function (as evidenced by ejection fraction) relative to vehicle treated *mdx* mice (Fig. 40B). The robust improvements in cardiac function were mirrored by a global decrease in histopathology of *mdx* hearts (Fig. 40C; vehicle: top panel, CDCs: middle panel, and CDC-XOs: bottom panel) concomitant with a significant reduction in interstitial fibrosis (Fig. 40D).

Example 28

[0261] Animals were treated as described in Example 27. Figures 41 & 42 reveal the effects of CDCs and CDC-XOs on the transcriptome, inflammation, oxidant stress, and regeneration of *mdx* hearts. Whole transcriptome analysis of RNA-sequencing data demonstrates that CDCs and CDC-XOs partially reverse the transcriptomic profile of *mdx* hearts, skewing gene expression toward WT hearts (Fig. 41A). Kyoto Encyclopedia of Genes and Genomes (KEGG) enrichment analysis of the 772 differentially regulated genes show a significant *up*regulation in cytokine-receptor interaction, complement and coagulation cascades, and several pathways involved in inflammation, such as NF-κB (data not shown). Therefore, the activation (phosphorylation) of NK-κB, a master transcriptional regulator of a host of pro-inflammatory genes, was probed. In *mdx* hearts, NF-κB is potently activated (Fig. 41B). Conversely, CDC and CDC-XO treatment decreased the protein levels of phosphorylated NF-κB (Fig. 41B), indicating a reduction in pro-inflammatory signaling. To determine if decreased NF-κB signaling had a physiological effect on inflammation in *mdx* hearts, cryosections of *mdx* hearts from vehicle (control; labeled *mdx*), CDC, and CDC-XO treated mice were immunostained for CD68, an activated macrophage marker, and visualized immunofluorescence by confocal microscopy. Relative to vehicle-treated *mdx* hearts, CDC and CDC-XO-treated *mdx* hearts contained significantly few $CD68^+$ macrophages (Fig. 41C&D) demonstrating a direct effect of CDCs and CDC-XOs to modulate inflammation in *mdx* hearts. Because hearts from *mdx* mice have been previously described to have mitochondrial dysfunction, assays for the protein expression of complexes involved in electron transport and oxidative phosphorylation were performed. Consistently, a modest, but significant, decrease in most electron transport chain complexes and ATP synthase (complex V) was demonstrated (Fig. 42A). In contrast, CDC and CDC-XO treatment restored protein expression of the electron transport chain complexes and ATP synthase (Fig. 42A). Mitochondrial dysfunction is associated with increases in cellular oxidant stress. The formation of protein-carbonyl adducts, an irreversible oxidative modification to proteins caused by severe oxidant stress, was tested. Treatment with CDCs and CDC-XOs reduced carbonylated protein accumulation to a level consistent with WT hearts (Fig. 42B). Lastly, testing was performed to determine if CDCs or CDC-XOs could induce cardiomyocyte proliferation, a marker of cardiac regeneration, when delivered intravenously. Compared to vehicle treated *mdx* hearts,

CDC and CDC-XO-treated *mdx* hearts 2.5-3-fold more Ki-67$^+$ cardiomyocytes, a protein exclusively expressed during cell division (Fig. 42C&D).

Example 29

[0262] Animals were treated as described in Example 27. Figure 43 shows the therapeutic benefits of intravenous delivery of CDCs and CDC-XOs are not exclusive to *mdx* hearts, they are also efficacious at improving skeletal muscle function. Given that skeletal muscles of *mdx* mice share common pathophysiological processes with *mdx* hearts, whether systemic delivery of CDCs and CDC-XOs would benefit skeletal muscles of *mdx* mice was tested. Vehicle-treated *mdx* mice exhibit a marked reduction isometric twitch and tetanic force of the diaphragm (Fig. 43A-C) and soleus (Fig. 43D-F), key respiratory and locomotor muscles respectively. Intravenous delivery of CDCs and CDC-XOs potently boosted isometric force produced by the diaphragm and soleus (Fig. 43A-F). Like *mdx* hearts, these improvements were mirrored by a decrease in histopathology (Fig. 43G; vehicle: left panel, CDCs: middle panel, and CDC-XOs: right panel) and related fibrosis (Fig. 43H). In parallel, CDC and CDC-XO treatment boosted the number of myofibers comprising the soleus of *mdx* mice (Fig. 43I).

Example 30

[0263] Animals were treated as described in Example 27. Figures 44&45 reveal the effects of CDCs and CDC-XOs on the transcriptome, and inflammation in the solei of *mdx* mice. Like *mdx* hearts, whole transcriptome analysis demonstrates that CDCs and CDC-XOs partially reverse the transcriptomic profile in the *mdx* mouse soleus (Fig. 44A). KEGG enrichment show a dramatic *up*regulation of pathways involved in inflammation in CDC (data not shown) and CDC-XO (Fig. 44B) treated *mdx* soleus. Fold change (relative to vehicle treated *mdx* soleus) of genes due to CDC and CDC-XO treatment involved in TNF and NF-κB signaling are depicted in Fig. 43C and Fig. 43D, respectively. Consistent, with vehicle treated *mdx* hearts, phosphorylated NF-κB was significant greater in vehicle treated *mdx* solei than WT solei (Fig. 45A). Next, we probed for CD68 immunohistochemistry on vehicle, CDC, and CDC-XO treated *mdx* solei cyrosections. Like vehicle treated *mdx* hearts, their soleus muscles are also infiltrated with CD68$^+$ macrophages. However, unlike CDC and CDC-XO treated *mdx* hearts, these treatments appear to boost CD68$^+$ macrophage accumulation in the soleus, an observation consistent with RNA-sequencing data (Fig. 45B&C). A careful inspection of the fascicular arrangement in these muscles (α-sarcomeric actin [green] channel in Fig. 45C) reveal that the increased accumulation of CD68$^+$ macrophages due to

CDC and CDC-XO treatment do not appear pathological. Indeed, these treatments boost contractile function of this muscle (Fig. 43D-F), and attenuate protein-carbonyl adducts (data not shown).

[0264] Figure 46 demonstrates the ability of CDCs and CDC-XOs (when delivered intravenously) to modestly increase the protein expression of the full-length dystrophin isoform in the soleus (Fig. 46A) and diaphragm (Fig. 46B) 3 weeks after a single dose.

Additional Background and Examples

[0265] As discussed above, several embodiments of the methods and compositions provided herein are based on the surprising discovery that, despite the finding that intravenous administration of cardiosphere-derived cells (CDCs) to *mdx* mice resulted in accumulation of the majority of CDCs in their lungs, functional improvements at dystrophic skeletal muscles were achieved as demonstrated by the various data presented herein, thereby enabling an effective treatment of a human subject suffering from muscular dystrophy, e.g., DMD, by administering a therapeutically effective amount of CDCs to a human subject suffering from skeletal muscular dystrophy.

[0266] The CDCs accumulated in the lungs may have released extracellular vesicles (EVs) including exosomes and microvesicles, as well as paracrine factors that through direct interactions with dystrophic skeletal muscle at, e.g., the leg, or through an indirect mechanism (e.g., immunomodulatory response and reducing chronic inflammation), reached a therapeutically effective amount to treat a subject in need thereof. As such, in this context and not wishing to be bound by theory, what is meant by "a therapeutically effective amount of CDCs" is a sufficient amount of CDCs administered to a subject to result in delivery of a sufficient amount of EVs to a targeted dystrophic skeletal muscle in a subject to increase and/or restore skeletal muscle function in the subject and to immune-modulate chronic inflammatory immune response.

[0267] Accordingly, one aspect of some embodiments provides a method of safely treating skeletal muscular dystrophy in a subject in need thereof, the method comprising administering to the subject a therapeutically effective amount of autologous or allogeneic CDCs and/or EVs, e.g., exosomes and microvesicles. In particular, said therapeutically effective amount of CDCs and/or EVs is sufficient to treat or alleviate a targeted dystrophic skeletal muscle of the subject. What is meant by "a targeted dystrophic skeletal muscle" in this context is that a therapeutically effective amount of CDCs and/or EVs is sufficient to treat or alleviate

dystrophinopathy and/or restore skeletal muscle function, of a particular dystrophic skeletal muscle in a subject at the site of a dystrophic skeletal muscle, rather than an accidental or inadvertent delivery of CDCs and/or EVs that might be secreted from CDCs that might not be in a sufficient amount to treat dystrophinopathy at the site of a dystrophic skeletal muscle.

[0268] Non-limiting examples of said skeletal muscular dystrophy include DMD and Becker muscular dystrophy, wherein one or more skeletal muscles of, e.g., the diaphragm, the arm and/or the leg is/are dystrophic. Non-limiting examples of a means to administer a therapeutically effective amount of CDCs and/or EVs in this context include intramuscular injection or infusion directly at a dystrophic skeletal muscle and systemic administration, in a single dose or multiple doses.

[0269] Another aspect provides a method of safely treating dystrophic cardiomyopathy, the method comprising systemically administering to the subject a therapeutically effective amount of CDCs. In particular, said therapeutically effective amount of CDCs is sufficient to treat or alleviate the subject's dystrophic heart muscle. Non-limiting examples of said dystrophic cardiomyopathy include heart failure secondary to, or associated with, an acute or chronic muscular dystrophy, e.g., DMD or Becker muscular dystrophy.

[0270] As discussed above, dystrophic tissues includes lack of, or deficient, dystrophin in skeletal and/or heart muscle.

[0271] In some embodiments, said subject is a mammal such as a human. Non-limiting examples of said systemic administration of CDCs include intravascular administration (e.g., intravenous or intra-arterial injection or infusion), intra-aortic administration, intraventricular administration (e.g., injection or infusion into the right or left ventricle or atrium), intrathecal administration, and intraperitoneal administration. Non-limiting examples of said intravenous administration of CDCs include jugular and/or femoral vein injection and/or infusion. Non-limiting examples of said administration of CDCs in multiple doses include administration of 2-10 doses at intervals of 1-5 months, e.g., 3 doses at intervals of about 3 months, or 5 doses at interval of about 1 week. Non-limiting examples of said administration of CDCs in multiple doses include three administrations at weeks 0, 6 and 12. Non-limiting examples of said therapeutically effective amount of CDCs include at least about 75-500 x 10^6 CDCs, e.g., about 75 x 10^6 CDCs, about 150 x 10^6 CDCs, about 300 x 10^6 CDCs, 400 x 10^6 CDCs, and 500 x 10^6 CDCs.

[0272] Some embodiments provide a formulation comprising CDCs for use in the treatment of skeletal muscular dystrophy and/or dystrophic cardiomyopathy according to the aforementioned methods.

[0273] Some embodiments use the aforementioned formulation for treating skeletal muscular dystrophy and/or dystrophic cardiomyopathy according to the aforementioned methods.

Cardiospheres

[0274] In some embodiments, cardiospheres are derived from cardiac tissue and include undifferentiated cardiac cells that grow as self-adherent clusters as described in WO 2005/012510, and Messina *et al.*, "Isolation and Expansion of Adult Cardiac Stem Cells From Human and Murine Heart," *Circulation Research*, 95:911-921 (2004), the disclosures of which are herein incorporated by reference in their entirety.

[0275] Briefly, heart tissue can be collected from a patient during surgery or cardiac biopsy. The heart tissue can be harvested from the left ventricle, right ventricle, septum, left atrium, right atrium, crista terminalis, right ventricular endocardium, septal or ventricle wall, atrial appendages, or combinations thereof. A biopsy can be obtained, *e.g.*, by using a percutaneous bioptome as described in, *e.g.*, U.S. Patent Application Publication Nos. 2009/012422 and 2012/0039857, the disclosures of which are herein incorporated by reference in their entirety. The tissue can then be cultured directly, or alternatively, the heart tissue can be frozen, thawed, and then cultured. The tissue can be digested with protease enzymes such as collagenase, trypsin and the like. The heart tissue can be cultured as an explant such that cells including fibroblast-like cells and cardiosphere-forming cells grow out from the explant. In some instances, an explant is cultured on a culture vessel coated with one or more components of the extracellular matrix (*e.g.*, fibronectin, laminin, collagen, elastin, or other extracellular matrix proteins). The tissue explant can be cultured for about 1, 2, 3, 4, or more weeks prior to collecting the cardiosphere-forming cells. A layer of fibroblast-like cells can grow from the explant onto which cardiosphere-forming cells appear. Cardiosphere-forming cells can appear as small, round, phase-bright cells under phase contrast microscopy. Cells surrounding the explant including cardiosphere-forming cells can be collected by manual methods or by enzymatic digestion. The collected cardiosphere-forming cells can be cultured under conditions to promote the formation of cardiospheres. In some aspects, the cells are cultured in cardiosphere-growth medium comprising buffered media, amino acids, nutrients, serum or serum replacement, growth factors including but not limited to EGF and bFGF,

cytokines including but not limited to cardiotrophin, and other cardiosphere promoting factors such as but not limited to thrombin. Cardiosphere-forming cells can be plated at an appropriate density necessary for cardiosphere formation, such as about 20,000-100,000 cells/mL. The cells can be cultured on sterile dishes coated with poly-D-lysine, or other natural or synthetic molecules that hinder the cells from attaching to the surface of the dish. Cardiospheres can appear spontaneously about 2-7 days or more after cardiosphere-forming cells are plated.

Cardiosphere-derived cells (CDCs)

[0276] In some embodiments, CDCs include a population of cells generated by manipulating cardiospheres in the manner as described in, *e.g.*, U.S. Patent Application Publication No. 2012/0315252, the disclosures of which are herein incorporated by reference in their entirety. For example, CDCs can be generated by plating cardiospheres on a solid surface which is coated with a substance which encourages adherence of cells to a solid surface of a culture vessel, *e.g.*, fibronectin, a hydrogel, a polymer, laminin, serum, collagen, or gelatin, and expanding same as an adherent monolayer culture. CDCs can be repeatedly passaged, *e.g.*, passaged two times or more, according to standard cell culturing methods.

Extracellular vesicles (EVs)

[0277] In some embodiments, EVs, including exosomes and microvesicles, include vesicles formed via a specific intracellular pathway involving multivesicular bodies or endosomal-related regions of the plasma membrane of a cell. EVs can range in size, for example, from approximately 20-150 nm in diameter. In some cases, they have a characteristic buoyant density of approximately 1.1-1.2 g/mL, and a characteristic lipid composition. Their lipid membrane may be rich in cholesterol and contain sphingomyelin, ceramide, lipid rafts and exposed phosphatidylserine. EVs express certain marker proteins, such as integrins and cell adhesion molecules, but generally lack markers of lysosomes, mitochondria, or caveolae. In some embodiments, the EVs contain cell-derived components, such as but not limited to, proteins, DNA and RNA (*e.g.*, microRNA and noncoding RNA). In some embodiments, EVs can be obtained from cells obtained from a source that is allogeneic, autologous, xenogeneic, or syngeneic with respect to the recipient of the exosomes.

[0278] In some embodiments, certain types of RNA, *e.g.*, microRNA (miRNA), are carried by EVs. miRNAs function as post-transcriptional regulators, often through binding to

complementary sequences on target messenger RNA transcripts (mRNAs), thereby resulting in translational repression, target mRNA degradation and/or gene silencing. For example, as described in WO 2014/028493, miR146a exhibits over a 250-fold increased expression in CDCs, and miR210 is upregulated approximately 30-fold, as compared to the EVs isolated from normal human dermal fibroblasts.

[0279] Examples of EVs derived from cardiospheres and CDCs are described in, *e.g.*, WO 2014/028493, the disclosures of which are herein incorporated by reference in their entirety. Methods for preparing EVs can include the steps of: culturing cardiospheres or CDCs in conditioned media, isolating the cells from the conditioned media, purifying the EVs by, *e.g.*, sequential centrifugation, and optionally, clarifying the EVs on a density gradient, *e.g.*, sucrose density gradient. In some instances, the isolated and purified EVs are essentially free of non-exosome components, such as components of cardiospheres or CDCs. EVs can be resuspended in a buffer such as a sterile PBS buffer containing 0.01-1% human serum albumin. The EVs may be frozen and stored for future use.

Example 31: Mouse CDC preparation

[0280] Some embodiments of the compositions and methods provided herein include CDCs prepared from a mammal such as a mouse or a human. In examples where mouse CDCs were used, mouse CDCs were expanded from wild-type strain-matched mouse hearts (C57BL/10ScSnJ wild type mouse heart) as described in, e.g., Smith, R. R. et al., Regenerative potential of cardiosphere-derived cells expanded from percutaneous endomyocardial biopsy specimens, *Circulation* 115, 896-908 (2007). Briefly, ventricular tissues were minced into ~1 mm explants, partially digested enzymatically and plated on adherent (fibronectin-coated) culture dishes. These explants spontaneously yielded outgrowth cells (explant-derived cells) which were harvested once confluent and plated in suspension culture (10^5 cells/mL on poly-D-lysine-coated dishes) to enable self-assembly of three-dimensional cardiospheres. Subsequent replating of cardiospheres on adherent culture dishes yielded CDCs which were used at passage 3, 4 or 5.

Example 32: Exercise capacity of *mdx* mice

[0281] As shown in Fig. 47, before treatment, a baseline measure of left ventricular ejection fraction in 8-10 month old *mdx* mice was obtained by echocardiography, and exercise

capacity was measured using treadmill exercise. CDC treatment or vehicle control was given at *t*=0 weeks. The CDC treatment included one of three doses of CDCs: 75,000 cells (injected intravenously into the jugular vein), 150,000 cells (injected intravenously into the jugular vein unless otherwise indicated), or 250,000 cells (injected intravenously into the femoral vein). The vehicle control included PBS (injected intravenously into the jugular vein). Left ventricular ejection fraction was measured 3 weeks after treatment. Exercise capacity was measured every week for 6 weeks following treatment. At the study conclusion, mice were sacrificed, isolated muscle function was measured on each mouse's soleus and diaphragm, and heart tissue was analyzed by Masson's trichrome staining to measure collagen deposition. The experimental protocol shown in Fig. 47 was used to generate the data in Figs. 48A, 48B, 49, and 50A-54, and described in Examples 32A-36B.

[0282] In one experiment, *mdx* mice received CDCs intravenously into either the jugular veins or femoral vein, to determine whether the route of administration had an effect on exercise capacity. Mice were treated with 150,000 CDCs in either the jugular (n=4) or femoral (n=4) vein, or received PBS vehicle without CDCs (n=10), at 0 weeks. Exercise capacity was assessed weekly, and is shown in Fig. 48A. Exercise capacity was assessed with an Exer-3/6 open treadmill (Columbus Instruments, Columbus, OH). For each mouse, after an acclimation period (10 m/min for 20 min), stepwise increases in average speed (2 m/min) were applied every two minutes during treadmill exercise until the mouse became exhausted (spending >10 seconds on a shocker; continuous nudging was used during treadmill to help mice stay on the track). Subsequently, the mouse was returned to its cage and the total distance traveled on the treadmill was recorded. Both treatment routes (jugular and femoral) resulted in similar increases in exercise capacity during the 6-week study period. * = $p<0.05$ versus control. Thus, in some embodiments, CDC treatment by systemic administration improves exercise capacity in a subject with a muscular dystrophy, such as DMD or Becker muscular dystrophy, involving dystrophinopathy of a skeletal muscle. A therapeutically effective administration includes intravenous injection into a blood vessel or vein such as the jugular vein or femoral vein.

[0283] A set of experiments was performed to determine effects of various CDC doses on exercise capacity, muscle function, body weight, and cardiac fibrosis, structure, and function (described in Examples 32-36B). Mice were treated with IV administration of 75,000 CDCs (n=8), 150,000 (n=8) CDCs, or 250,000 CDCs (n=4), or PBS vehicle (n=12), at 0 weeks and exercise

capacity was assessed weekly with Exer-3/6 open treadmill. For each mouse, after an acclimation period (10 m/min for 20 min), stepwise increases in average speed (2 m/min) were applied every two minutes during treadmill exercise until the mouse became exhausted (spending >10 seconds on shocker; continuous nudging was used during treadmill to help mice stay on the track). Subsequently, the mouse was returned to the cage and the total distance traveled by the mouse was recorded. The results are shown graphically in Fig. 48B. After an initial increase in exercise capacity 1-3 weeks after treatment, the exercise capacity of mice treated with 75K CDCs returned to that of PBS-treated mice. Mice treated with 150K and 250K CDCs showed increased exercise capacity over the course of the 6 week study compared to mice treated with 75K or PBS, indicating a dose response. * = $p<0.05$ versus control. All of these results indicate that in some embodiments, doses of about 75,000, 100,000, 125,000, 150,000, 200,000 250,000 CDCs, or more, such as about 500,000 or 1 x 10^6 CDCs, are therapeutically effective for improving exercise capacity in a subject with muscular dystrophy, such as DMD or Becker muscular dystrophy, involving dystrophinopathy of a skeletal muscle. These results also indicate that in some embodiments, ranges including and/or spanning the aforementioned numbers of CDCs, are therapeutically effective for improving exercise capacity in a subject with muscular dystrophy, such as DMD or Becker muscular dystrophy, involving dystrophinopathy of a skeletal muscle. These results also indicate that in some embodiments, a dose of about 150,000, 200,000 250,000, 500,000, or 1 x 10^6 CDCs, or more CDCs may be even more effective than a dose of 75,000 CDCs. Thus, in some embodiments, systemic administration of about 75,000 to about 250,000 CDCs, or of about 150,000 to about 250,000 CDCs may be used to improve a subject's exercise capacity, including running capacity.

[0284] The therapeutically effective doses exemplified here and in the other examples may be increased or adjusted in accordance with the size and/or body weight of the subject to be treated. For example, where a dose of about 75,000 to about 250,000 CDCs is therapeutically effective for a mouse, a therapeutically effective dose for a human may also be about 75,000 to about 250,000 CDCs, but may also be adjusted in accordance with the body weight of an average human to include a dose such as about 1.86 x 10^8 to about 6.2 x 10^8 CDCs (to adjust from a typical mouse weight of 25 g to an average human body weight of 62 kg).

Example 33: *In vitro* isolated muscle function

[0285] Effects on muscle function of various doses of CDCs administered systemically were also determined. The same mice that were used to generate the data shown in Fig. 48B were deeply anesthetized with ketamine/xylazine (80 mg/kg and 10 mg/kg body weight IP). For each mouse, the diaphragm muscle was rapidly excised, and the animal was euthanized. Following a left costal margin skin and muscle incision, a section of the midcostal hemidiaphragm was transferred to a preparatory Sylgar lined dish containing cold Ringer's and a narrow 3-4 mm wide strip of diaphragm was isolated maintaining fiber attachments to the rib and central tendon intact which were tightened with a silk suture and mounted vertically in the tissue bath. One end of the diaphragm was secured to a clamp at the bottom of the dish and one end was attached to a calibrated force transducer (Cambridge Technology Model 300B, Watertown, MA). A micromanipulator linked to the system was used to adjust muscle length. Platinum plate electrodes placed on each side of the muscle were used for direct muscle stimulation (Grass Model S88 stimulator; Quincy, MA) using 0.2 msec duration monophasic rectangular pulses of constant current delivered at supramaximal intensity. Muscle length was adjusted until maximum isometric twitch force response measurements were obtained. Isometric contractile properties were determined at optimal length (Lo). Peak twitch force (Pt) was determined from a series of single pulses. Force/frequency relationships were measured at stimulus frequencies ranging from 5-150 pulses per second (pps). The stimuli were presented in trains of 1 sec duration with an interval of at least 1 min intervening between each stimulus train. Muscle forces generated, including Pt and maximum tetanic force (Po), were normalized for the estimated physiological cross-sectional areas (CSA) of the muscle segment (CSA = muscle weight/1.056 x Lo; where 1.056 g/cm^3 represents the density of muscle) and expressed in Newtons (N)/cm^2. As shown in Fig. 49, diaphragm muscle function tended to be increased in mice treated with 75K (n=8), 150K (n=8) compared to PBS vehicle (n=6). 250K (n=4) CDCs had a higher impact on diaphragm muscle function compared to 150K CDCs and 75K CDCs, indicating a dose response. The data for the 250K dose was statistically significant versus the PBS control treatment ($p<0.05$). Thus, in some embodiments, systemic administration of CDCs improves muscle function, including skeletal muscle function, in a subject with muscular dystrophy, such as DMD or Becker muscular dystrophy, involving dystrophinopathy of a skeletal muscle. Therapeutically effective doses for improving muscle

function include but are not limited to about 75,000 to about 250,000 CDCs, about 150,000 to about 250,000 CDCs, or about 250,000 or more CDCs.

Example 34: *Mdx* mouse body weight

[0286] Mice treated with CDCs were weighed weekly immediately after exercise to determine whether CDC treatment had any effect on body mass. Body weight data are shown in Figs. 50A-50B. No difference in body weight was observed between groups. Thus, in some embodiments, a therapeutically effective dose of CDCs may be systemically administered without affecting a subject's body mass or weight.

Example 35: Masson's trichrome stain of mdx mouse hearts from PBS or CDC-treated mice

[0287] As described in Example 31, mice treated with CDCs were sacrificed 6 weeks after treatment. Paraffin-embedded sections of each heart were used for histology to identify the effect of CDC treatment on cardiac fibrosis. Masson's trichrome staining (HT15 Trichrome Stain [Masson] Kit; Sigma-Aldrich, St. Louis, MO) was performed for evaluation of fibrosis. As shown in Fig. 51, left ventricular heart tissue from PBS-treated mice exhibited more fibrosis and collagen deposition compared to mice treated with 150K CDCs as shown by the decrease in blue in the CDC-treated mouse heart sections. Thus, in some embodiments, systemically administering CDCs decreases or prevents fibrosis, including cardiac or left ventricular fibrosis in a subject with muscular dystrophy, such as DMD or Becker muscular dystrophy, involving dystrophinopathy of a skeletal muscle. A therapeutically effective dose for decreasing or preventing cardiac fibrosis includes at least 150,000 CDCs.

[0288] The histology slides used to generate the images in Fig. 51 were recut and restained with Masson's trichrome. Whole-heart sections of the recut and restained slides are shown in Fig. 53. Similar results were seen in the whole-heart sections shown in Fig. 53 as for the images shown in Fig. 51. Accordingly, in some embodiments, systemic administration of CDCs prevents or decreases fibrosis throughout the whole heart. Therapeutically effective doses for preventing or decreasing fibrosis throughout the whole heart include about 75,000 to about 250,000 CDCs, about 150,000 to about 250,000 CDCs, or about 250,000 CDCs. Additionally, no adverse effects on overall cardiac structure were seen in the hearts of mice treated with CDCs. Accordingly, in some embodiments, a therapeutically effective amount of CDCs does not adversely affect a subject's cardiac structure.

Example 36: Change in ejection fraction of *mdx* mice from baseline to 3 weeks after injection

[0289] As shown in Fig. 52A (and also Fig. 47), echocardiographic studies were performed 1-3 days before treatment and 3 weeks after treatment using the Vevo 3100 Imaging System (VisualSonics, Toronto, Canada) to determine effects of CDCs on cardiac function. After induction of light general anesthesia, the heart was imaged at the level of the greatest left ventricular (LV) diameter. LV ejection fraction (EF) was measured with VisualSonics version 3.0.0 software from 2-dimensional long-axis views. Treatment with 150,000 CDCs did not decrease the ejection fraction (Fig. 52B). Therefore, in some embodiments, a therapeutically effective dose of CDCs may be administered to a subject with muscular dystrophy, such as DMD or Becker muscular dystrophy, involving dystrophinopathy of a skeletal muscle, without adversely affecting the subject's heart function.

Example 37: Change in ejection fraction of SCID mice with permanent LAD ligation

[0290] To determine whether various routes of administration could beneficially affect heart function, human CDCs were administered to SCID mice by three separate administration routes: intramuscular (IM), femoral vein, or right ventricle. Administration by all three routes resulted in a positive change in left ventricular ejection fraction (Fig. 54). The change was statistically significant in all three groups compared to mice that received a control treatment. Intramuscular and IV administration routes were equally effective, indicating efficacy with IV administration. Accordingly, in some embodiments, treatment with human CDC improves cardiac function in a subject with SCID. A therapeutically route of administration includes intramuscular injection, systemic intravenous injection into the femoral vein, or cardiac injection such as right ventricular injection.

Example 38: Biodistribution of CDCs after jugular vein administration in wild type mice evaluated using human Alu sequence qPCR method

[0291] One purpose of the study in this example was to determine the biodistribution of CDCs after systemic delivery. Human CDCs were administered systemically to wild-type mice via intravenous injection into the jugular vein. Making the biodistribution determination included measuring the abundance of DNA containing the human Alu sequence, a transposable element abundant in most human DNA and generally absent from mouse DNA. The abundance of DNA

containing the human Alu sequence was determined using qPCR on tissues collected 10 minutes and 24 hours after CDC administration.

CDC preparation

[0292] Human CDCs were obtained in a manner similar to mouse CDCs as described hereinabove. After a flask was rinsed with volume of culture medium equal to the amount of culture medium in a cell solution, the cell solution was centrifuged at 1000 rpm (197 x g) for 5 minutes to pellet cells in the cell solution. CDCs were resuspended in Iscove's Modified Dulbecco's Media (IMDM) with no phenol red and no additional supplementation, then counted using a iNCYTO C-chip disposable hemocytometer. CDCs were diluted to 1.5 x 10^6 cells/mL in IMDM with no phenol red and no additional supplementation. CDCs were kept on ice prior to injection, or the cell pellet was frozen at -20°C for tissue spiking studies.

qPCR method validation

[0293] Genomic DNA was isolated from 1 x 10^6 CDCs at passage 5 using a DNeasy Blood and Tissue Kit (Qiagen). Ten-fold serial dilutions of the CDC DNA were prepared in sterile water and qPCR was performed using Taqman Fast Advanced Master Mix (ThermoFisher) with custom Alu primers and a custom Alu probe (from ThermoFisher). The DNA sequences of the probe and primers are as follows:

[0294] Forward: 5′-GTCAGGAGATCGAGACCATCCT-3′,

[0295] Reverse: 5′-AGTGGCGCAATCTCGGC-3′,

[0296] Probe: 5′-6-FAM-AGCTACTCGGGAGGCTGAGGCAGGA-MGB-3′

[0297] The qPCR reactions were performed in a on a QuantStudio 6 Flex Real-Time PCR (RT-PCR) system (ThermoFisher). Ct values were plotted versus the log of the number of CDCs in each qPCR sample. Linear regression analysis was performed using GraphPad Prism 5 and the slope of the line was used to calculate the efficiency of the qPCR using the equation: % efficiency = $-1+10^{(-1/\text{slope})}$ x 100.

Tissue spiking curves

[0298] Dilutions of DNA isolated from human CDCs were spiked into DNA isolated from naïve 8-12 week old C57BL/6J mouse tissue. qPCR was run in triplicate on a QuantStudio 6 Flex RT-PCR system with 1 μL spiked DNA. The qPCR reactions included Taqman Fast Advanced Master Mix and the same primers/probe as described above under "qPCR method validation" for the Alu sequence, and a mouse β-actin (ThermoFisher, Mm00607939_s1) Taqman

primer was used as a housekeeping gene for normalizing Ct values. ΔCt was calculated by subtracting the Ct value for β-actin from the Ct value for Alu from each sample. ΔCt was plotted against the known number of cells in the 1 μL qPCR sample. Linear regression analysis was done using GraphPad Prism 5.

Mouse injection and tissue harvest

[0299] C57BL/6J mice (8-12 weeks old, Jackson Laboratory) were injected with 100 μL human CDCs in IMDM (1.5 x 10^6 cells/mL) in the jugular vein under anesthesia with inhaled isofluorane. This dose of CDCs utilized had been effective for *mdx* mice when administered by jugular vein injection. After 10 minutes (n=8) or 24 hours (n=8), mice were sacrificed by cervical dislocation. Blood was collected from the submandibular vein, followed by removal of the heart, lungs, spleen, liver, diaphragm, and soleus muscle. Tissues were also collected from two control mice that did not undergo cell injection. Tissues were washed in PBS before being frozen at -80°C. EDTA was added to blood as an anticoagulant at a final concentration of 0.05 M prior to freezing at -80°C.

Alu and β-actin qPCR

[0300] Tissue samples were thawed, weighed, and cut into small pieces for homogenization. Average tissue weights, amounts of tissue used for homogenization, and amounts of tissue used for DNA isolation are listed in Table 1. DNA was isolated using a DNeasy Blood and Tissue Kit (Qiagen), per the instructions from the DNeasy Kit manufacturer. DNA was eluted from the DNeasy column with 100 μL elution buffer. qPCR was performed as described above for tissue spiking curves.

Data analysis

ΔCt was calculated by subtracting the Ct value of β-actin from the Ct value of Alu for each sample. The slope and y-intercept from a standard curve were used to calculate the log of the number of cells in the qPCR sample. The number of cells per gram of tissue was calculated by multiplying the number of cells in the qPCR sample by a factor specific to the tissue, accounting for the amount of tissue used for the DNA isolation and the final volume of eluted DNA (Table 1). Triplicates were averaged and cells per gram of tissue were graphed for each organ at each time point. Significance was determined using a 1-tailed student's T-test with $p \leq 0.05$.

[0301] Referring to Table 1, the weight of each tissue was measured and the average was taken to approximate tissue weight. In most cases, the whole tissue was homogenized, except

for the liver which was larger than the other tissues. From the homogenized tissue, an equivalent of 10-25 mg was taken for DNA isolation. The factor used to calculate CDCs per gram of tissue is based on 1 µL used for qPCR out of 100 µL purified DNA and the amount of tissue used for DNA isolation.

Table 1: Tissue weights and DNA isolation information

Tissue	Approximate tissue weight (mg)	Amount homogenized	Amount used for DNA isolation (mg)	Factor to calculate CDCs per g tissue
Lung	175	whole tissue	25	4000
Liver	1300	250 mg	25	4000
Heart	130	whole tissue	25	4000
Soleus	10	whole tissue	whole tissue	10000
Diaphragm	40	whole tissue	25	4000
Spleen	80	whole tissue	15	6666

qPCR method validation

[0302] To validate the qPCR primers and assess the linear range of the assay, human CDC DNA was isolated from a known number of cells. Serial dilutions were prepared and qPCR was performed using the Alu primer. As shown in Fig. 55A, this assay is linear in the range of 0.0025 to 2500 cells per qPCR sample, which can encompass all study samples and can detect DNA from less than 1 cell.

Tissue spiking curves - results

[0303] Spiking studies were done in each tissue of interest to remove any tissue-specific variability due to β-actin levels in each tissue. As shown in Fig. 55B, standard curves were prepared in the lungs, liver, heart, spleen, diaphragm, blood, and soleus muscle, by spiking a known amount of CDC DNA into naïve tissue DNA, and Table 2 summarizes the slope, intercept, and R^2 for each line. These standard curves were used to calculate the amount of CDC DNA in the qPCR of study samples.

Table 2: Summary of tissue spiking curves

Tissue	Slope	Intercept	R^2
Lung	-3.72	1.36	0.9932
Liver	-3.471	1.02	0.9982
Blood	-3.601	-3.011	0.9979
Heart	-3.662	-0.5318	0.997
Soleus	-3.582	-0.1151	0.9958
Diaphragm	-3.574	0.4034	0.9977
Spleen	-3.588	3.678	0.9975

CDC biodistribution in WT mice 10 minutes and 24 hours after jugular vein administration

[0304] C57BL/6J mice were injected with 150,000 human CDCs by jugular vein administration. At 10 minutes (n=8) or 24 hours (n=8) after injection, each mouse was euthanized, and tissues were removed (Fig. 56A). Tissues were homogenized, DNA was isolated, and qPCR was performed using the Alu sequence and mouse β-actin primers described above.

[0305] As shown in Fig. 56B, the majority of human CDCs were found in the lungs (155,000 ± 12,500 cells/g tissue in 10 minutes). Less than 1% of infused CDCS were found distributed among all other tissues, with 120 ± 47 CDCs/g tissue in the liver 10 minutes after CDC infusion. Blood, heart, and soleus muscle also contained CDCS above background levels (67 ± 15, 19 ± 4, 14 ± 2 cells/g tissue, respectively), but were not as high as in the lungs. 24 hours after administration, ~23% of the CDCs in the lung remained (36,000 ± 7,900 cells/g tissue). Low levels of CDCs remained in the liver, blood, heart, spleen, and soleus (31 ± 4, 15 ± 6, 11 ± 4, 17 ± 5, and 23 ± 11 cells/g tissue, respectively). Rapid clearance of cells may be due in part to immune system clearance by WT mice, but more studies would be needed to confirm this hypothesis.

[0306] After jugular vein administration, human CDCs were rapidly trapped in mouse lungs with less than 1% of injected cells remaining in the rest of the tested tissues. CDCs were cleared rapidly with only ~22-26% of the cells in the lungs, liver or blood at 10 minutes remaining after 24 hours. A lower CDC clearance ratio was observed in the heart (58% of the cells found 10 minutes after administration remain 24 hours later) and in the soleus. In fact, more cells per gram of tissue were found in the soleus 24 hours after cell delivery than after 10 minutes. These results indicate that in some embodiments, even though systemic administration of CDCs leads to the majority of the CDCs entering the lungs, some CDCs do arrive at the heart and skeletal muscles such as the soleus and diaphragm. Therefore, in some embodiments, at least some therapeutic

effects on the heart and skeletal muscle of systemic CDC administration may be due to direct effects on the heart and skeletal muscle within those tissues.

Example 39: Biodistribution and clearance of CDCs after jugular vein administration in SCID mice evaluated using human Alu sequence qPCR method

[0307] One purpose of the study in this example was to determine the biodistribution and clearance of CDCs in severe combined immunodeficiency (SCID) mice after systemic delivery to the jugular vein. The biodistribution of human CDCs was determined by measuring the human Alu sequence. Biodistribution and clearance of CDCs were determined using qPCR on tissues collected 24 hours, 1 week, and 3 weeks after jugular vein administration in the SCID mice (Fig. 57A). SCID mice were chosen for this study because their compromised immune system would limit immune reaction against human CDCs, so longer time points could be studied if an immune response would otherwise have cleared the CDCs from the body sooner.

[0308] The methods relating to CDC preparation, qPCR method validation, and tissue spiking curves for this study were performed in the same manner as described in Example 39.

Mouse injection and tissue harvest

[0309] Male 8-12-week-old SCID mice (Jackson Laboratory) were injected with 100 μL CDCs in IMDM (1.5 x 10^6 cells/mL) into the jugular vein under anesthesia with inhaled isofluorane. After 24 hours (n=4), 1 week (n=8), or 3 weeks (n=8), blood was collected from the submandibular vein, followed by removal of the heart, lungs, spleen, liver, diaphragm, soleus muscle, and testes. Tissues were also collected from two control mice that did not undergo cell injection. Tissues were washed in PBS before freezing at -80°C. EDTA was added to blood as an anticoagulant to a final concentration of 0.05 M prior to freezing at -80°C.

[0310] The methods relating to Alu and β-actin qPCR and data analysis for this study were performed in the same manner as described in Example 38, Figs. 55A-55B, and Table 2. Table 3 is the same as Table 1, except that data relating to testes is included in Table 3 but not Table 1.

Table 3: Tissue weights and DNA isolation information

Tissue	Approximate tissue weight (mg)	Amount homogenized	Amount used for DNA isolation (mg)	Factor to calculate CDCs per g tissue
Lung	175	whole tissue	25	4000
Liver	1300	250 mg	25	4000
Heart	130	whole tissue	25	4000
Soleus	10	whole tissue	whole tissue	10000
Diaphragm	40	whole tissue	25	4000
Spleen	80	whole tissue	15	6666
Testes	190	whole tissue	25	4000

CDC biodistribution in SCID mice 24 hours, 1 week, and 3 weeks after jugular vein administration

[0311] As described above, SCID mice were injected with 150,000 human CDCs by jugular vein administration. 24 hours (n=4), 1 week (n=8), and 3 weeks (n=8) after injection, mice were sacrificed and their tissues were removed. Tissues were homogenized, DNA was isolated, and qPCR was performed using primers for the Alu sequence and mouse β-actin described in Example 38.

[0312] As shown in Figs. 57B and 57C, the majority of CDCs were found in the lungs (217,000 ± 71,000 CDCs/g tissue in 24 hours). Less than 1% of infused CDCs were found distributed among all other tissues. Liver and blood contained CDCs above background (50 ± 15, 39 ± 8 cells/g tissue, respectively) 24 hours after CDCs administration. 4% of the CDCs found in the lungs at 24 hours remained (8,600 ± 1900 cells/g tissue) 1 week after administration. Interestingly, more CDCs tended to be found in the heart (7,700 ± 5,000 at 1 week vs. 110 ± 58 at 24 hours), diaphragm (107 ± 82 vs. 42 ± 18), and spleen (170 ± 80 vs. 107 ± 37) 1 week after administration than were found in those tissues 24 hours after administration. The increase in CDCs found in those tissues 1 week after administration suggests that in some embodiments, cells are freed from the lungs to redistribute to other tissues, and become notably lodged in the heart, the first organ that would be encountered after exiting the lung via the pulmonary vein. None of the tissues tested had a statistically significant number of cells present 3 weeks after CDC administration compared to vehicle, suggesting most CDCs are cleared within 3 weeks after delivery.

[0313] This study confirms the findings of the biodistribution study performed in WT mice (see Example 38), wherein CDCs were trapped in the lungs and relatively few CDCs distributed to other tissues. Compared to 24 hours post administration in WT mice, SCID mice do not clear CDCs as rapidly (36,000 ± 7,900 cells/g tissue in WT mice vs. 218,000 ± 71,000 in SCID mice present at 24 hours), likely due to the immunocompromised nature of SCID mice.

[0314] This study shows that CDCs are trapped in the lungs 24 hours after cell administration by the jugular vein. A similar CDC biodistribution was observed in immunodeficient SCID mice and in WT C57BL/6 mice at 24 hours, suggesting that although the immune system could be responsible for the faster clearance observed in immune-competent mice, it does not have a significant impact on cell distribution.

[0315] Around 4% of the CDCs found in the lungs 24 hours after jugular vein administration, remained 1 week later. This study shows a possible redistribution within 1 week after cell delivery with more cells found in the heart, spleen, and diaphragm at 1 week versus 24 hours. Thus, the results indicate that in some embodiments, even though systemic administration of CDCs leads to a portion of the CDCs entering the lungs, according to several embodiments, some CDCs arrive at the heart and skeletal muscles (by way of non-limiting example, the soleus and diaphragm). Therefore, in some embodiments, at least some therapeutic effects on the heart and skeletal muscle of systemic CDC administration may be due to effects on the heart and skeletal muscle due to CDCs that are localized within those tissues.

Example 40: Dose-dependent safety and efficacy of CDCs in an acute myocardial infarction (AMI) porcine model using intravenous administration

[0316] The purpose of this study was to investigate a maximum tolerable dose (MTD) for CDCs and a dose efficacy response of CDCs. In this non-limiting example, intravenous administration was used in an AMI pig model, which is a widely used model for AMI.

[0317] ***CDC preparation***

[0318] Sinclair mini pig CDCs (pCDCs) were produced and formulated in a manner similar to mouse CDCs and human CDCs (hCDCs) as described hereinabove. Pig hearts were harvested and dissected. Pieces of both the atria and the septum were isolated and minced into explant pieces. These explants were plated on cell bind 1-stacks with 20% growth media. After 3-4 days, explant-derived cells (EDCs) began to grow around each explant. EDCs were harvested

and frozen in CS10 in 2mL cryovials until ready to be used. The EDCs were thawed at 37°C until only a small amount of ice remained in the vial. The cell solution was added dropwise to a small volume of 20% media (~10mLs). The cells were centrifuged at ~280G for 5 minutes to remove any residual CS10. The cells were resuspended, counted, and plated on fibronectin-coated Nunc triple flasks at approximately 3-6 x 10^6 cells per flask. pCDCs were grown in 20% media supplemented with hyclone serum up to P5 and P6. Cells were lifted and frozen in CryoStor CS10. Frozen cells were thawed at 37°C until only a small amount of ice remained in the vial. The cells were resuspended in the following administration buffer:

- CryoStor®CS10 (22.5 mL), heparin (2.5 mL), nitroglycerin (250 µL); and
- 5% human serum albumin (103 mL), HypoThermosol® (13.5 mL), CS10 (13.5 mL) (This concentration is proportional to the human equivalent dose. The volume was changed after an optimal volume of 130 mL was determined for IV infusion.).

[0319] Cells were administered over 45 minutes for most doses to keep cell concentrations relatively consistent. Cells delivered in a volume of 130 mL were also delivered over 45 minutes.

Animal model

[0320] Myocardial infarction was induced in Yucatan mini pigs by a 90 minute occlusion of the left anterior descending (LAD) artery using an angioplasty balloon, followed by 30 minutes of reperfusion as previously described (Kanazawa, Tseliou et al. 2015). Animals then underwent a baseline left ventriculogram (LV gram) to assess changes in cardiac function (as indicated by change in ejection fraction), and were then infused with vehicle (CryoStor®CS10, n=10) or allogeneic CDCs (n=18). Three CDC doses were administered sequentially: 50 x 10^6 (n=8), 100 x 10^6 (n=3), and 200 x 10^6 (n=3). Infusions took place using a Swan-Ganz catheter (6-8 French) placed in the right ventricular outflow tract (RVOT). An additional group (n=4) animals were injected with 200 x 10^6 CDCs using femoral vein infusion. Two days after infusion, animals underwent a follow-up LV gram. Troponin I (TnI) levels were assessed by chemiluminescence with an Abbot Architect i2000SR, at baseline and 48 hours to identify any myocardial tissue damage. Briefly, the blood samples were spun down to collect plasma, and once the plasma was collected, it was analyzed with the Abbot Architect i2000SR. Animals underwent physical exams 24 and 48 hours after administration. One animal was administered 200 x 10^6 CDCs via femoral

vein infusion and then followed up two weeks later. This animal was intended to show the long-term effects of CDCs.

Histopathology analysis

[0321] Heart and lung tissues were subjected to histology. Gentian Violet and Thioflavin T dyes were injected into the left atrium prior to animal sacrifice to assess area at risk (AAR) and microvascular obstruction (MVO) in the heart. Excised hearts were sliced and stained with triphenyl tetrazolium chloride (TTC) to measure infarct size (IS). Lungs from two pigs RVOT injected with vehicle or 200M CDCs were collected and infused with 4% paraformaldehyde. After 48 hours in 4% PFA, tissue samples were collected from the anterior and posterior areas, as illustrated in Fig. 58). Fifteen samples were collected from each lung, and paraffin embedded. 5 μm tissue slices on slides were stained with H&E.

Results

[0322] The first animal infused at the 50 x 10^6 dose was infused over the course of 15 minutes as opposed to the 45 minutes used for all subsequent animals. This pig experienced a persistent decrease in oxygen saturation during infusion (SpO_2 decreased from 100% to 76%). During a physical exam 24 hours post-infusion, thoracic auscultation revealed normal lung sounds. At the 48 hour endpoint, this animal continued to display a decreased SpO_2 from baseline (85%). As a result, the infusion time was increased to 45 minutes for all subsequent animals. One animal infused with the 100 x 10^6 dose displayed a transient decrease in SpO_2 (98% to 81%), which returned to baseline 20 minutes into the infusion. This animal was normal on a follow-up physical exam. One animal infused with the 200 x 10^6 dose displayed a slight transient decrease in SpO_2 (100% to 94%) but remained within the range of normal for SpO_2. Cardiac enzyme (i.e. TnI) increases were moderate and similar for vehicle and CDC treated animals. As shown in Fig. 59, TnI increases did not statistically correlate with CDC dose. Instead, there was a trend for CDC treatment to decrease TnI, indicating that in some embodiments, systemic CDC administration does not cause cardiac tissue damage, and may prevent or decrease cardiac tissue damage. As shown in Figs. 60-62, AAR, NR/AAR, and TTC/AAR were similar among groups. This provides further evidence that the degree of myocardial damage 48 hours post-infusion was not negatively impacted by CDC treatment in this study. As shown in Fig. 63, EF trended toward improvement when CDCs were administered at the 100 x 10^6 and 200 x 10^6 doses. However, femoral vein administration of 200 x 10^6 cells showed a decrease in EF. Overall, these results indicate that in

some embodiments, systemic administration of CDCs into, for example, the RVOT or femoral vein, does not cause cardiac tissue damage or dysfunction, and may prevent or decrease cardiac tissue damage or dysfunction.

[0323] Lungs from a pig injected with vehicle or 200 x 10^6 CDCs into the RVOT were collected 48 hours after the ischemia/reperfusion event and product administration, and fixed in paraformaldehyde for histological analysis. 32 samples were obtained, paraffin embedded, sliced and analyzed after H&E stain. Lung surfaces as well as section surfaces revealed lack of evident lesions. 68 slides from 2 pigs RVOT injected with vehicle or with 200 x 10^6 CDCs were analyzed by an independent pathologist. H&E slides analyzed from pig injected with vehicle or injected with CDCs, displayed normal lung structures without evident histological abnormalities. No CDCs were found in blood vesicles or other lung areas. Thus, in some embodiments, systemic administration of CDCs does not adversely affect lung tissue.

[0324] Of the different doses of cells administered, the minimum effective dose when CDCs were delivered through RVOT was 100 x 10^6, as a higher dose (200 x 10^6) did not add any apparent additional benefit. Both doses showed similar effects on ejection fraction of the AMI model. Scar size was similar across all conditions. However, pigs that were injected with 200 x 10^6 CDCs into the femoral vein showed a limited EF improvement. This suggests that in some embodiments, administration via different routes may have different efficacies.

[0325] Histological analysis of the lung samples showed no tissue damage in pigs with 200 x 10^6 cells administered via RVOT or using the femoral vein route. Administration of the cells via the RVOT is a more direct path from the heart to the lungs than, for example, the femoral vein, and administration of CDCs by that route would be expected in some embodiments to show a greater effect CDC administration by the femoral vein.

[0326] Results from this study illustrate that systemic administration of CDCs is reasonably safe (i.e., not generally associated with more than a few, mild, transient adverse events during infusion) up to a human equivalent dose of at least 400 x 10^6 (200 x 10^6 dose in pigs).

[0327] This study showed that by systemically delivering 100 x 10^6 cells shows an efficacious improvement in EF in an AMI porcine model. No significant differences in terms of efficacy were observed between pigs delivered with 100 x 10^6 or 200 x 10^6 cells. Accordingly, in some embodiments, a therapeutically effective dose includes 1 x 10^5, 1 x 10^6, 1 x 10^7, 1 x 10^8, 2 x

10^8, 5 x 10^8, 1 x 10^9, or 1 x 10^{10} CDCs, and prevents or decreases cardiac dysfunction, and tissue damage in the heart and/or lungs of a subject undergoing a cardiac injury.

[0328] The evidence in the studies in this example supports the conclusion that in some embodiments, a maximum effective dose may be between 100 x 10^6 and 200 x 10^6 CDCs (human equivalent does of between 200 x 10^6 and 400 x 10^6 CDCs). Further, administering these doses did not result in any toxicological effect on the lung tissue of the subjects to whom the doses were administered.

Example 41: CDC interaction with human T cells

[0329] One purpose of the study in this example was to determine the immunological activity of CDCs linked to human allogeneic T cells. The study was conducted with HLA-genotyped human peripheral blood mononuclear cells (PBMC) (n=3) and human $CD3^+$ T cells (n=2) isolated from PBMC. CDCs were prepared in a manner described above.

CDC immune phenotype

[0330] CDCs (10^5 cells) at steady state were stained with antibodies specific for immune relevant molecules or their respective isotype controls. Cells were acquired on a Canto II BD FACS and analyzed by FlowJo software. All of the cells expressed significant levels of HLA class I molecules but were negative for HLA II molecules (Fig. 64).

[0331] A modest percentage of cells displayed a dim expression of non-classical HLA I molecules HLA-E and HLA-G. A good proportion of cells expressed moderate levels of co-stimulatory CD86 and co-stimulatory/regulatory CD274 (PD-L1) molecules while few cells displayed dim expression of co-stimulatory CD80 and co-stimulatory/regulatory CD275 (ICOS-L) molecules. Nearly 65% of CDCs also showed considerable expression of NK cells activating receptor NKG2D ligands (ULBP and MIC-A/B). Thus, in some embodiments, at least some immune-stimulatory or immune-modulatory markers may be present in CDCs.

The capacity of CDCs to stimulate T cells in allogeneic setting

[0332] Tailored one-way mixed lymphocyte cultures was used to investigate the capacity of CDCs to stimulate allogeneic T cells. Briefly, human HLA-mismatched PBMC were prepared from blood samples of 3 different healthy donors by centrifugation on a Ficoll-Hypaque density gradient. Responding unfractionated PBMC ($1x10^5$) labeled with carboxyfluorescein succinimidyl ester (CFSE) (2.5μM for 10 minutes) were co-cultured in RPMI-10% FBS in U-

bottom 96-wells plates with either HLA-mismatched mitomycin-C-treated stimulatory PBMC ($1x10^5$) (AlloPBMC) used as positive-control or mitomycin-C-treated CDCs ($1x10^4$).

[0333] At the end of 5-days co-cultures, the expression of two T-cell activation markers, CD69 and HLA-DR, was monitored by staining with conjugated anti-CD3, anti-CD4, anti-CD8-APC, anti-CD69, anti-HLA-DR; T-cell proliferation by loss of CFSE labeling; and cell death by 7AAD staining. The results in Fig. 66 show slight staining in CDCs, but not as pronounced as for the AlloPBMC positive control. Accordingly, in some embodiments, CDCs may have a slight capacity to stimulate allogeneic T cells.

[0334] As seen in Fig. 66, both $CD4^+$ and $CD8^+$ T cells up-regulated, more or less, at least one of the two activation markers in response to allogeneic CDCs. The up-regulation of HLA-DR was more pronounced than CD69. Thus, in some embodiments, CDCs can activate T cells in unfractionated PBMC. However, compared to allogeneic PBMC-induced activation (positive control), the observed up-regulation of these markers is in general very weak albeit for expression of HLA-DR by Donor A.

[0335] It was then determined whether this activation would be able to result in T cell proliferation. By monitoring CFSE, it was observed that CDCs might be able to elicit a weak $CD4^+$ T cells proliferation, however in a donor dependent manner. The observed proliferation seems to be in line with expression of activation markers as shown in Fig. 66. For Fig. 67B, only T cells from unfractionated PBMC Donor A demonstrated significant expression of both CD69 and HLA-DR and were able to proliferate in response to CDC. T cells from unfractionated PBMC Donor C only showed significant expression of HLA-DR, whereas Donor D expressed neither CD69 nor HLA-DR, and both did not demonstrate any significant proliferation in response to CDCs. In contrast, CDCs did not elicit any substantial response in $CD8^+$ T cells, as shown in Figs. 67A-67B. Taken together, in some embodiments, CDCs seem to induce a weak response, much weaker than that observed with an allogeneic PMBC control, in $CD4^+$ T cells. While the response can vary to some degree among donors, as shown in Fig. 67C, according to some embodiments, systemic administration of a therapeutically effective amount of CDCs does not activate $CD4^+$ or $CD8^+$ T cells, or any significant immune response.

[0336] The CDC-induced activation and proliferation of purified $CD3^+$ T cells (Donor C and A) were evaluated using the same experimental settings described above. Briefly, responding allogeneic T ($1x10^5$) labeled with CFSE (2.5μM for 10 minutes) were co-cultured in

RPMI-10% FBS in U-bottom 96-wells plates with either HLA-mismatched mitomycin-C-treated stimulatory PBMC ($1x10^5$) (AlloPBMC) or CDC ($1x10^4$) and five days later, their activation (expression of CD69 and HLA-DR) and proliferation (CFSE loss) were monitored. $CD4^+$ and $CD8^+$ T cells from both donors up-regulated, more or less, the expression of HLA-DR activation marker rather than CD69. However, this activation did not result in any significant proliferation of either CD4 or CD8 T cells, as shown in Fig. 68. Thus, in some embodiments, the administration of CDCs results in a surprisingly weak or absent immune response, or does not activate an immune response, despite being re-exposed to allogeneic CDCs.

Immune-modulation by CDCs

[0337] The capacity of CDCs to modulate an ongoing immune response in an allogeneic setting was then investigated because a lack of activation of an immune response may indicate an improved safety profile with decreased side effects in response to CDC treatment. To this end, HLA-mismatched unfractionated CFSE-labeled PBMC ($1x10^5$) were stimulated with PHA (1 μg/ml) in the absence or presence of CDCs ($1x10^4$) to see whether the CDCs would enhance the PHA stimulation, in U-bottom 96 well plates and allogeneic T cell proliferation was evaluated by monitoring CFSE. CDC considerably down regulated PHA-induced proliferation of both $CD4^+$ and $CD8^+$ T cells, as shown in Fig. 69. These results indicate that in some embodiments, CDCs surprisingly decrease immune stimulation, and do not enhance it.

[0338] Therefore, similar experiments were conducted using purified $CD3^+$ T cells from two donors (Donor C and A). The modulation of PHA-induced CD69 and HLA-DR expression on these HLA-mismatched T cells, as well as the modulation of their PHA-induced proliferation, were evaluated.

[0339] While significantly down-regulating the PHA-induced CD69, CDCs significantly increased the expression of HLA-DR on both $CD4^+$ and $CD8^+$ T cells. This modulation of activation markers resulted in strong inhibition of both $CD4^+$ and $CD8^+$ T cell proliferation. The inhibition of $CD4^+$ T cell proliferation was more pronounced than that observed with $CD8^+$ T cells. Thus, despite the inter-donor variability and within the limit of results obtained with two donors only, CDCs appear to be potent immunomodulators. HLA-DR is a marker of effector regulatory T cells (Treg). Therefore the observed increase in HLA-DR expression might suggest an eventual expansion of regulatory T cells induced by the presence of CDC, which might explain the strong inhibition of observed on-going T cells proliferation. These results are in line

with the above data analyzing the induction of allogeneic T cells activation and proliferation by CDC, as shown in Fig. 70. Overall, these results indicate that in some embodiments, a therapeutically effective dose of allogeneic CDCs can surprisingly downregulate an immune response.

Example 42: CDC-derived extracellular vesicles (CDC-EVs) interaction with T cells

[0340] One purpose of the study in this example was to determine the immunological activity of CDC-EVs linked to T cells activation and regulation.

Characterization of CDC-EVs & immune phenotype

[0341] The expression of exosome informative markers was analyzed in CDC-EVs using western blotting. CDC-EVs (20µl = 10µg) were lysed using RIPA buffer and loaded in 10% SDS-Page gels, then transferred to nitrocellulose membrane. Membranes were blocked with 5% BSA, then hybridized with specific antibodies against HSP70, CD81, CD63, ALIX, HLA II and β-actin. CDCs and dendritic cells (DC) lysates as well as exosome-free supernatant (SN) were used as controls. CDC-EVs expressed expected exosome markers CD81, CD63 and ALIX, while SN was completely negative (Fig. 71).

[0342] CDC-EVs were next analyzed for the surface expression of immune relevant markers. CDC-EVs (30µl=15µg) were coupled to 5µl Latex beads (4µm). CDC-EVs/beads were treated successively with 100 mM glycine and 2% BSA buffers in order to block any eventual non-specific binding of these EVs/beads with antibodies or with beads. After washing, EVs/beads were stained with specific antibodies against relevant immune molecules acquired on Canto II BD Facs and analyzed by FlowJo software. Beads incubated with the same amount of respective antibodies were used as a control.

[0343] Compared to a bead-antibody control, CDC-EVs expressed HLA class I molecules and CD86, but were negative for HLA II and CD80 molecules (Fig. 72). CDC-EVs seem to express the co-stimulatory PD-L1 molecule but not the ICOS-L. NK activating receptor ligands were remarkably expressed on the CDC-EVs. Significant expression of both EV markers CD81 and CD63 was detected. Thus, in some embodiments, at least some immune-stimulatory or immune-modulatory markers may be present in CDC-EVs.

The capacity of CDCs and CDC-EVs to activate T cells in allogeneic setting

[0344] PBMC were prepared from blood samples of 3 different healthy donors by centrifugation on a Ficoll-Hypaque density gradient and cryopreserved for use in different experiments. T cell activation and proliferation in response to CDC and CDC-EVs were investigated by monitoring the expression of two T cells activation markers, CD69 and HLA-DR, and the level of CFSE by flow cytometry, respectively. Briefly, responding PBMC ($1x10^5$) labeled with CFSE (2.5μM for 10 minutes) were co-cultured in RPMI-10% FBS in U-bottom 96-wells plates with either HLA-mismatched mitomycin-C-treated stimulatory PBMC ($1x10^5$) or HLA-mismatched CDC ($1x10^4$) or with CDC-EVs at different doses as indicated, as shown in Fig. 73A. At the end of 5-days co-cultures staining with conjugated anti-CD3, anti-CD4, anti-CD8-APC, anti-CD69, anti-HLA-DR and 7AAD monitored the activation, proliferation, and cell death of T cells. The results show some staining in CDC-EVs, but not as much as for the AlloPBMC positive control. Accordingly, in some embodiments, CDC-EVs may be capable of stimulating allogeneic T cells.

[0345] As shown in Fig. 74, compared to control, CDCs and CDC-EVs seem to be able to elicit weak $CD4^+$ T cell proliferation but did not elicit any substantial response in $CD8^+$ T cells. The observed response was much weaker than that observed with allogeneic PMBC control.

[0346] Accordingly, the CDC- and CDC-EV-induced activation and proliferation of purified $CD3^+$ T cells (2 different donors) were evaluated using the same experimental settings described above. Briefly, responding allogeneic T ($1x10^5$) labeled with CFSE (2.5μM for 10 minutes) were co-cultured in RPMI-10% FBS in U-bottom 96-wells plates with either HLA-mismatched mitomycin-C-treated stimulatory PBMC ($1x10^5$) or CDCs ($1x10^4$) or with CDC-EVs at different doses as indicated. A weak activation and proliferation of $CD4^+$ T cells was only observed with CDC-EVs but not with CDCs, as shown in Fig. 75. However, the magnitude of both activation and proliferation compared to that obtained when unfractionated-PBMC were used was fairly lower. Thus, in some embodiments, the administration of CDCs and/or CDC-EVs results in a surprisingly weak or absent immune response, or does not activate an immune response.

[0347] Together these results also indicate that in some embodiments, the observed CDC-EV-induced activation and proliferation of T cells occurs mainly via an indirect pathway that may involve antigen presenting cells such as monocyte/macrophages and dendritic cells (DC).

Indirect T cells activation and proliferation in response to allogeneic EVs

[0348] Monocytes were isolated from blood samples obtained from two different healthy donors. Isolated-monocytes were then stimulated for 6 days with a combination of GM-CSF (20 ng/ml) and IL4 (20 ng/ml) to allow their differentiation to dendritic cells (DC). Differentiation of monocytes with GM-CSF+IL4 generates immature DCs (iDC) marked by moderate expression of HLA II, CD80, and CD86 molecules, absence of CD16 (marker of monocytes/macrophages), and low expression of TLR-2. These monocyte-derived iDC were then incubated overnight with HLA-mismatched CDC-EVs.

[0349] iDC cultured with EVs displayed features of mature DC (mDC); they up-regulated their HLA II, CD80 and CD86 molecules, which is recognized as mDC properties, as shown in Fig. 76. Then $1x10^4$ of iDCs or iDCs that were in contact with EVs (iDC-EVs) were co-cultured with autologous T cells ($1x10^5$) in U-bottom 96 wells plates for another 6 days. Autologous T cells co-cultured with iDC or iDC-EVs where analyzed for their expression of CD69 and HLA-DR, and for their proliferation. Although the response of T cells from two different donors was variable, as a whole iDC-EV were more potent in activating and inducing the proliferation of T cells than iDCs alone, as shown in Fig. 77. Compared to direct CDC-EV-induced T cell proliferation, the magnitude of indirect CDC-EV-induced T cells proliferation was fairly higher.

[0350] The capacity of CDC-EVs to stimulate T cells when presented by mature DC (mDC) was evaluated. Given that mDC have a very low phagocytic activity and to ensure appropriate uptake of EVs and based on previous experience of phagocytizing apoptotic bodies, the maturation of DC was induced by treating iDC and iDC-EVs overnight with IFNγ (500 IU/ml), which is a recognized inducer of DC maturation. Compared to iDC, these mDC showed higher expression of HLA II, CD80 and CD86, and higher expression of TLR-2, which are features of mDC. The presence of CDC-EVs during iDC maturation to mDC further up-regulated HLA II, CD86, CD80, and TLR-2 molecules, as shown in Fig. 78, indicating that CDC-EVs may enhance DC maturation.

[0351] mDC or mDC-EVs were then co-cultured with autologous T cells ($1x10^5$) fin U-bottom 96-wells plates or 6 days and their activation (expression of CD69 and HLA-DR), and proliferation was analyzed. Again the responses from two donors, were variable but as a whole mDC-EVs were more potent in activating and inducing the proliferation of T cells than mDCs

alone. Compared to iDC-EVs-induced response, mDC-EV-induced T cell activation and proliferation for the same donor was higher.

[0352] The ensemble of these results in regards to T cells activation and proliferation suggests that CDC-EVs can activate and induce the proliferation of T cells through the indirect pathway without ruling out at least some activation of the direct pathway. Thus, in several embodiments, an indirect pathway is activated. In other embodiments, the direct pathway is partially activated. In still additional embodiments, a combination of direct and indirect pathways is activated.

Immune-modulation by CDCs and CDC-EVs

[0353] Although CDCs or CDC-EVs may enhance DC maturation, this does not mean that they would necessarily results in an adverse reaction within a subject. To evaluate this, the capacity of CDCs and CDC-EVs to modulate an ongoing immune response in an allogeneic setting was investigated. HLA-mismatched unfractionated CFSE-labeled PBMC ($1x10^5$) were stimulated with PHA (1 μg/ml) in the absence or presence of CDCs ($1x10^4$) or various doses of CDC-EVs as shown in the upper panel of Fig. 80. The experiment was conducted in U-bottom 96 well plates, and allogeneic T cell proliferation was evaluated by monitoring CFSE. Both CDCs and CDC-EVs were able to down regulate PHA-induced $CD4^+$ and $CD8^+$ T cell proliferation. CDC-EVs-induced down regulation of T cells proliferation was dose dependent, and at the highest used dose ($20x10^9$ particles) CDC-EVs were more potent in down regulating ongoing response than their parental cells, as shown in Fig. 80.

[0354] The CDC- and CDC-EV-induced immune modulation is likely through direct effects since similar results were obtained when purified $CD3^+$ T cells were used instead of PBMC within the same experimental settings. Indeed, CDCs and CDC-EVs were able to down regulate PHA-induced expression of CDC69 and/or HLA-DR on T cells obtained from 2 different donors, as shown in Fig. 81.

[0355] As shown in Fig. 82, down-modulation of T cells activation markers by CDCs and CDC-EVs resulted in a pronounced down regulation of PHA-induced $CD4^+$ and $CD8^+$ T proliferation. Similarly, as shown in Fig. 83, despite inter-donor variability and within the limit of results obtained with two donors only, both CDCs and CDC-EVs are potent immune modulators.

[0356] These studies of capacity of CDC-EVs to induce immune-modulation demonstrated that they are potent immune-modulators. Accordingly, in some embodiments, the administration of CDCs and/or CDC-EVs surprisingly suppresses an immune response, overall.

Example 43: Additional improvement with multiple administrations of allogeneic CDCs compared with single administration

[0357] In some cases, because CDCs and CDC-EVs may suppress an immune response, they may be administered repeatedly to a subject without an immune response severely dampening their therapeutic effects or resulting in an inflammatory response. One purpose of the study in this example was to evaluate whether multiple systemic administrations of allogeneic CDCs could result in an additive or enhanced effect compared to a single dose. For example, multiple administrations may promote an additional improvement in muscle activity and exercise capabilities in subjects with muscular dystrophy, as is modeled in *mdx* mice. Thus, a goal was to analyze immune responses after multiple administrations of allogeneic CDCs.

[0358] Cells derived from heart explants were cultured in ultra-low adherent plates to obtain cardiospheres, and then seeded in fibronectin coated plates to produce CDCs. Aged *mdx* mice (8-10 months of age) were IV treated with three doses of CDCs, six weeks apart (systemic administrations via the jugular vein at weeks 0, 6 and 12), and their exercise capacity was analyzed weekly for 14 weeks. The dose used in this experiment was 150,000 syngeneic CDCs (n=8), 150,000 allogeneic CDCs (n=6), or PBS as a control (n=6). The presence or absence of allo-antibodies was also analyzed to determine the extent of immune activation that the CDCs may have caused.

[0359] The repeated systemic dosing of syngeneic or allogeneic CDCs resulted in an increase in exercise capability after each administration in *mdx* mice, as shown in Figs. 84A-84C. These results indicate that in some embodiments, a therapeutically effective dose delivered in multiple systemic administrations enhances the therapeutic benefit when compared to a single administration. Surprisingly, CDC administration resulted in a low immunogenic profile with weak production of allo-antibodies, indicating that in some embodiments, multiple administrations of syngeneic and/or allogeneic CDCs does not result in an immune response. In some embodiments, the enhanced benefit of multiple administrations compared to a single administration results from the low immunogenic profile and/or weak production of allo-

antibodies because the low immunogenic profile and weak production of allo-antibodies allows more CDCs to remain in the body, and/or allows the CDCs to remain in the body longer so the greater number or duration of CDCs can exert their beneficial effects to a greater extent. For example, a strong immune response might have otherwise prevented the second dose from enhancing the therapeutic effect because the immune response might have destroyed the CDCs in the second administration before they could exert their beneficial effects. In some embodiments, several systemic administrations of CDCs are given, where at least one of the additional administrations enhances the benefit of the first administration of CDCs.

[0360] In another example, multiple administrations of syngeneic and/or allogeneic CDCs exert a greater beneficial effect on the heart, such as reducing cardiac fibrosis, cardiac tissue damage and cardiac remodeling, and improving cardiac or ventricular function, compared to a single CDC administration, at least partially as a result of lack of or relatively weak immune response to the CDCs.

[0361] To further assess the interaction of an immune response with multiple CDC administrations, another experiment was included in which CDCs were administered with or without a corticosteroid to suppress the immune system and inflammation. 8-10-month-old *mdx* mice were given PBS vehicle (n=6), PBS vehicle + steroid (n=7), CDCs (n=7), or CDCs + steroid (n=8). The CDCs were administered at a dose of 150,000 CDCs per mouse per administration. Steroid (prednisone, 1 mg/kg/day) was given for 5 days during each week of CDC and/or PBS administration. The steroid, CDCs, and/or vehicle were administered twice, once at week 0, and the second time at week 6. Each administration included a systemic intravenous injection into the jugular vein. Steroid administration did not impact the CDCs efficacy, and a similar improvement in exercise capability was observed with or without steroids, as shown in Fig. 85A. Allo-antibodies against CDCs in blood were measured by flow cytometry. As shown in Figs. 85B and 85C, CDCs had a low immunogenic profile with and without steroids (see also Fig. 86). These results are in line with a lack of an immune response to systemic CDC administration because if an immune response prevented or decreased the therapeutic benefits of one or more CDC administrations, then the steroid would have been expected to enhance the CDCs' therapeutic benefits by reducing that immune response. Thus, in some embodiments, a lack of an immune response or a weak immune response enables additional CDCs to be administered multiple times, and thereby exert enhanced

therapeutic effects, with a minimized or non-existent immune response to the CDCs, as compared to a single administration.

[0362] These data demonstrate that repeat dosing of CDCs is effective in producing additional exercise improvement in *mdx* mice. Although allogeneic CDCs are recognized by the immune system, their low immunogenic profile and immune-regulatory capabilities allow them to be effectively administered multiple times.

[0363] Although the foregoing has been described in some detail by way of illustrations and examples for purposes of clarity and understanding, it will be understood by those of skill in the art that modifications can be made without departing from the spirit of the present disclosure. Therefore, it should be clearly understood that the forms disclosed herein are illustrative only and are not intended to limit the scope of the present disclosure, but rather to also cover all modification and alternatives coming with the true scope and spirit of the embodiments of the invention(s).

[0364] It is contemplated that various combinations or subcombinations of the specific features and aspects of the embodiments disclosed above may be made and still fall within one or more of the inventions. Further, the disclosure herein of any particular feature, aspect, method, property, characteristic, quality, attribute, element, or the like in connection with an embodiment can be used in all other embodiments set forth herein. Accordingly, it should be understood that various features and aspects of the disclosed embodiments can be combined with or substituted for one another in order to form varying modes of the disclosed inventions. Thus, it is intended that the scope of the present inventions herein disclosed should not be limited by the particular disclosed embodiments described above. Moreover, while the invention is susceptible to various modifications, and alternative forms, specific examples thereof have been shown in the drawings and are herein described in detail. It should be understood, however, that the invention is not to be limited to the particular forms or methods disclosed, but to the contrary, the invention is to cover all modifications, equivalents, and alternatives falling within the spirit and scope of the various embodiments described and the appended claims. Any methods disclosed herein need not be performed in the order recited. The methods disclosed herein include certain actions taken by a practitioner; however, they can also include any third-party instruction of those actions, either expressly or by implication. For example, actions such as "administering an antigen-binding protein" include "instructing the administration of an antigen-binding protein." In addition, where

features or aspects of the disclosure are described in terms of Markush groups, those skilled in the art will recognize that the disclosure is also thereby described in terms of any individual member or subgroup of members of the Markush group.

[0365] The ranges disclosed herein also encompass any and all overlap, sub-ranges, and combinations thereof. Language such as "up to," "at least," "greater than," "less than," "between," and the like includes the number recited. Numbers preceded by a term such as "about" or "approximately" include the recited numbers. For example, "about 90%" includes "90%." In some embodiments, at least 95% homologous includes 96%, 97%, 98%, 99%, and 100% homologous to the reference sequence. In addition, when a sequence is disclosed as "comprising" a nucleotide or amino acid sequence, such a reference shall also include, unless otherwise indicated, that the sequence "comprises", "consists of" or "consists essentially of" the recited sequence.

[0366] Terms and phrases used in this application, and variations thereof, especially in the appended claims, unless otherwise expressly stated, should be construed as open ended as opposed to limiting. As examples of the foregoing, the term 'including' should be read to mean 'including, without limitation,' 'including but not limited to,' or the like.

[0367] The indefinite article "a" or "an" does not exclude a plurality. The term "about" as used herein to, for example, define the values and ranges of molecular weights means that the indicated values and/or range limits can vary within ±20%, e.g., within ±10%. The use of "about" before a number includes the number itself. For example, "about 5" provides express support for "5". Numbers provided in ranges include overlapping ranges and integers in between; for example a range of 1-4 and 5-7 includes for example, 1-7, 1-6, 1-5, 2-5, 2-7, 4-7, 1, 2, 3, 4, 5, 6 and 7.

CLAIMS

1. A method of improving skeletal muscle isometric force production in a skeletal muscle of a subject with muscular dystrophy in need of treatment for skeletal muscle myopathy, the method comprising:

administering to the subject a first dose of a composition comprising a therapeutically effective amount of cardiosphere-derived cells (CDCs),

wherein the therapeutically effective amount of the first dose ranges from about 1 x 10^7 to about 1 x 10^9 CDCs;

waiting a first period of time after administration of said first dose,

wherein said first period of time is between about 1 and 6 months;

administering to the subject a second dose of a composition comprising a therapeutically effective amount of cardiosphere-derived cells (CDCs),

wherein the therapeutically effective amount of the second dose ranges from about 1 x 10^7 to about 1 x 10^9 CDCs;

waiting a second period of time after administration of said second dose,

wherein said second period of time is between about 1 and 6 months;

administering to the subject at least one additional dose of a composition comprising a therapeutically effective amount of cardiosphere-derived cells (CDCs),

wherein the therapeutically effective amount of the at least one additional dose ranges from about 1 x 10^7 to about 1 x 10^9 CDCs;

waiting at least one additional period of time after administration of said at least one additional dose,

wherein said at least one additional period of time is between about 1 and 6 months;

wherein said administrations result in an improvement in exercise capacity or muscle function,

wherein said CDCs are allogeneic with respect to said subject,

wherein said administrations do not induce a significant immune response in the subject, and

wherein said administrations comprise systemic administration.

2. The method according to Claim 1, wherein said skeletal muscular dystrophy is:

a) Duchenne muscular dystrophy (DMD) involving dystrophinopathy of a skeletal muscle; and/or

b) Becker muscular dystrophy involving dystrophinopathy of a skeletal muscle.

3. The method according to Claim 1 or 2,

wherein said first period of time is about three months, said second period of time is about three months, and said at least one additional period is about three months.

4. The method according to any one of Claims 1 to 3, wherein said therapeutically effective amount of CDCs is, or is at least:

a) 450×10^6 CDCs;

b) 300×10^6 CDCs; or

c) 150×10^6 CDCs.

5. The method according to any one of Claims 1 to 4, wherein said therapeutically effective amount of CDCs is, or is at least:

a) about 150 x 10^6 CDCs; or

b) about 75 x 10^6 CDCs.

6. The method according to any one of Claims 1 to 5, wherein said CDCs are allogeneic human CDCs, and the subject is a human subject.

7. The method according to any one of Claims 1 to 6, wherein said systemic administration is via intravenous injection.

8. The method according to Claim 7, wherein said administrations alter expression of one or more markers of T cell activation or proliferation.

9. The method according to any one of Claims 1 to 8,

wherein said systemic administration comprises injection into the right ventricle of the subject's heart, or injection into the left ventricle of the subject's heart.

10. The method according to any one of Claims 1 to 9, wherein said skeletal muscle comprises a skeletal muscle of the diaphragm, the arm, or the leg.

.

Figure 1.

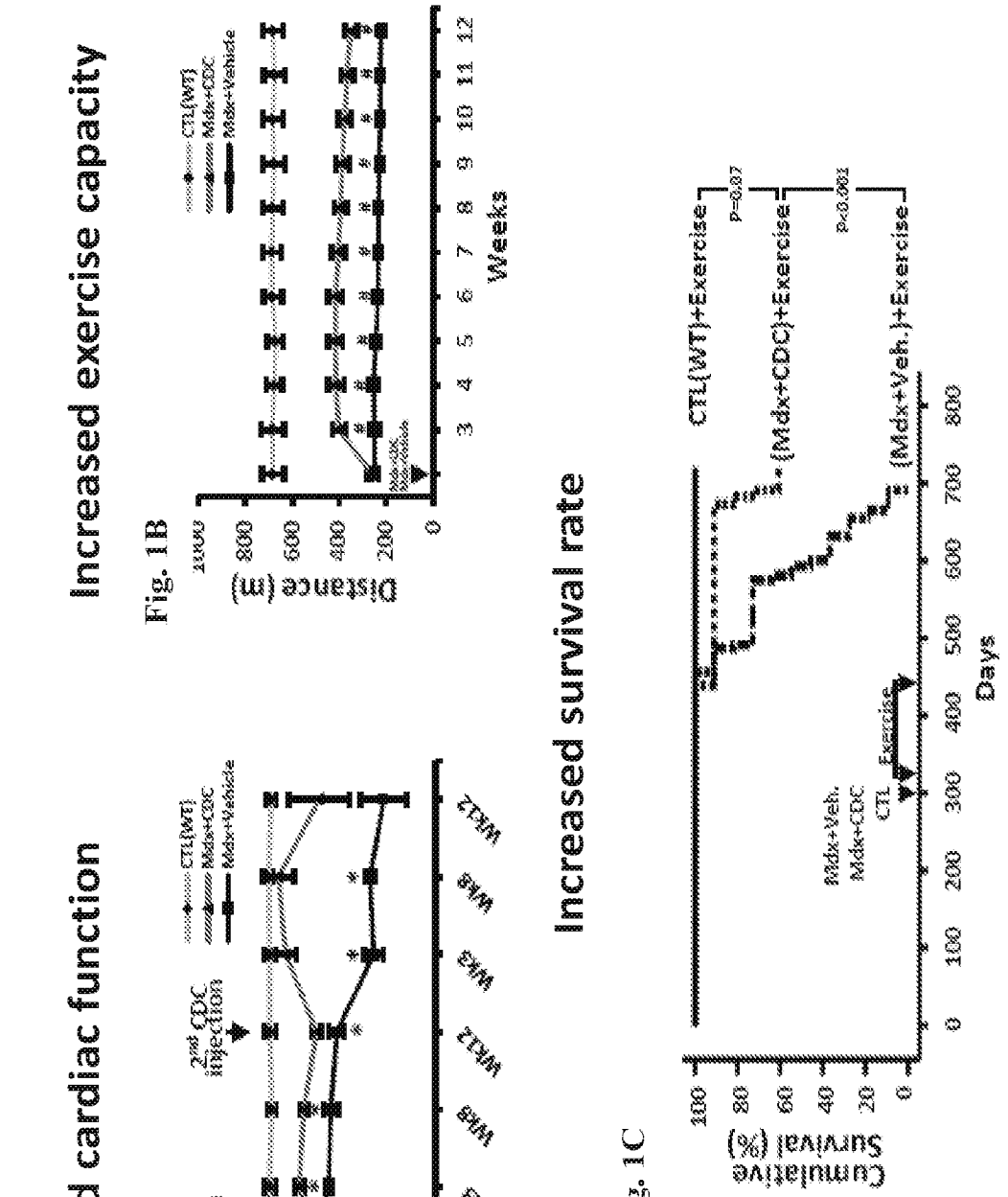
Improved cardiac function
Fig. 1A
CTL(WT)
Mdx+CDC
Mdx+Vehicle
1st CDC injection
2nd CDC injection
EF (%)
baseline
Wk1
Wk2
Wk3
Wk8
Wk12
Wk24
Increased exercise capacity
Fig. 1B
Distance (m)
Weeks
Increased survival rate
Fig. 1C
CTL(WT)+Exercise
(Mdx+CDC)+Exercise
(Mdx+Veh.)+Exercise
P=0.07
P<0.001
Mdx+Veh.
Mdx+CDC
CTL
Exercise
Cumulative Survival (%)
Days

Figure 1.

Fig. 1D

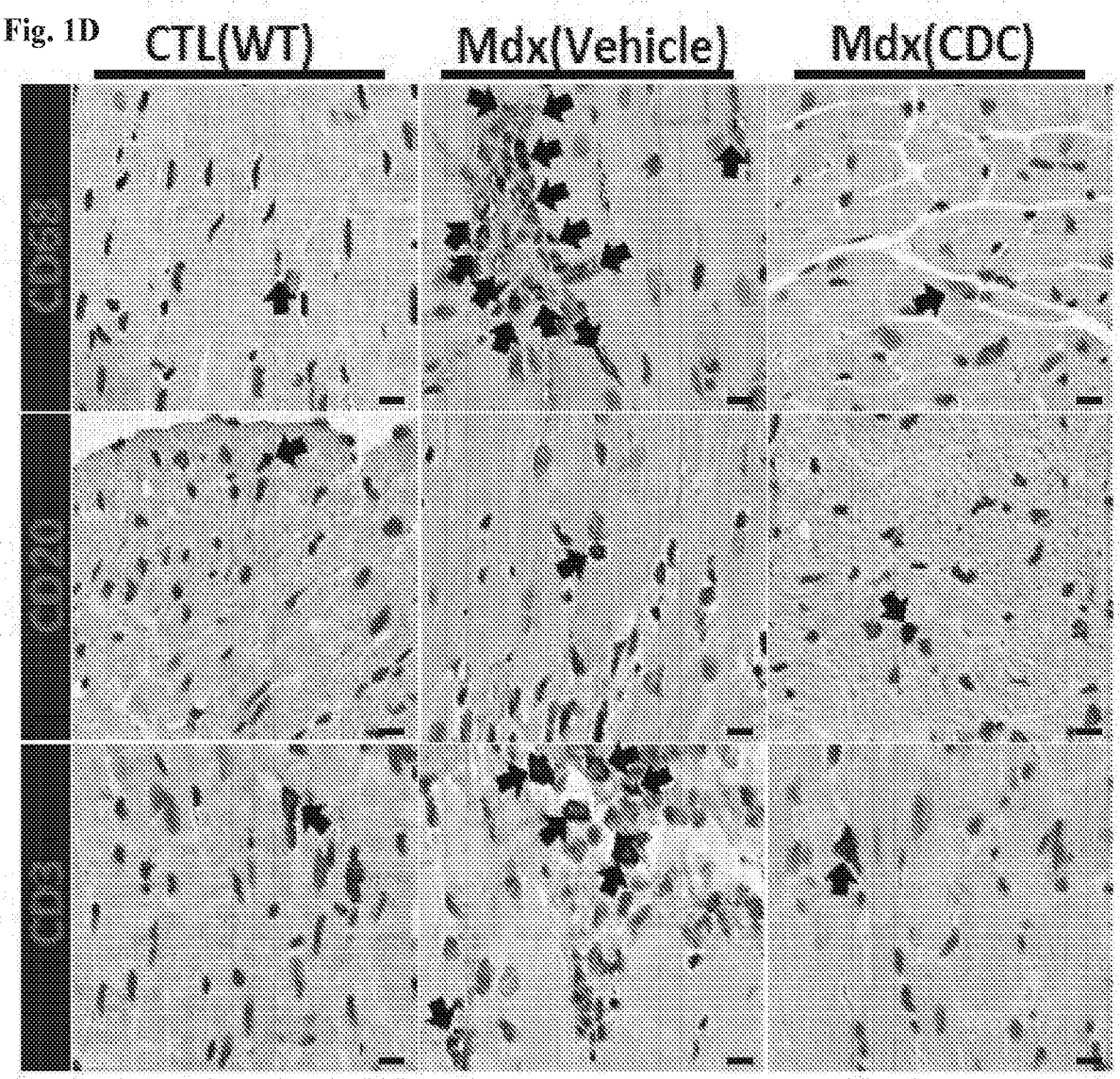

Figure 1.

Fig. 1E

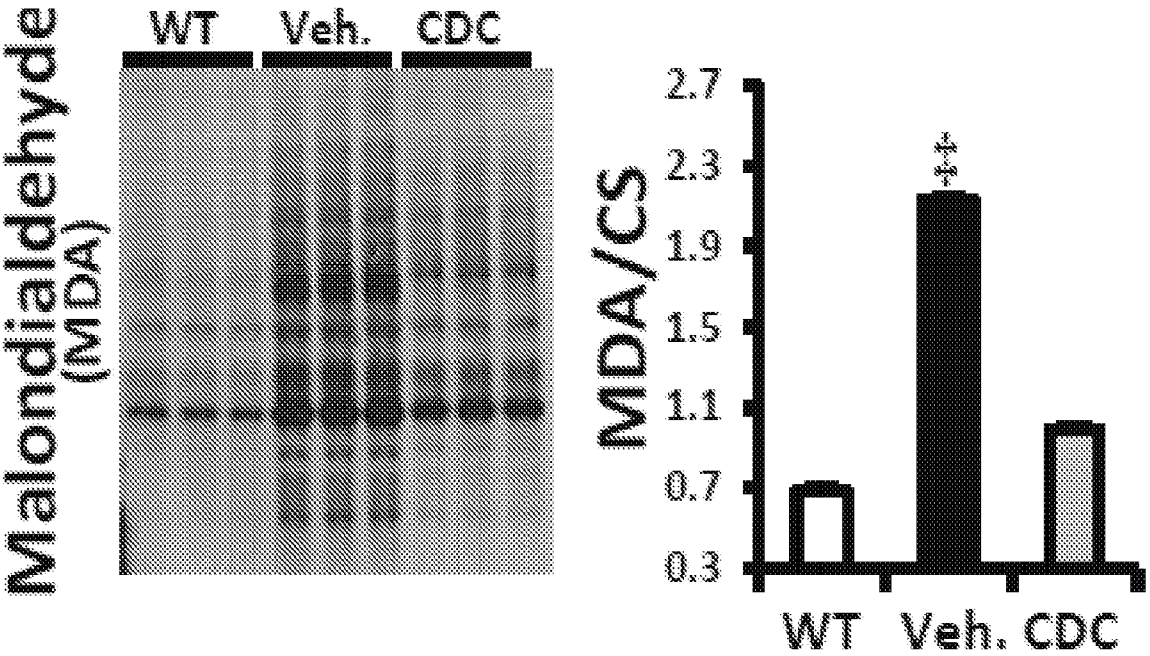

Figure 1.

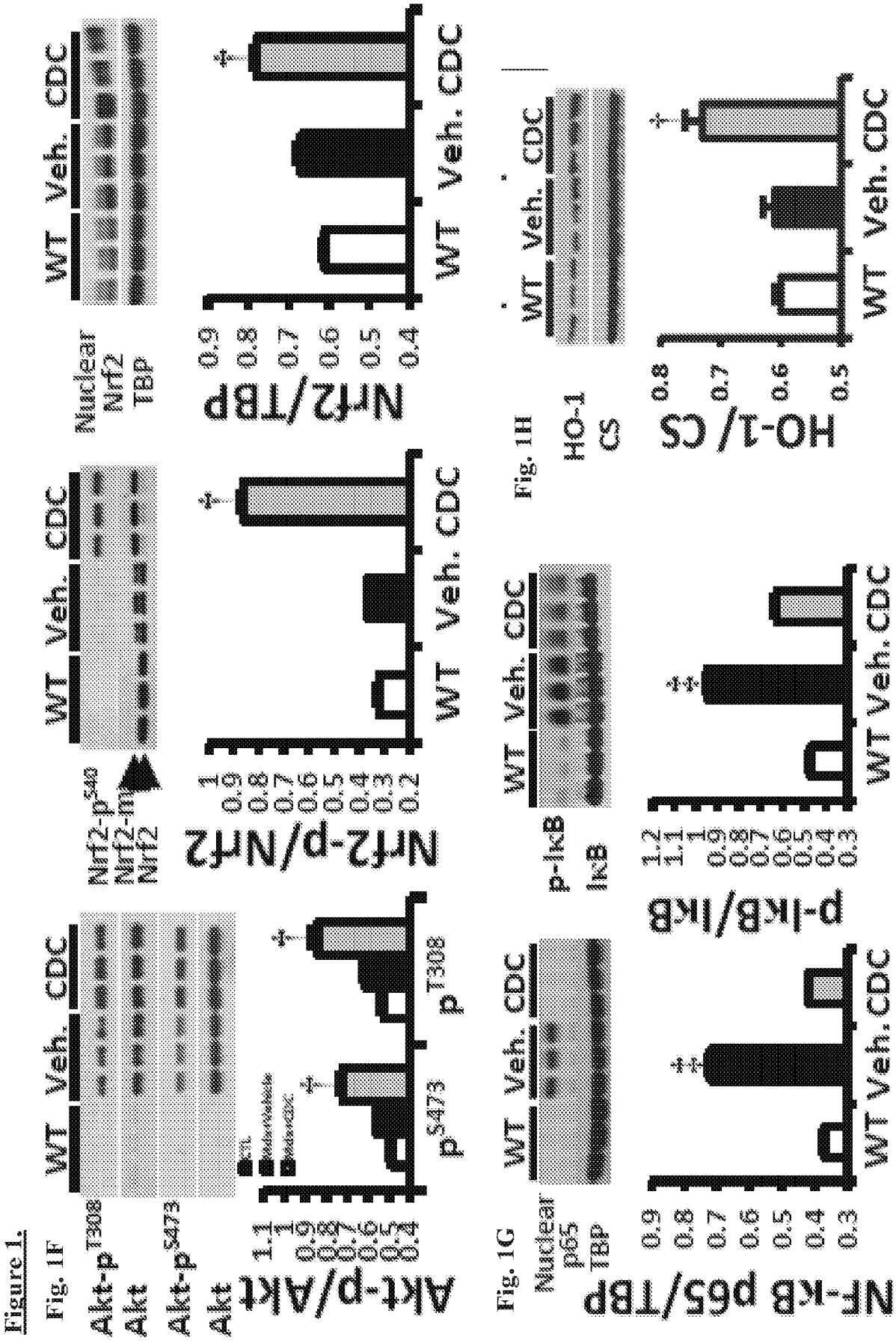
Fig. 1F
WT Veh. CDC
Akt-p^{T308}
Akt
Akt-p^{S473}
Akt
Akt-p/Akt
p^{S473}
p^{T308}
Nrf2-p^{S40}
Nrf2-m
Nrf2
Nrf2-p/Nrf2
Nuclear
Nrf2
TBP
Nrf2/TBP
Fig. 1G
Nuclear
p65
TBP
NF-κB p65/TBP
p-IκB
IκB
p-IκB/IκB
Fig. 1H
HO-1
CS
HO-1/ CS

Figure 1.

Fig. 1I

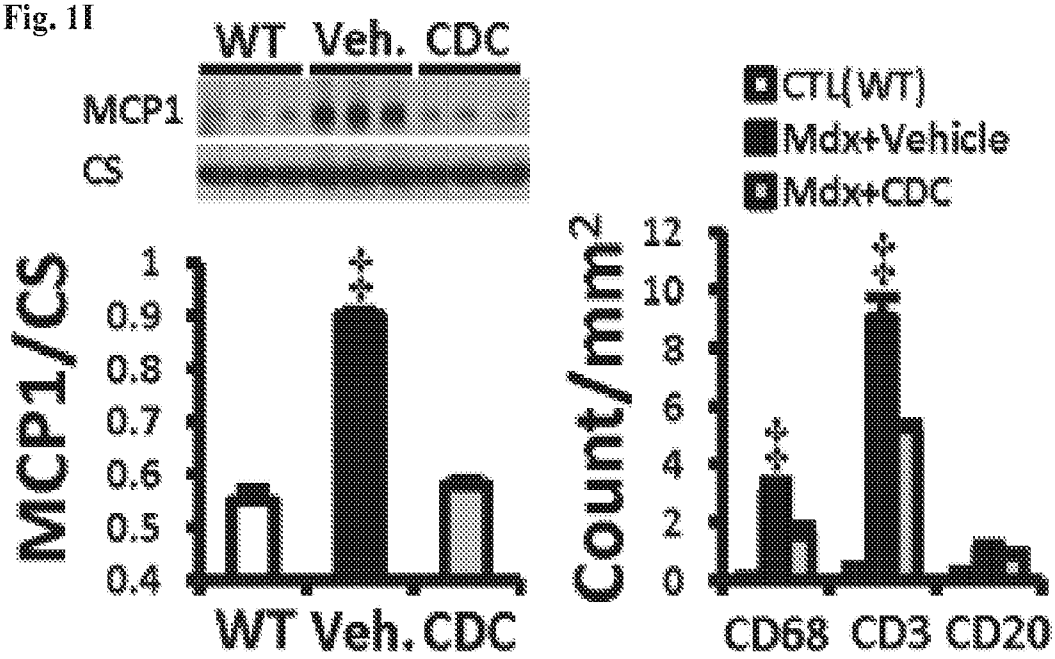

Figure 1.

Fig. 1J

Figure 2.

Fig. 2A

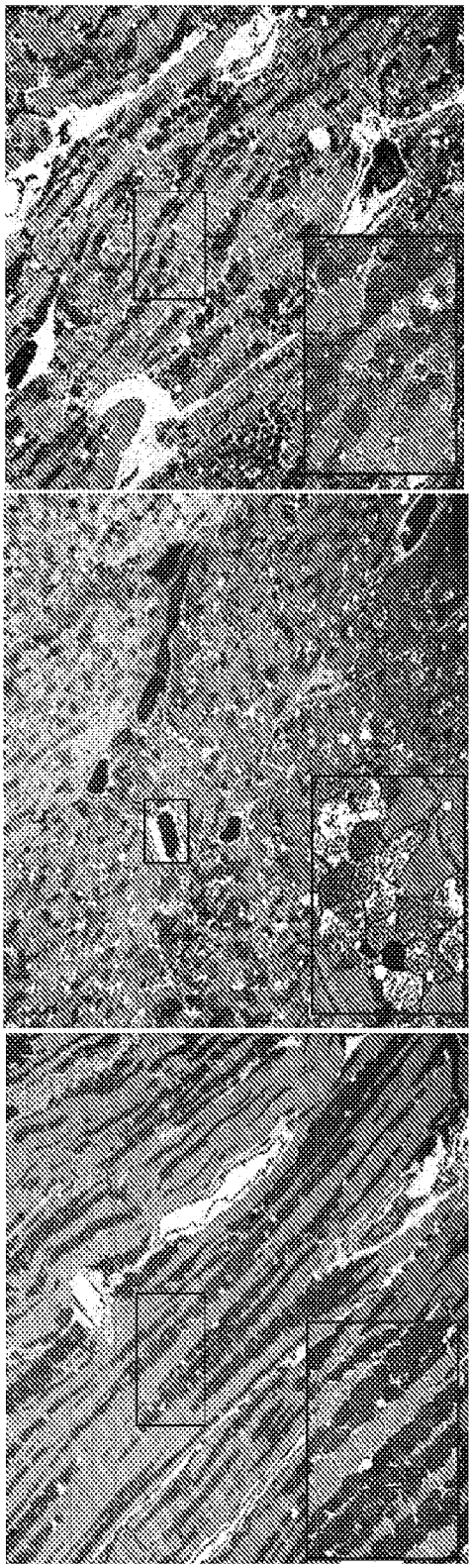

Figure 2.

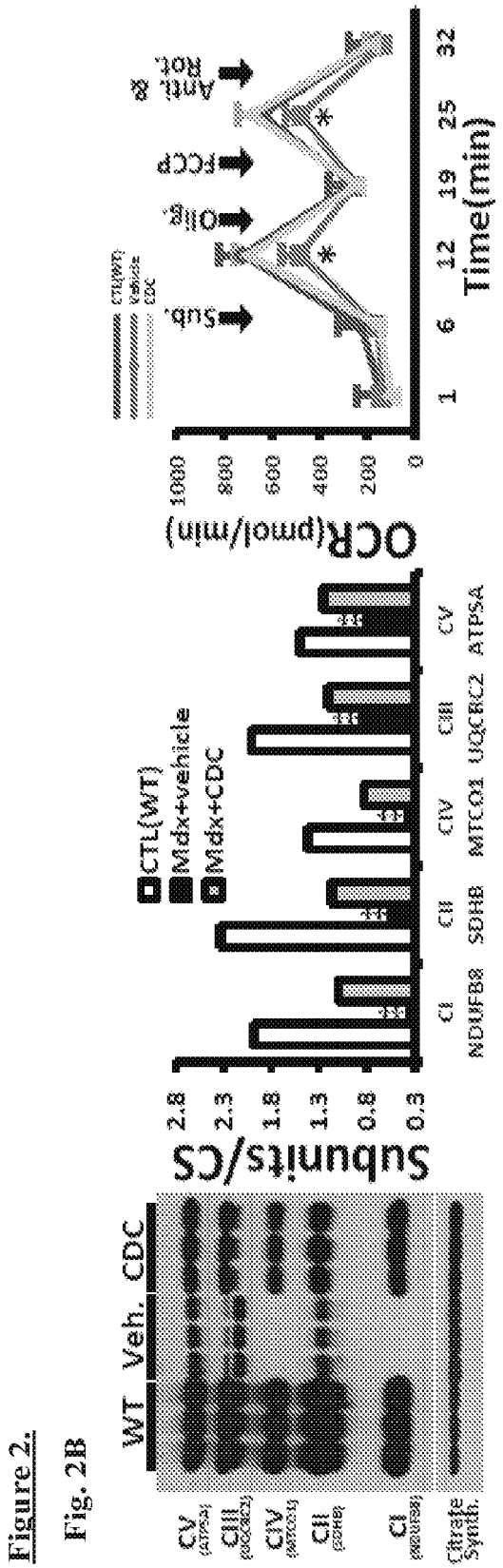
Fig. 2B
WT
Veh.
CDC
CV (ATPSA)
CIII (UQCRC2)
CIV (MTCO1)
CII (SDHB)
CI (NDUFB8)
Citrate Synth.
Subunits/CS
2.8
2.3
1.8
1.3
0.8
0.3
CTL(WT)
Mdx+vehicle
Mdx+CDC
CI
CII
CIV
CIII
CV
NDUFB8
SDHB
MTCO1
UQCRC2
ATPSA
OCR(pmol/min)
1000
800
600
400
200
0
1
6
12
19
25
32
Time(min)
Sub.
Oligo.
FCCP
Anti. & Rot.

Figure 3.

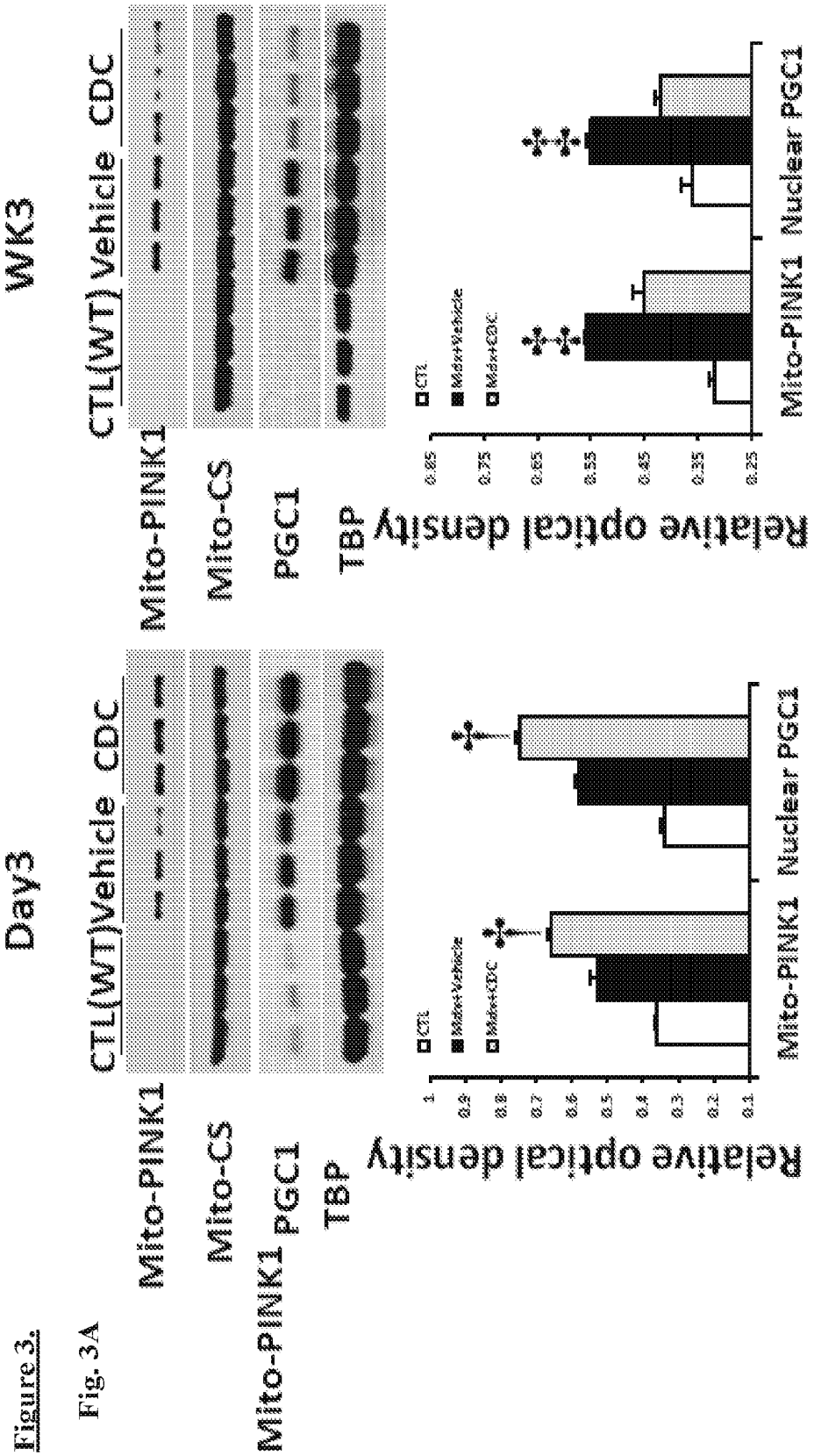
Fig. 3A
Day3
CTL(WT)Vehicle CDC
Mito-PINK1
Mito-CS
PGC1
TBP
Relative optical density
CTL
Mdivi+Vehicle
Mdivi+CDC
Mito-PINK1
Nuclear PGC1
WK3
CTL(WT) Vehicle CDC
Mito-PINK1
Mito-CS
PGC1
TBP
Relative optical density
CTL
Mdivi+Vehicle
Mdivi+CDC
Mito-PINK1
Nuclear PGC1

Figure 3.

Fig. 3B

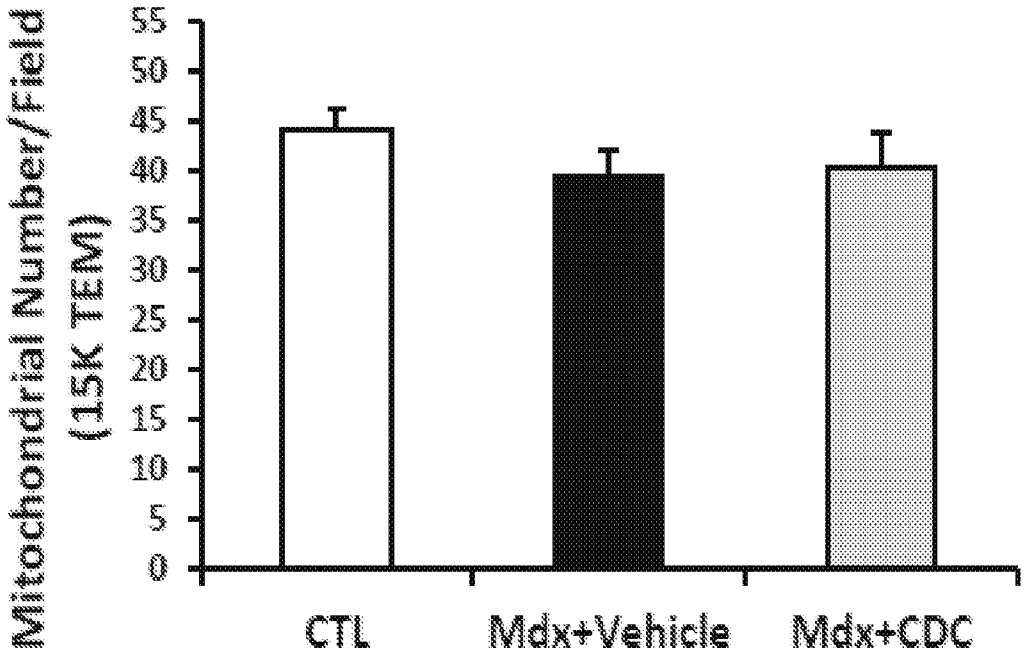

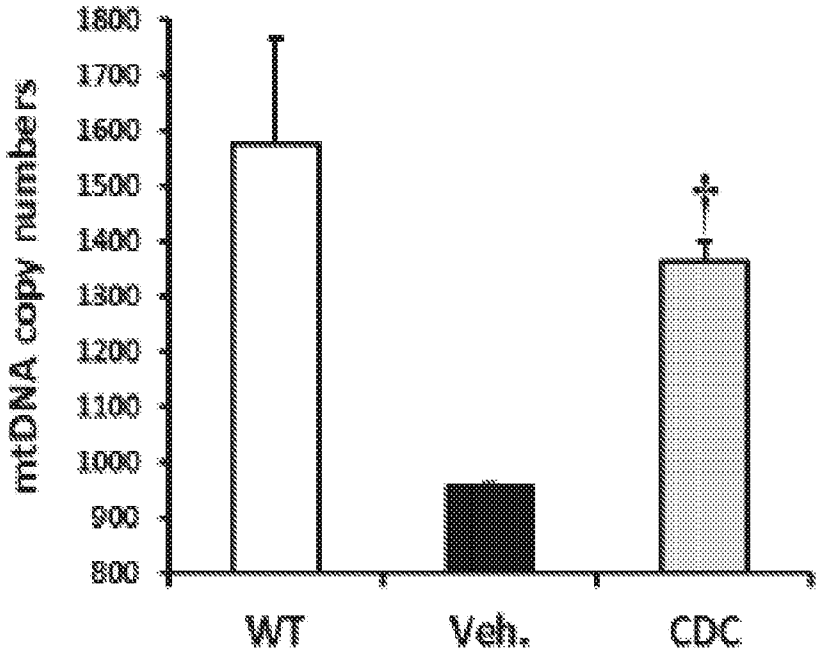

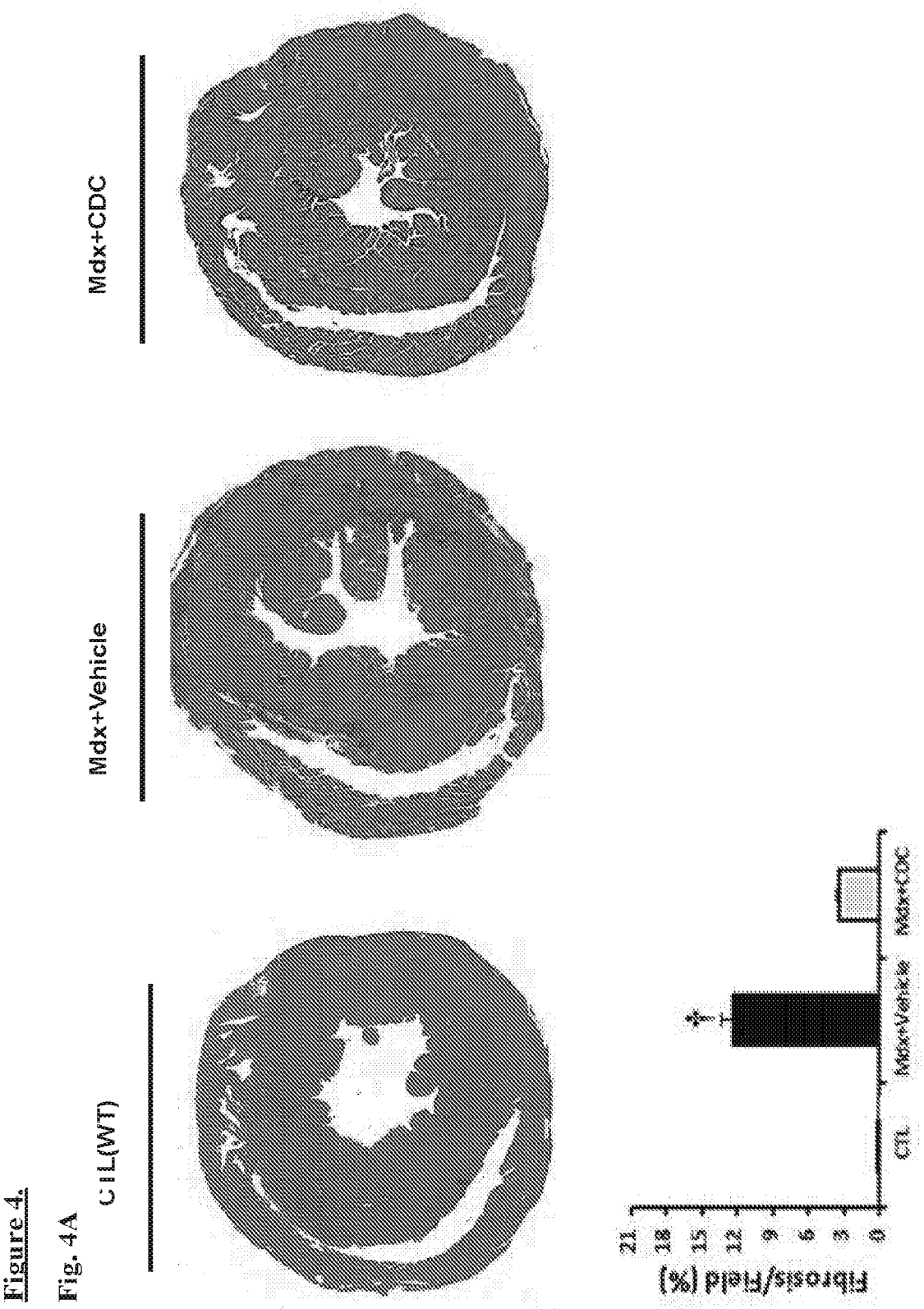

Figure 4.

Fig. 4A

Figure 4.

Fig. 4B

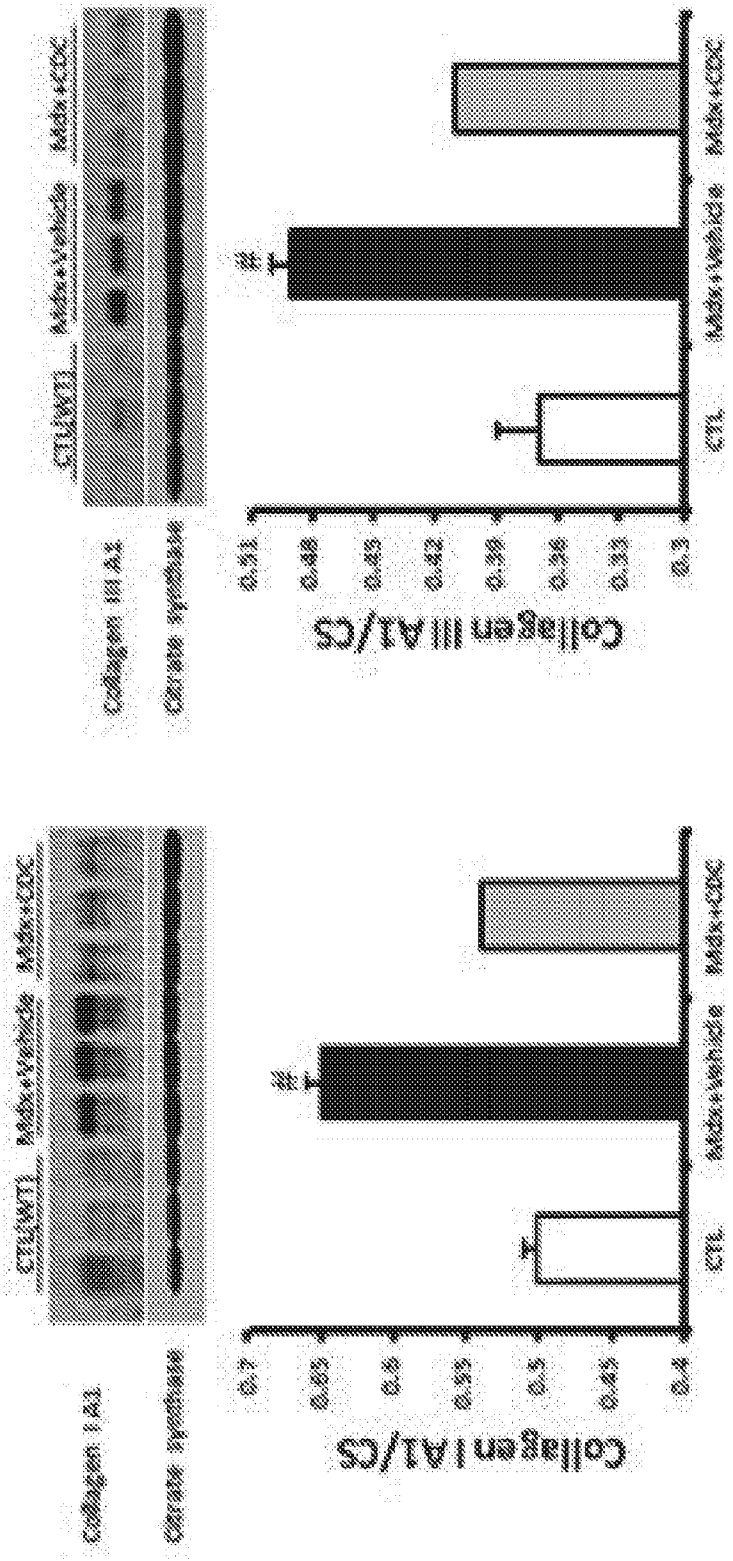

Figure 5.

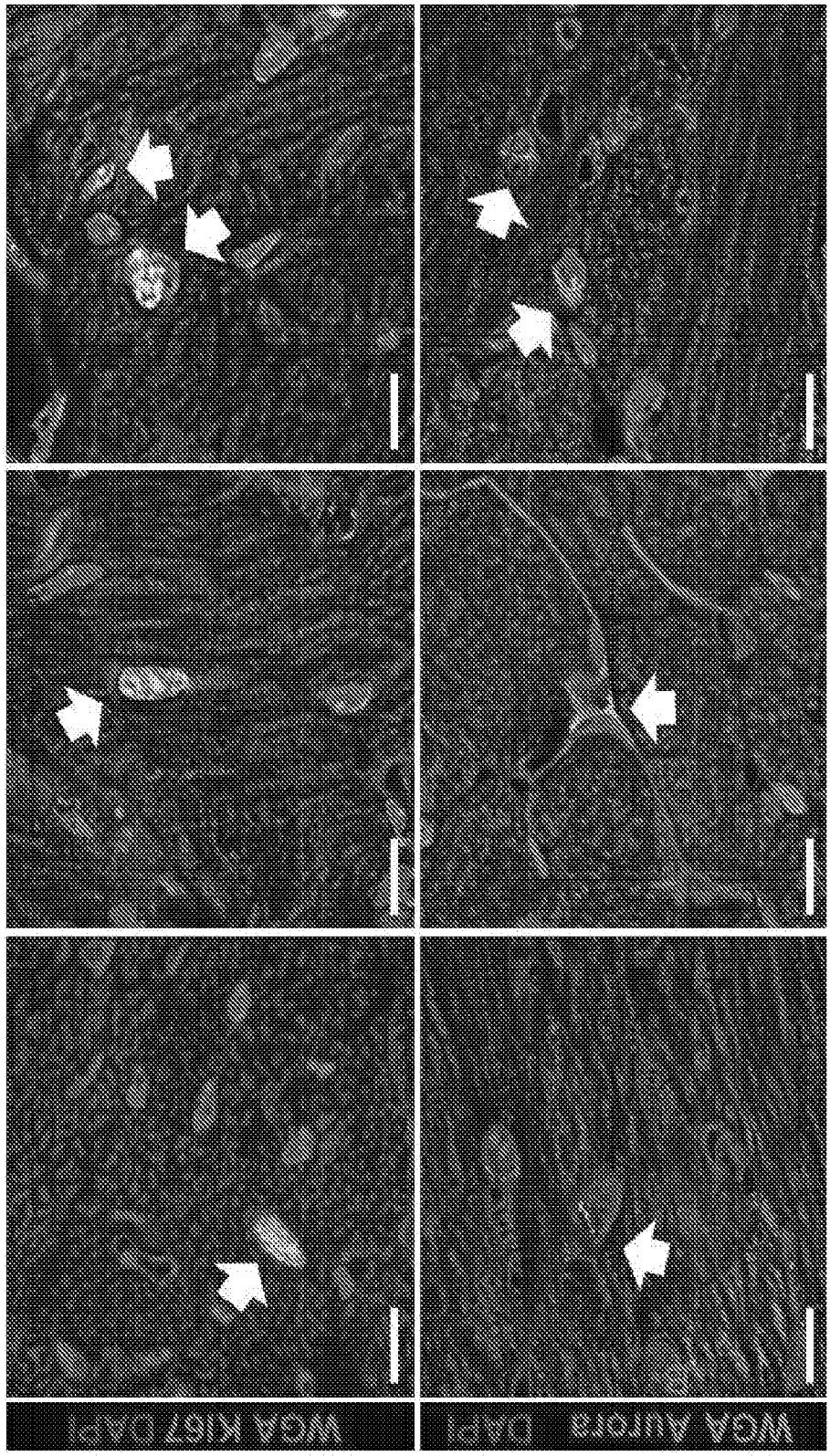
Fig. 5A
CTL (WT)
MDX+Vehicle
MDX+CDC
WGA Ki67 DAPI
WGA Aurora DAPI

Figure 5.

Fig. 5B

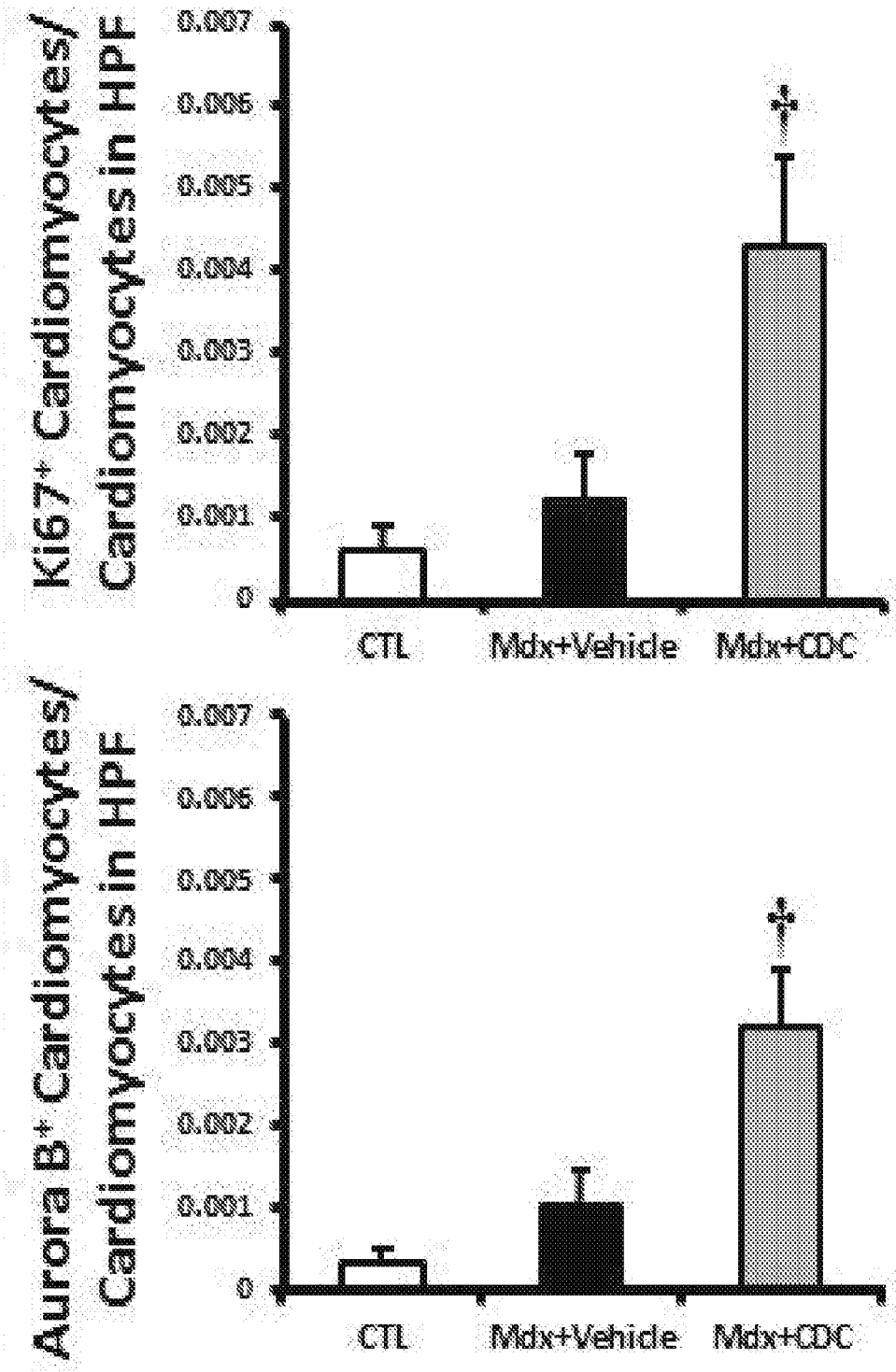

Figure 6.

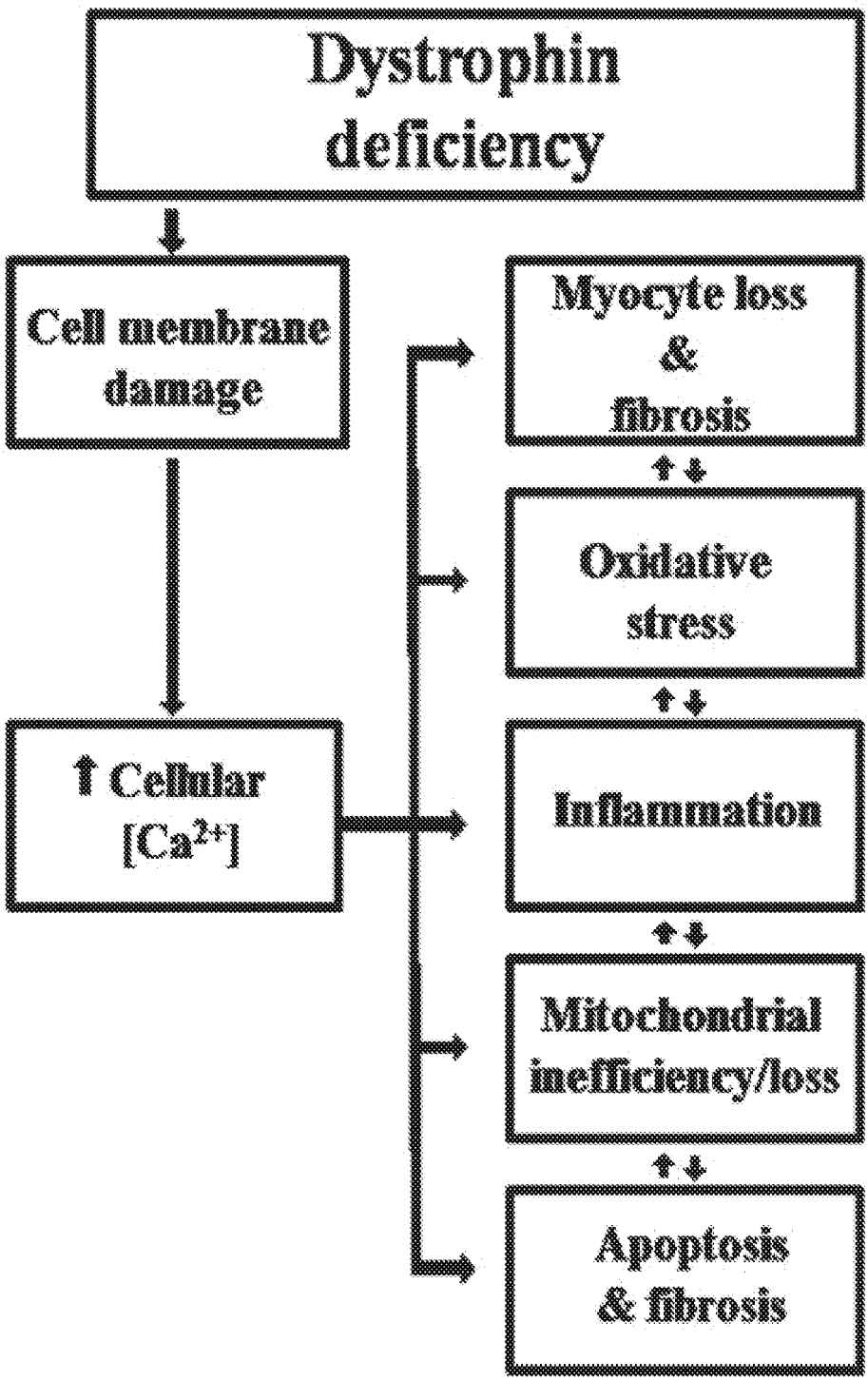
Dystrophin deficiency
Cell membrane damage
↑ Cellular [Ca2+]
Myocyte loss & fibrosis
Oxidative stress
Inflammation
Mitochondrial inefficiency/loss
Apoptosis & fibrosis

Figure 7.

Fig. 7A

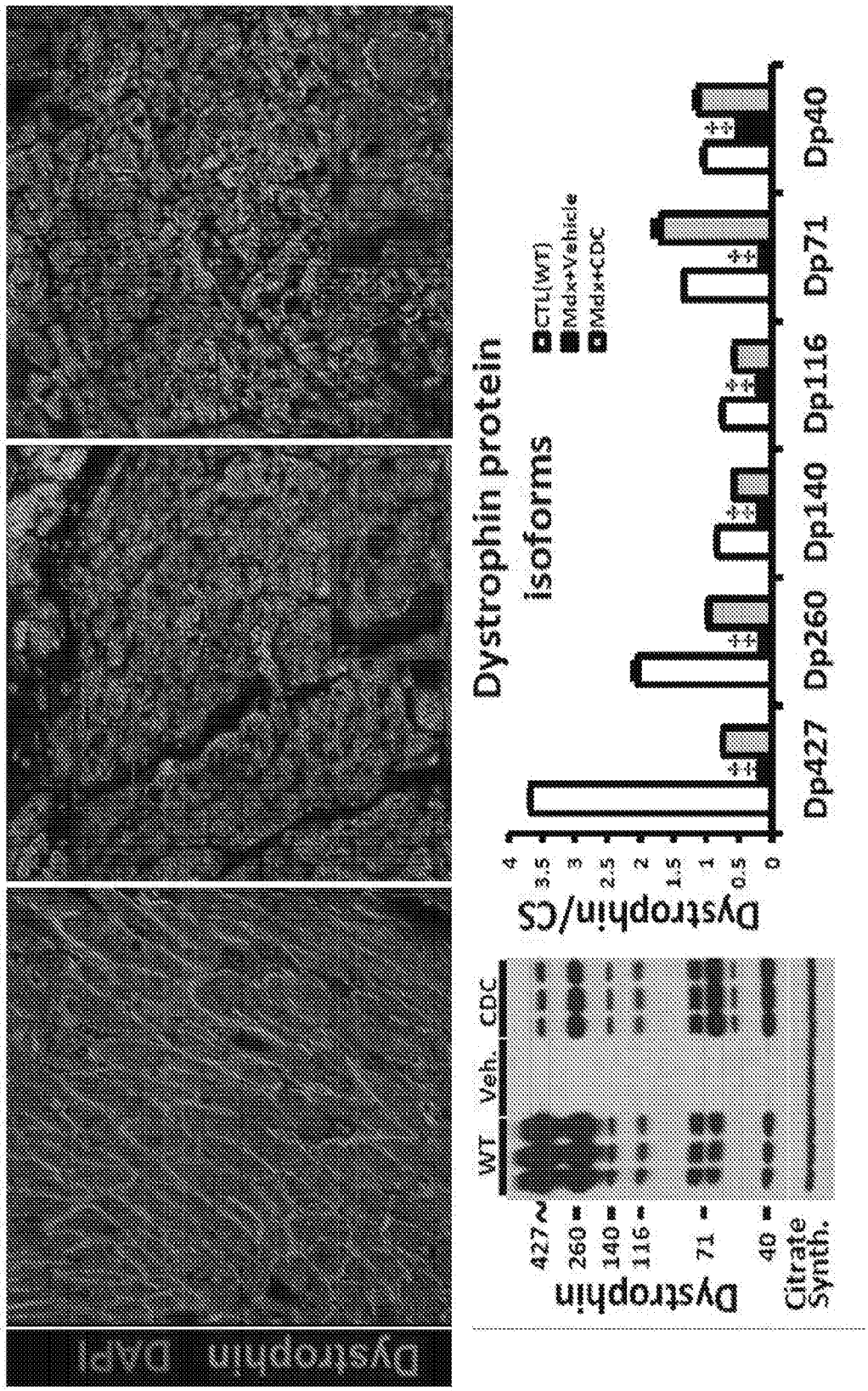

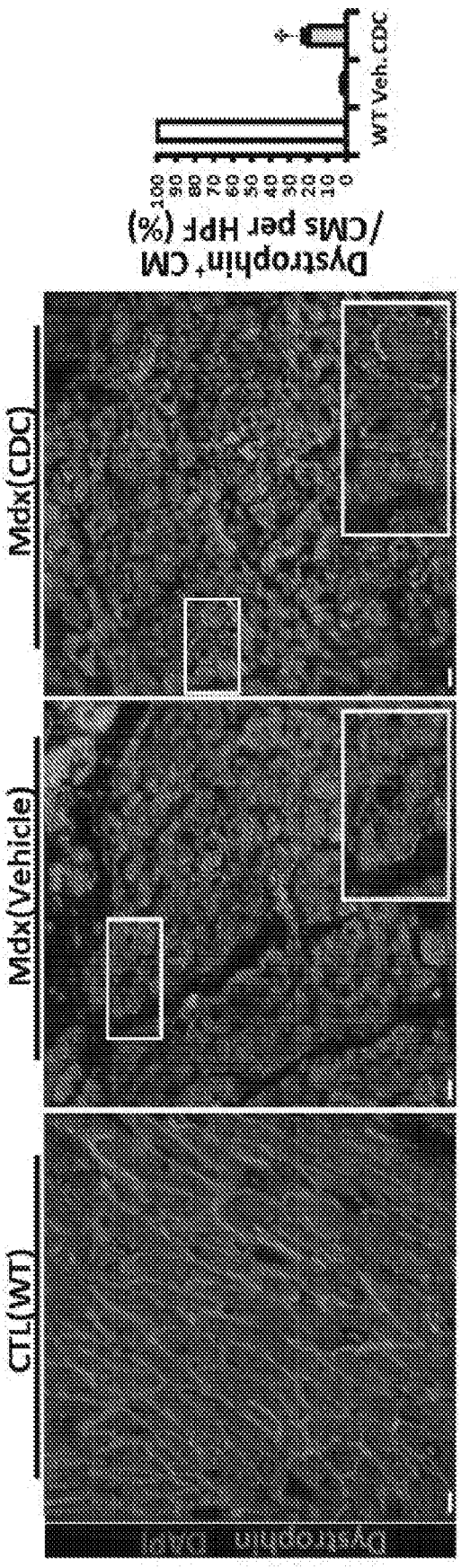

Figure 7.

Fig. 7B

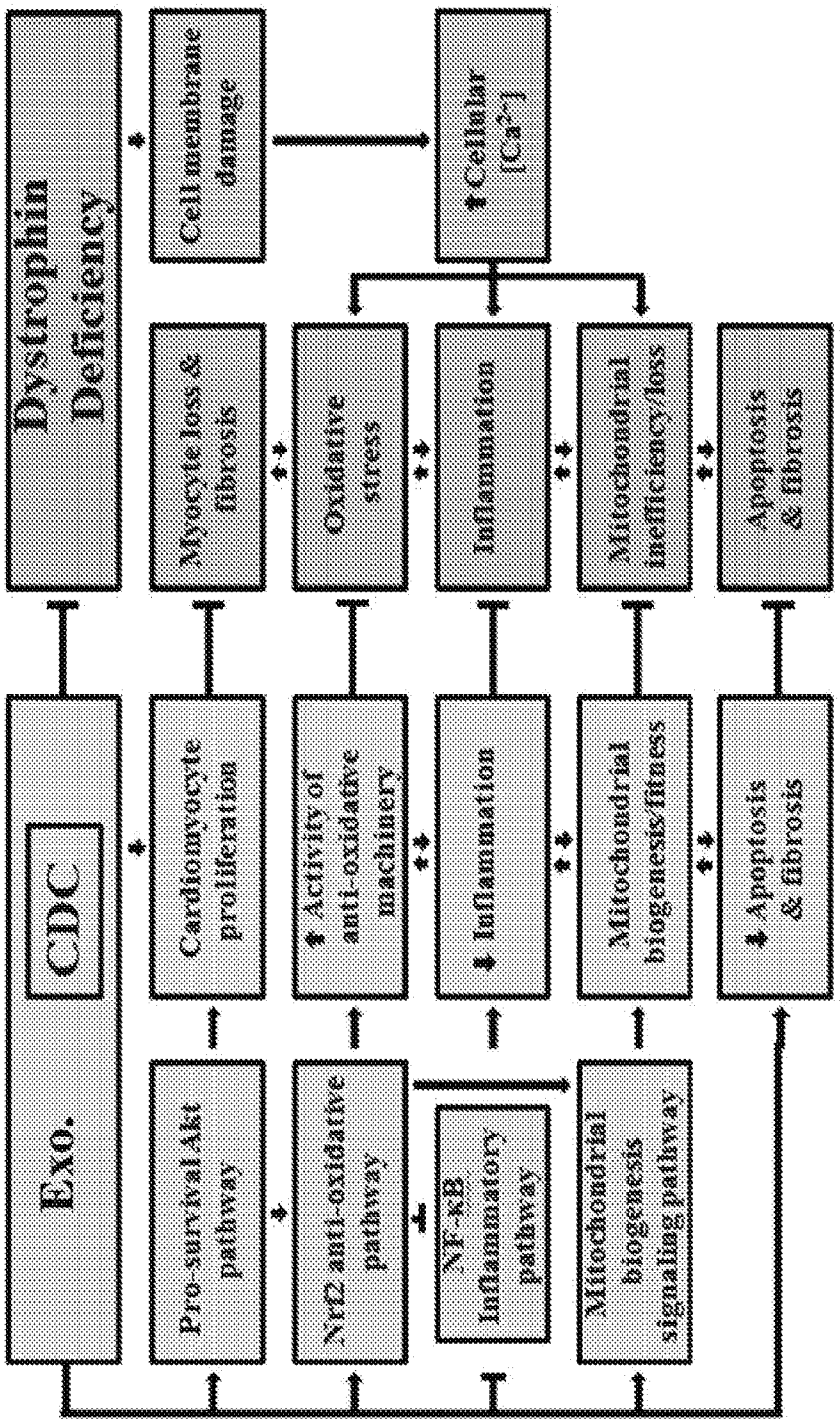
Dystrophin Deficiency
Cell membrane damage
↑Cellular [Ca2+]
Myocyte loss & fibrosis
Oxidative stress
Inflammation
Mitochondrial inefficiency/loss
Apoptosis & fibrosis
Exo.
CDC
Cardiomyocyte proliferation
↑ Activity of anti-oxidative machinery
↓ Inflammation
Mitochondrial biogenesis/fitness
↓ Apoptosis & fibrosis
Pro-survival Akt pathway
Nrf2 anti-oxidative pathway
NF-κB Inflammatory pathway
Mitochondrial biogenesis signaling pathway

Figure 8.

Figure 9.

Fig. 9A

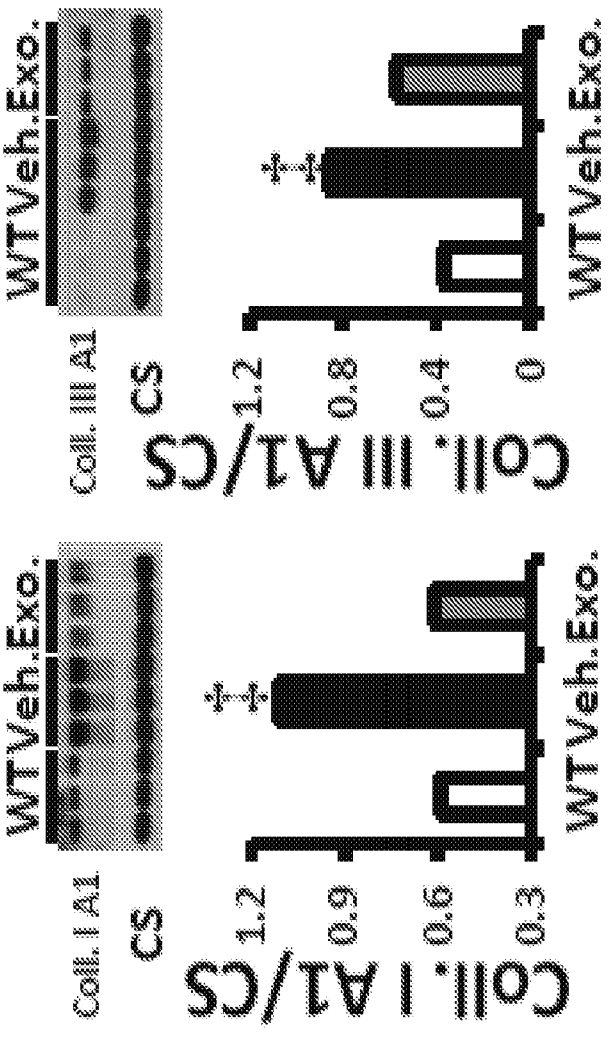

Figure 9.

Fig. 9B

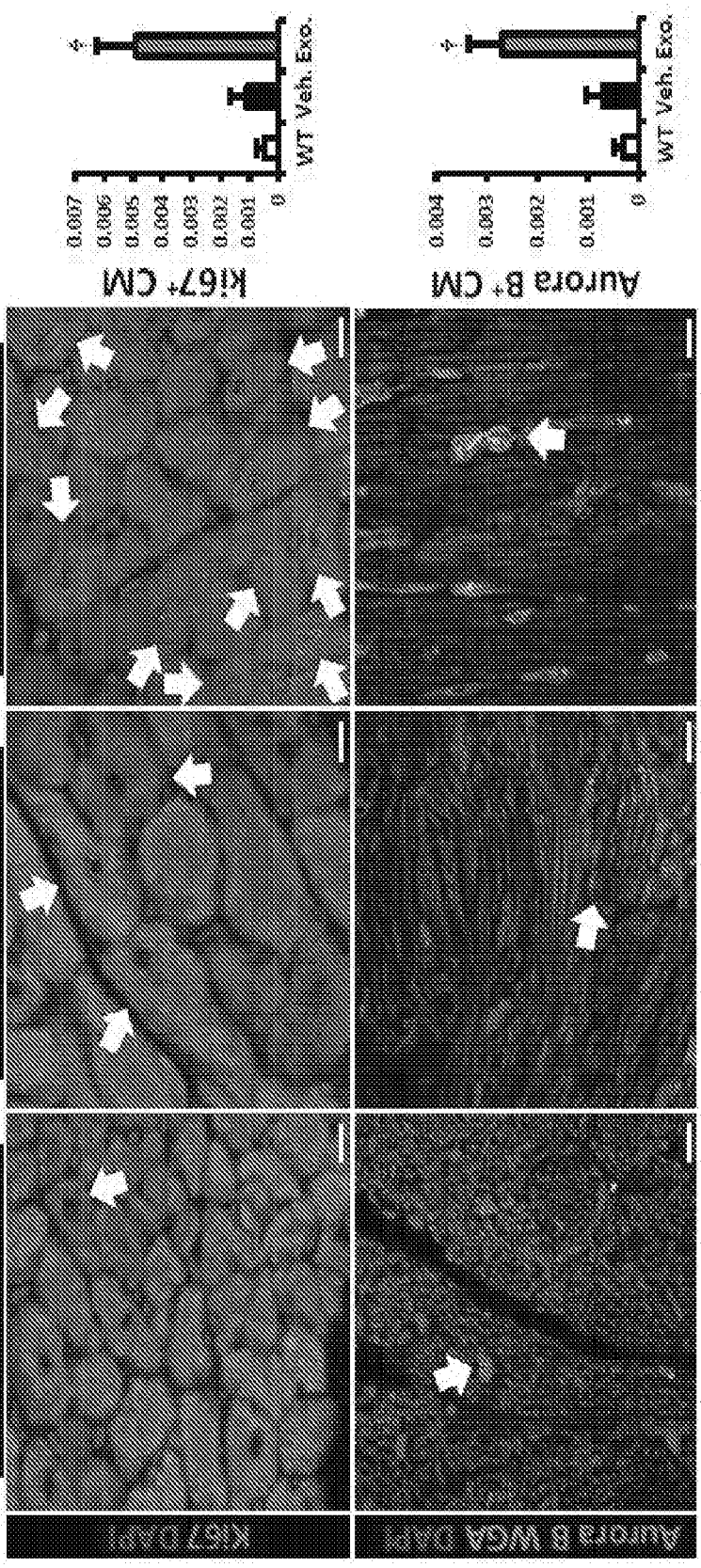

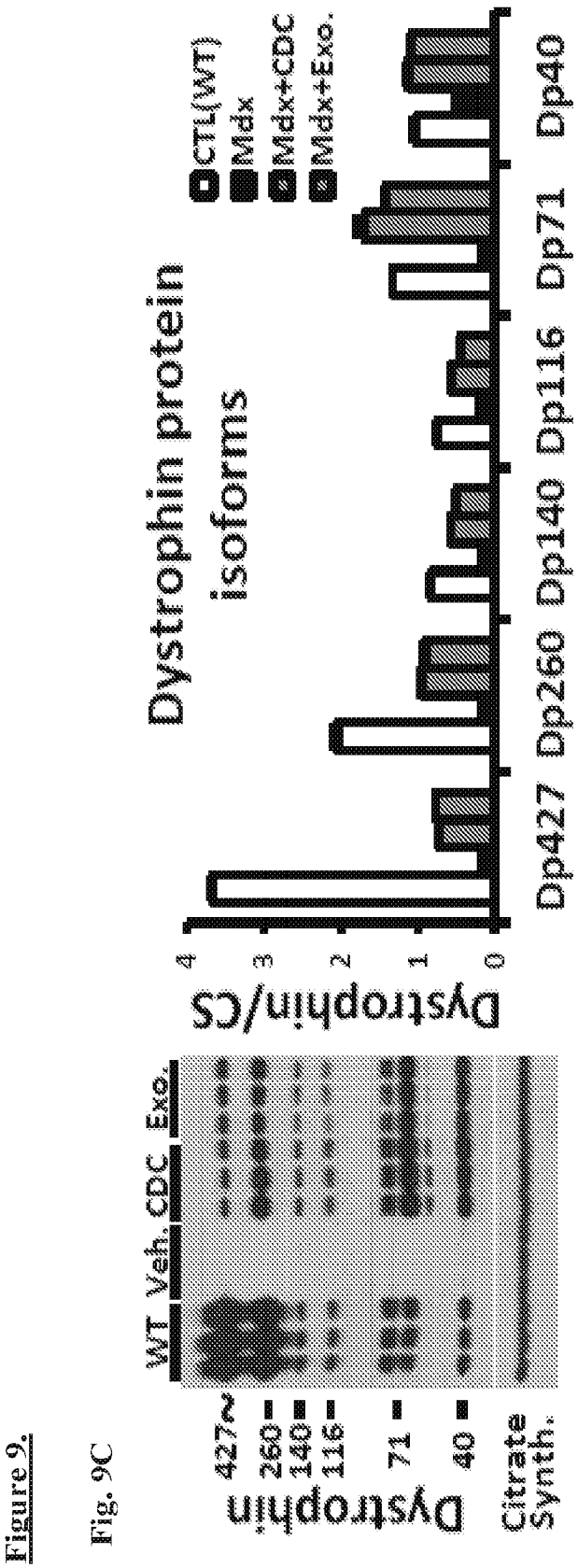

Figure 9.

Fig. 9C

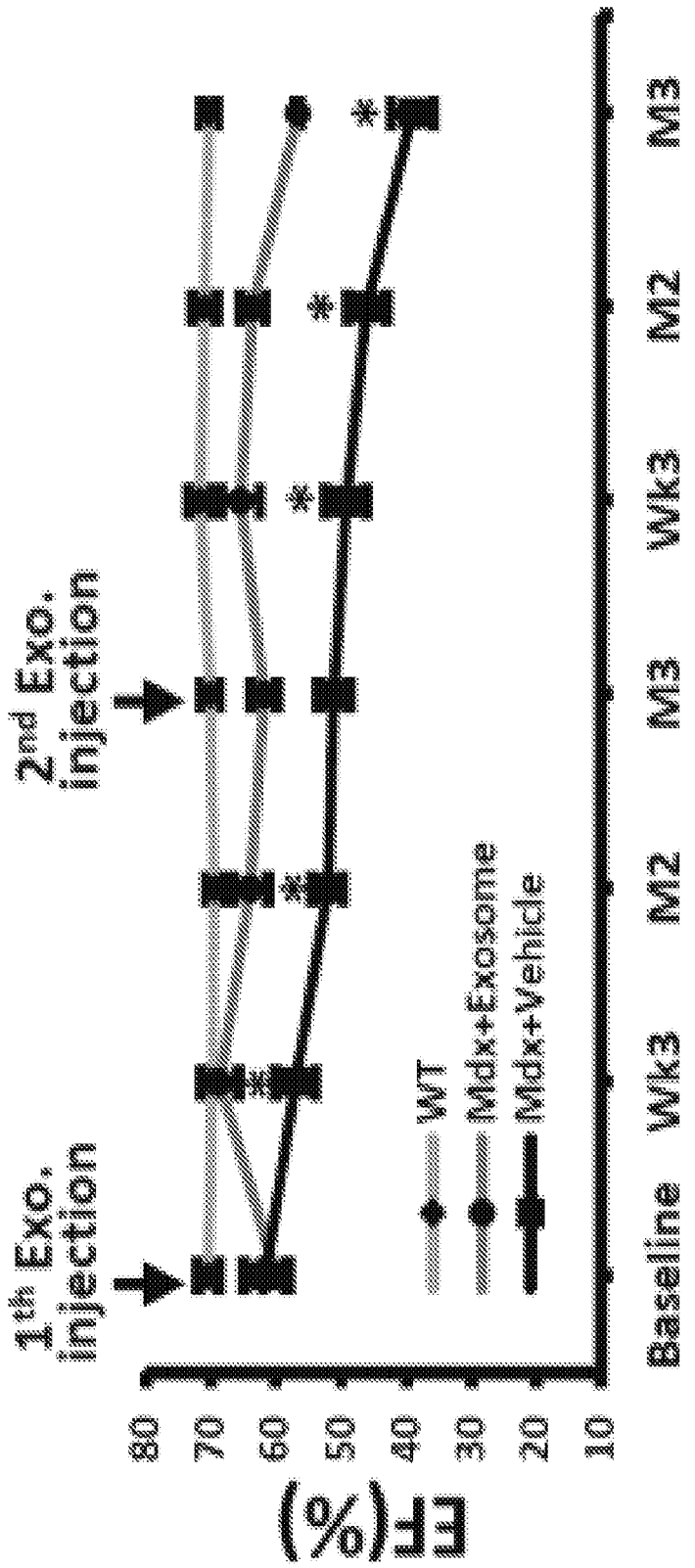

Figure 9.

Fig. 9D

Figure 10.

Fig. 10A

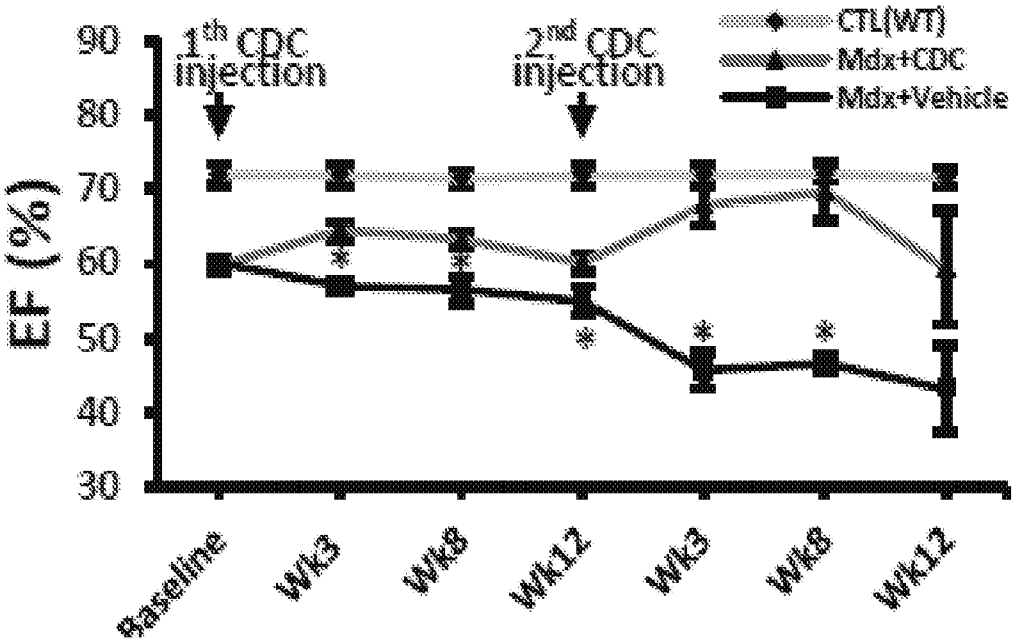

Fig. 10B

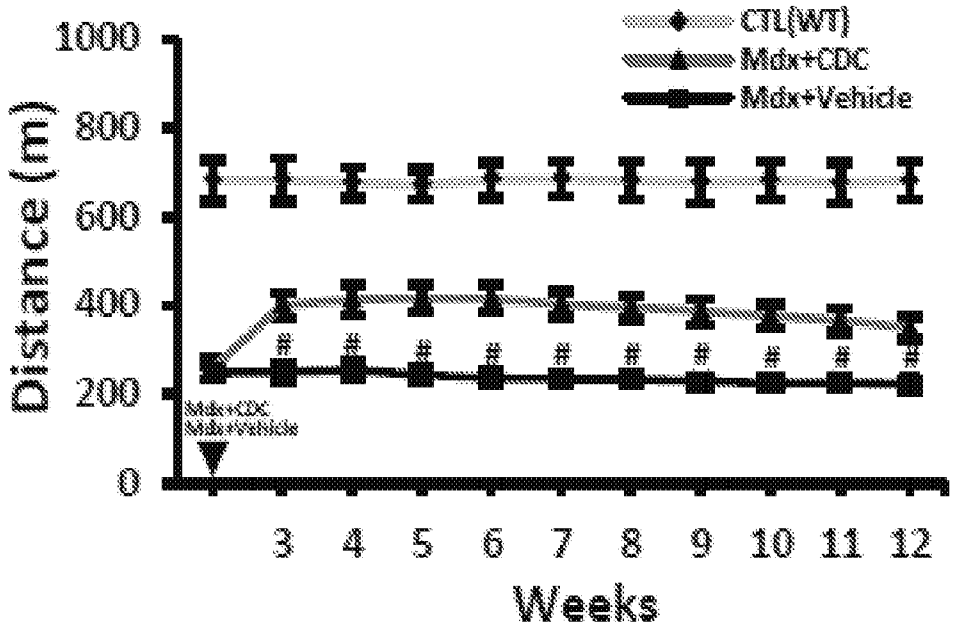

Figure 11.

Fig. 11A

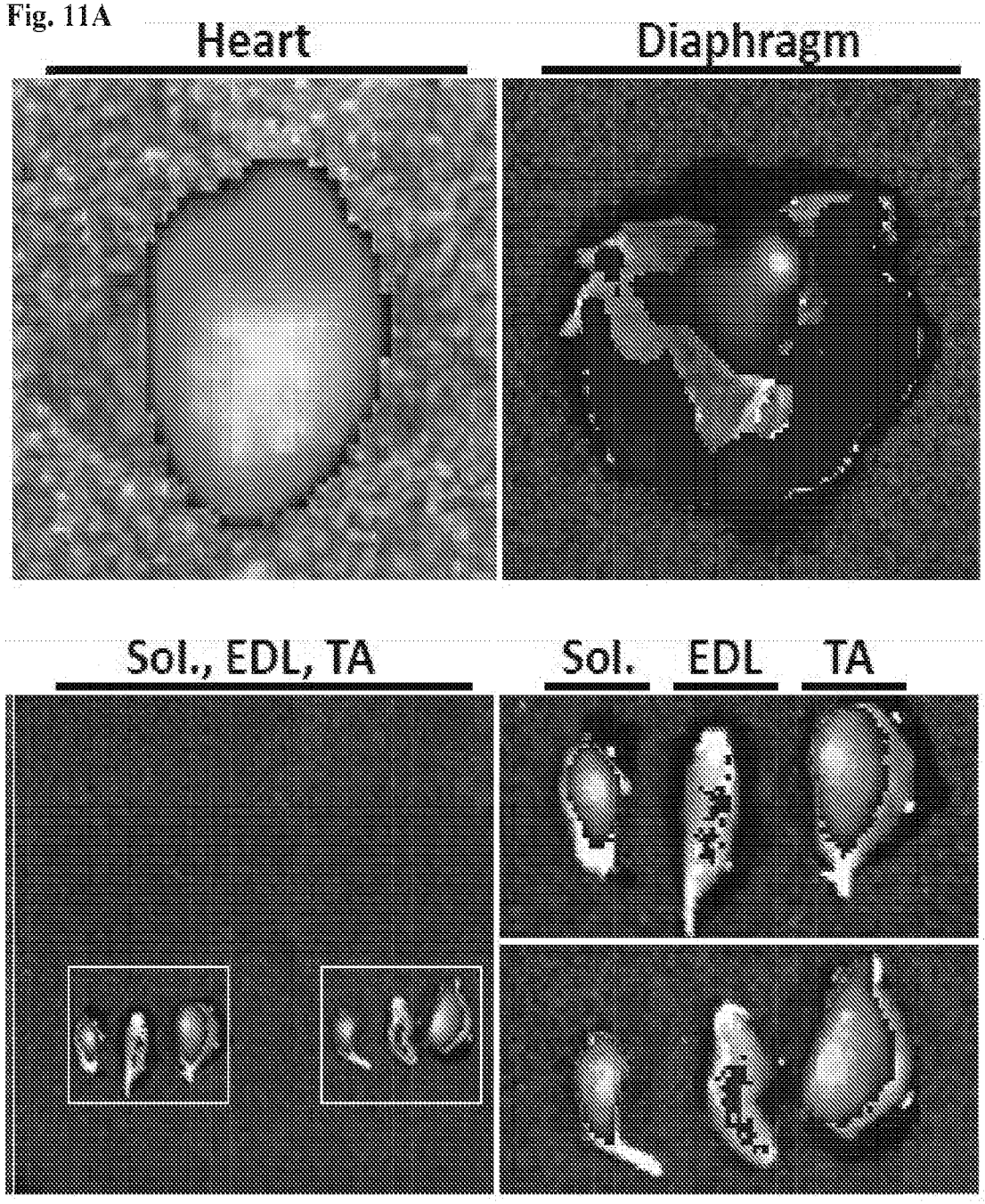

Figure 11.

Fig. 11B

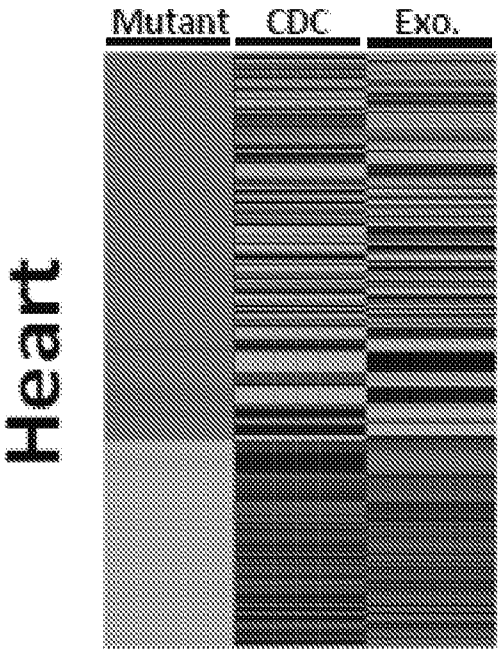

Fig. 11C

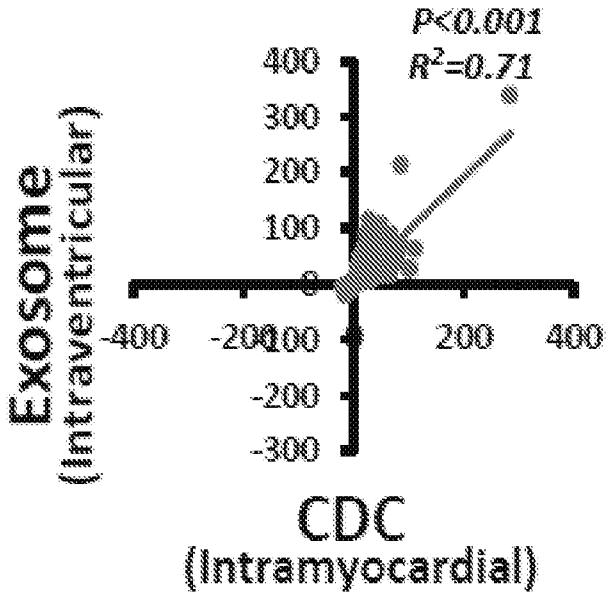

Fig. 11D

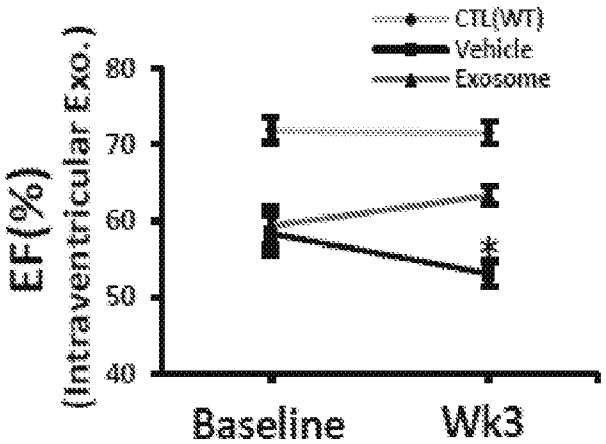

Fig. 11E

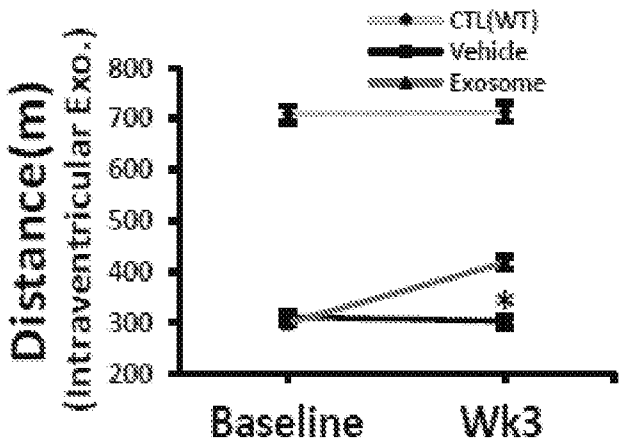

Figure 11.

Fig. 11F

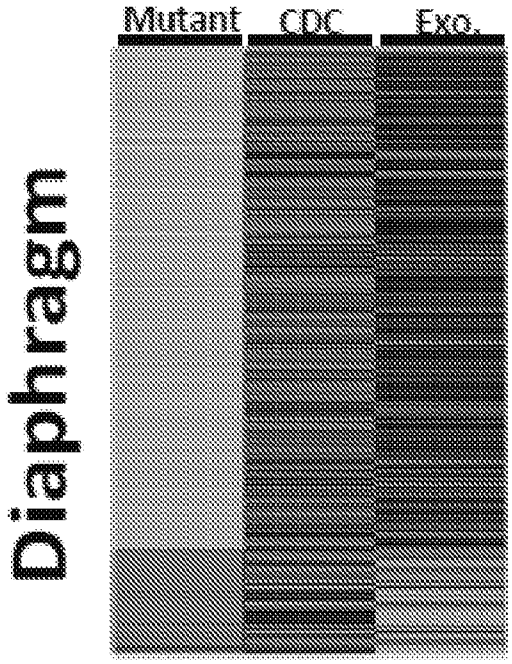

Fig. 11G

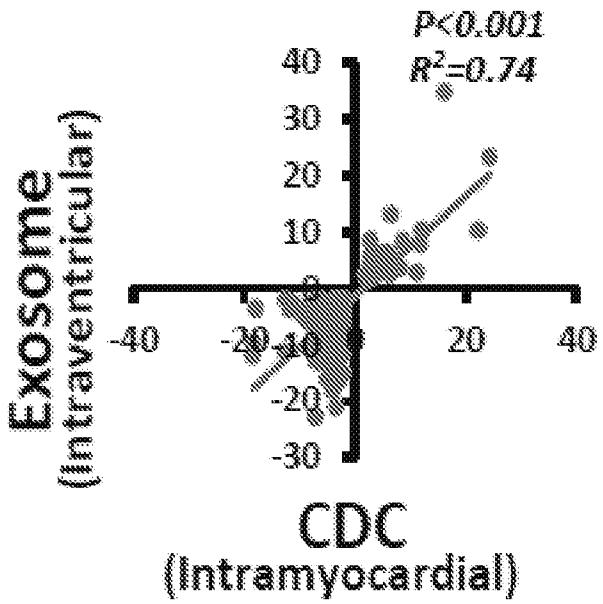

Fig. 11H

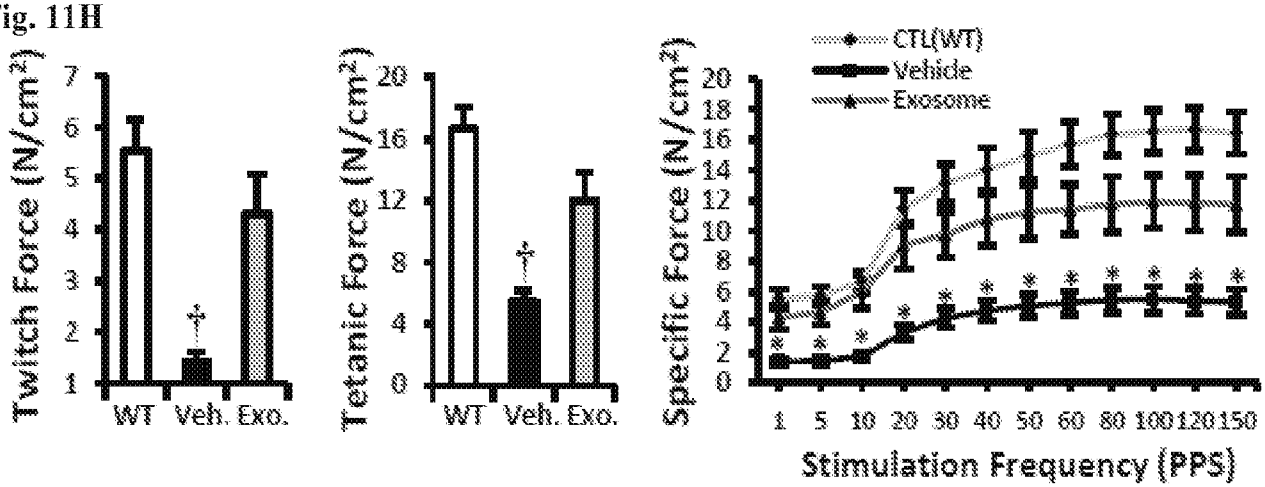

Figure 11.

Fig. 11I

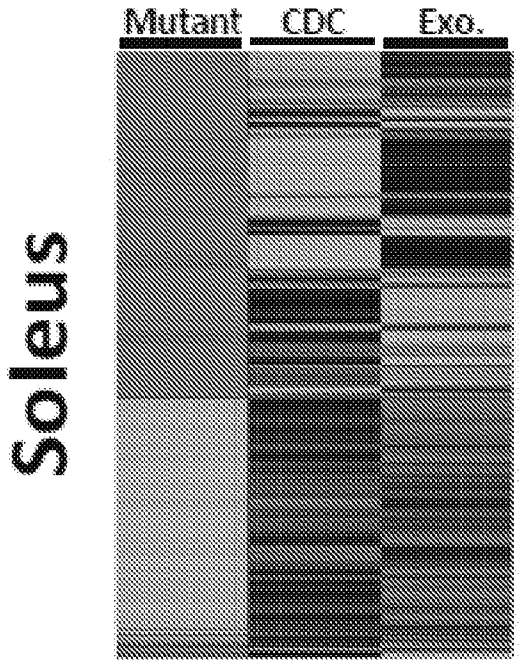

Fig. 11J

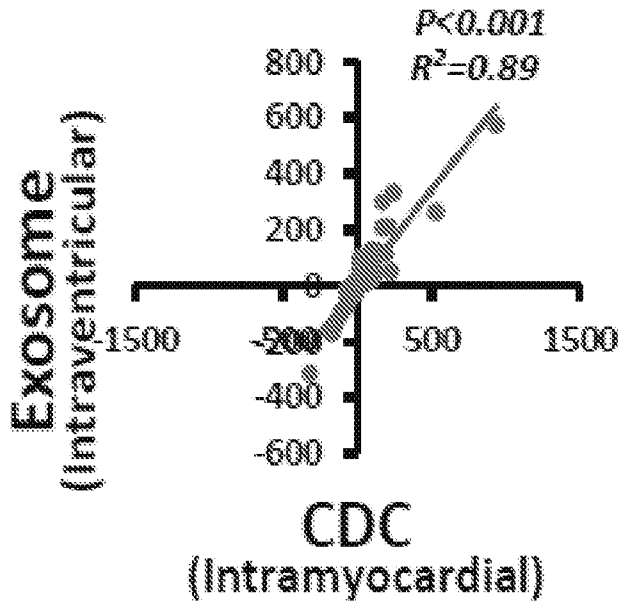

Fig. 11K

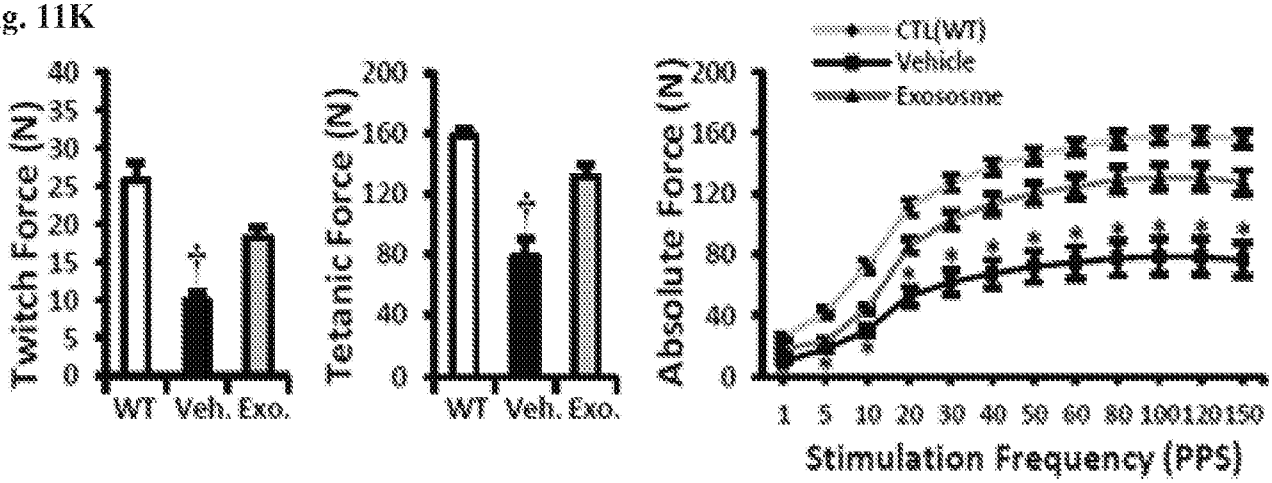

Figure 11.

Fig. 11L

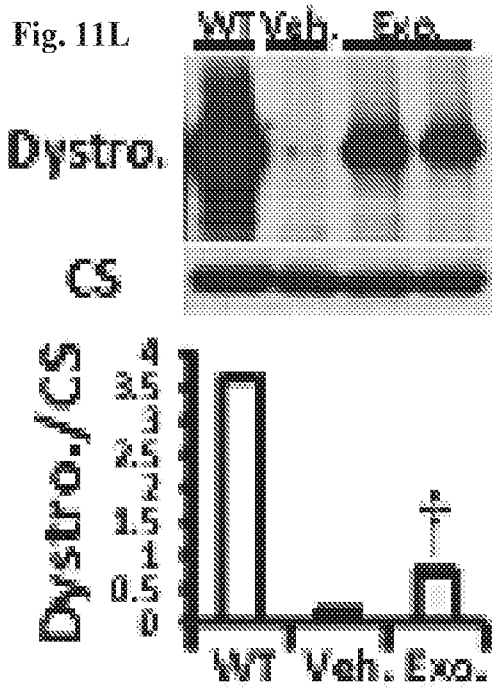

Fig. 11M

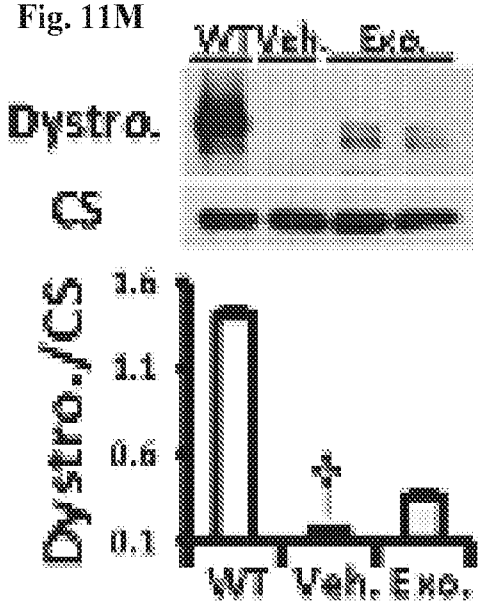

Fig. 11N

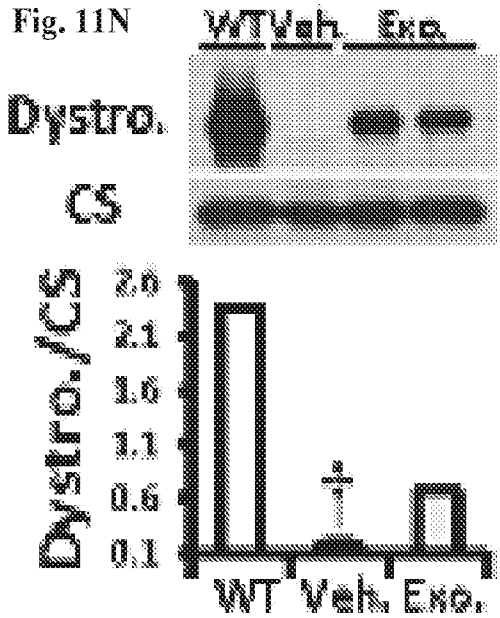

Figure 12.

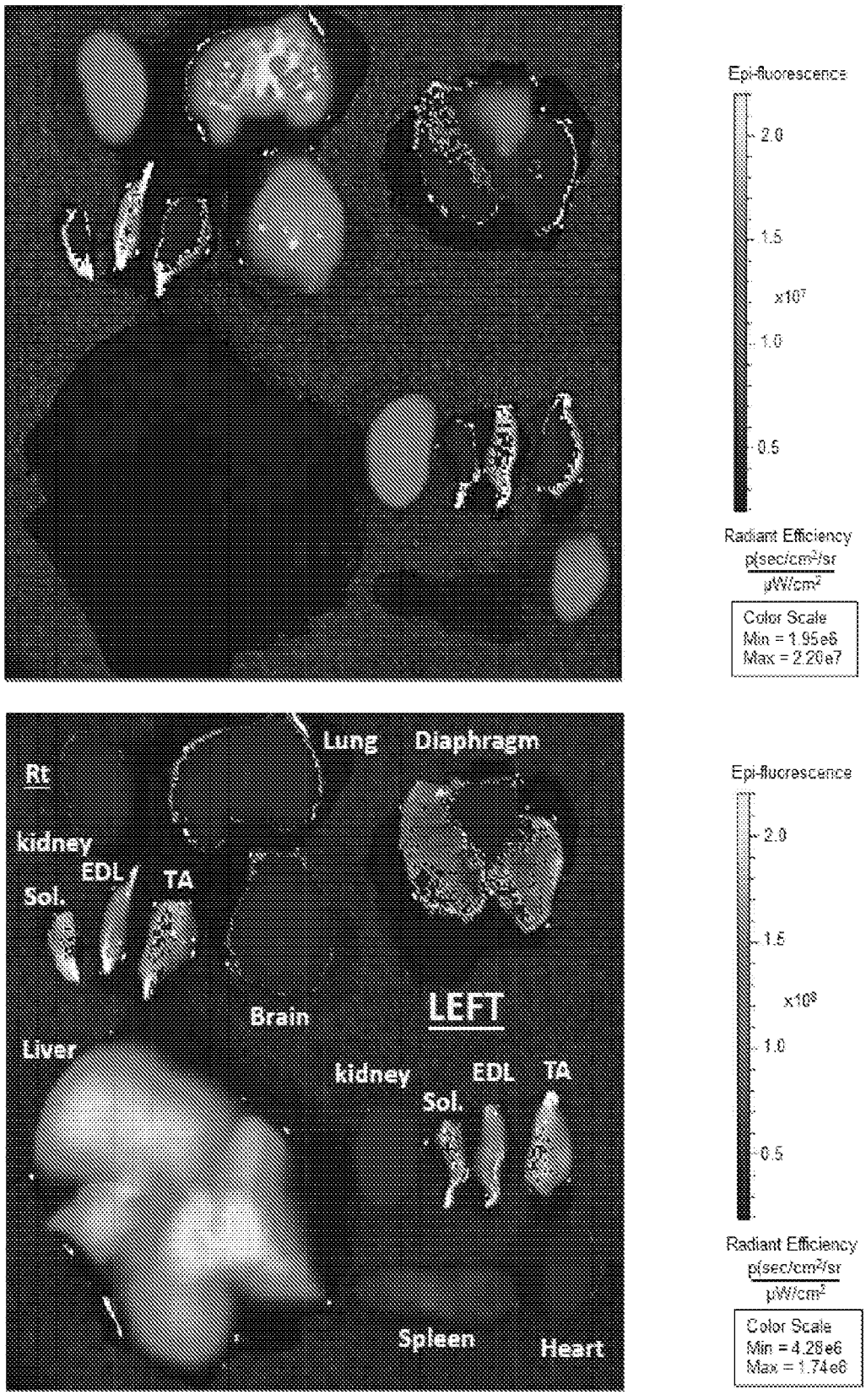
Epi-fluorescence
2.0
1.5
x10⁷
1.0
0.5
Radiant Efficiency
p(sec/cm²/sr
µW/cm²
Color Scale
Min = 1.95e6
Max = 2.20e7
Lung
Diaphragm
Rt
kidney
EDL
TA
Sol.
Brain
LEFT
Liver
kidney
EDL
TA
Sol.
Spleen
Heart
Epi-fluorescence
2.0
1.5
x10⁸
1.0
0.5
Radiant Efficiency
p(sec/cm²/sr
µW/cm²
Color Scale
Min = 4.28e6
Max = 1.74e8

Figure 13.

Fig. 13A

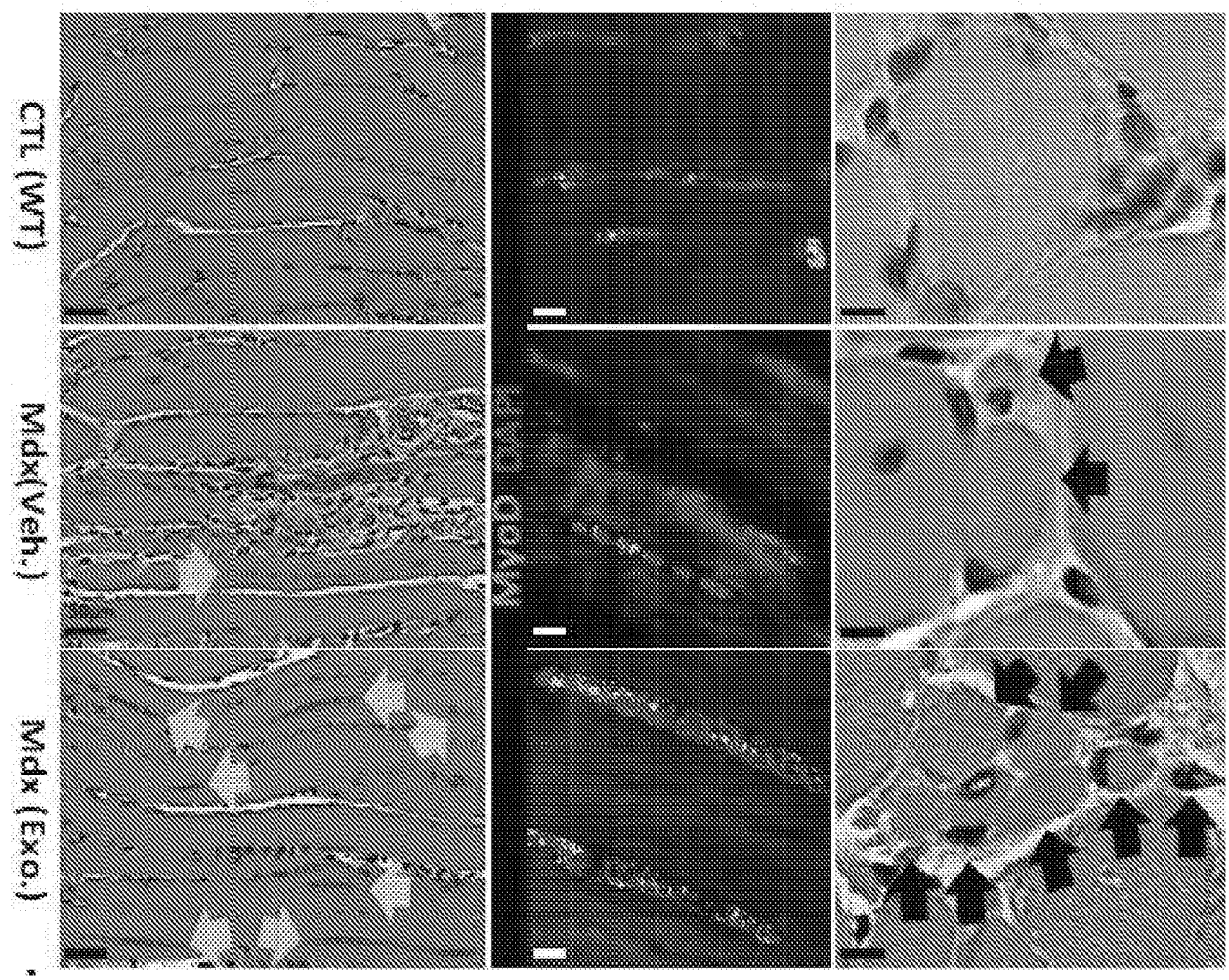

Figure 13.

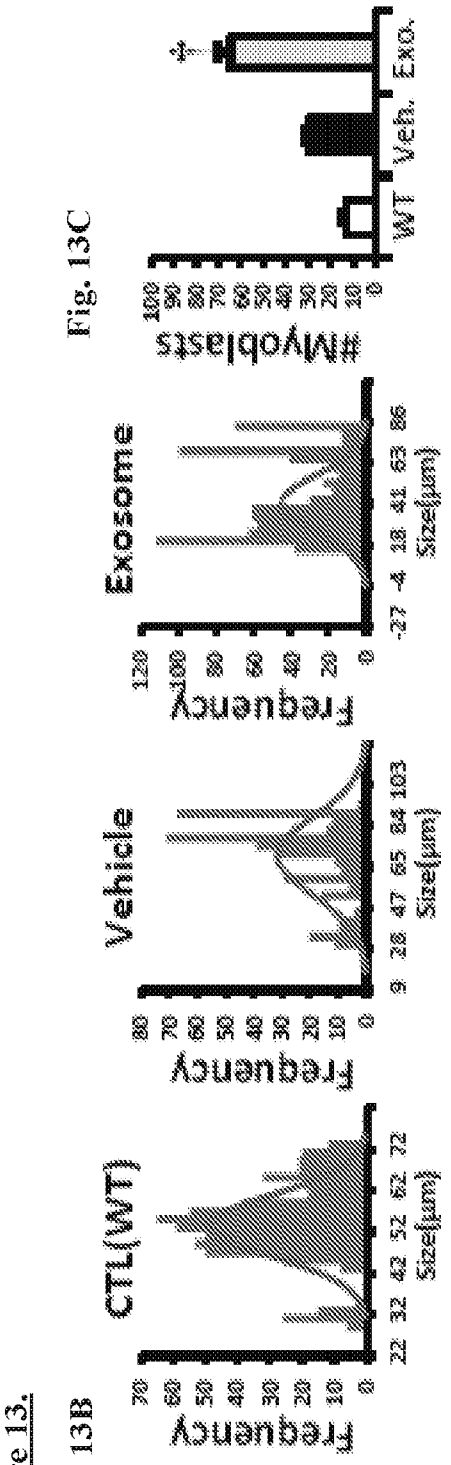
Fig. 13B
CTL(WT)
Frequency
Size(μm)
Vehicle
Exosome
Fig. 13C
#Myoblasts
WT
Veh.
Exo.

Figure 13.

Fig. 13D

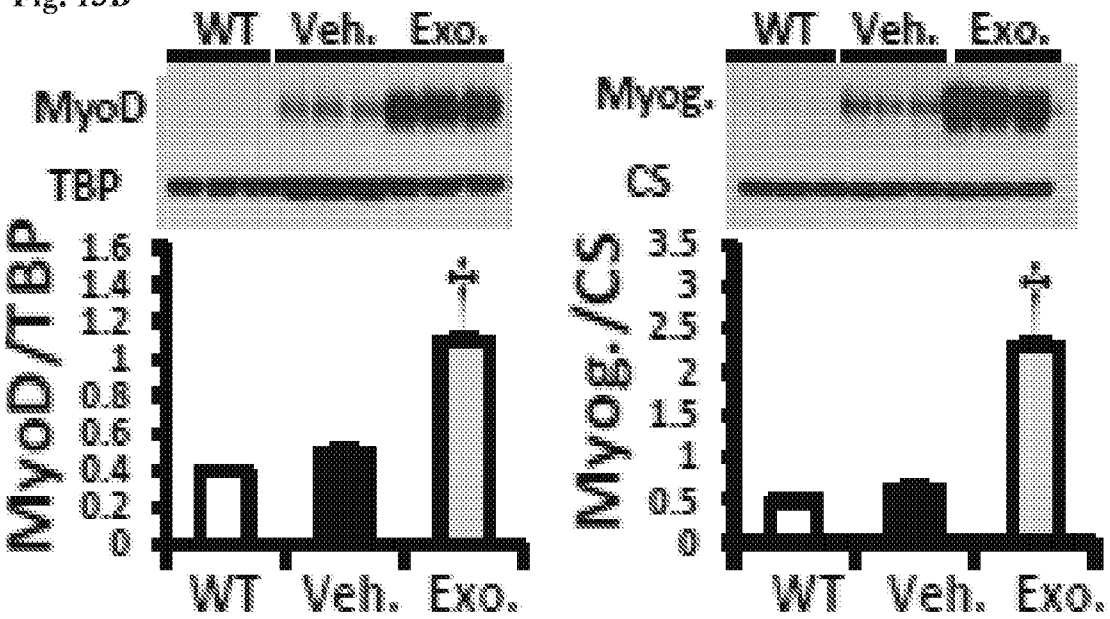

Fig. 13E

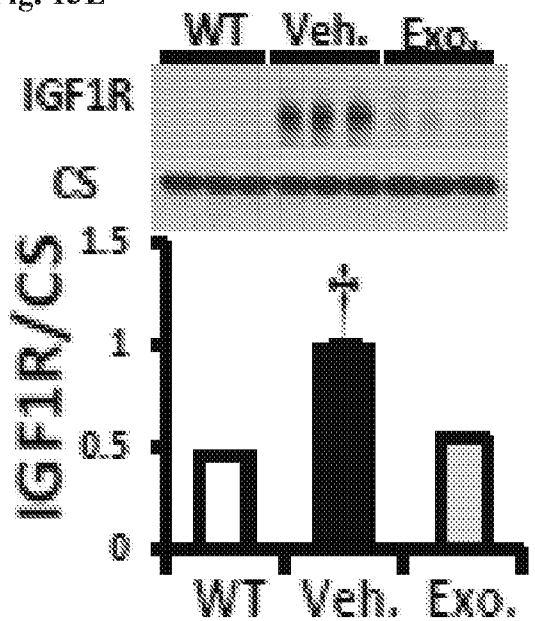

Fig. 13F

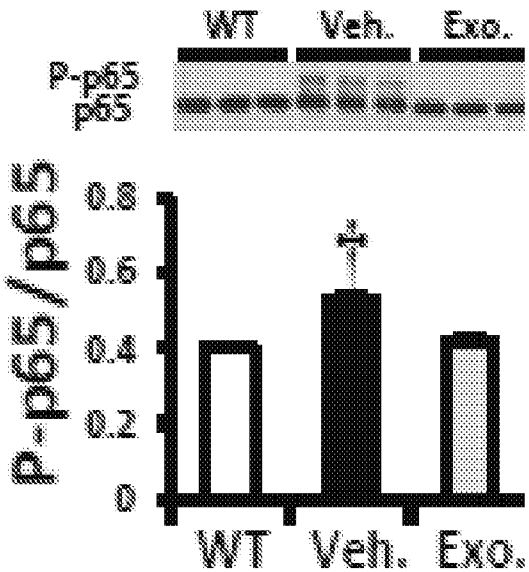

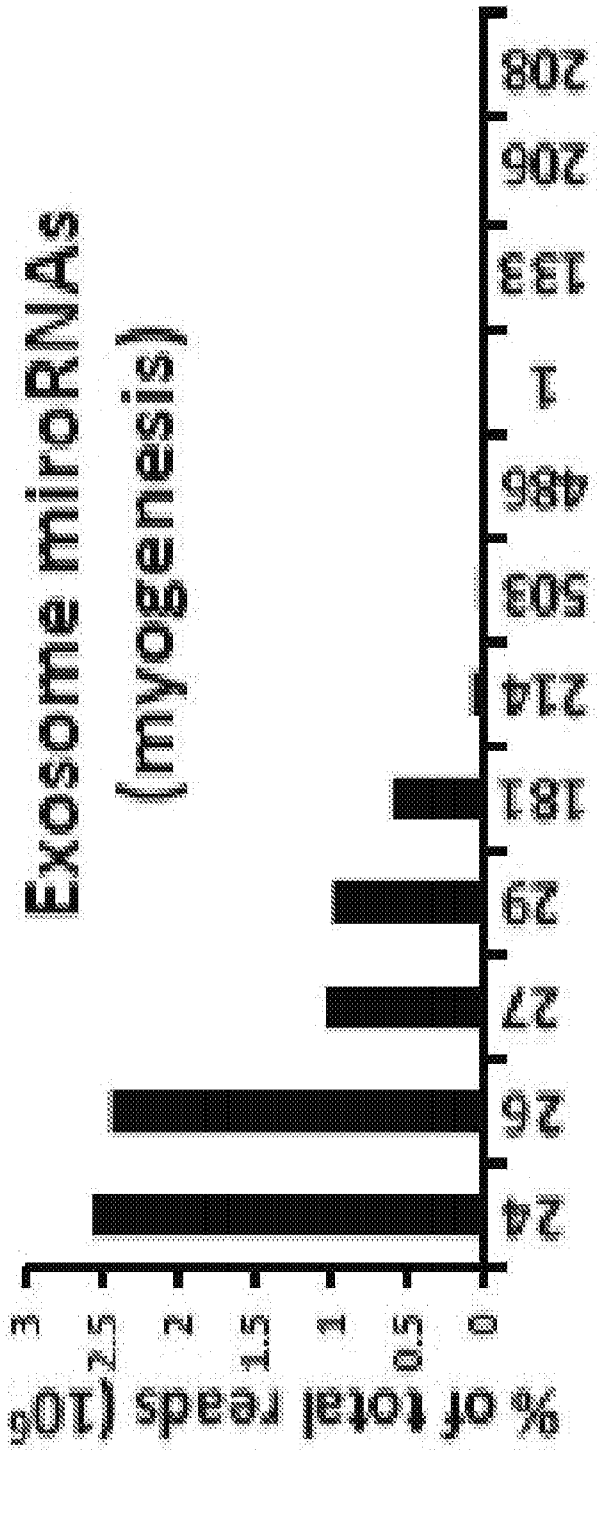

Figure 13.

Fig. 13G

Figure 13.

Fig. 13H

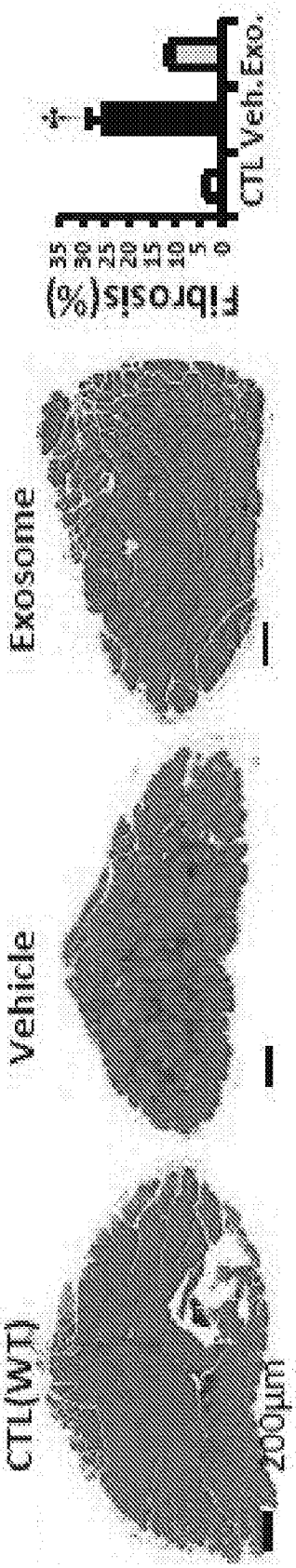

Fig. 13I

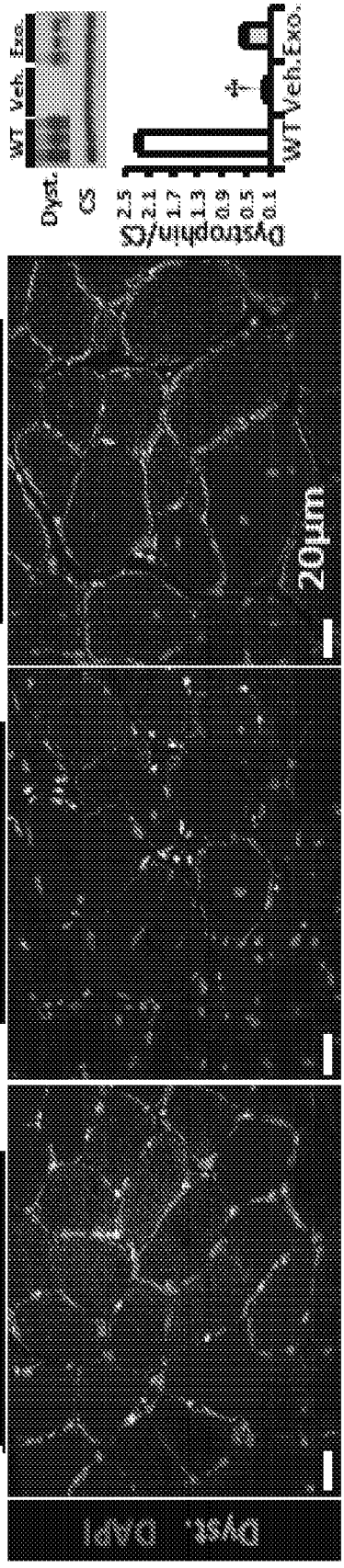

Figure 13.

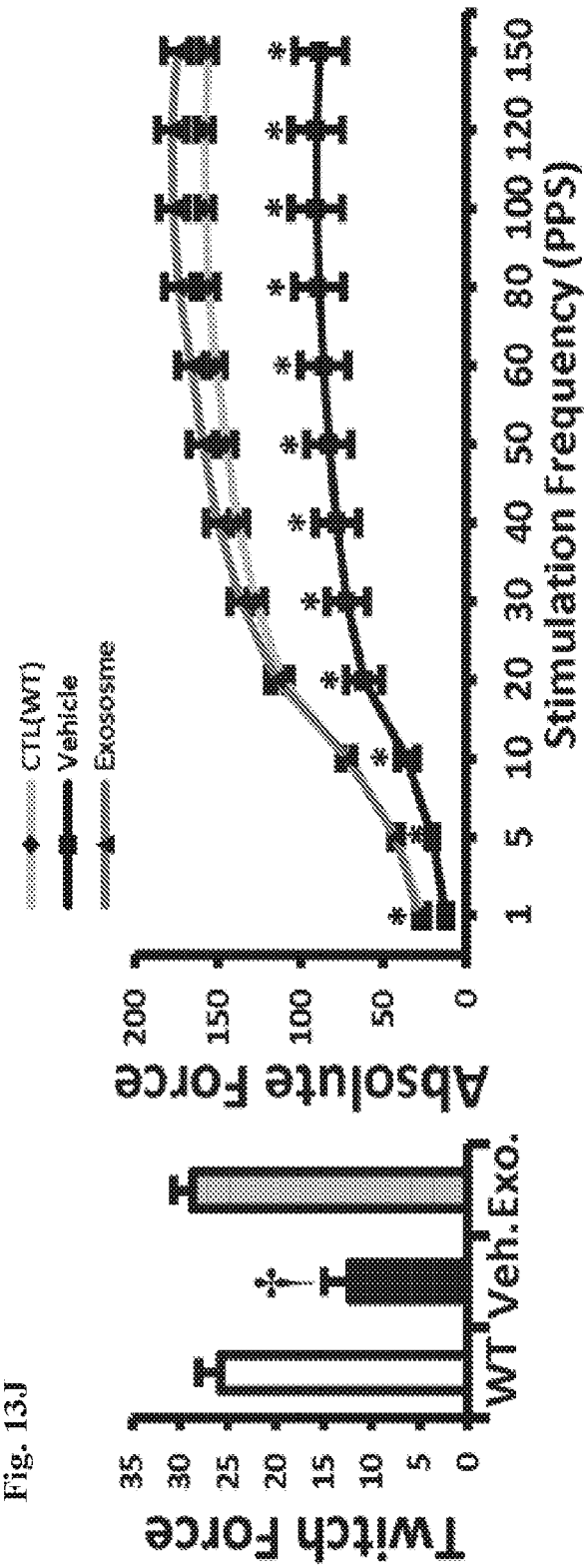

Fig. 13J

Figure 14.

Fig. 14A

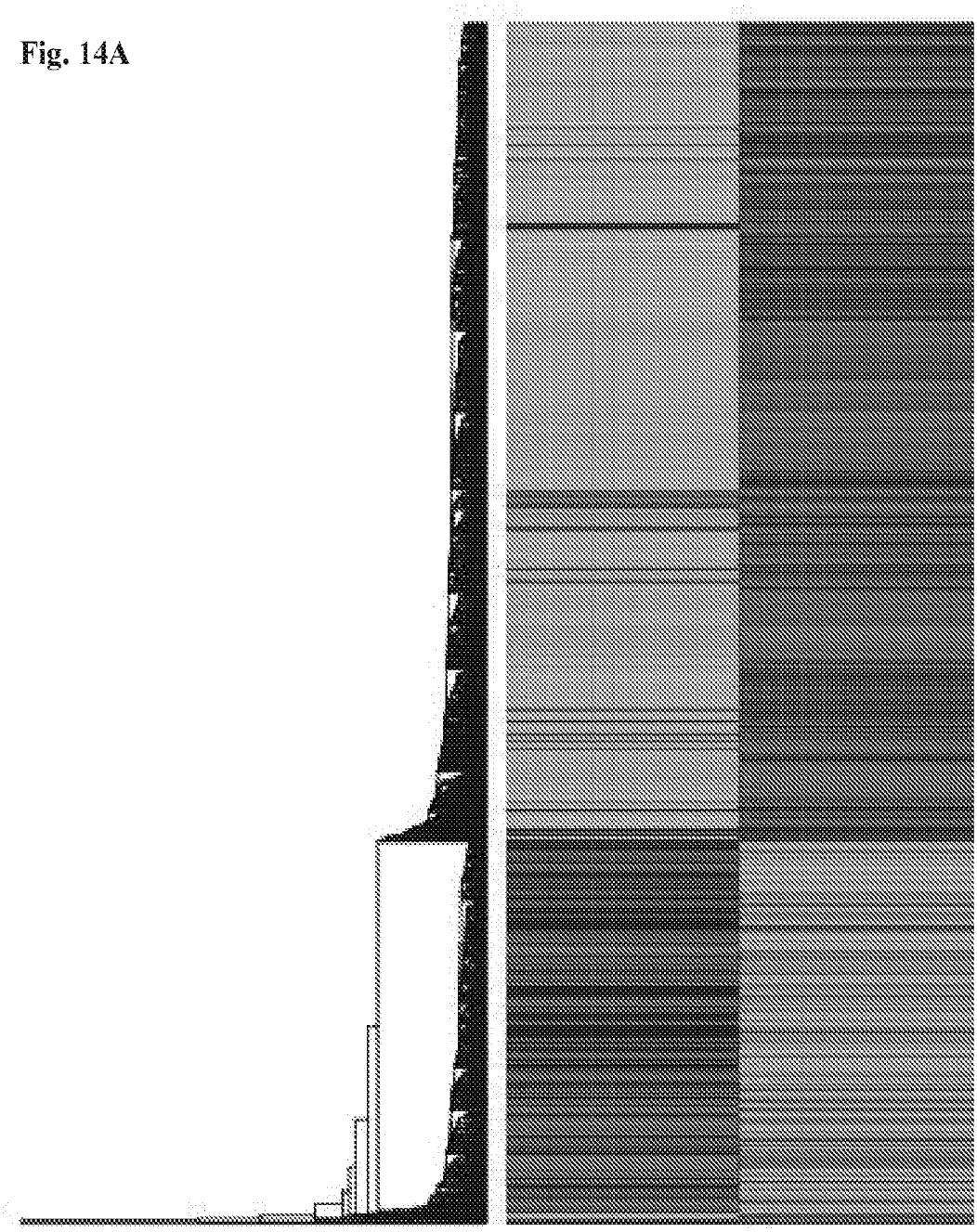

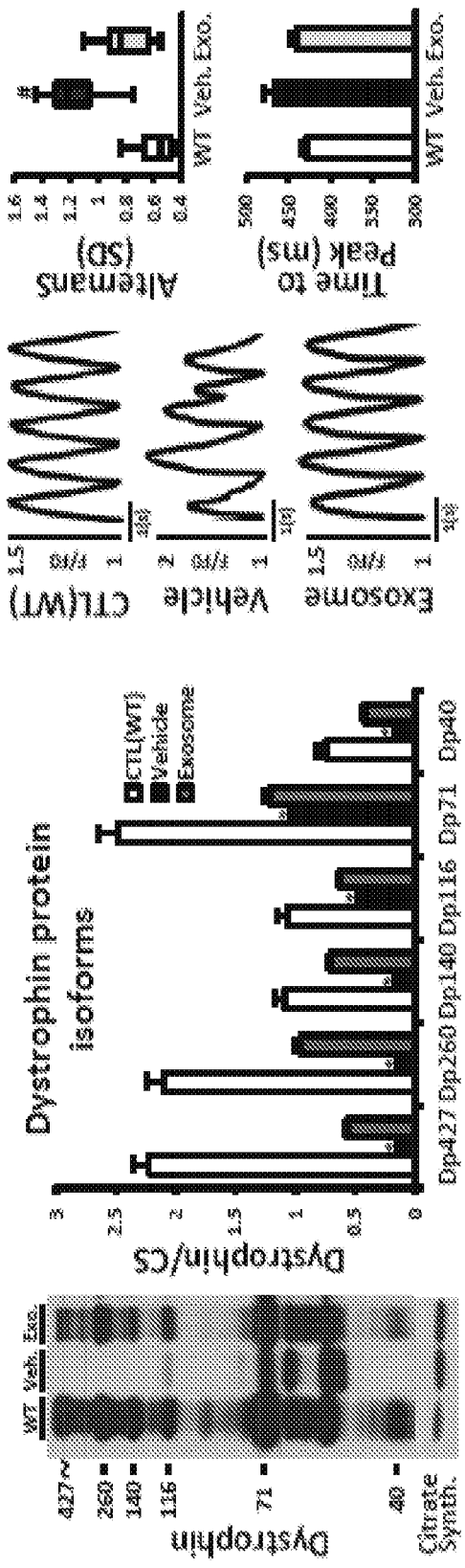

Figure 14.

Fig. 14B

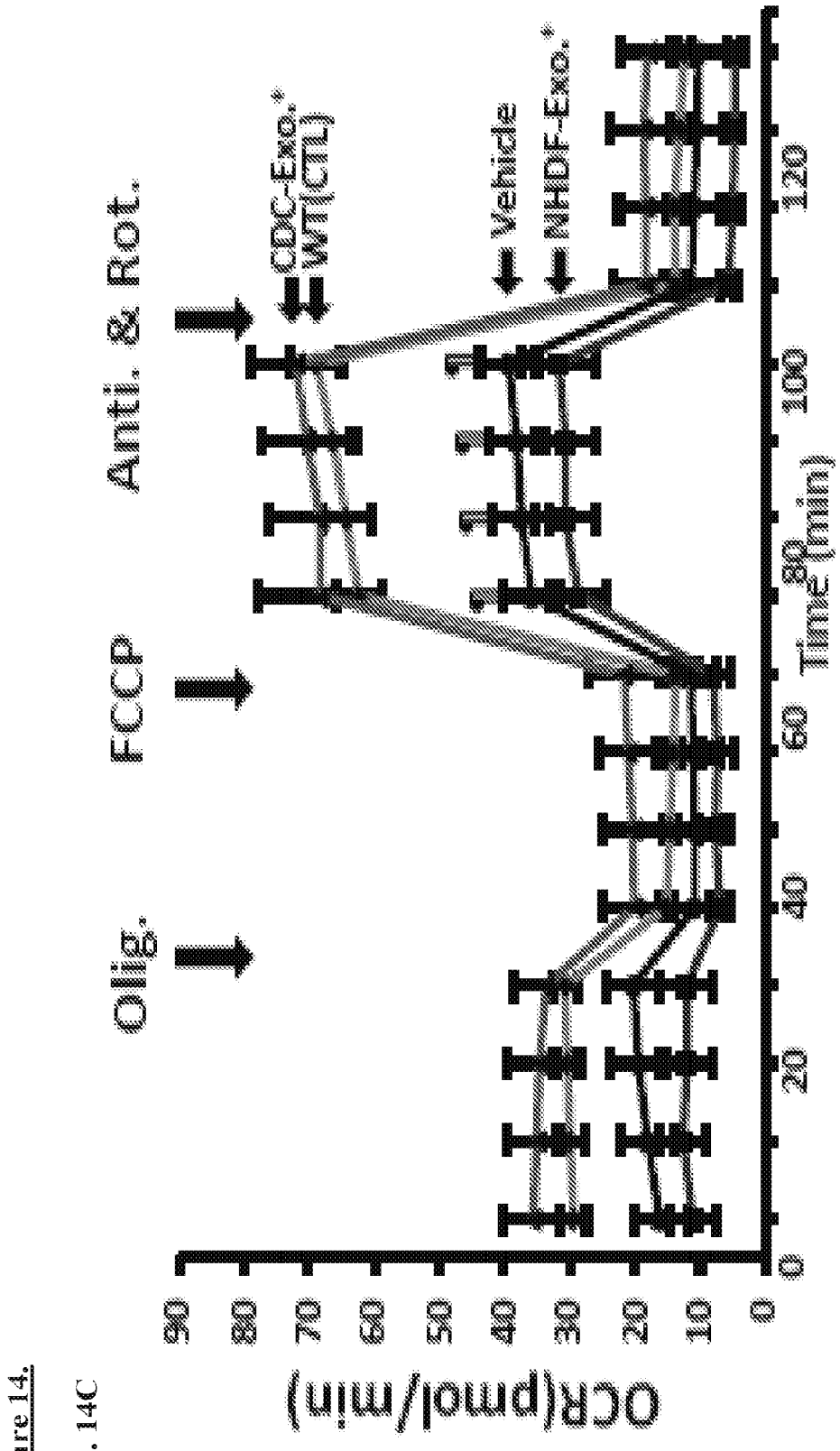

Figure 14.

Fig. 14C

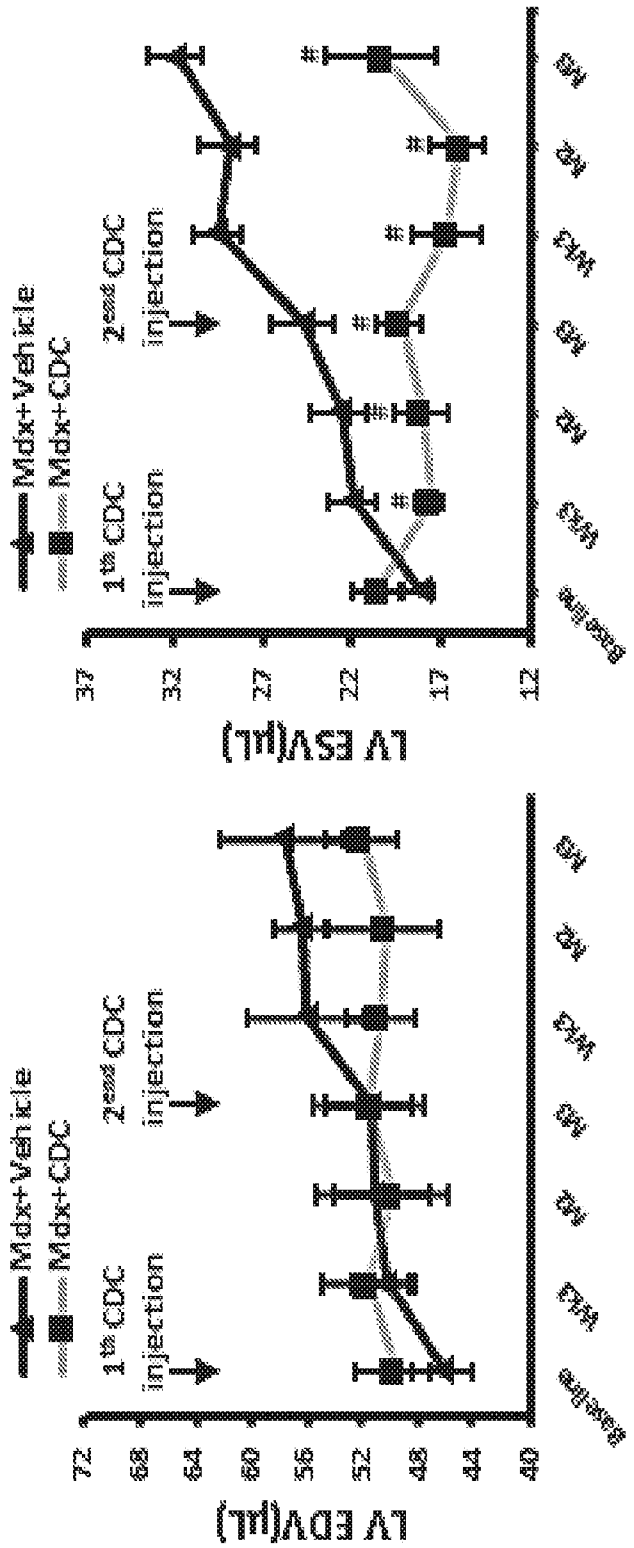
Mdx+Vehicle
Mdx+CDC
1th CDC injection
2end CDC injection
LV EDV(μL)
LV ESV(μL)
Baseline
4th
7th
14th
21th
28th

Figure 15.

Figure 16.

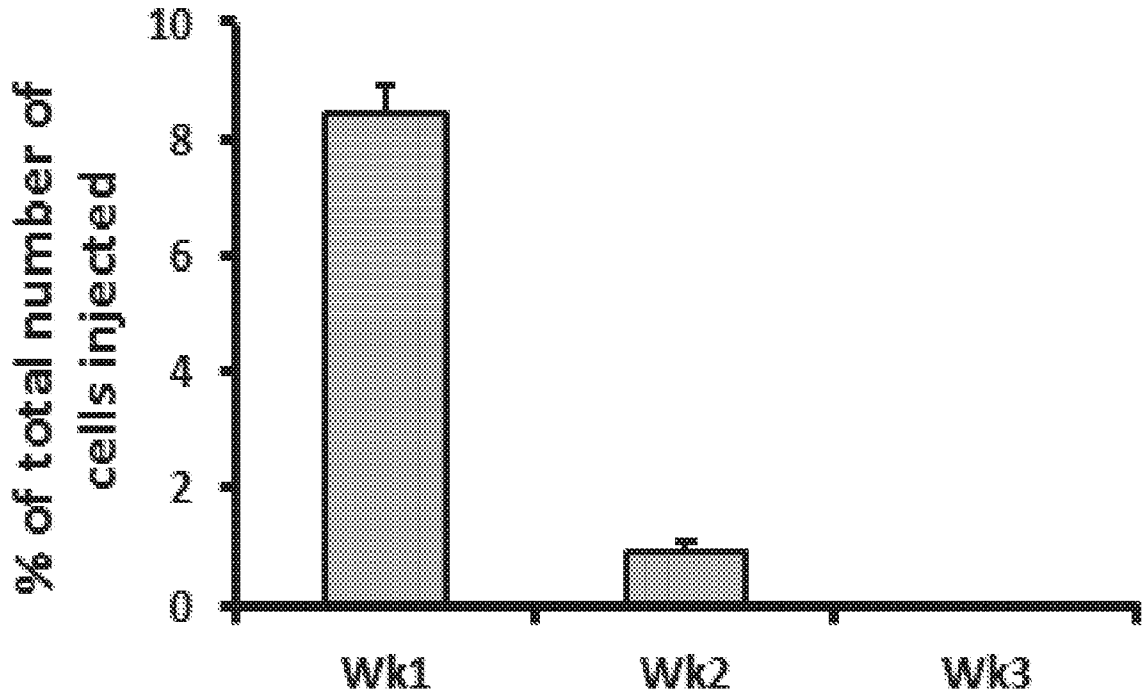

Figure 17.

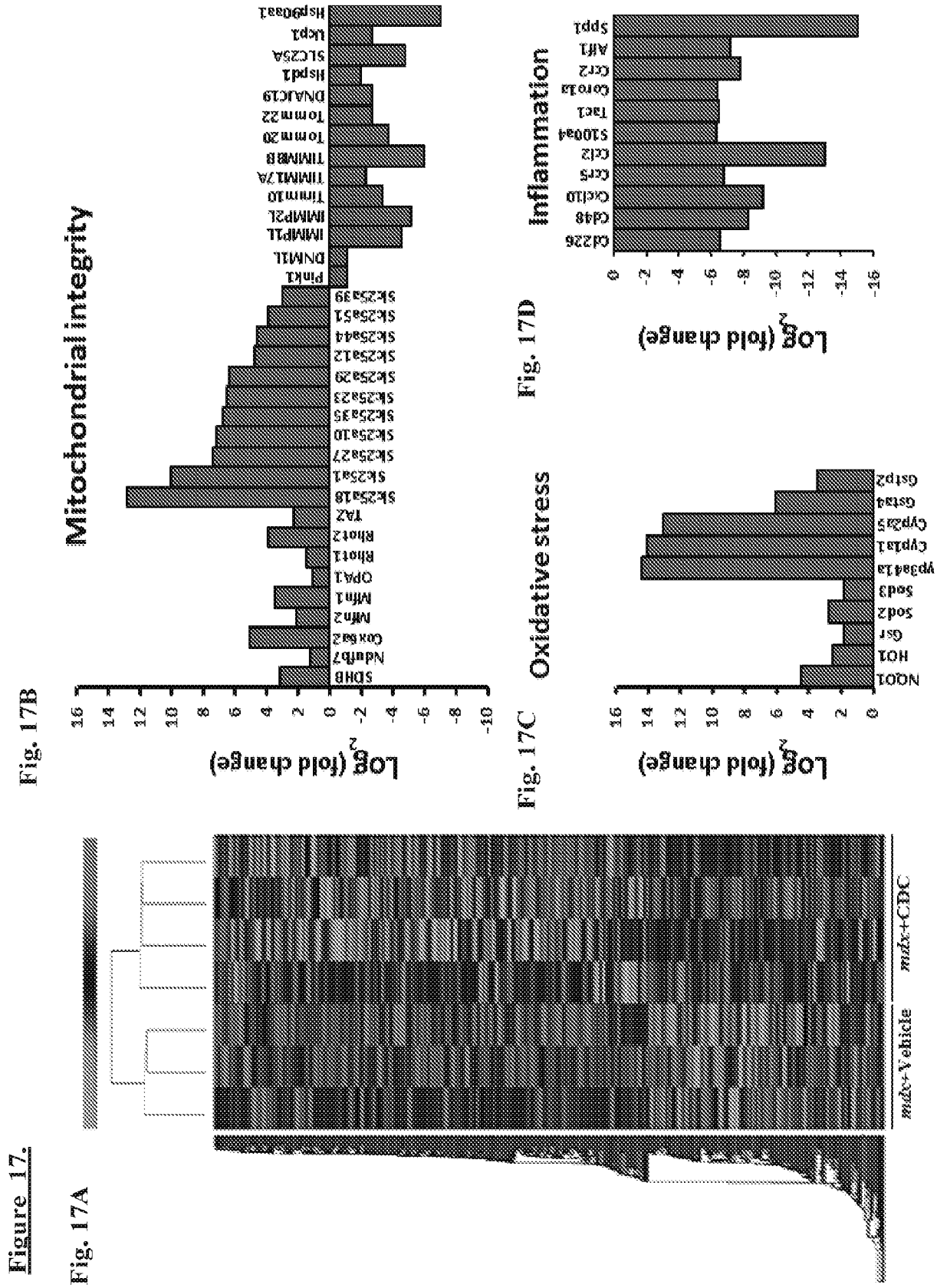
Fig. 17A
mdx+Vehicle
mdx+CDC
Fig. 17B
Mitochondrial integrity
Log2 (fold change)
SDHB
Ndufb7
Cox6a2
Mfn2
Mfn1
OPA1
Rhot1
Rhot2
TA2
Slc25a18
Slc25a1
Slc25a27
Slc25a10
Slc25a35
Slc25a23
Slc25a29
Slc25a12
Slc25a44
Slc25a51
Slc25a39
Pink1
DNM1L
IMMP1L
IMMP2L
Timm10
TIMM17A
TIMM8B
Tomm20
Tomm22
DNAJC19
Hspd1
SLC25A
Lkp1
Hspb0aa1
Fig. 17C
Oxidative stress
Log2 (fold change)
NQO1
HO1
Gsr
Sod2
Sod3
Cyp3a1a
Cyp1a1
Cyp2b5
Gsta4
Gstp2
Fig. 17D
Inflammation
Log2 (fold change)
Ccl26
Ccl48
Ccl10
Ccr5
Ccl2
S100a4
Tac1
Cxcl3a
Ccr2
Aif1
Spp1

Figure 18.

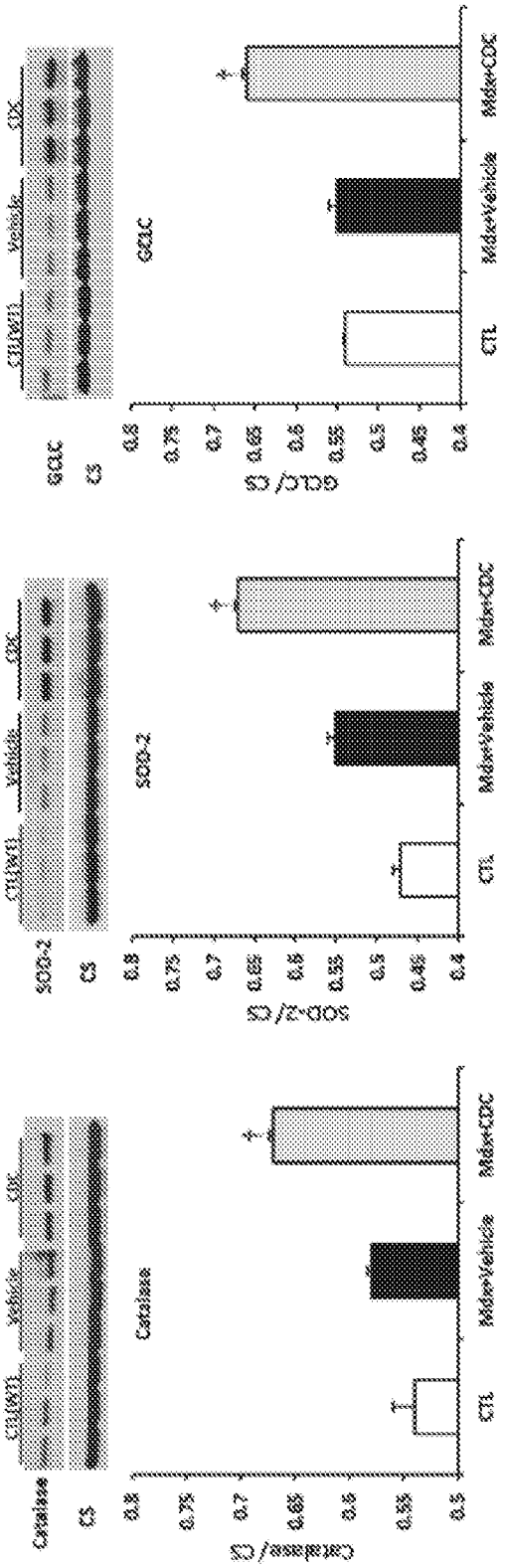
Catalase
CS
CTL(WT)
Vehicle
CDC
Catalase
CTL
Mdx+Vehicle
Mdx+CDC
Catalase/CS
SOD-2
CS
SOD-2
SOD-2/CS
GCLC
CS
GCLC
GCLC/CS

Figure 19.

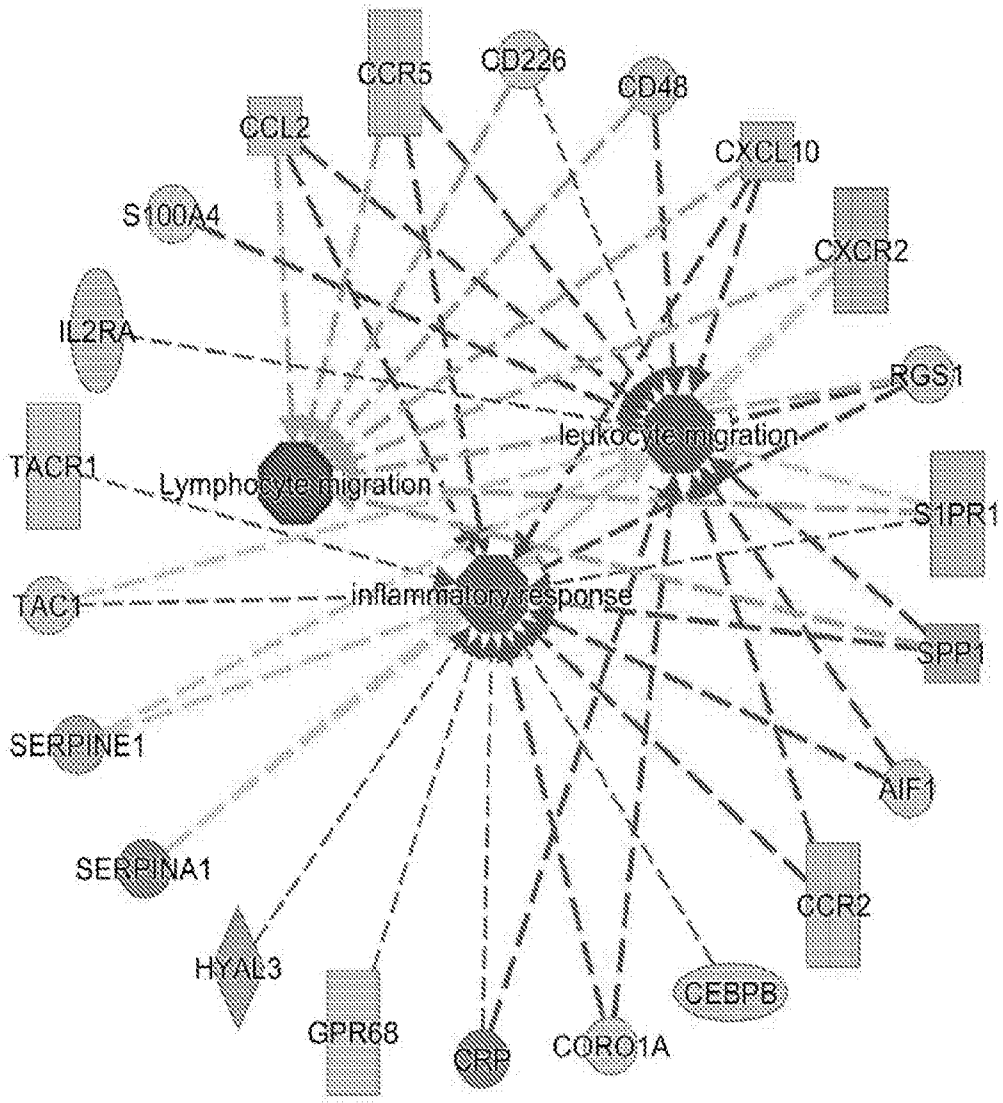
CCR5
CD226
CD48
CCL2
CXCL10
S100A4
CXCR2
IL2RA
RGS1
leukocyte migration
TACR1
Lymphocyte migration
S1PR1
TAC1
inflammatory response
SPP1
SERPINE1
AIF1
SERPINA1
CCR2
HYAL3
CEBPB
GPR68
CRP
CORO1A

Figure 20.

Fig. 20A
Mdx+Vehicle

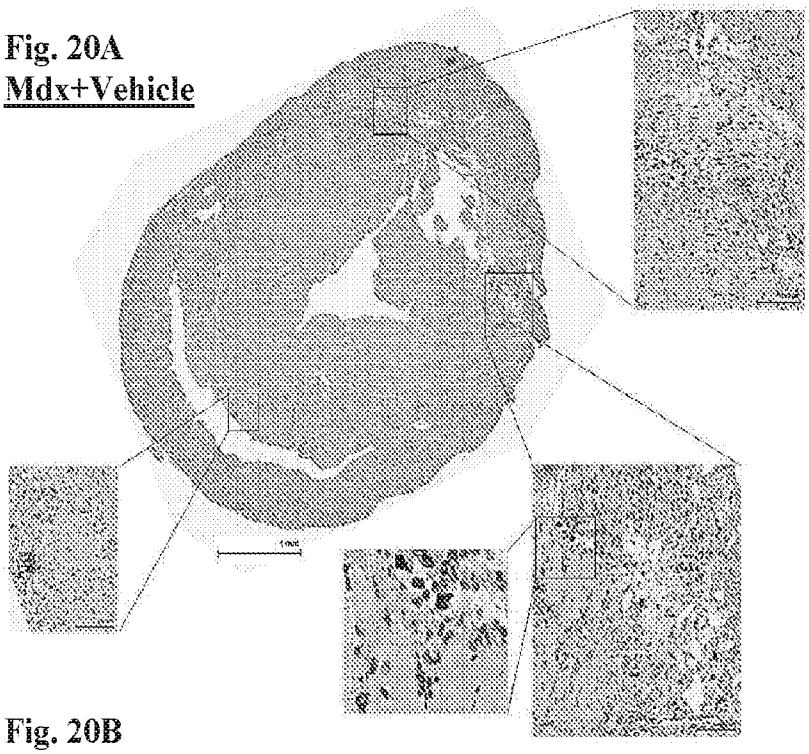

Fig. 20B
Mdx+CDC

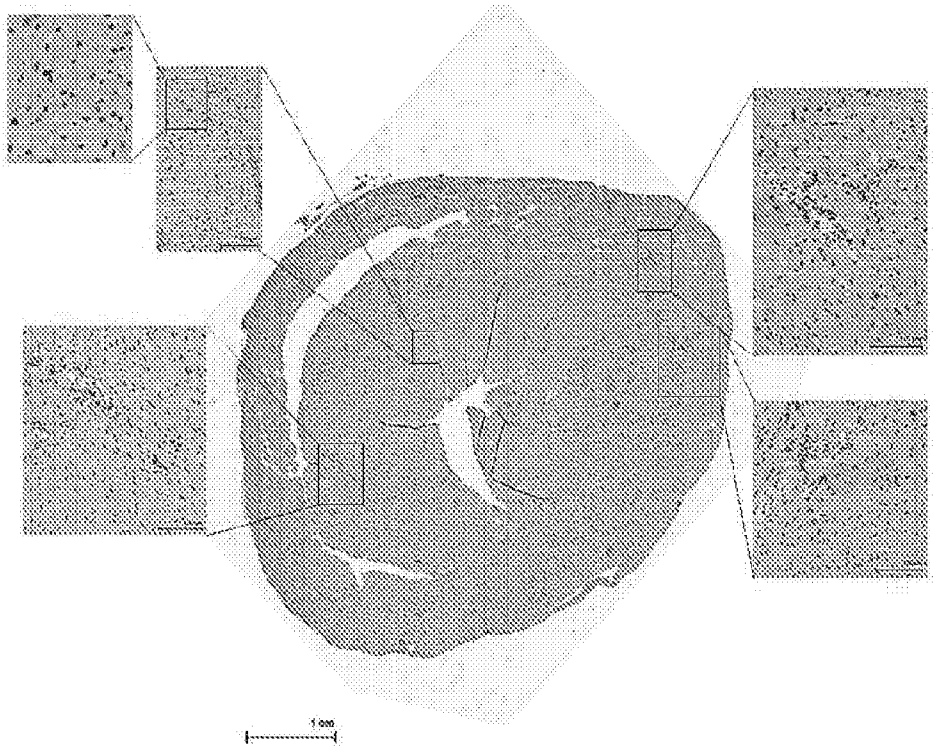

Figure 20.

Fig. 20C
CTL(WT)

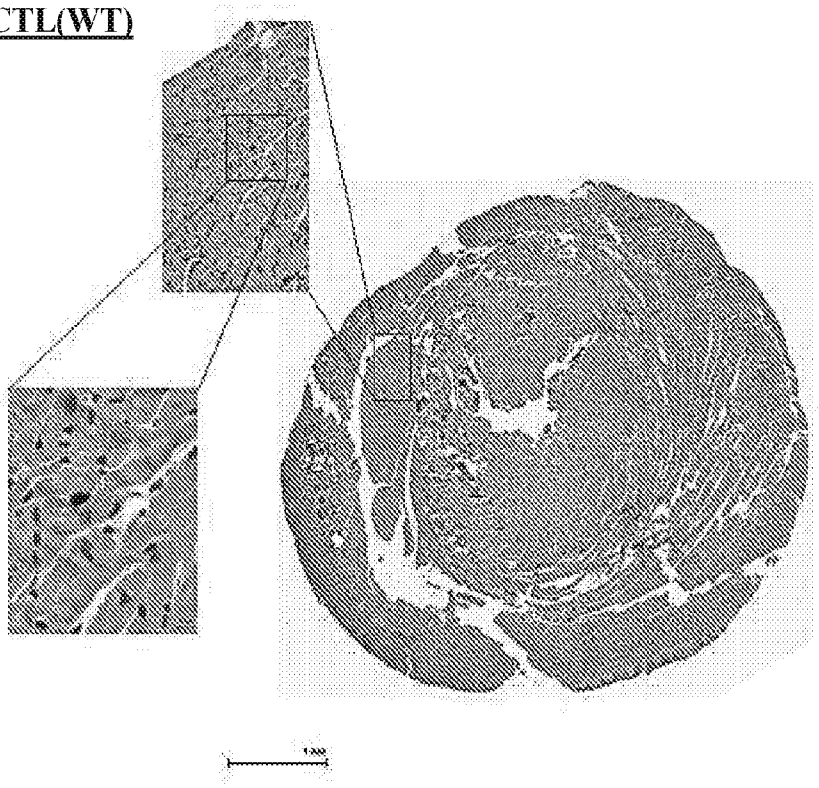

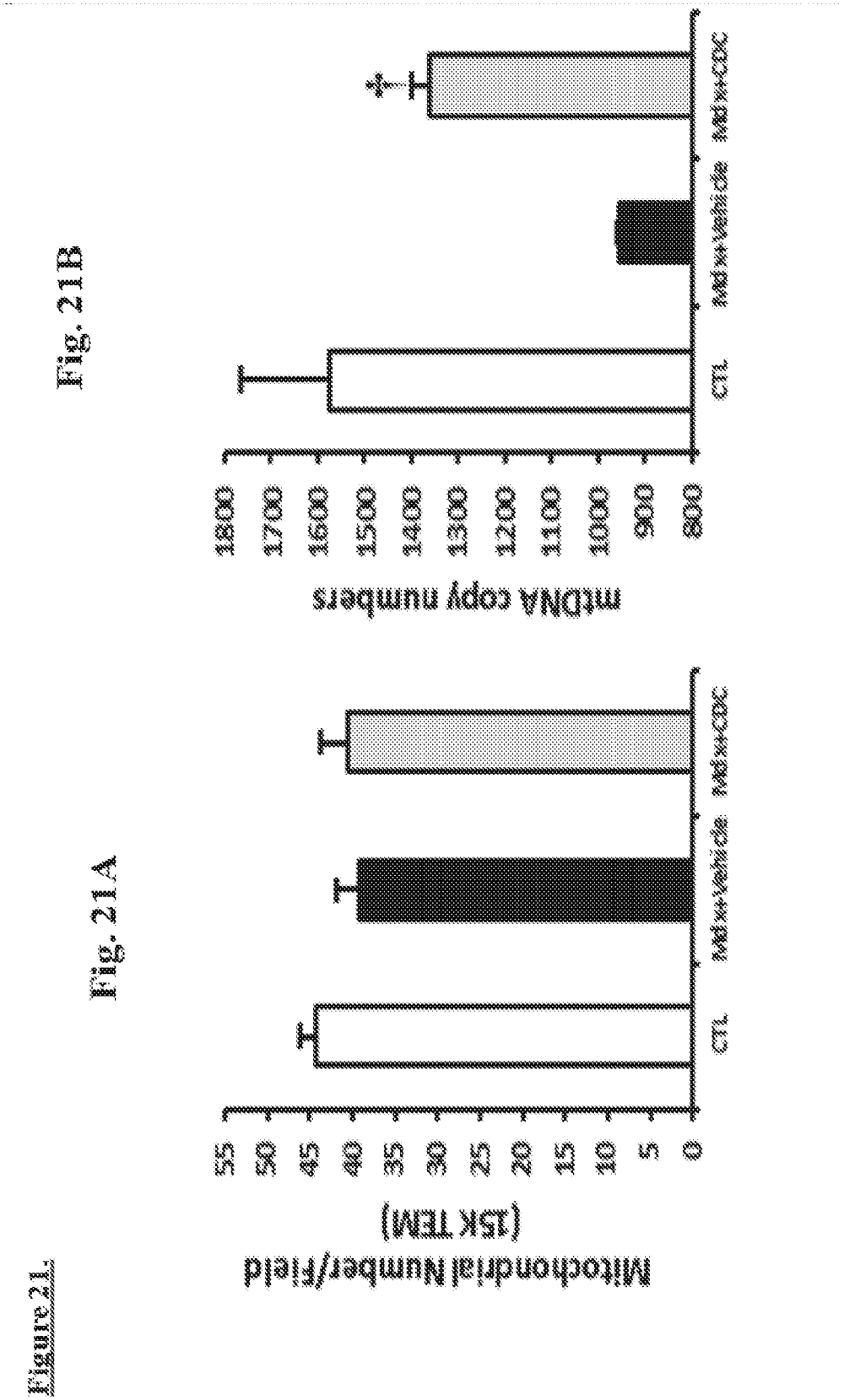
Fig. 21B
mtDNA copy numbers
1800
1700
1600
1500
1400
1300
1200
1100
1000
900
800
CTL
Mdx+vehicle
Mdx+CDC
*
Fig. 21A
Mitochondrial Number/field
(15K TEM)
55
50
45
40
35
30
25
20
15
10
5
0
CTL
Mdx+vehicle
Mdx+CDC

Figure 21.

Figure 22.

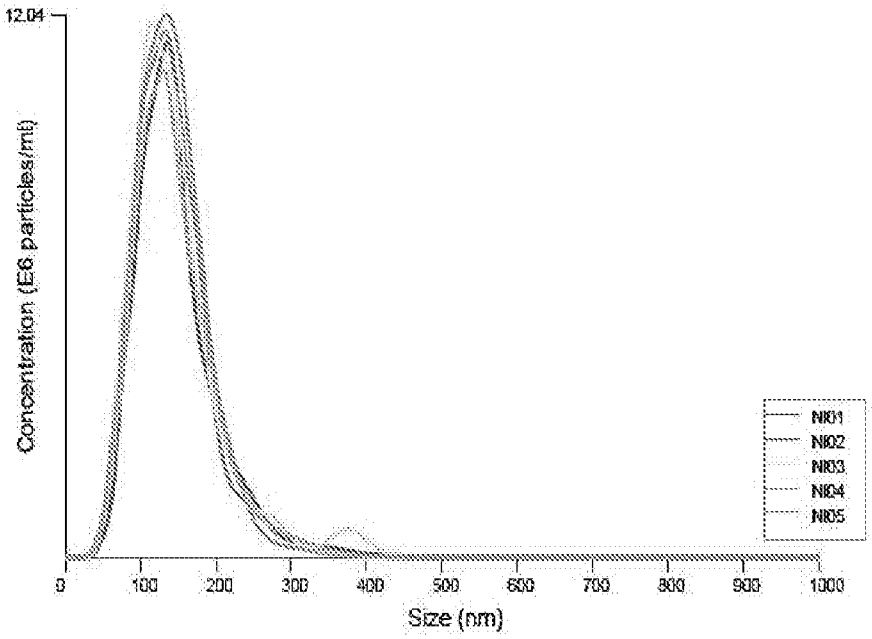

Size / Concentration

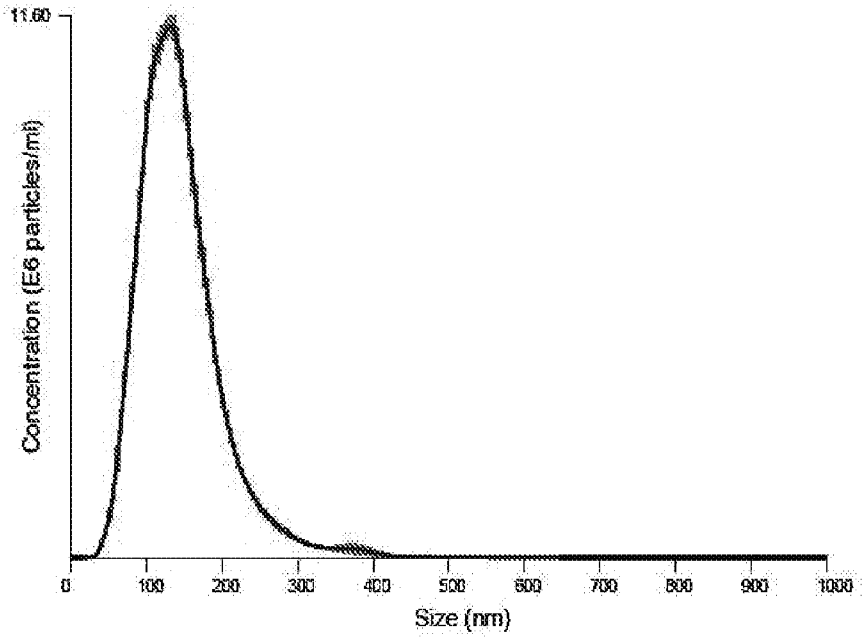

Averaged Size / Concentration
Red error bars indicate +/- 1 standard error of the mean

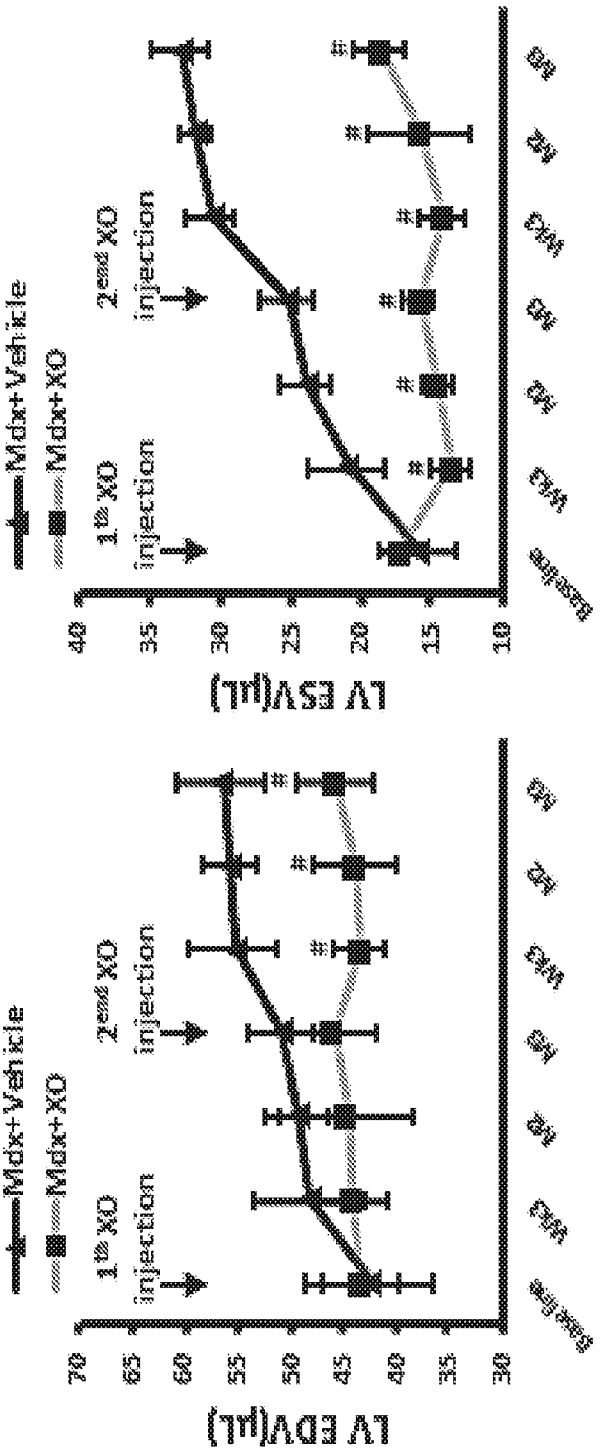
Mdx+Vehicle
Mdx+XO
1st XO injection
2end XO injection
LV EDV(μL)
LV ESV(μL)
Baseline
1M
2M
3M
4M
5M
6M
#

Figure 23.

Figure 24.

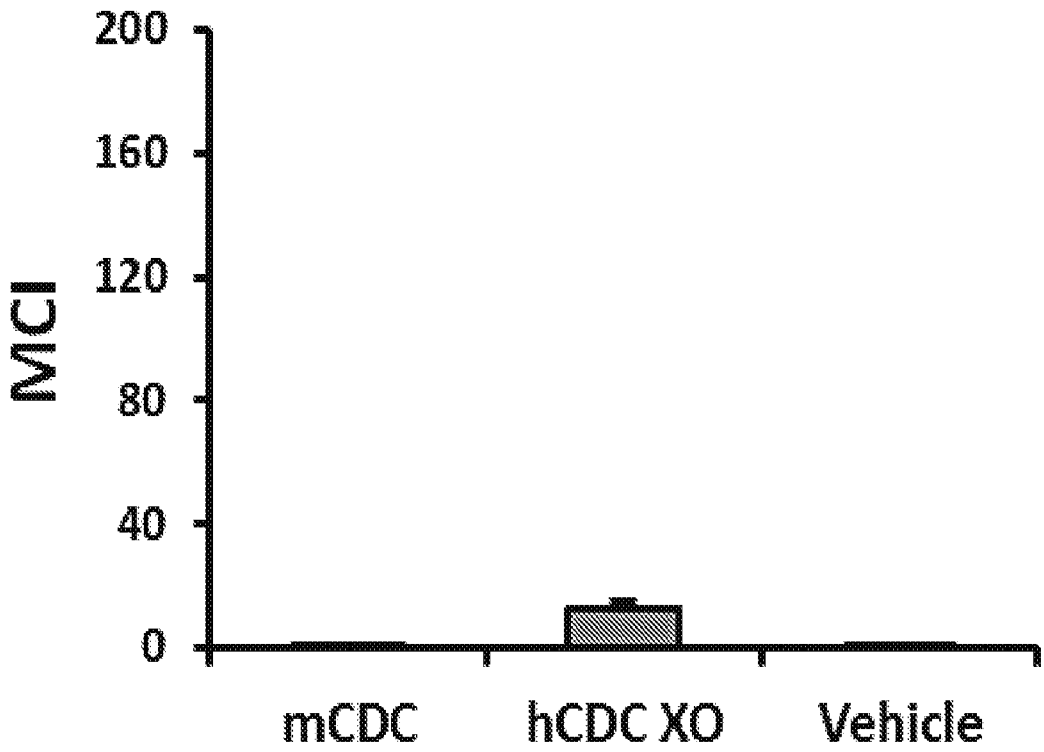

Figure 25.

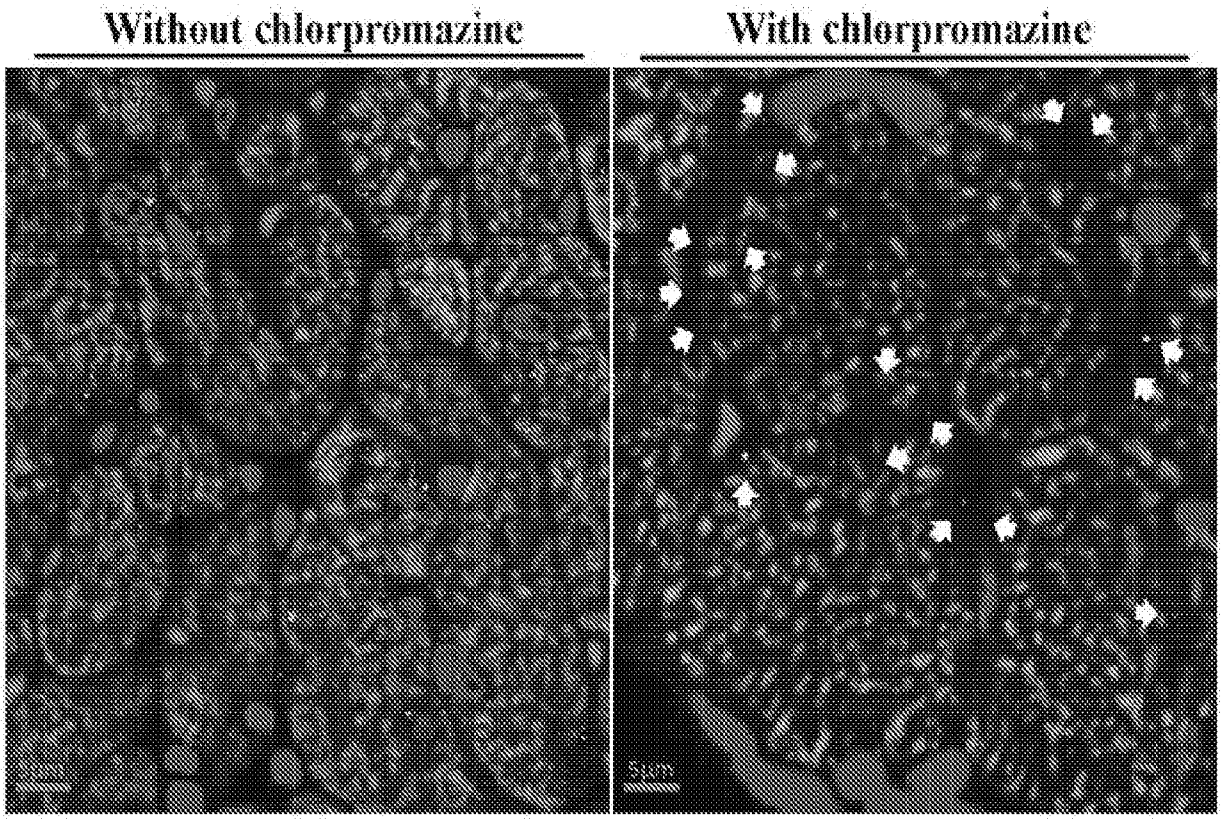

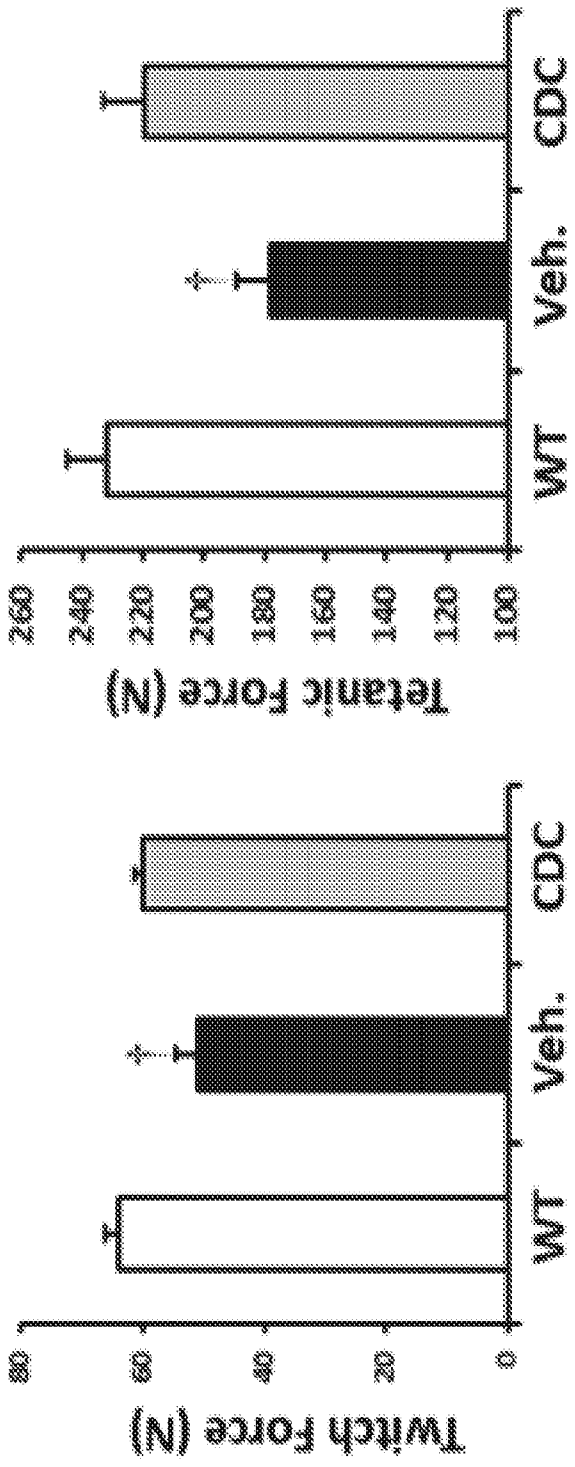
Twitch Force (N)
80
60
40
20
0
WT
Veh.
CDC
Tetanic Force (N)
260
240
220
200
180
160
140
120
100
WT
Veh.
CDC

Figure 26.

Figure 27.

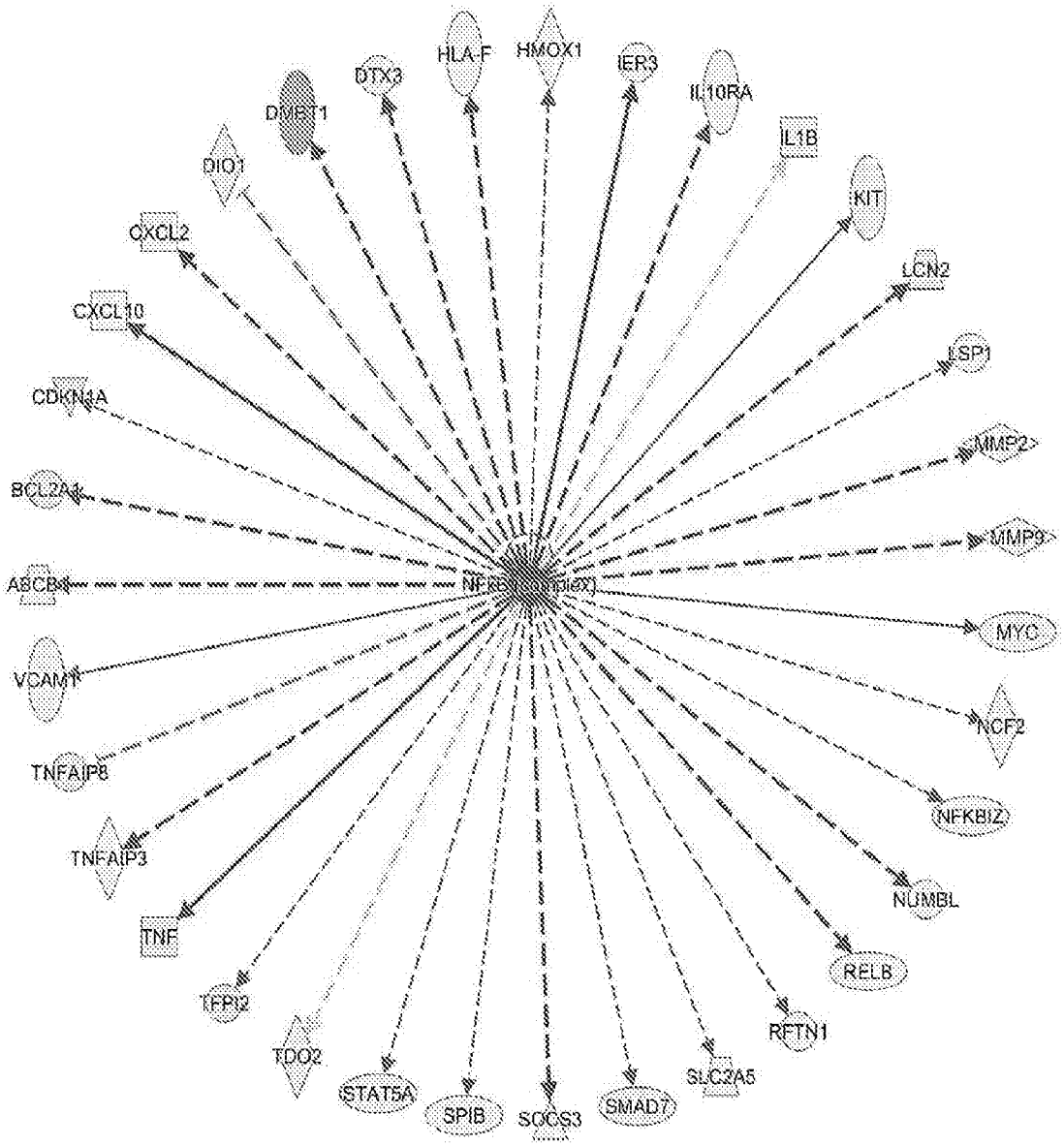
HLA-F
HMOX1
IER3
DTX3
IL10RA
DUSP1
IL1B
DIO1
KIT
CXCL2
LCN2
CXCL10
LSP1
CDKN1A
MMP2
BCL2A1
MMP9
ABCB4
NFKB
MYC
VCAM1
NCF2
TNFAIP8
NFKBIZ
TNFAIP3
NUMBL
TNF
RELB
TFPI2
RETN1
TDO2
SLC2A5
STAT5A
SMAD7
SPIB
SOCS3

Figure 28.

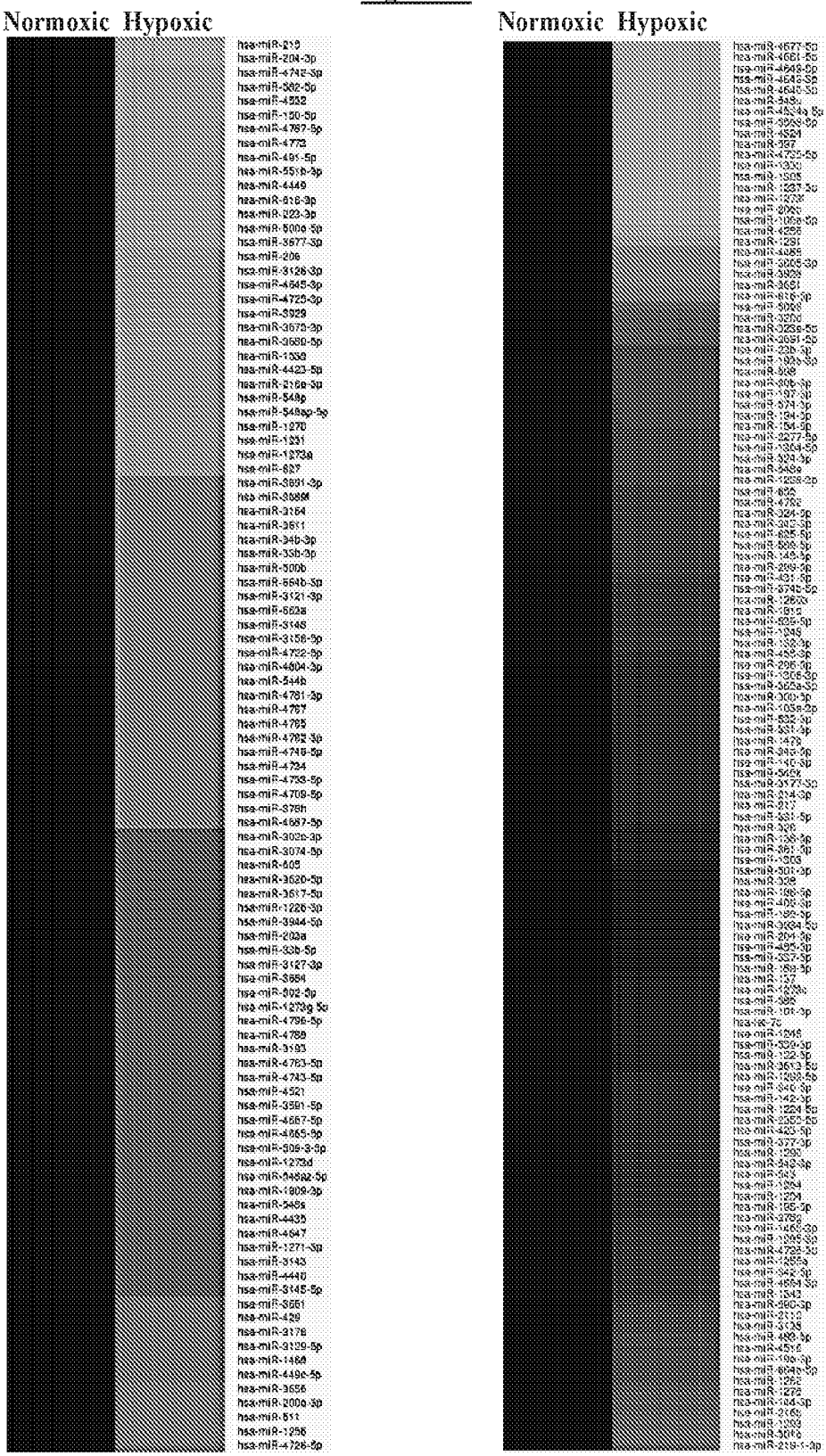

Figure 29.

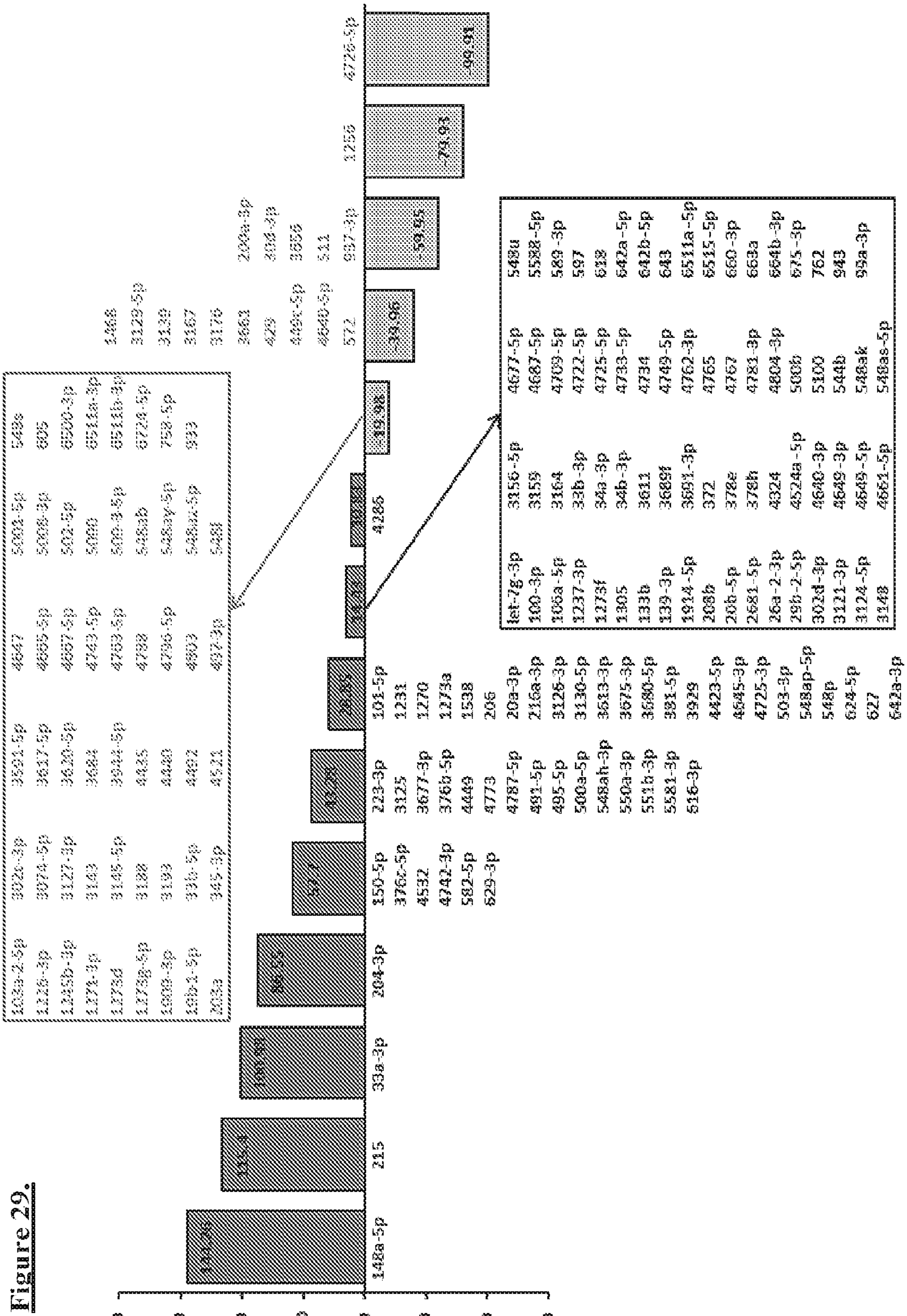
Fold Change
200
150
100
50
0
-50
-100
-150
144.26
115.4
100.98
86.55
57.7
43.28
28.85
14.43
10.83
-19.98
-39.96
-59.95
-79.93
-99.91
148a-5p
215
33a-3p
204-3p
150-5p 376c-5p 4532 4742-3p 582-5p 629-3p
223-3p 3125 3677-3p 376b-5p 4449 4773 4787-5p 491-5p 495-5p 500a-5p 548ah-3p 550a-3p 551b-3p 5581-3p 616-3p
101-5p 1231 1270 1273a 1538 206 20a-3p 216a-3p 3126-3p 3130-5p 3613-3p 3675-3p 3680-5p 381-5p 3929 4423-5p 4645-3p 4725-3p 503-3p 548ap-5p 548p 624-5p 627 642a-3p
4286
1468 3129-5p 3139 3167 3176 3661 429 449c-5p 4640-5p 572
200a-3p 30d-3p 3656 511 937-3p
1256
4726-5p
103a-2-5p 1226-3p 1245b-3p 1271-3p 1273d 1273g-5p 1909-3p 19b-1-5p 203a
302c-3p 3074-5p 3127-3p 3143 3145-5p 3188 3193 33b-5p 345-3p
3591-5p 3617-5p 3620-5p 3684 3944-5p 4435 4440 4492 4521
4647 4665-5p 4667-5p 4743-5p 4763-5p 4788 4796-5p 4803 497-3p
5001-5p 5008-3p 502-5p 5090 509-3-5p 548ab 548ay-5p 548az-5p 548f
548s 605 6500-3p 6511a-3p 6511b-3p 6724-5p 758-5p 933
let-7g-3p 100-3p 106a-5p 1237-3p 1273f 1305 133b 139-3p 1914-5p 208b 20b-5p 2681-5p 26a-2-3p 29b-2-5p 302d-3p 3121-3p 3124-5p 3148
3156-5p 3159 3164 33b-3p 34a-3p 34b-3p 3611 3689f 3691-3p 372 378e 378h 4324 4524a-5p 4640-3p 4649-3p 4649-5p 4661-5p
4677-5p 4687-5p 4709-5p 4722-5p 4725-5p 4733-5p 4734 4749-5p 4762-3p 4765 4767 4781-3p 4804-3p 5006 5100 544b 548ak 548as-5p
548u 5588-5p 589-3p 597 618 642a-5p 642b-5p 643 6511a-5p 6515-5p 660-3p 663a 664b-3p 675-3p 762 943 99a-3p

Figure 30.

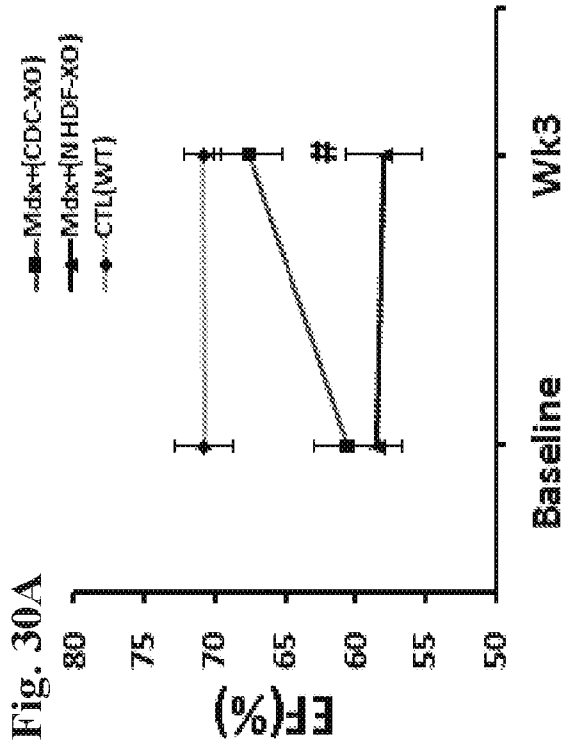
Fig. 30A
EF(%)
80
75
70
65
60
55
50
Baseline
Wk3
Mdx+(CDC-XO)
Mdx+(NHDF-XO)
CTL(WT)
#

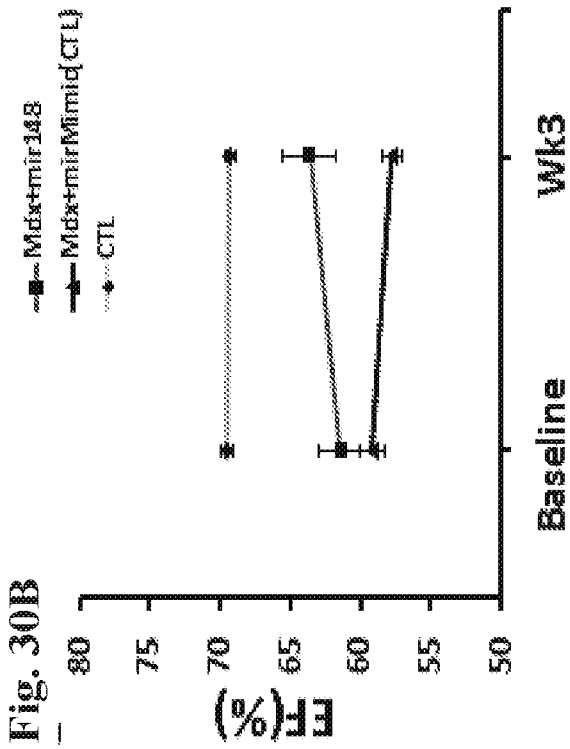
Fig. 30B
EF(%)
80
75
70
65
60
55
50
Baseline
Wk3
Mdx+mir148
Mdx+mirMimid(CTL)
CTL

Figure 31.

Fig. 31A

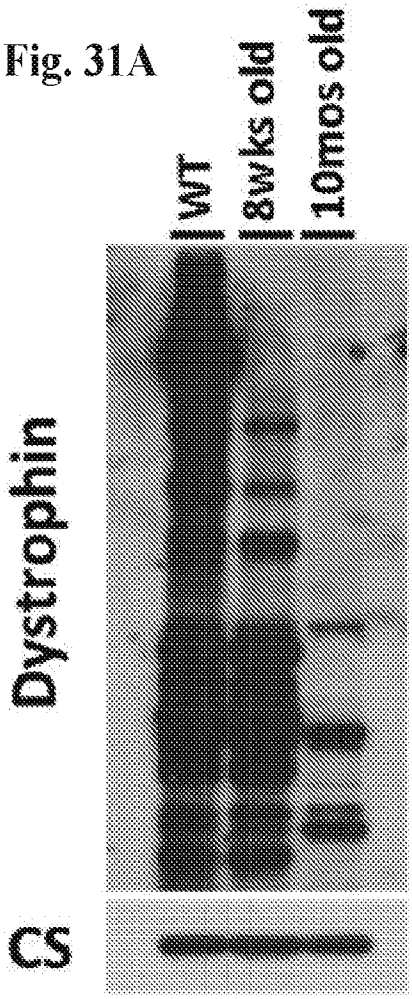

Fig. 31B

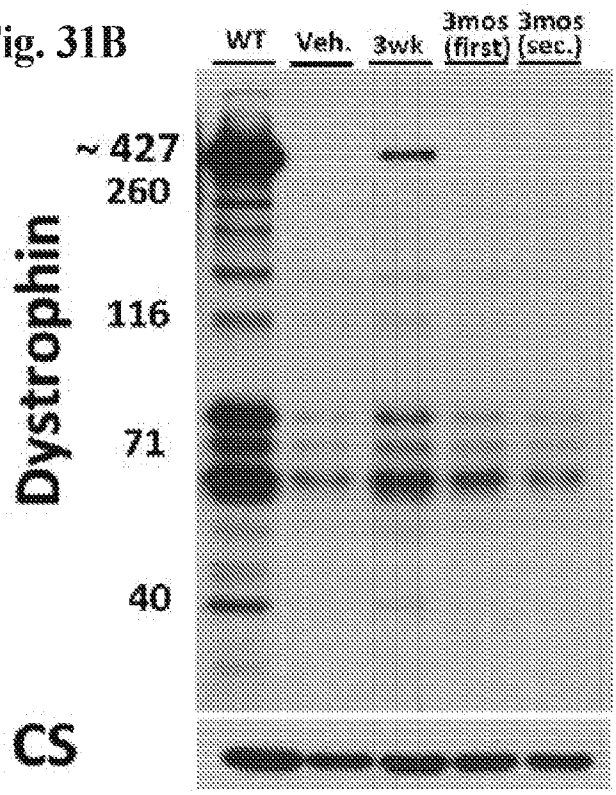

Figure 32.

Fig. 32A

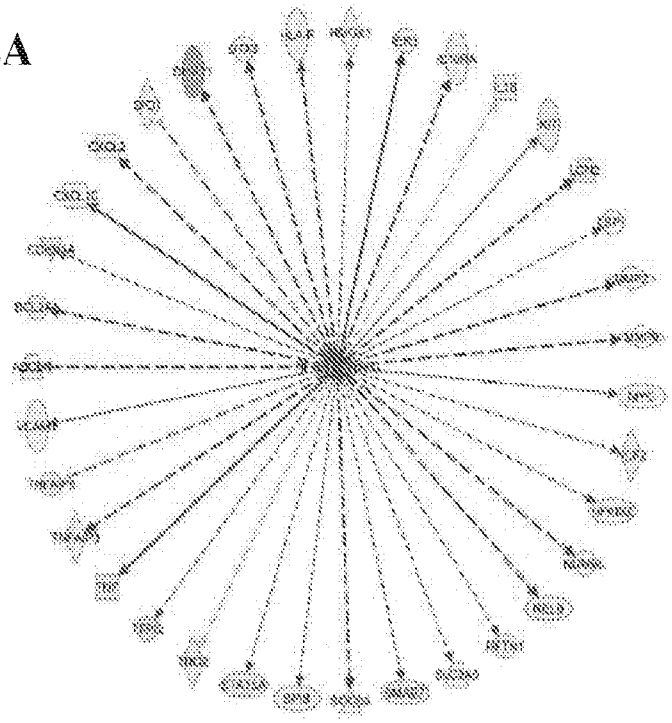

Fig. 32B

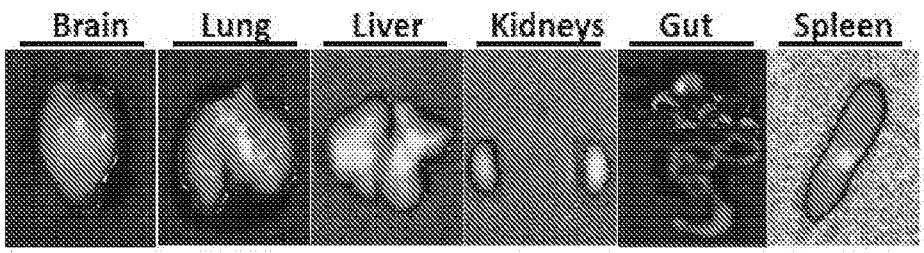

Fig. 32D

Fig. 32C

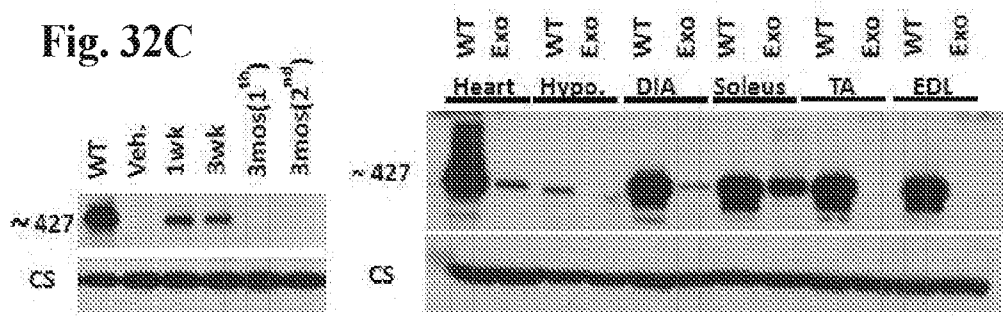

Figure 33.

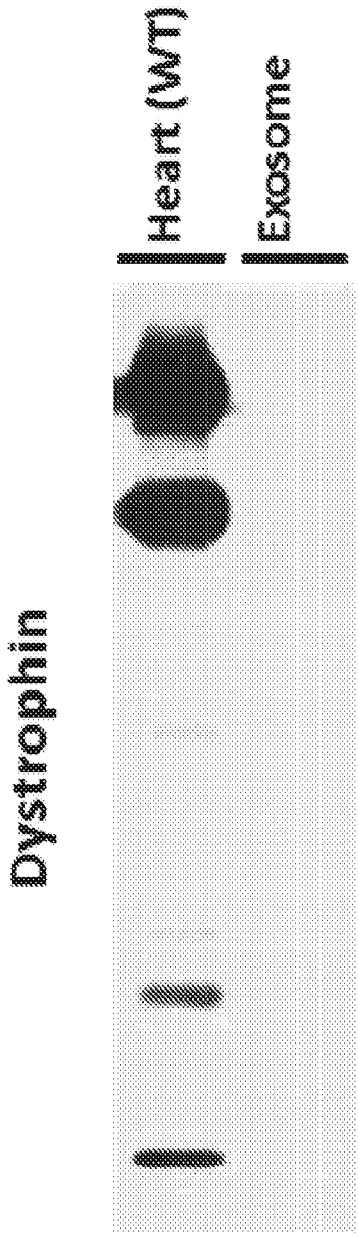

Figure 34.

Fig. 34A

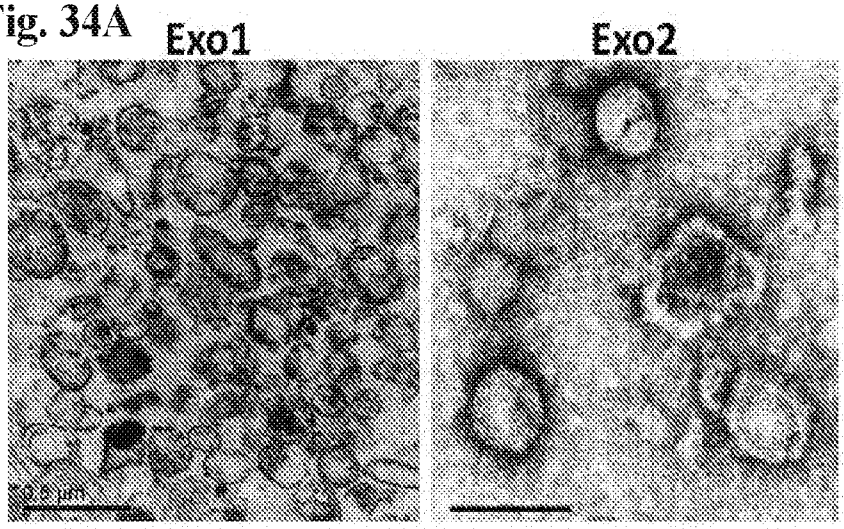

Fig. 34B

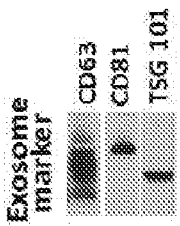

Fig. 34C

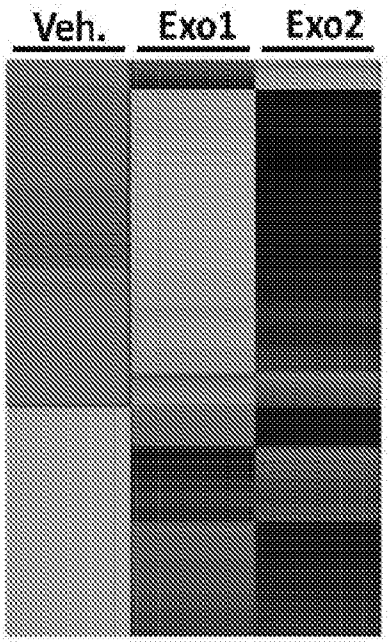

Fig. 34D

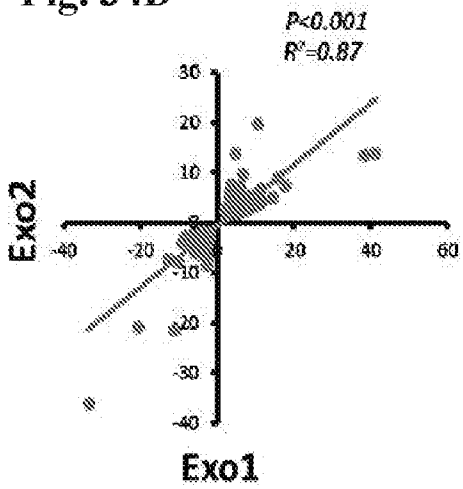

Figure 35.

Fig. 35A

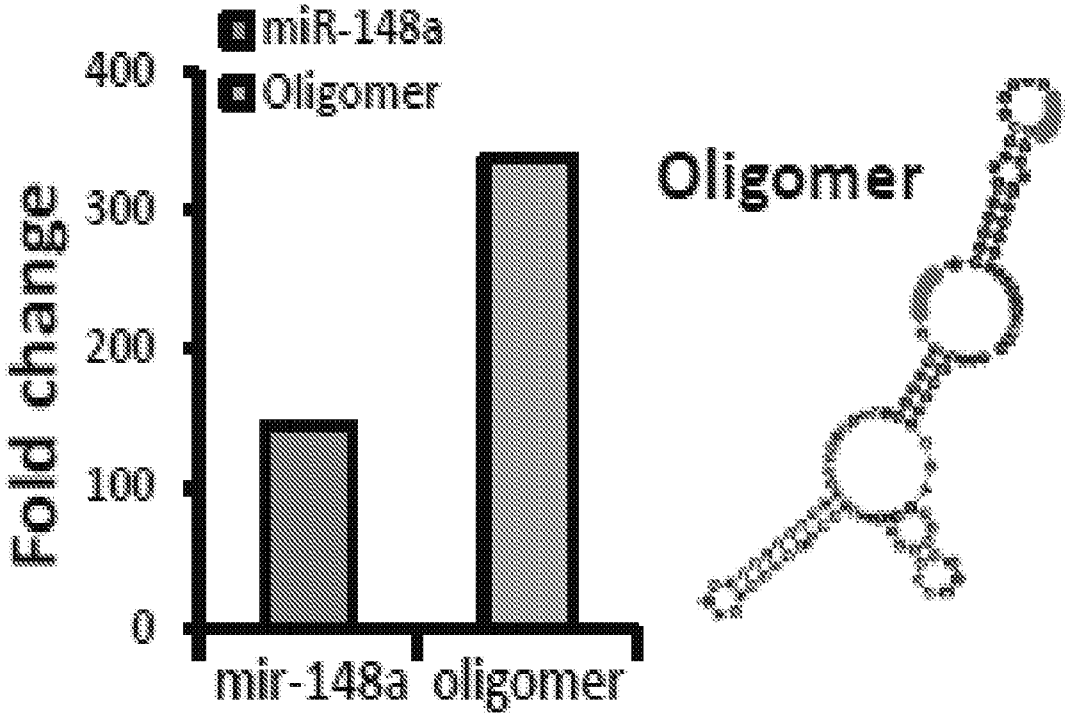

Figure 35.

Fig. 35B

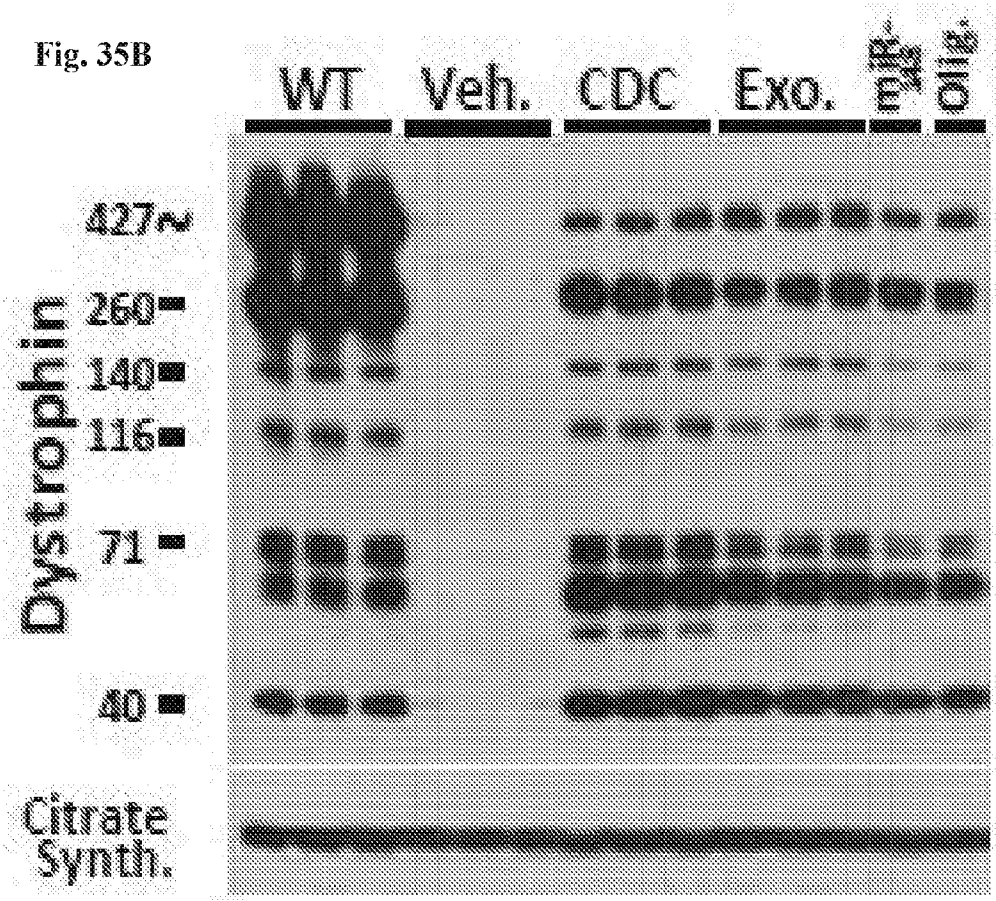

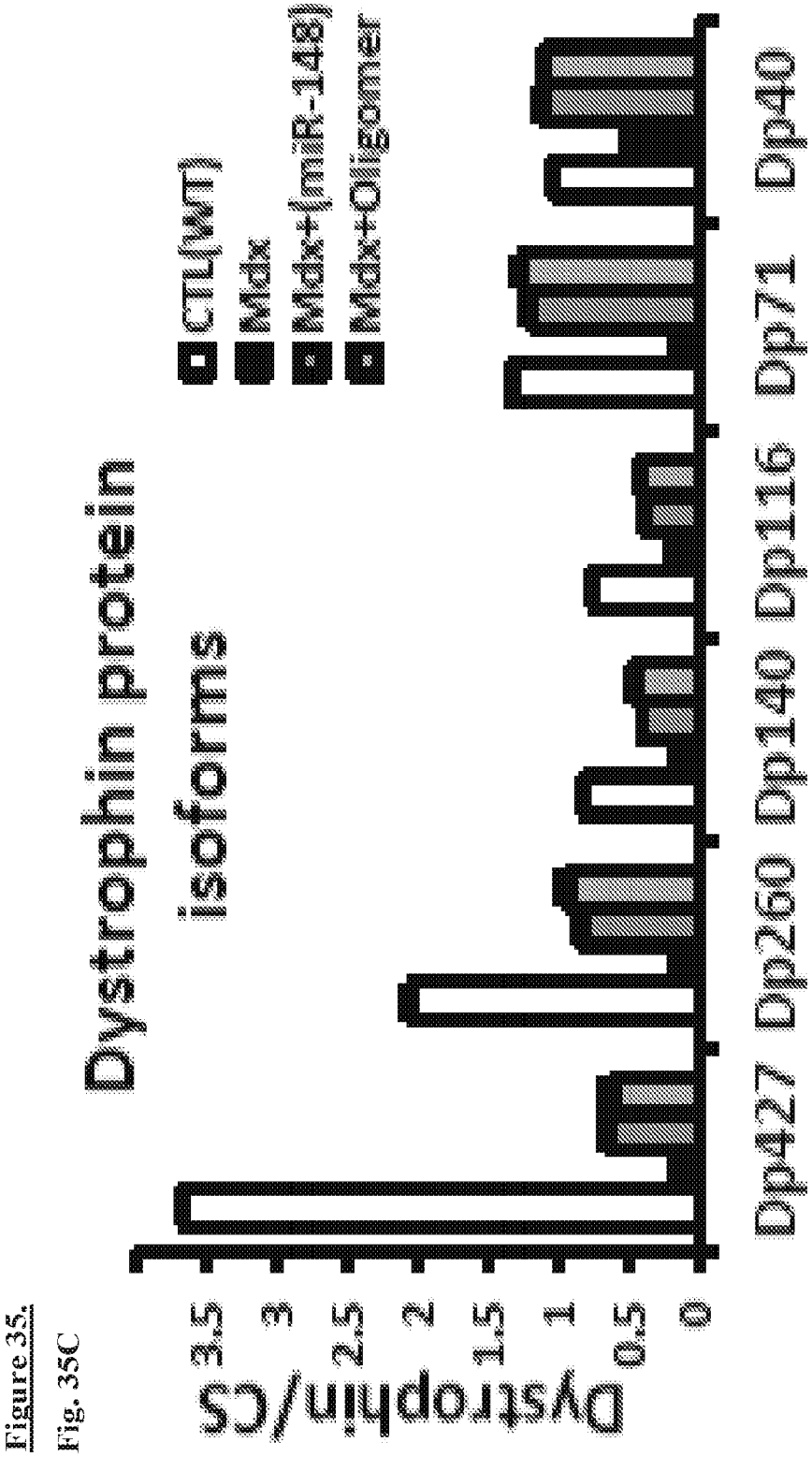

Figure 35.

Fig. 35C

Figure 36.

Fig. 36A

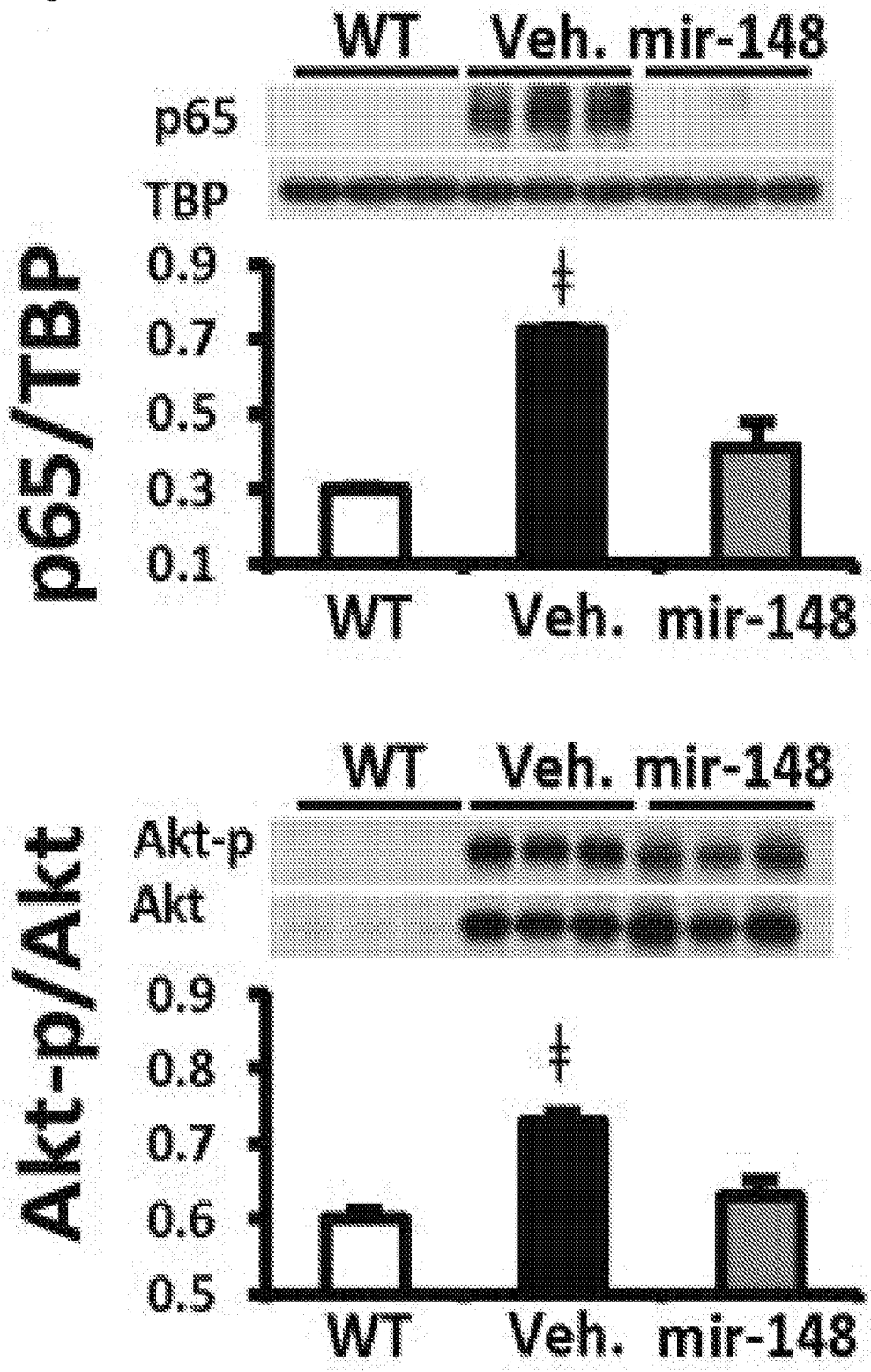

Figure 36.

Fig. 36B

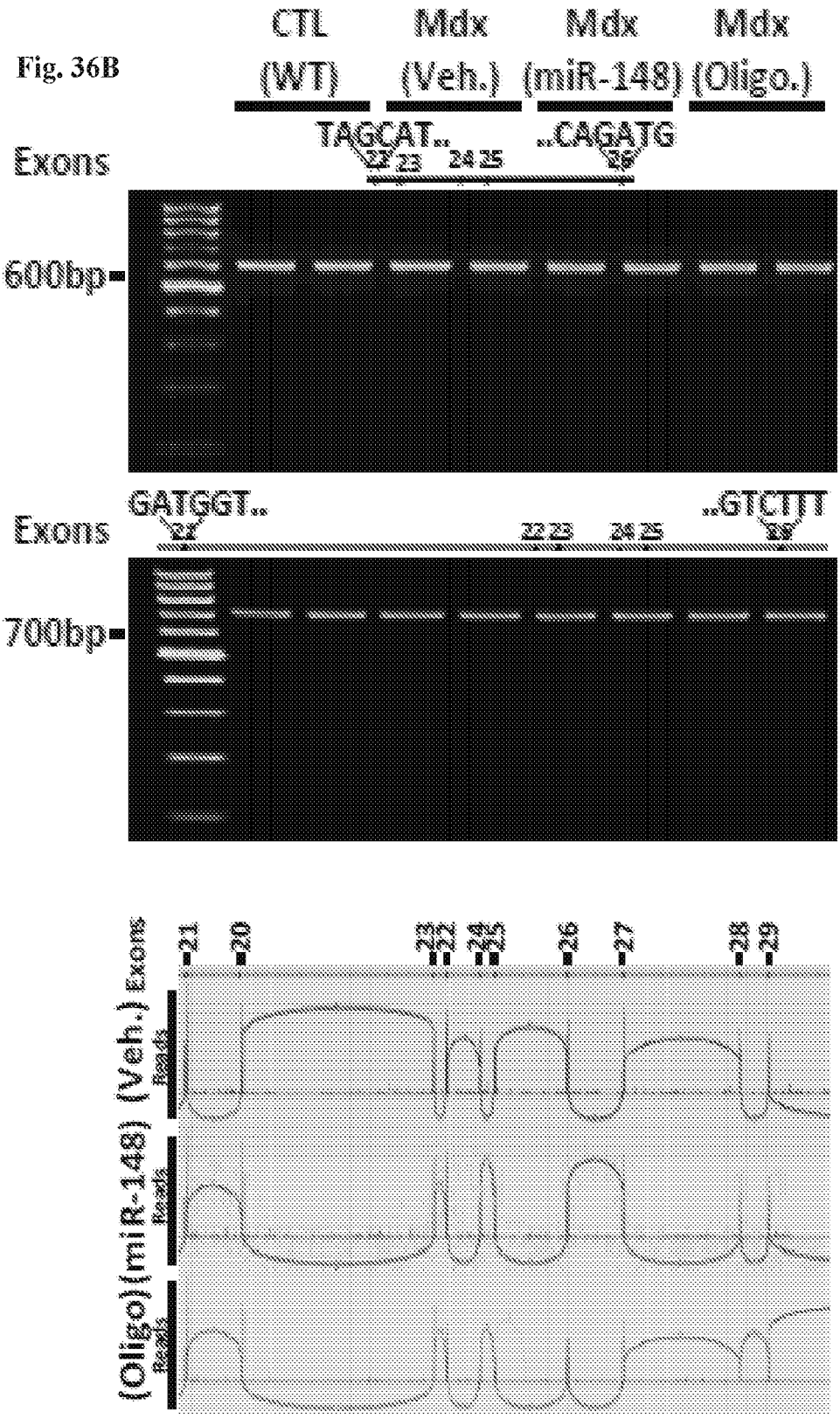

Figure 37.

Fig. 37A

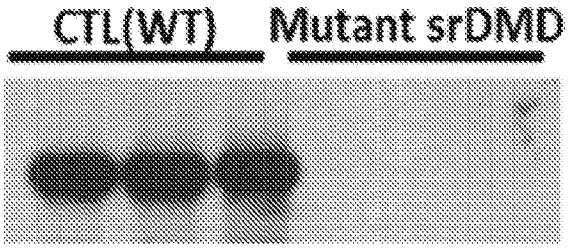

Fig. 37B

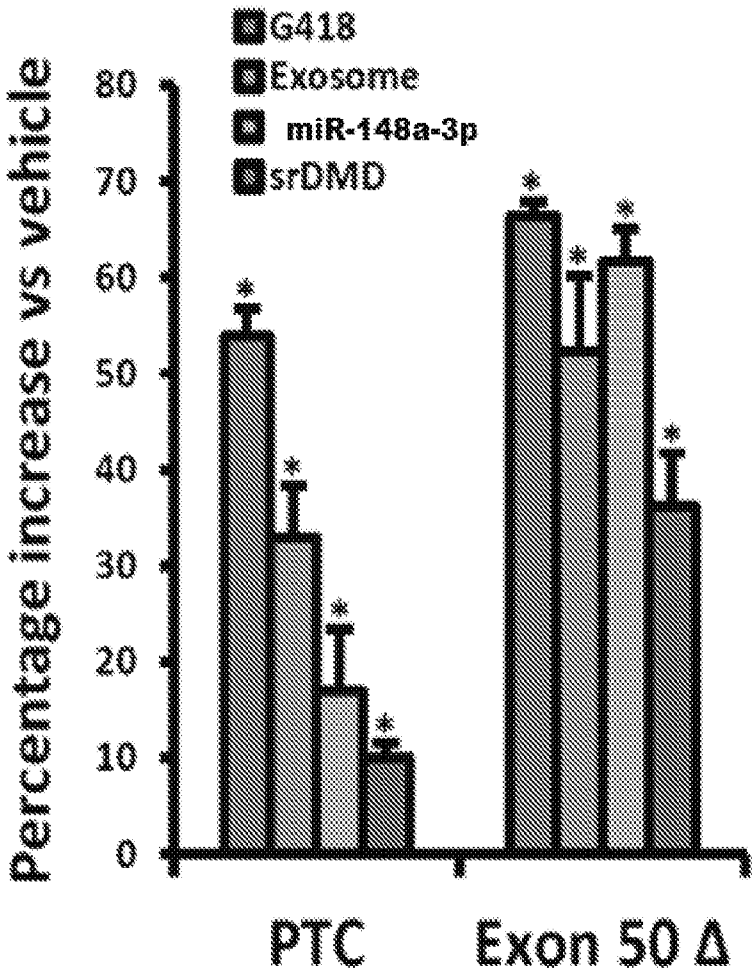

Figure 38.

Fig. 38A

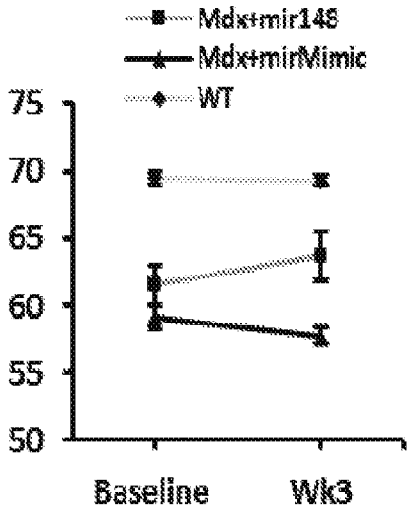

Fig. 38B

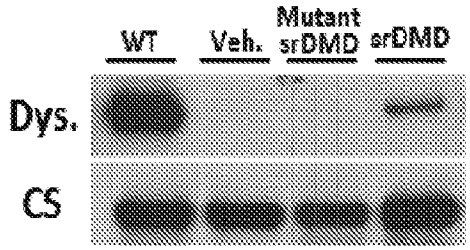

Figure 39.

Fig. 39A

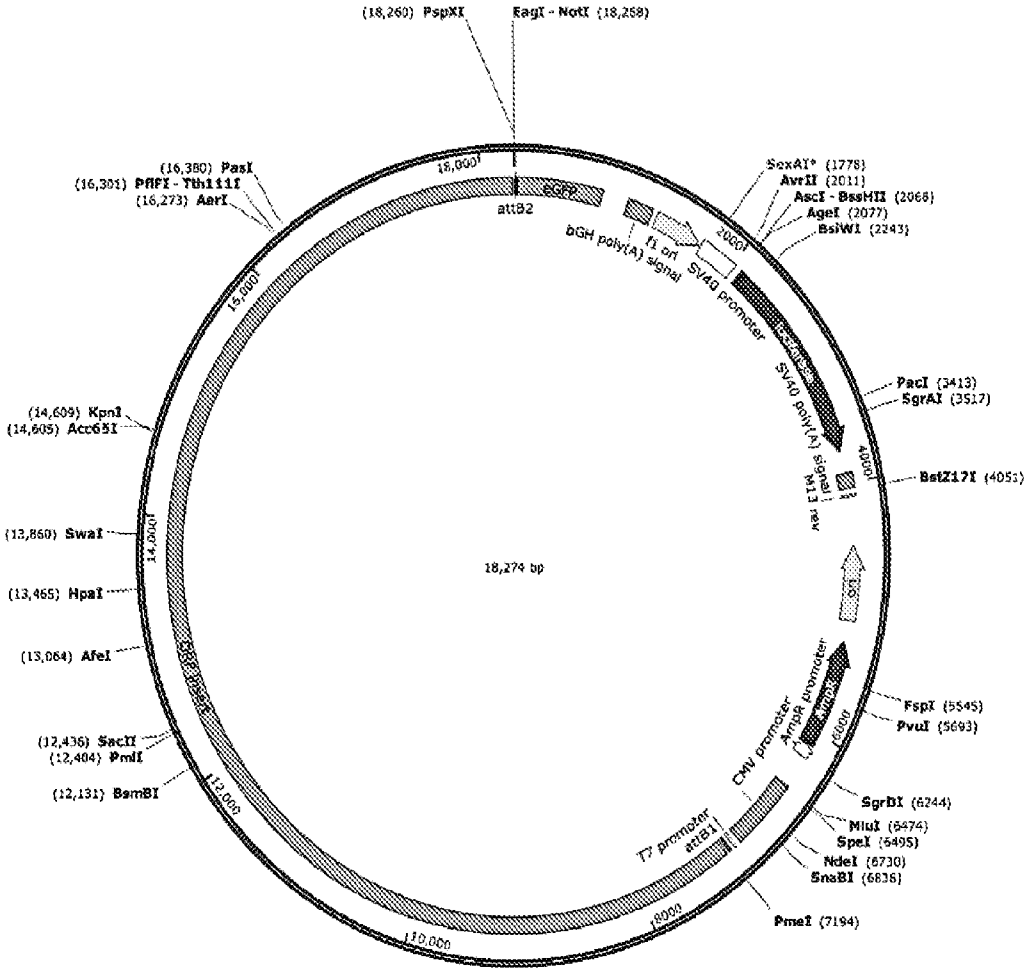

Fig. 39B

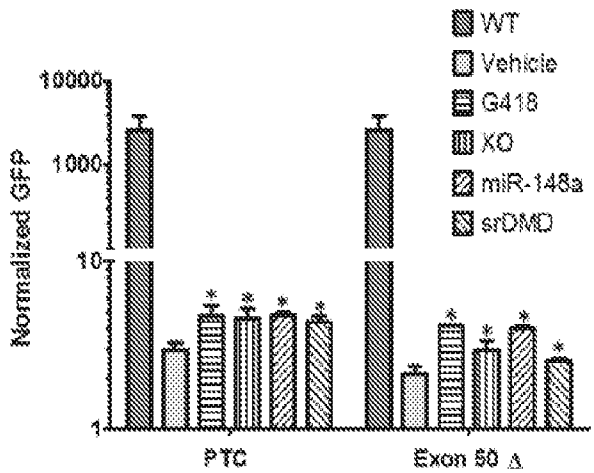

Figs. 40A-D

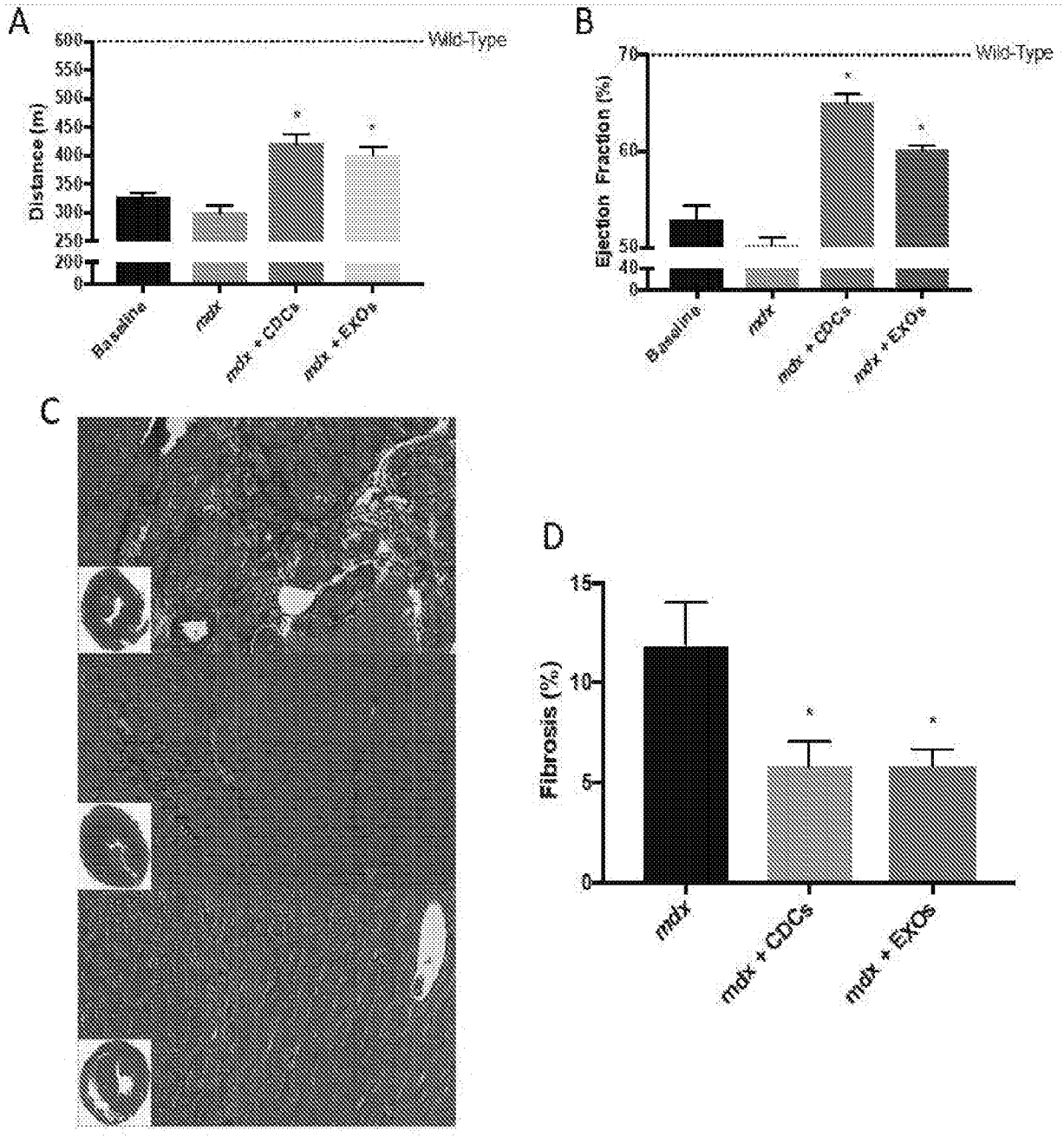
A
Wild-Type
Distance (m)
600
550
500
450
400
350
300
250
200
0
Baseline
mdx
mdx + CDCs
mdx + EXOs
B
Wild-Type
Ejection Fraction (%)
70
60
50
40
0
Baseline
mdx
mdx + CDCs
mdx + EXOs
C
D
Fibrosis (%)
15
10
5
0
mdx
mdx + CDCs
mdx + EXOs

Figs. 41A-D

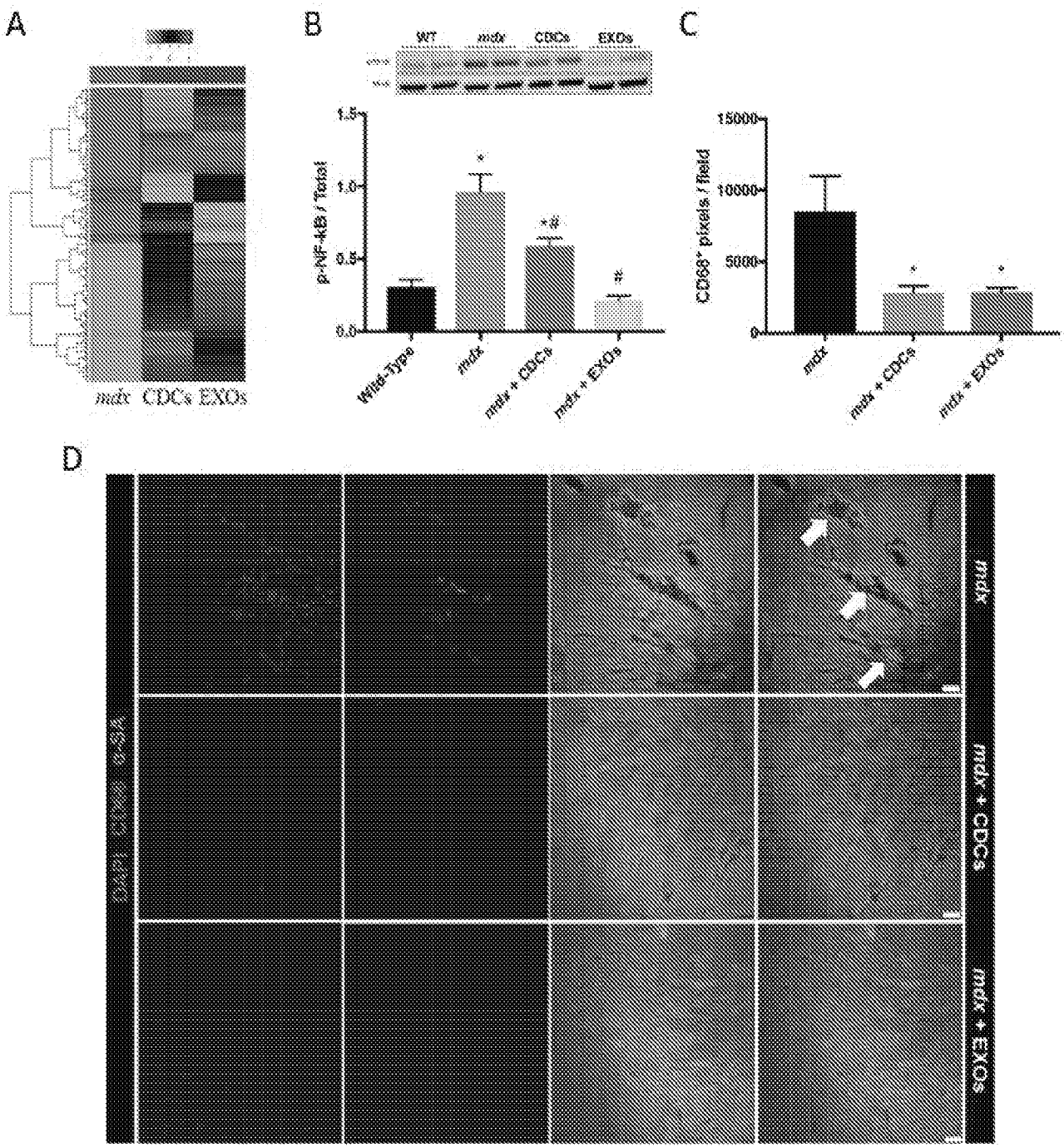
A
mdx CDCs EXOs
B
WT
mdx
CDCs
EXOs
p-NF-kB / Total
Wild-Type
mdx
mdx + CDCs
mdx + EXOs
C
CD68+ pixels / field
mdx
mdx + CDCs
mdx + EXOs
D
Wild-Type
mdx
mdx + CDCs
mdx + EXOs

Fig. 42A

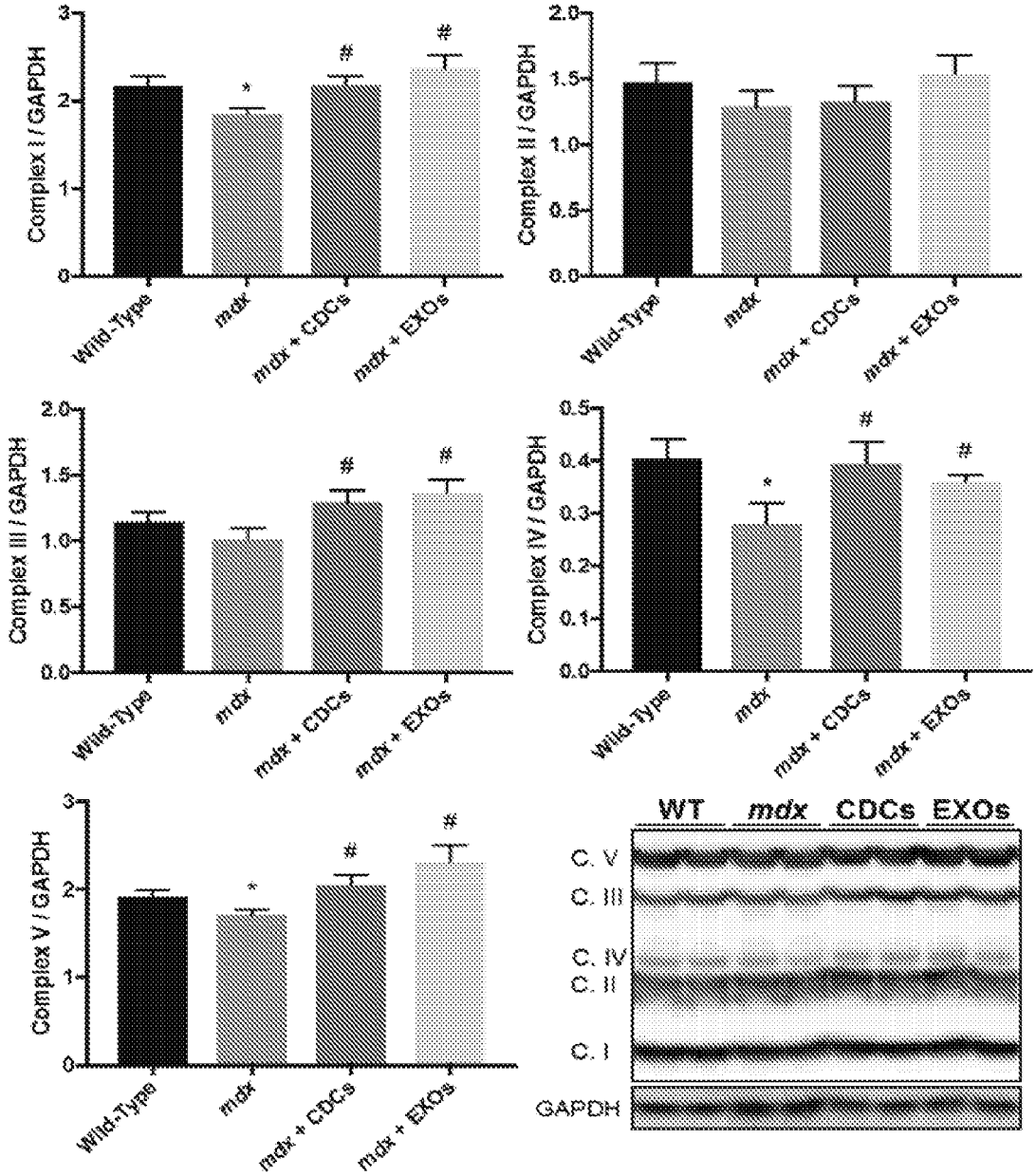
Complex I / GAPDH
Complex II / GAPDH
Complex III / GAPDH
Complex IV / GAPDH
Complex V / GAPDH
Wild-Type
mdx
mdx + CDCs
mdx + EXOs
WT
mdx
CDCs
EXOs
C. V
C. III
C. IV
C. II
C. I
GAPDH

Fig. 42B

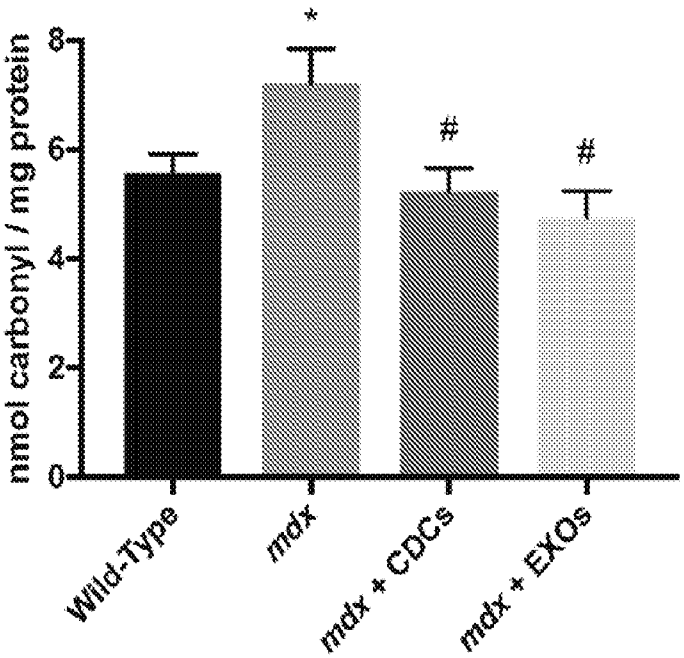

Fig. 42C

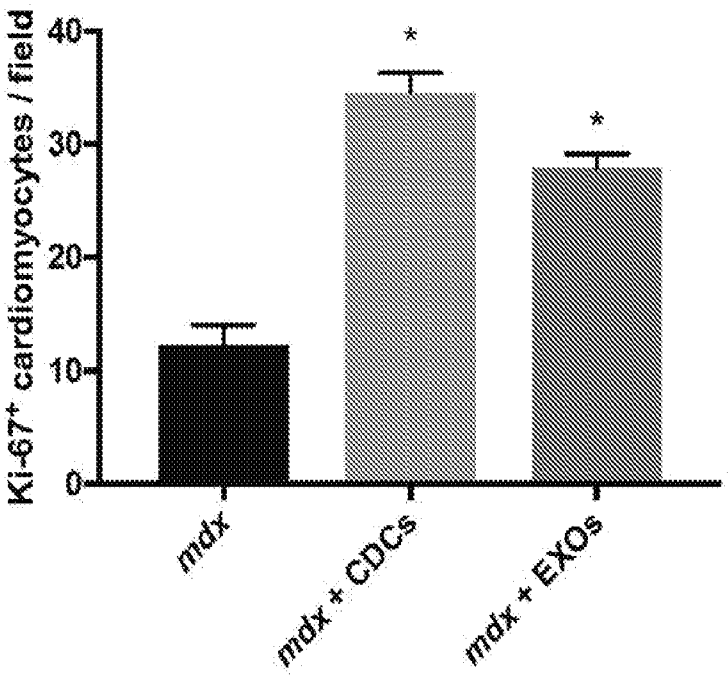

Fig. 42D

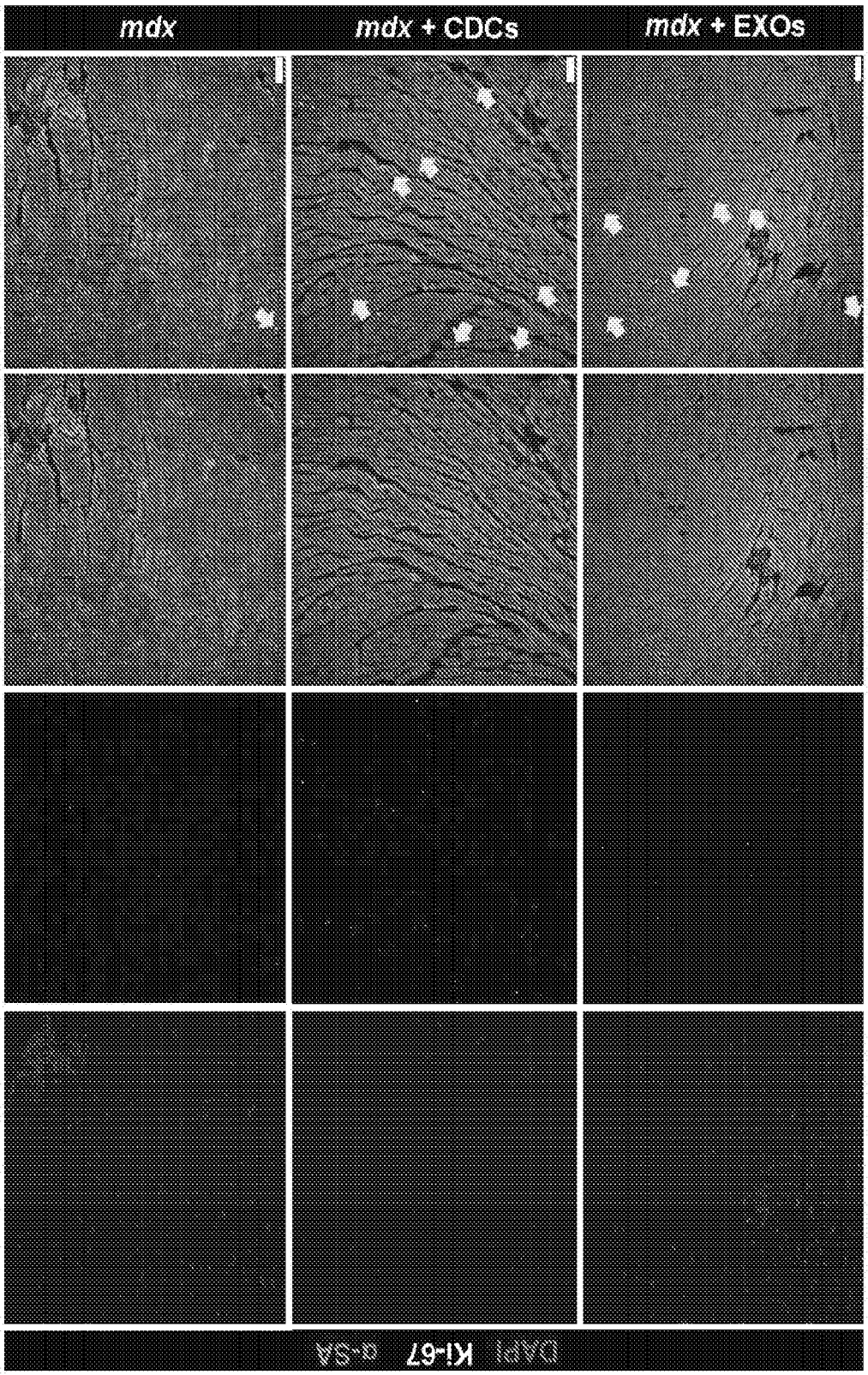

Figs. 43A-F

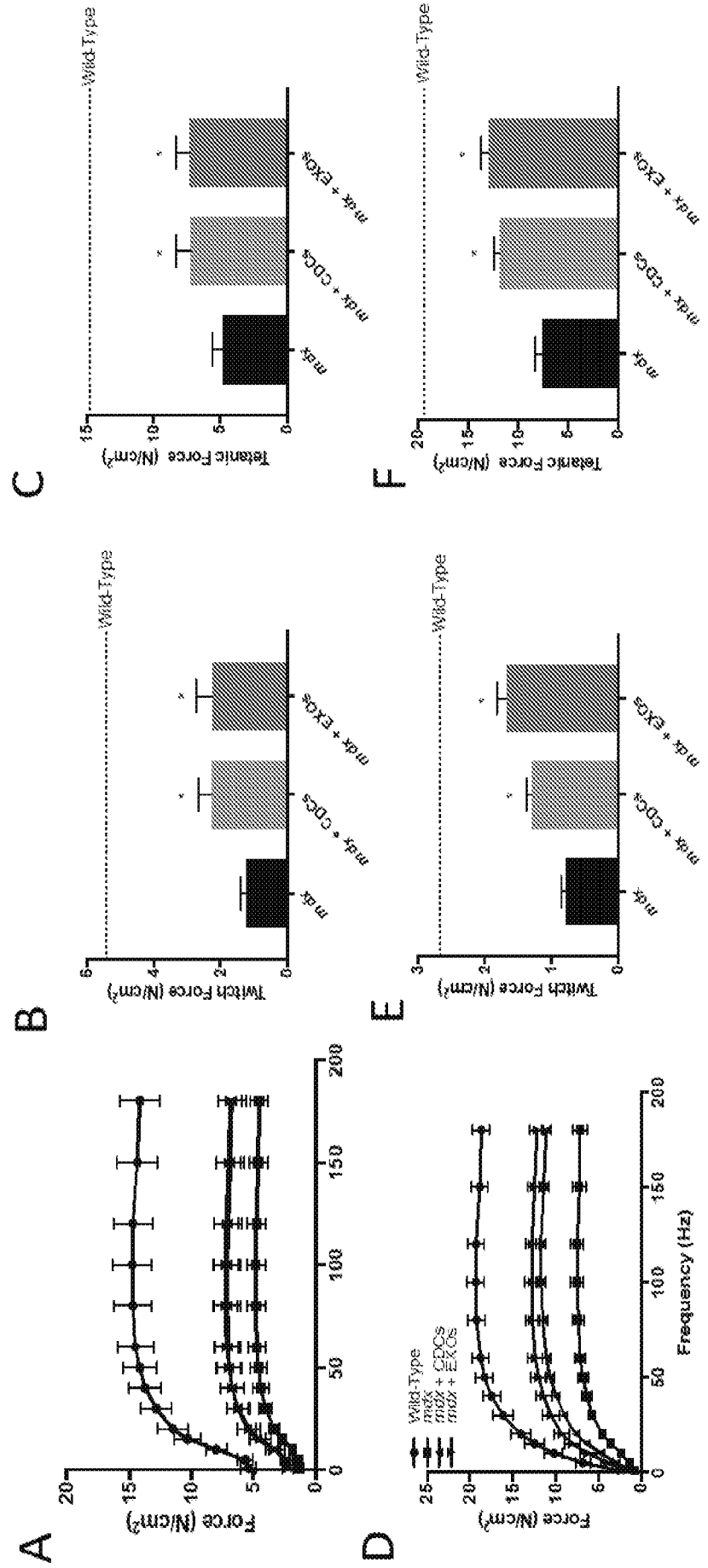
A
B
C
D
E
F
Force (N/cm²)
Twitch Force (N/cm²)
Tetanic Force (N/cm²)
Frequency (Hz)
Wild-Type
mdx
mdx + CDCs
mdx + EXOs

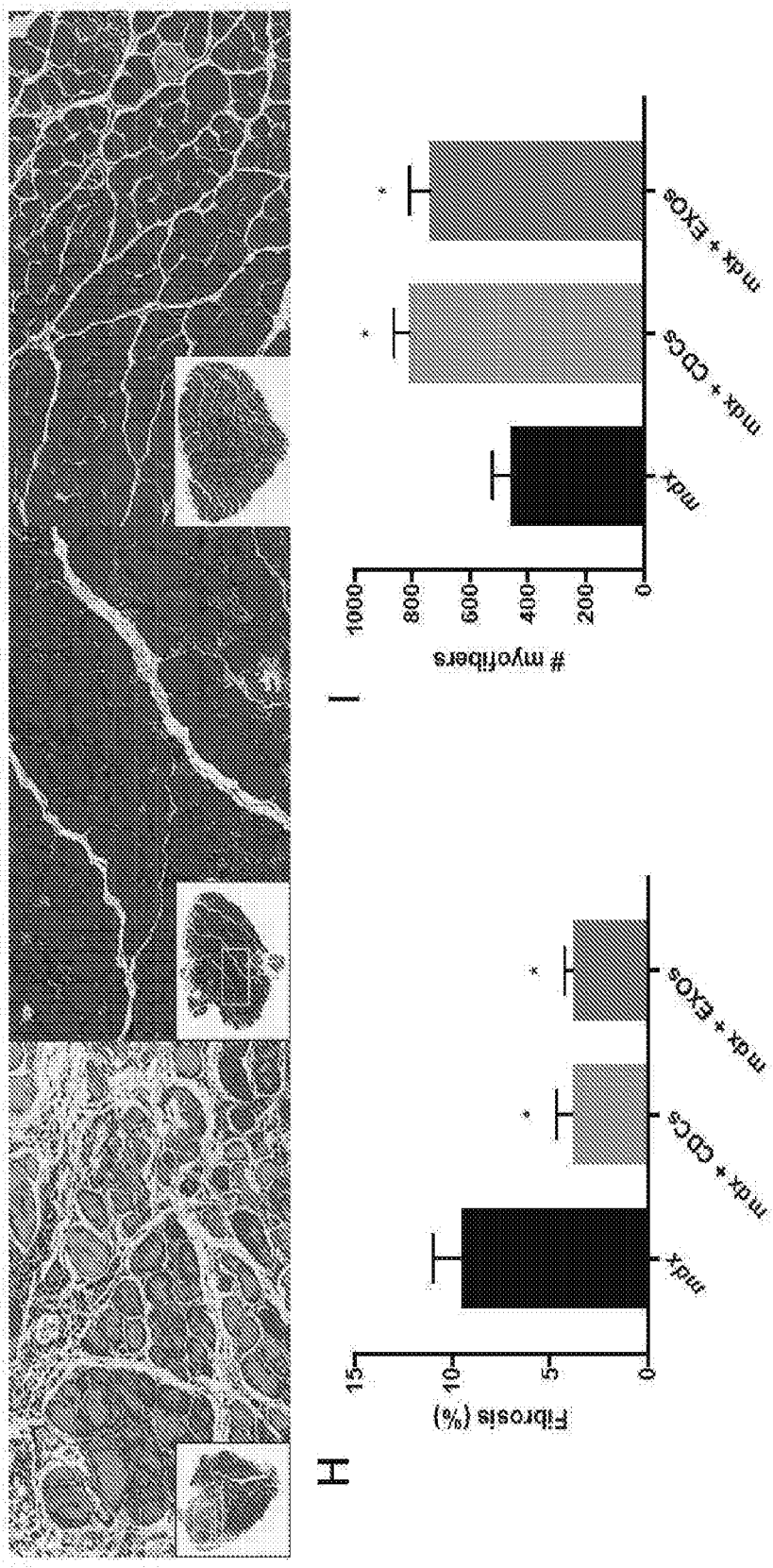
G
H
Fibrosis (%)
15
10
5
0
mdx
mdx + CDCs
mdx + EXOs
I
myofibers
1000
800
600
400
200
0
mdx
mdx + CDCs
mdx + EXOs

Figs. 43G-I

Figs. 44A-B

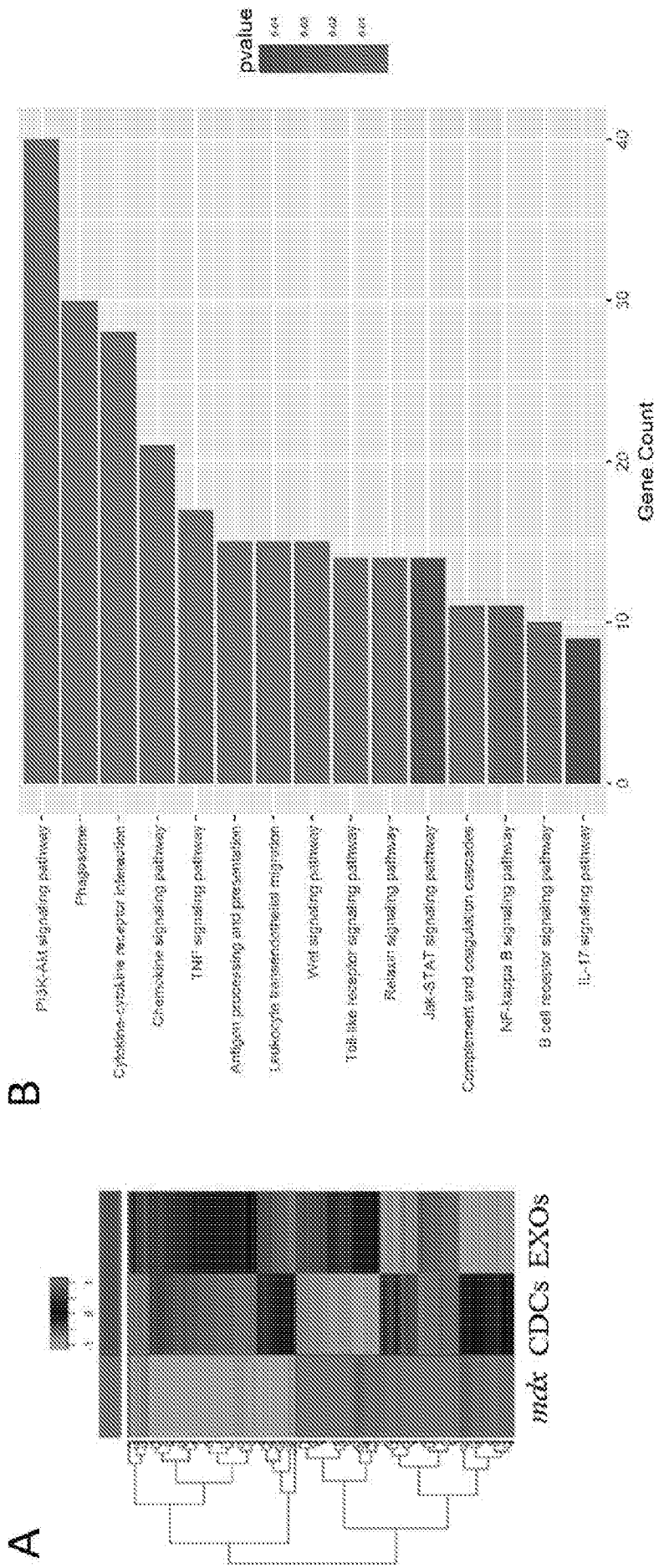
A
mdx CDCs EXOs
B
PI3K-Akt signaling pathway
Phagosome
Cytokine-cytokine receptor interaction
Chemokine signaling pathway
TNF signaling pathway
Antigen processing and presentation
Leukocyte transendothelial migration
Wnt signaling pathway
Toll-like receptor signaling pathway
Relaxin signaling pathway
Jak-STAT signaling pathway
Complement and coagulation cascades
NF-kappa B signaling pathway
B cell receptor signaling pathway
IL-17 signaling pathway
0
10
20
30
40
Gene Count
pvalue

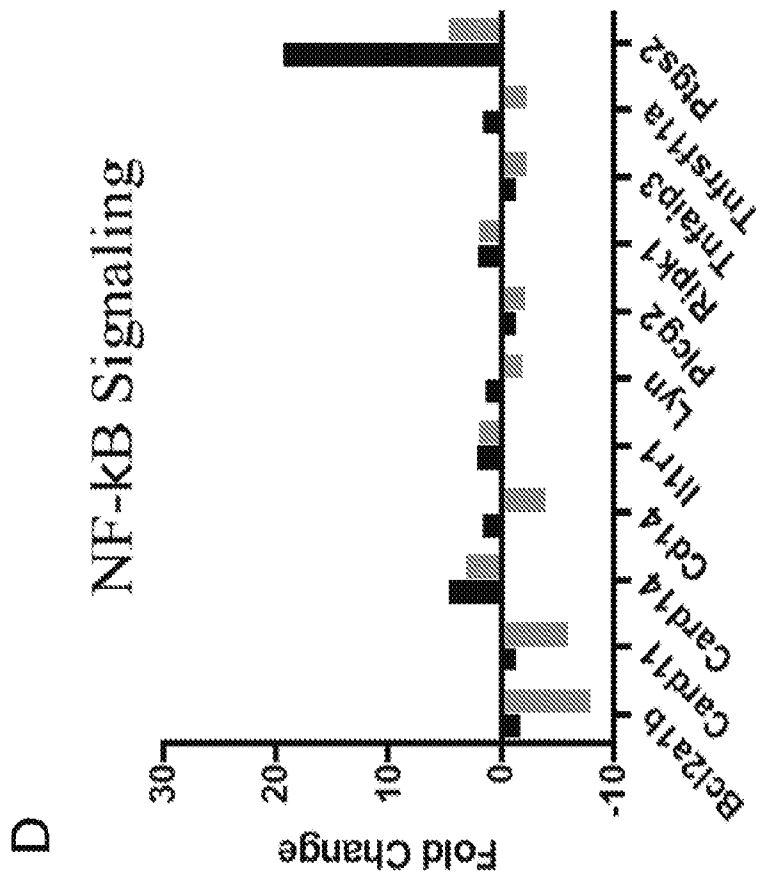
D
NF-kB Signaling
Fold Change
30
20
10
0
-10
Bcl2a1b
Card11
Card14
Cd14
Il1rl
Lyn
Plcg2
Ripk1
Tnfaip3
Tnfrsf1a
Ptgs2

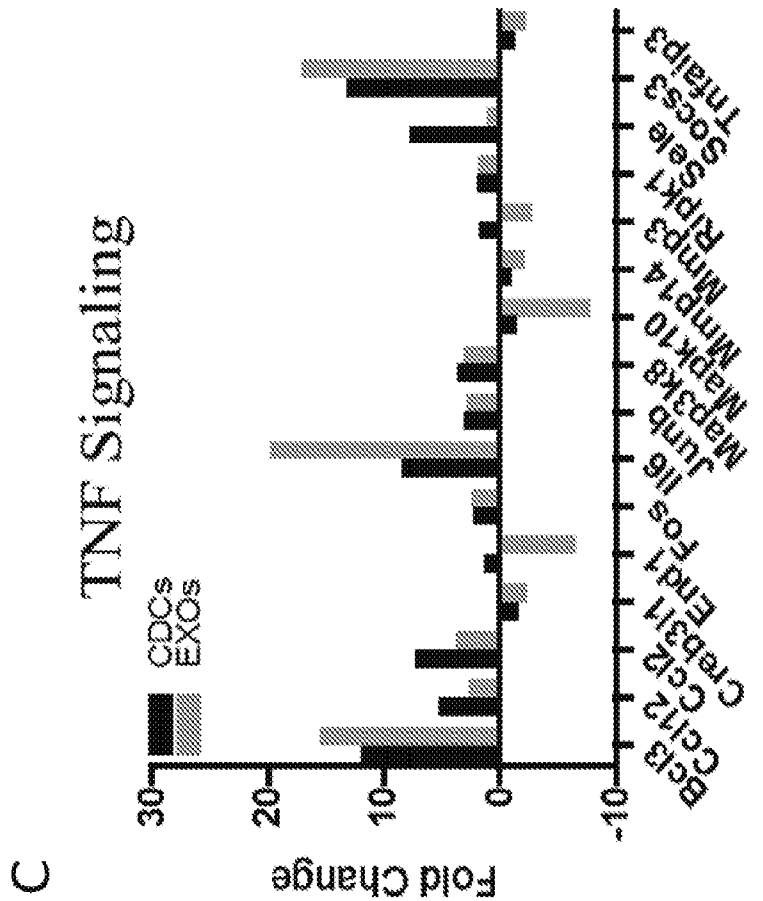
C
TNF Signaling
CDCs
EXOs
Fold Change
30
20
10
0
-10
Bcl3
Ccl2
Ccl2
Crebbp
Ctnd1
Fos
Il6
Jund
Map3k8
Mapk10
Mmp14
Mmp3
Ripk1
Socs3a
Socs3
Tnfaip3

Figs. 44C-44D.

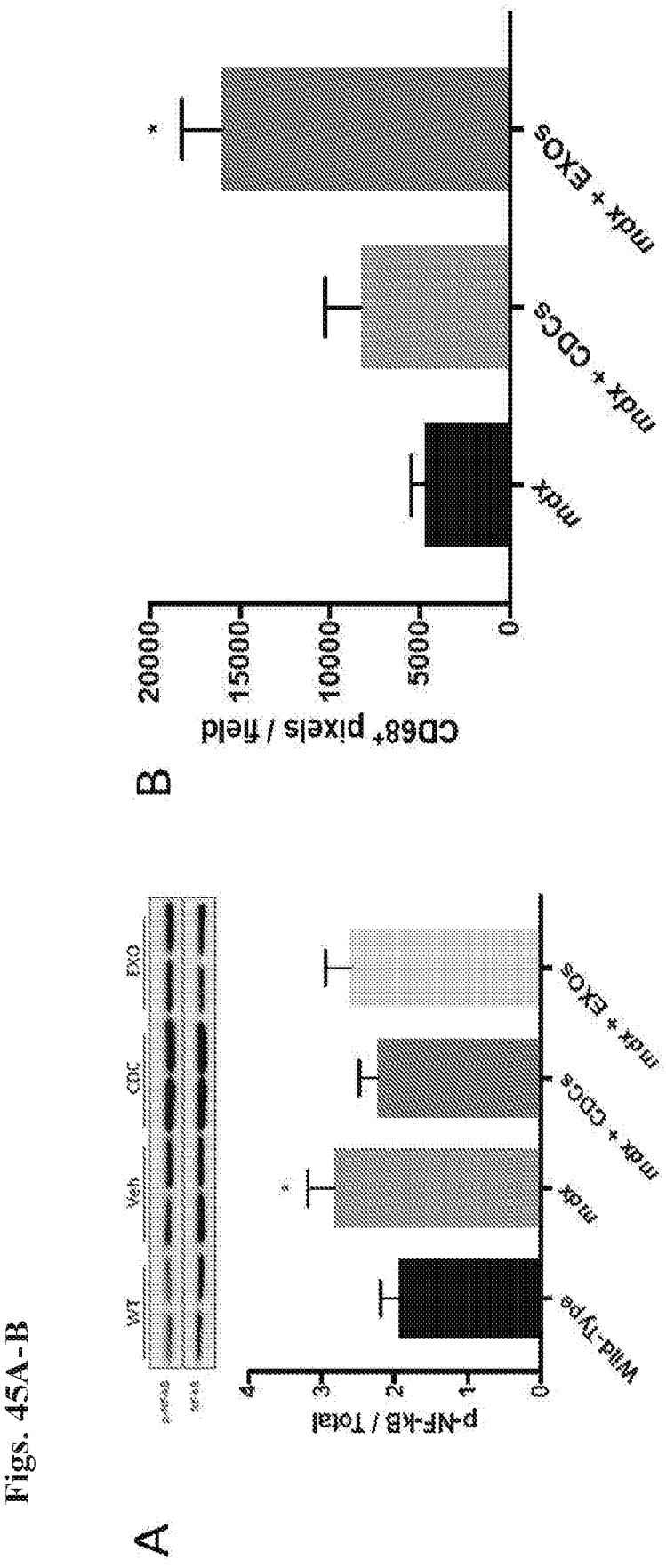
A
WT
Veh
CDC
EXO
p-NF-κB / Total
Wild-Type
mdx
mdx + CDCs
mdx + EXOs
B
CD68+ pixels / field
mdx
mdx + CDCs
mdx + EXOs

Figs. 45A-B

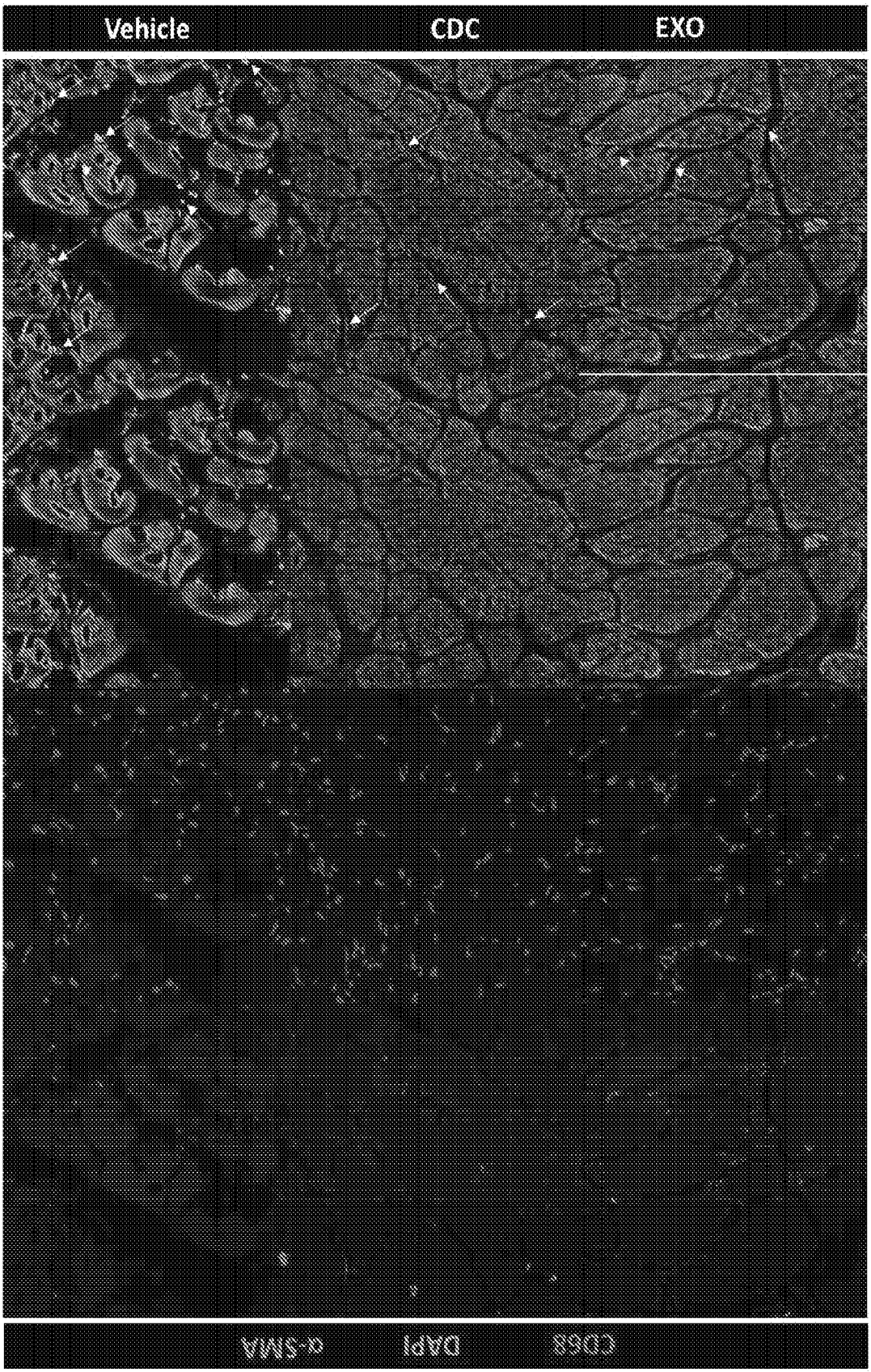

Fig. 45C

Figs. 46A-B

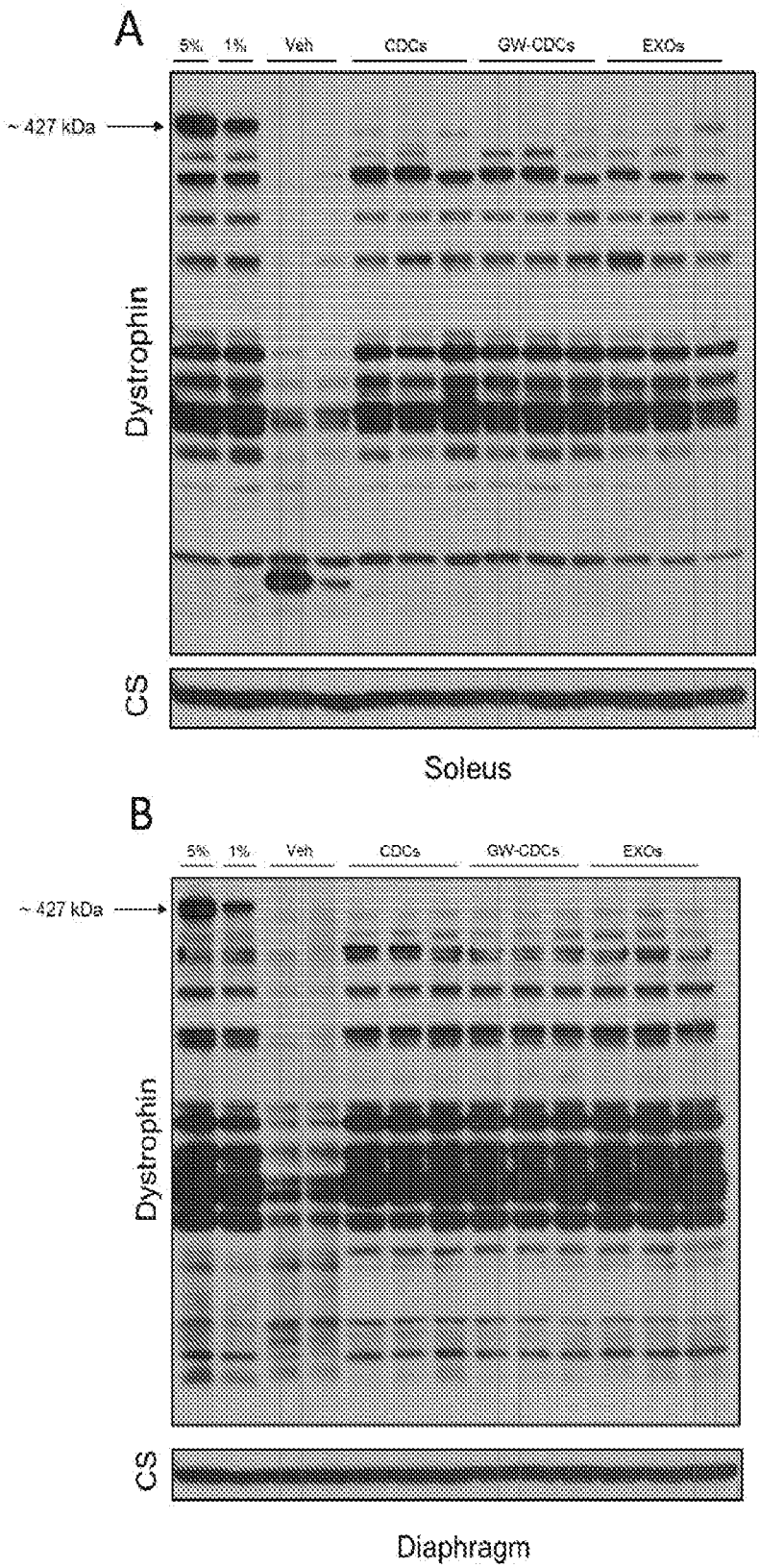
A
5%
1%
Veh
CDCs
GW-CDCs
EXOs
~ 427 kDa
Dystrophin
CS
Soleus
B
5%
1%
Veh
CDCs
GW-CDCs
EXOs
~ 427 kDa
Dystrophin
CS
Diaphragm

Fig. 47

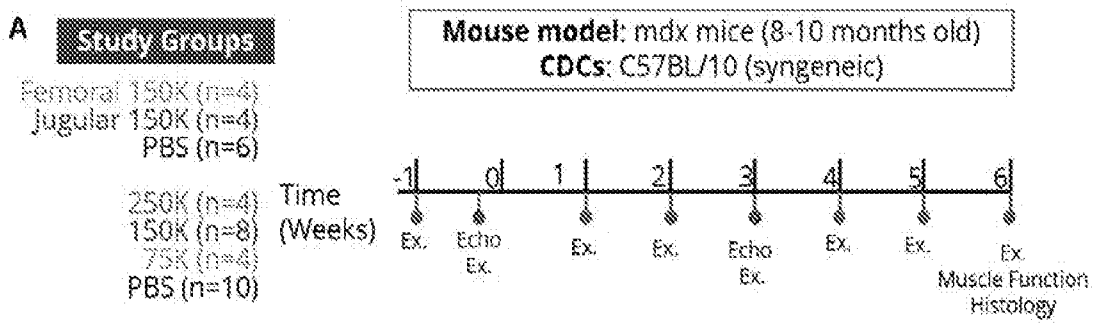
A
Study Groups
Femoral 150K (n=4)
Jugular 150K (n=4)
PBS (n=6)
250K (n=4)
150K (n=8)
75K (n=4)
PBS (n=10)
Time (Weeks)
Mouse model: mdx mice (8-10 months old)
CDCs: C57BL/10 (syngeneic)
-1
0
1
2
3
4
5
6
Ex.
Echo Ex.
Ex.
Ex.
Echo Ex.
Ex.
Ex.
Ex.
Muscle Function Histology

Fig. 48A

Mouse model:	Mdx mice (8-10 months old)
CDCs:	C57BL/10 (syngeneic)
Dose:	150K
Injection route:	Jugular or Femoral
Injection time:	Week 0

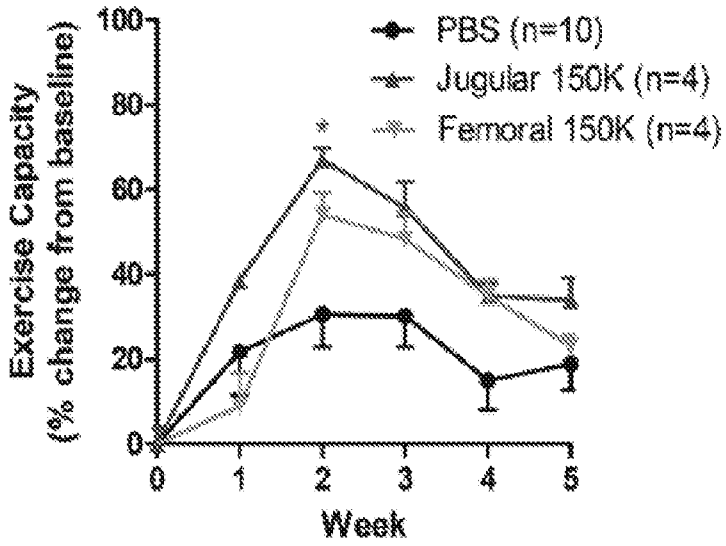

Fig. 48B

Mouse model:	Mdx mice (8-10 months old)
CDCs:	C57BL/10 (syngeneic)
Dose:	75K, 150K, or 250K
Injection route:	PBS, 150K, 75K: Jugular 250K: Femoral
Injection time:	Week 0

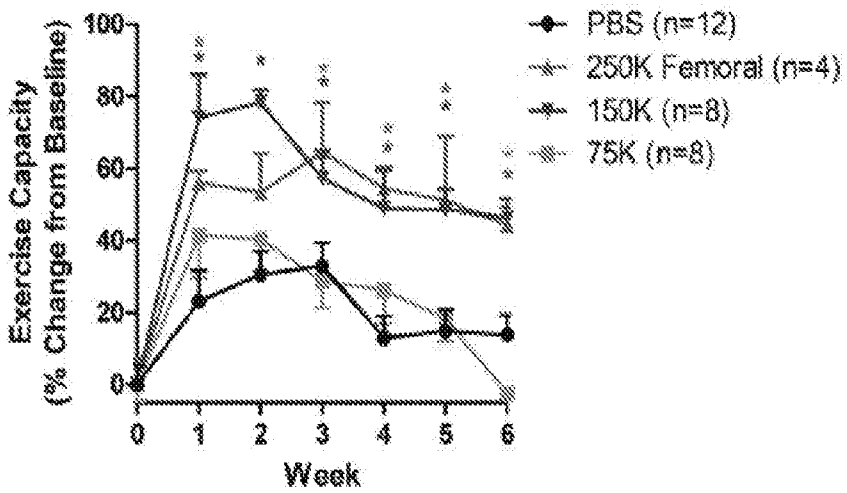

Fig. 49

Mouse model:	Mdx mice (8-10 months old)
CDCs:	C57BL/10 (syngeneic)
Dose:	75K, 150K, or 250K
Injection route:	PBS, 150K, 75K: Jugular 250K: Femoral
Injection time:	Week 0

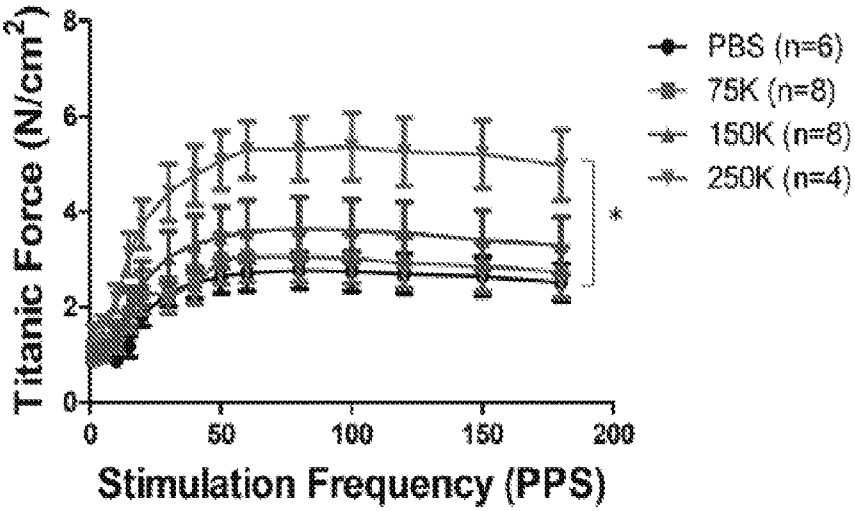

Fig. 50A

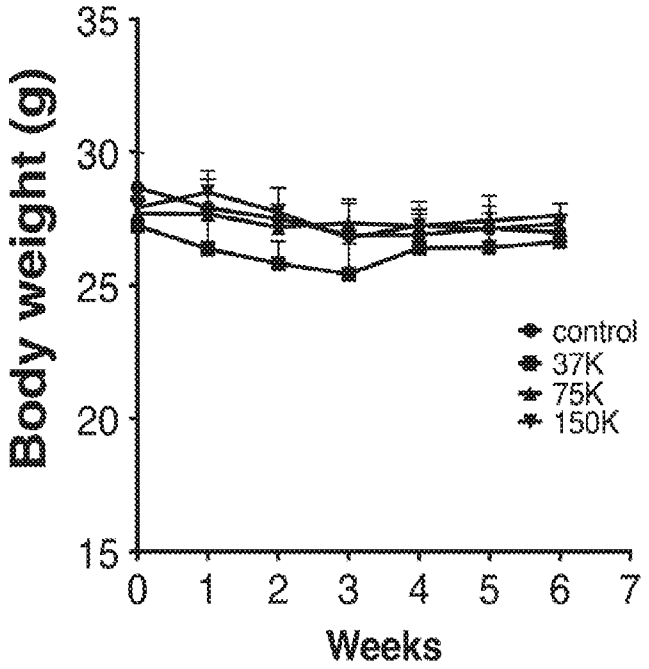

Fig. 50B

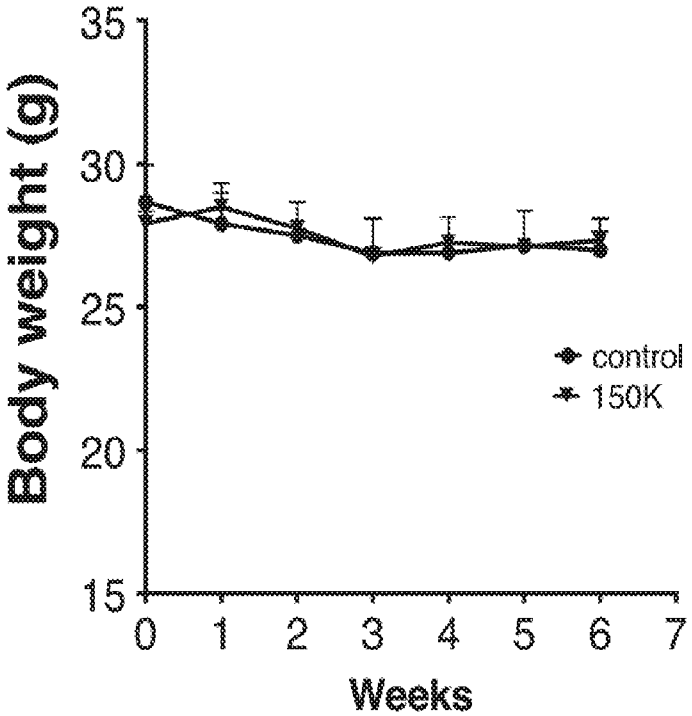

Fig. 51

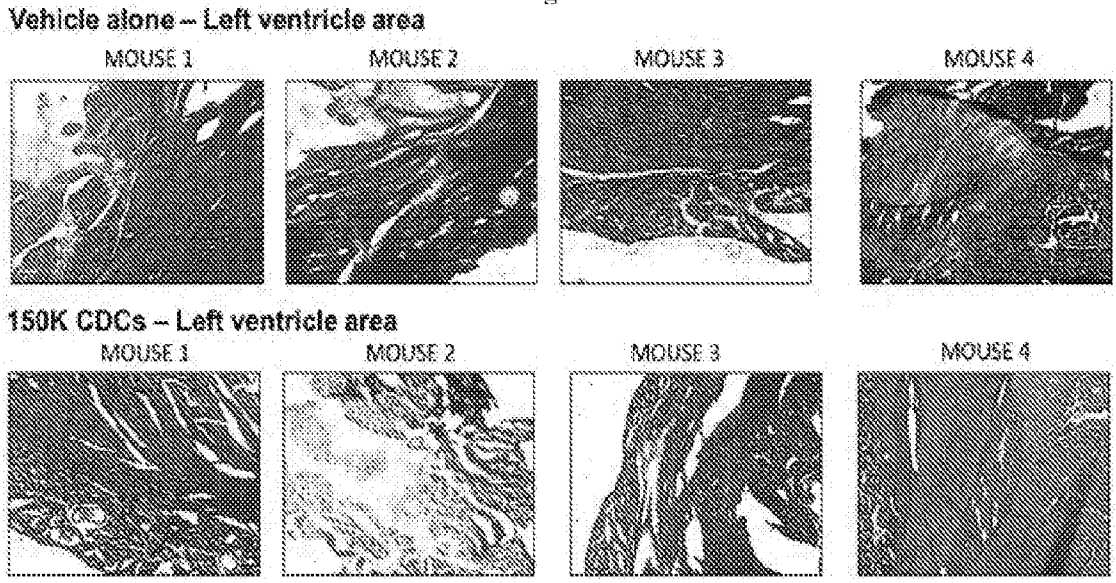
Vehicle alone – Left ventricle area
MOUSE 1
MOUSE 2
MOUSE 3
MOUSE 4
150K CDCs – Left ventricle area
MOUSE 1
MOUSE 2
MOUSE 3
MOUSE 4

Fig. 52A

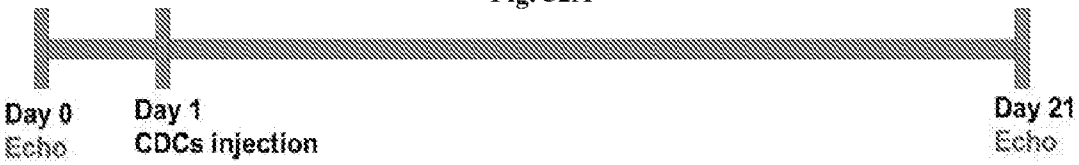

Fig. 52B

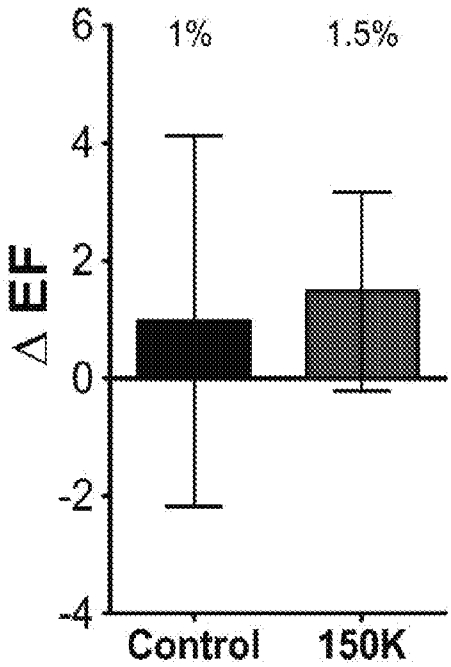

Fig. 53

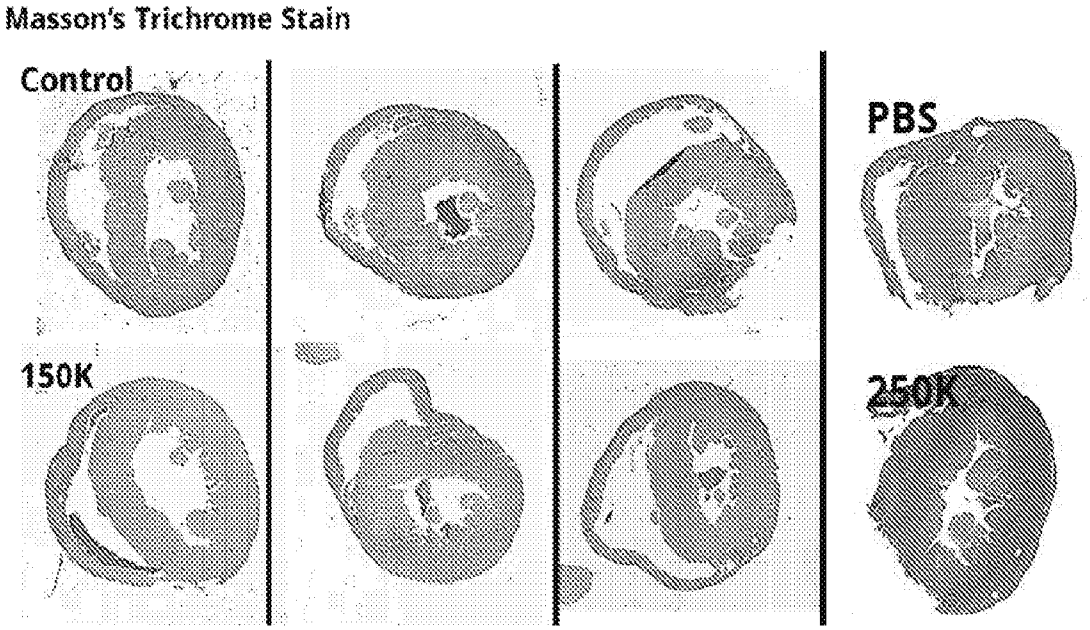

Fig. 54

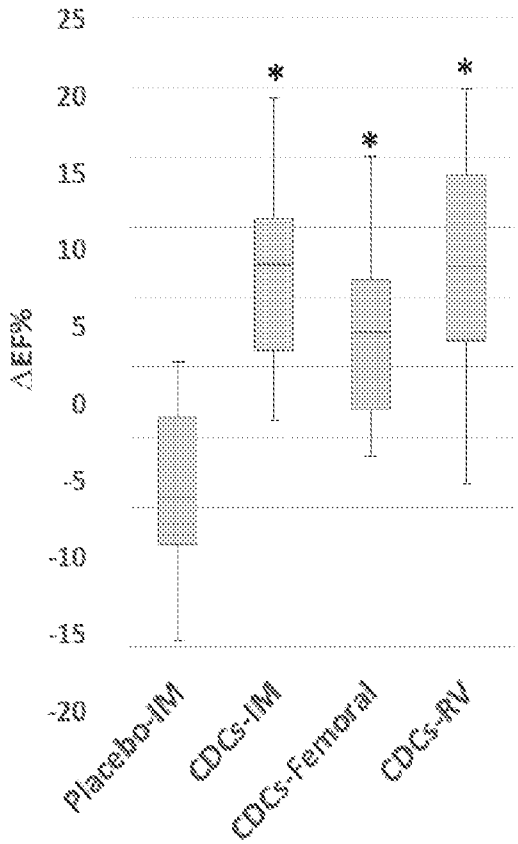
25
20
15
10
5
0
-5
-10
-15
-20
ΔEF%
*
*
*
Placebo-IM
CDCs-IM
CDCs-Femoral
CDCs-RV

Fig. 55A

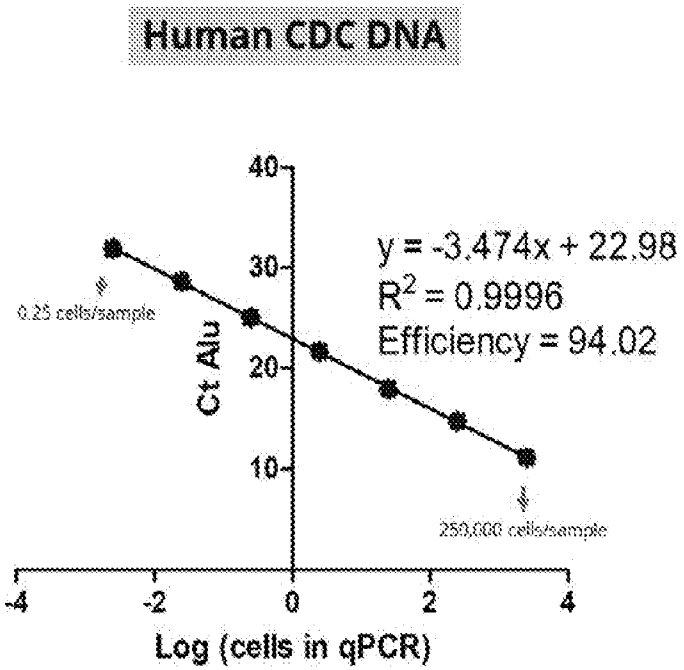

Fig. 55B

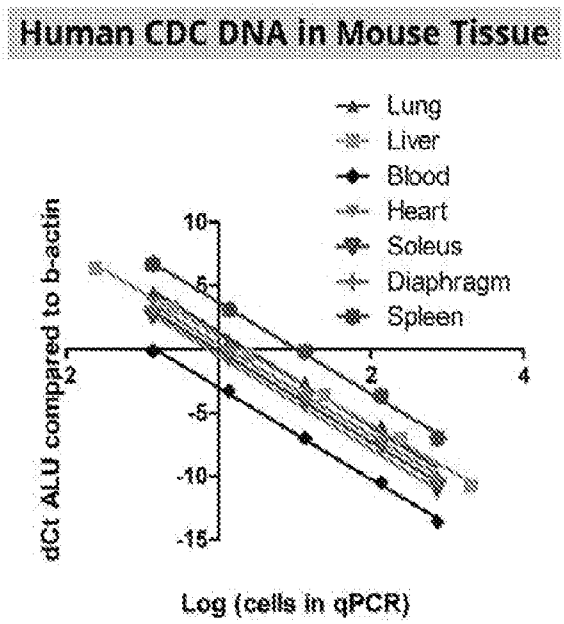

Fig. 56A

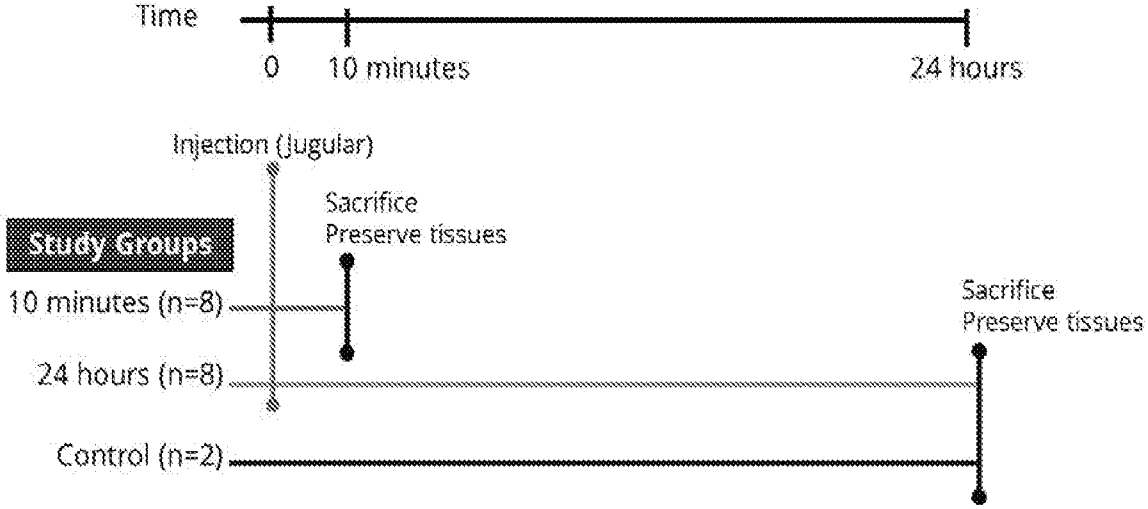

Fig. 56B

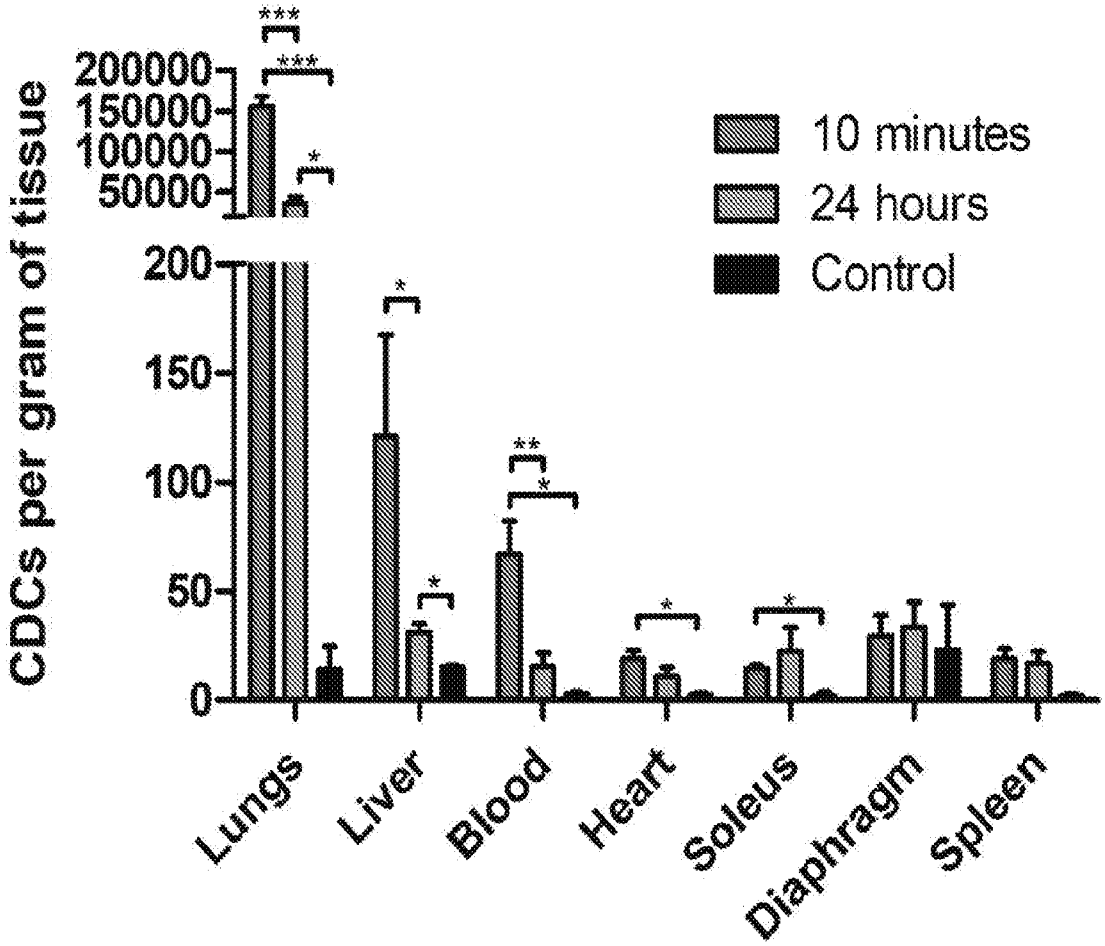

Fig. 57A

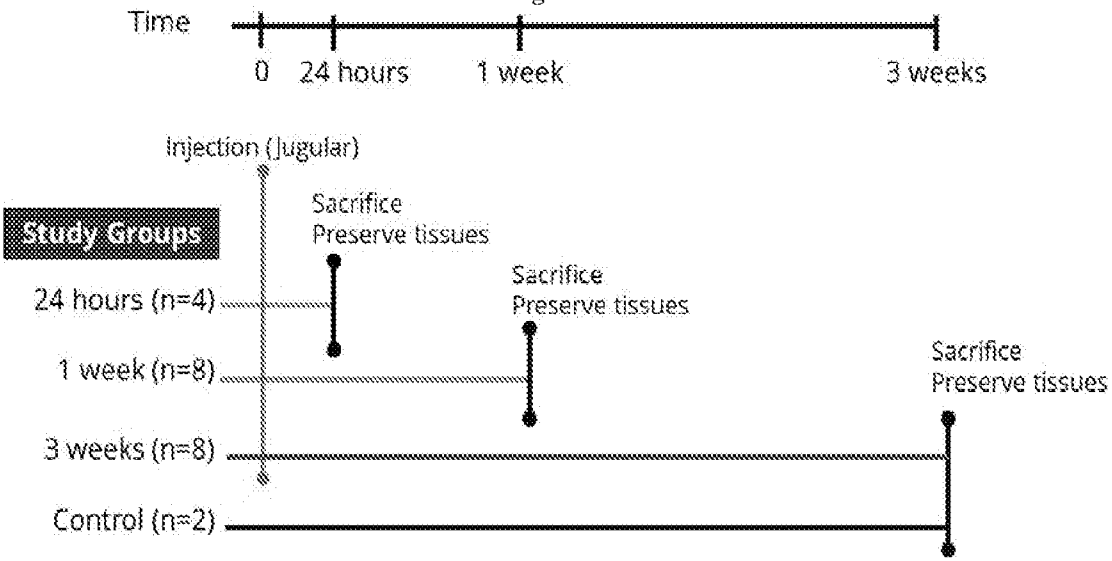

Fig. 57B

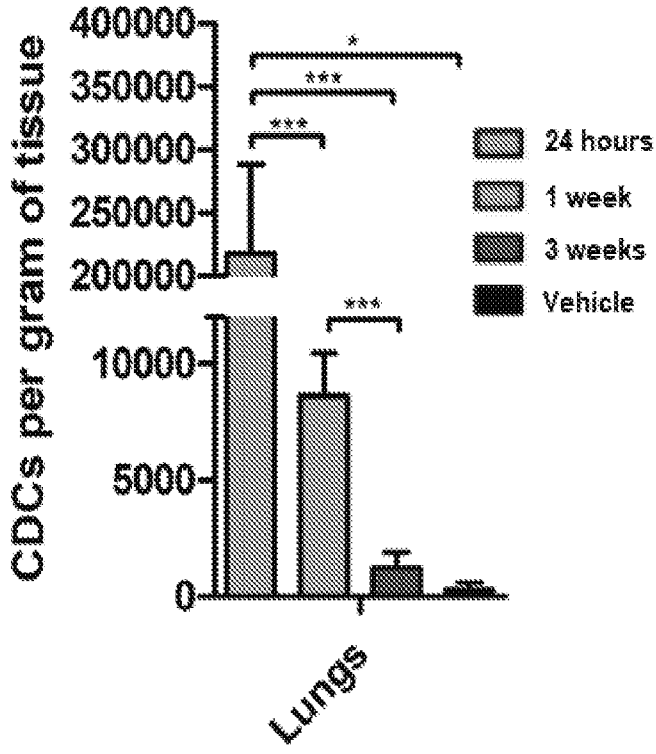

Fig. 57C

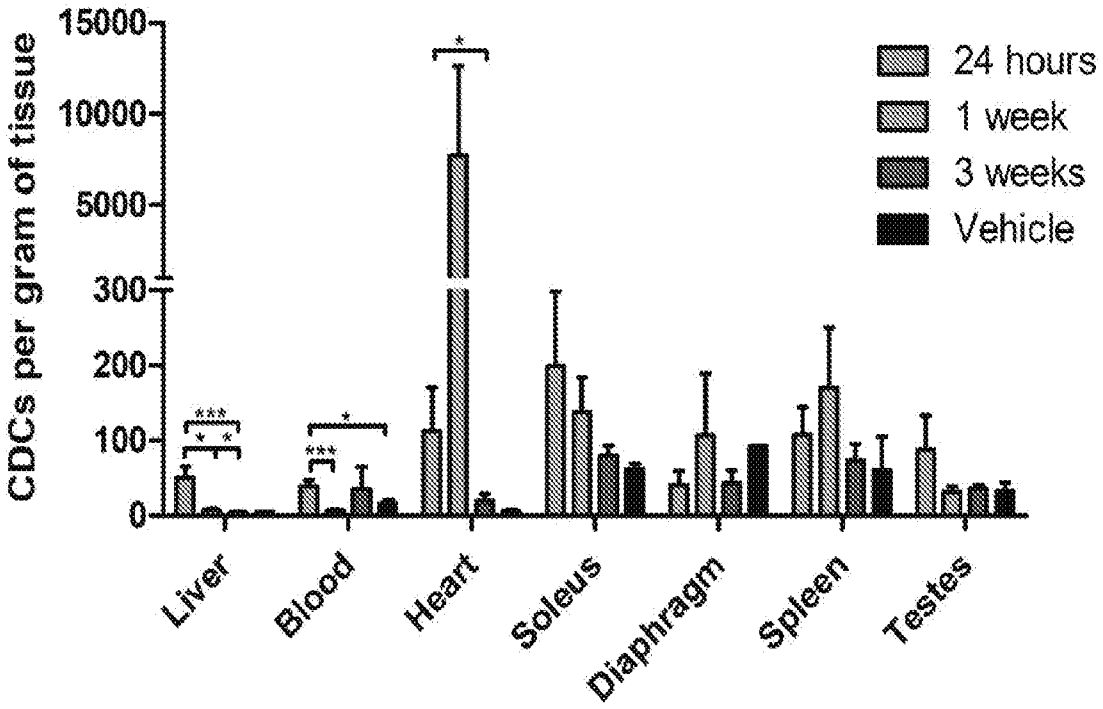
CDCs per gram of tissue
15000
10000
5000
300
200
100
0
24 hours
1 week
3 weeks
Vehicle
***
*
***
*
*
Liver
Blood
Heart
Soleus
Diaphragm
Spleen
Testes

Fig. 58

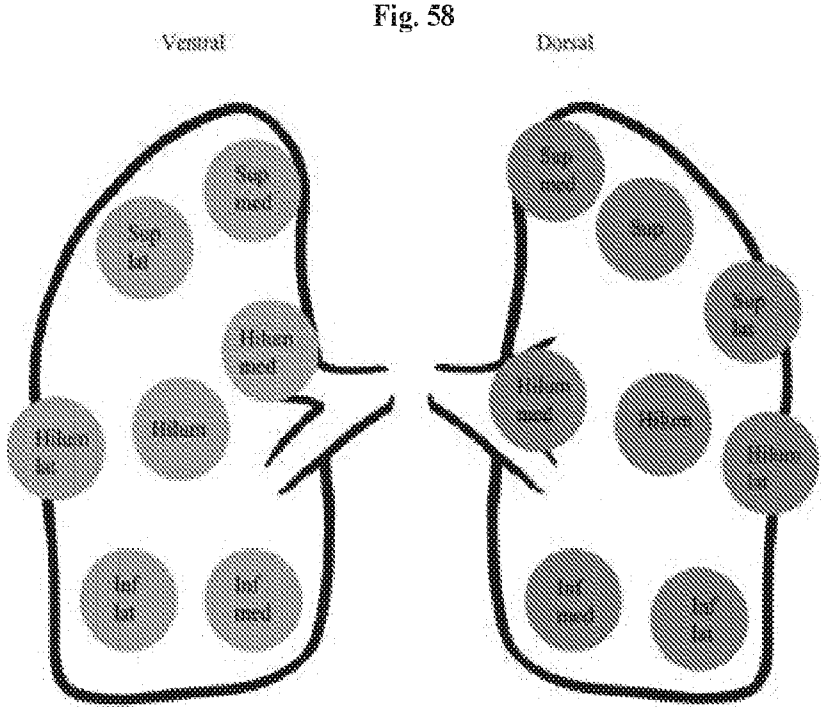
Ventral
Dorsal

Fig. 59

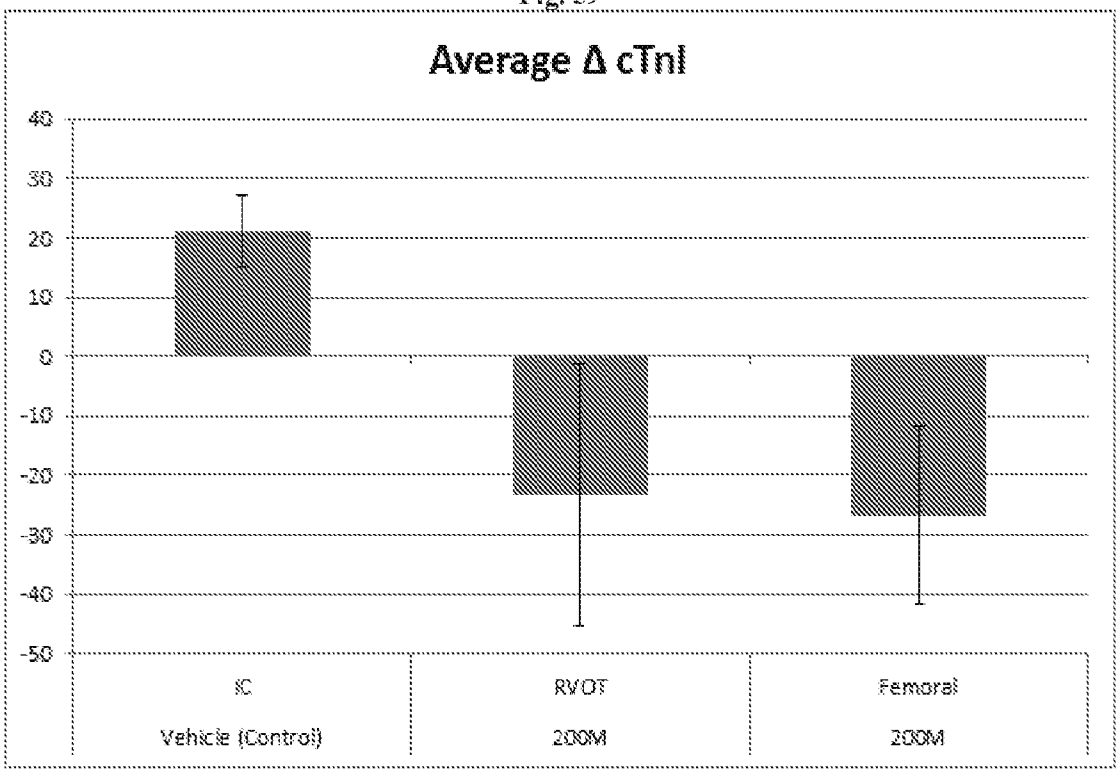
Average Δ cTnI
40
30
20
10
0
-10
-20
-30
-40
-50
IC
Vehicle (Control)
RVOT
200M
Femoral
200M

Fig. 60

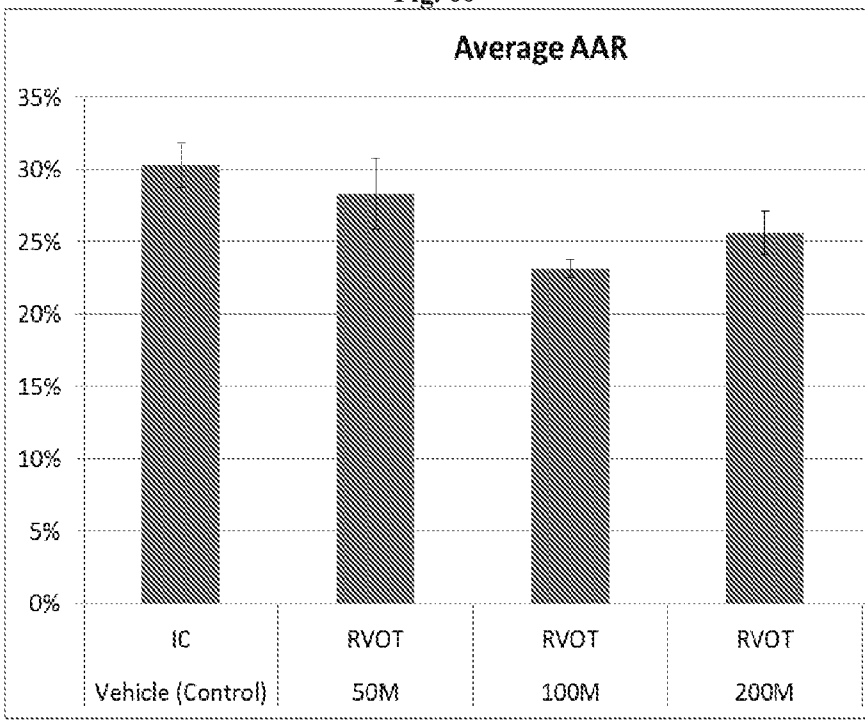
Average AAR
35%
30%
25%
20%
15%
10%
5%
0%
IC
Vehicle (Control)
RVOT
50M
RVOT
100M
RVOT
200M

Fig. 61

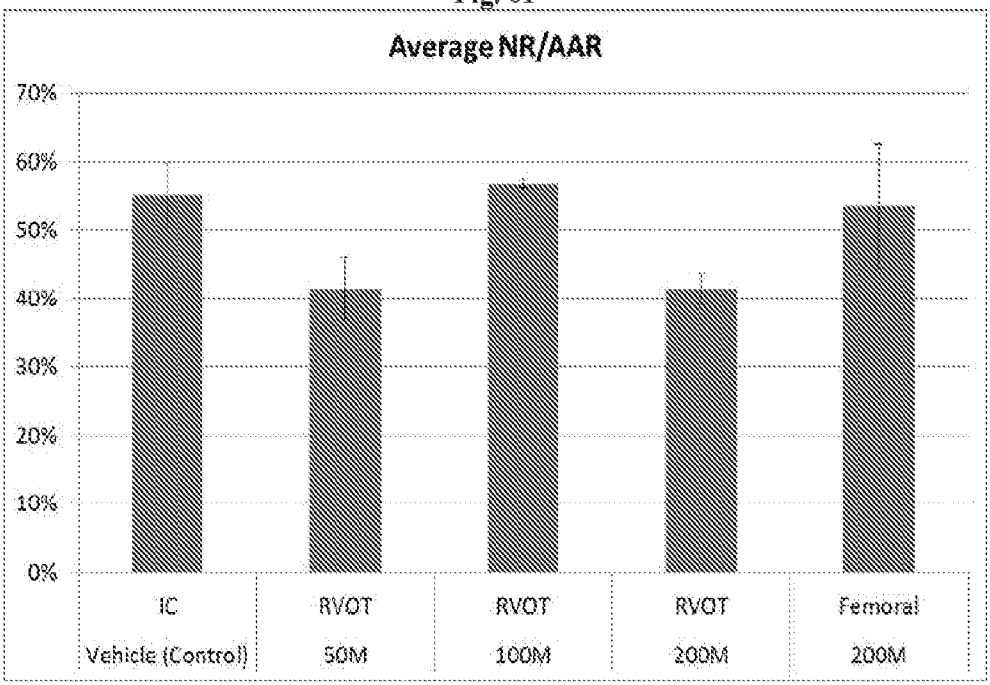
Average NR/AAR
70%
60%
50%
40%
30%
20%
10%
0%
IC
Vehicle (Control)
RVOT
50M
RVOT
100M
RVOT
200M
Femoral
200M

Fig. 62

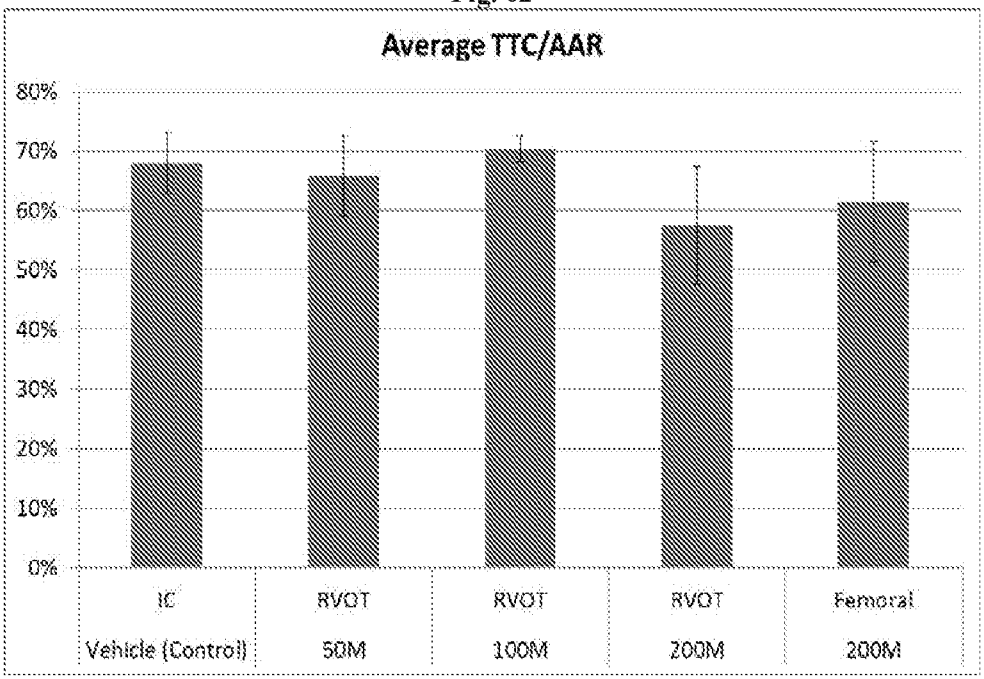
Average TTC/AAR
80%
70%
60%
50%
40%
30%
20%
10%
0%
IC
Vehicle (Control)
RVOT
50M
RVOT
100M
RVOT
200M
Femoral
200M

Fig. 63

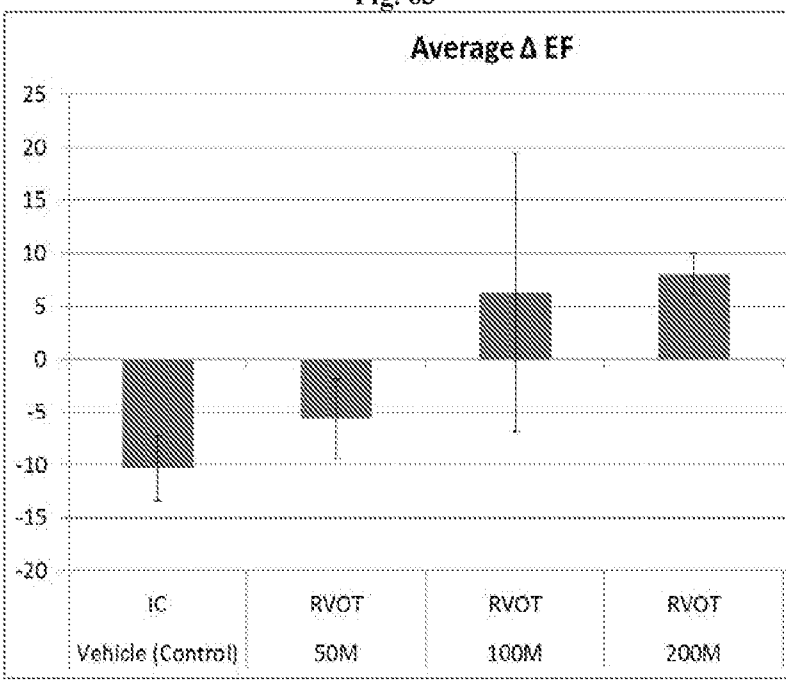
Average Δ EF
25
20
15
10
5
0
-5
-10
-15
-20
IC
Vehicle (Control)
RVOT
50M
RVOT
100M
RVOT
200M

Fig. 64

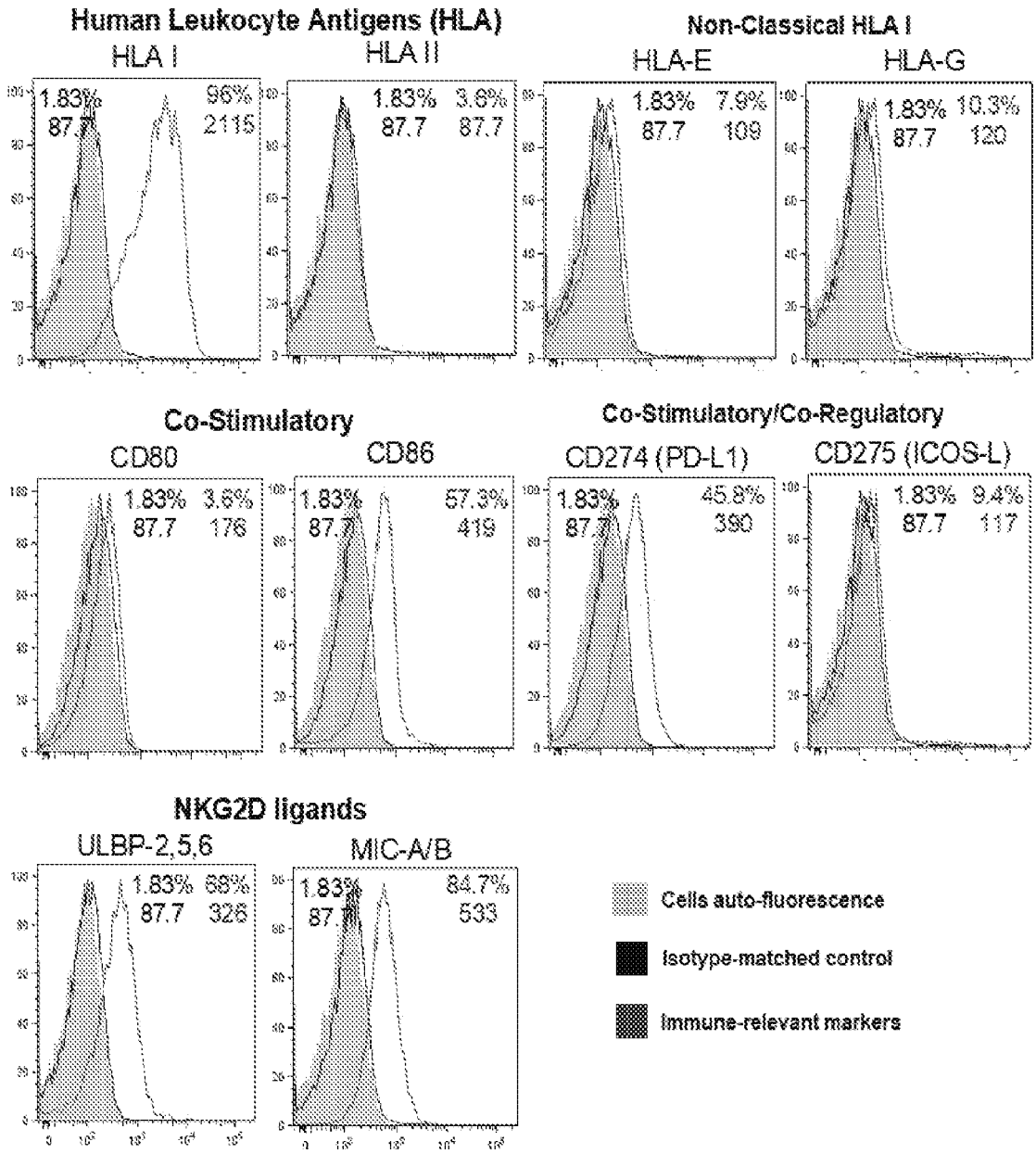
Human Leukocyte Antigens (HLA)
HLA I
1.83% 96%
87.7 2115
HLA II
1.83% 3.6%
87.7 87.7
Non-Classical HLA I
HLA-E
1.83% 7.9%
87.7 109
HLA-G
1.83% 10.3%
87.7 120
Co-Stimulatory
CD80
1.83% 3.6%
87.7 176
CD86
1.83% 57.3%
87.7 419
Co-Stimulatory/Co-Regulatory
CD274 (PD-L1)
1.83% 45.8%
87.7 390
CD275 (ICOS-L)
1.83% 9.4%
87.7 117
NKG2D ligands
ULBP-2,5,6
1.83% 68%
87.7 326
MIC-A/B
1.83% 84.7%
87.7 533
Cells auto-fluorescence
Isotype-matched control
Immune-relevant markers

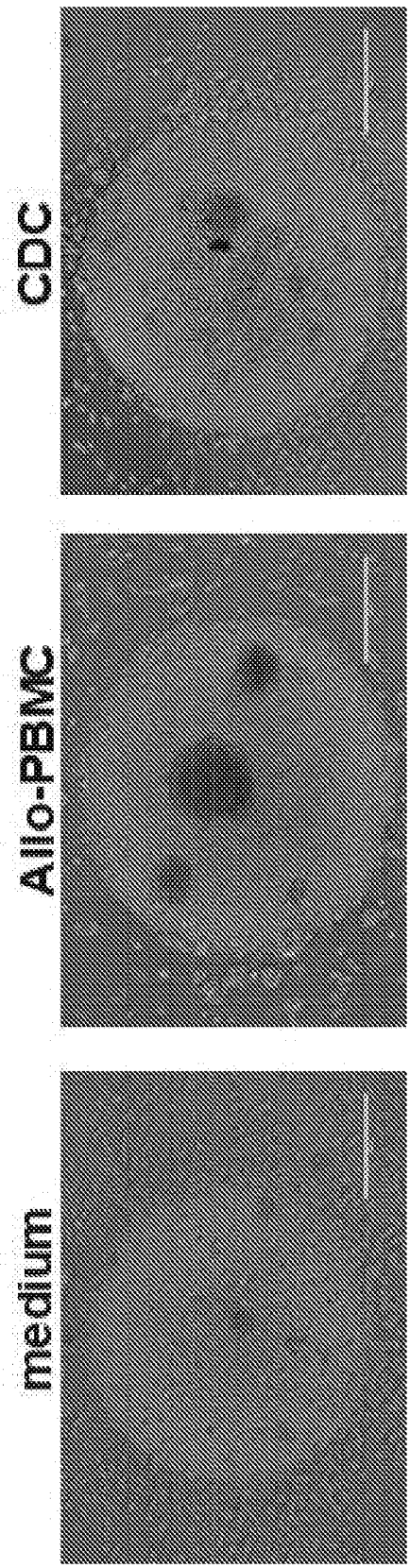

Fig. 65

Fig. 66

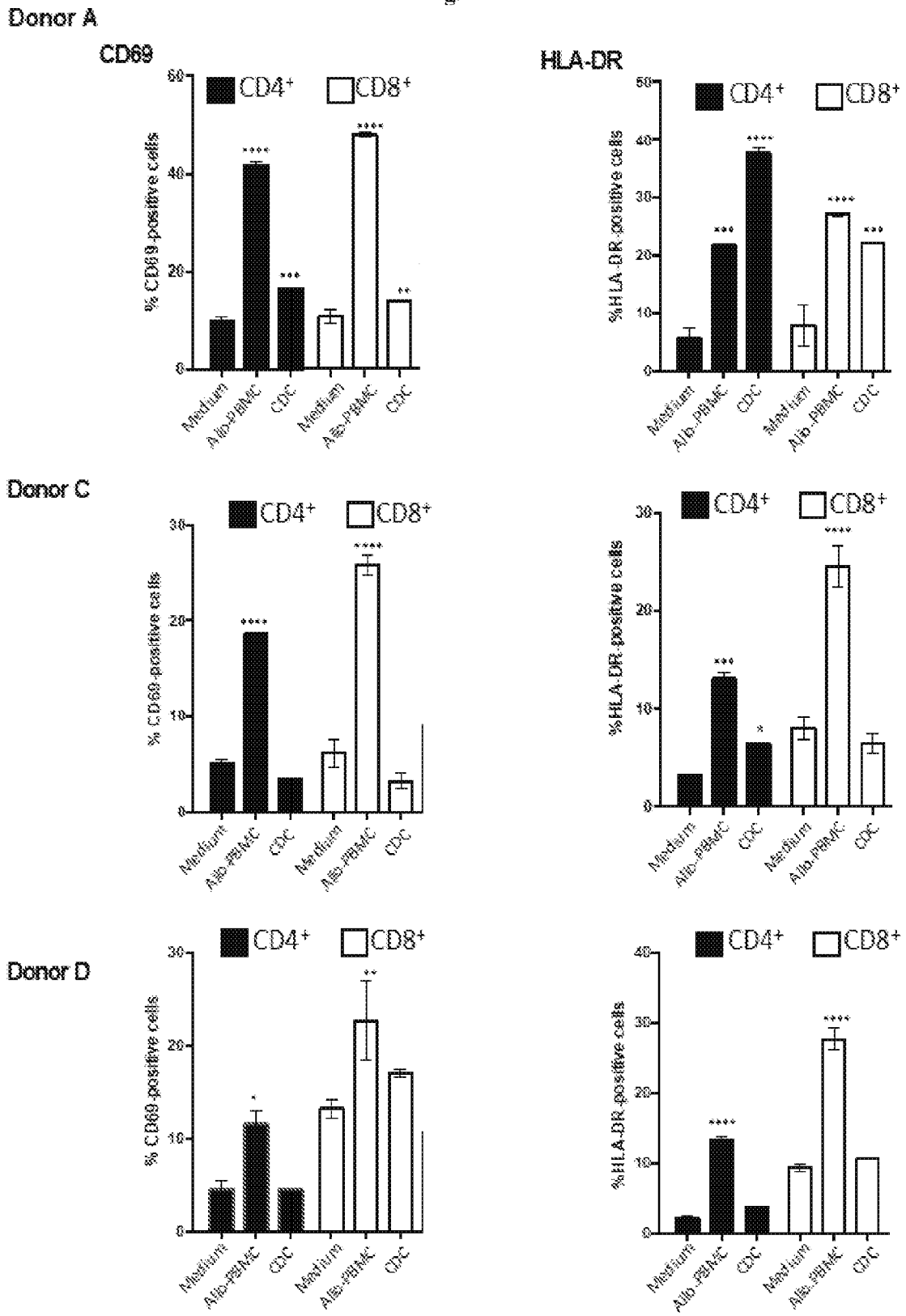
Donor A
CD69
HLA-DR
CD4+
CD8+
% CD69-positive cells
%HLA-DR-positive cells
Donor C
Donor D
Medium
Allo-PBMC
CDC

Fig. 67A

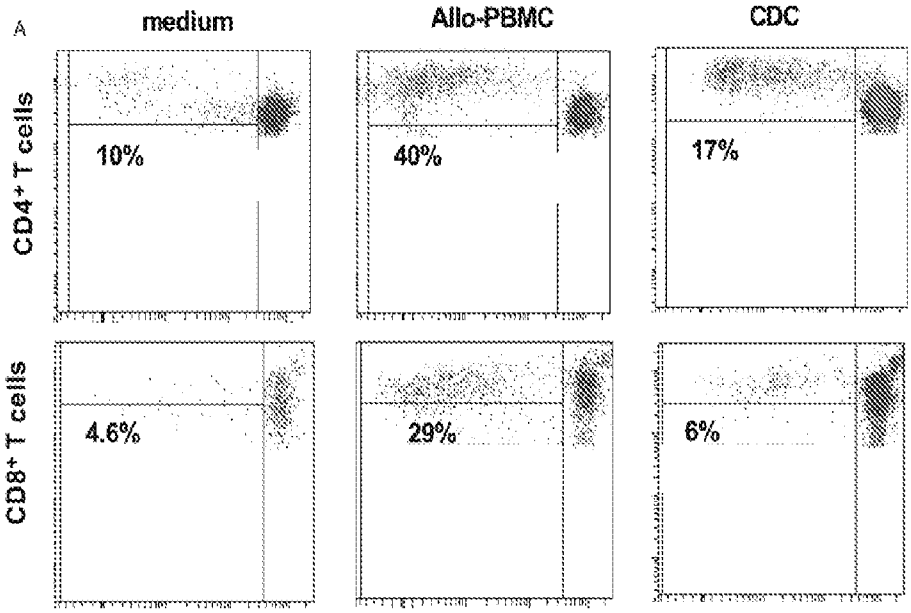

Fig. 67B

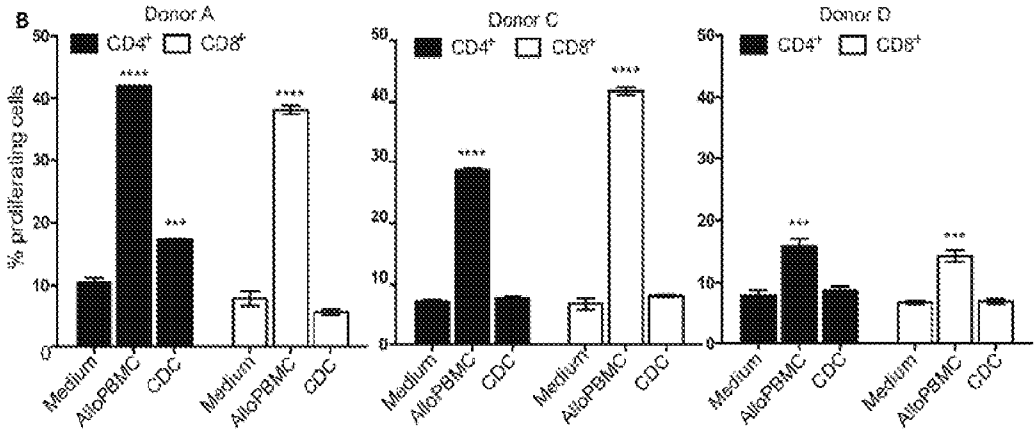

Fig. 67C

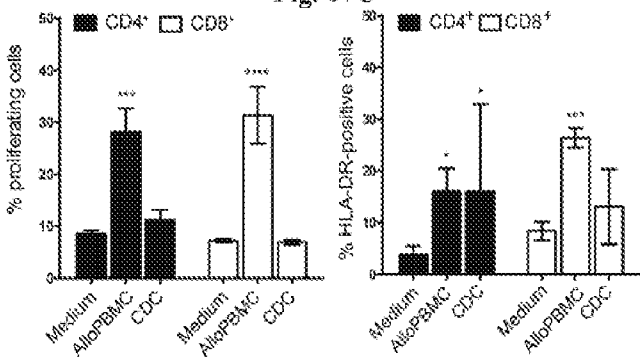

Fig. 68

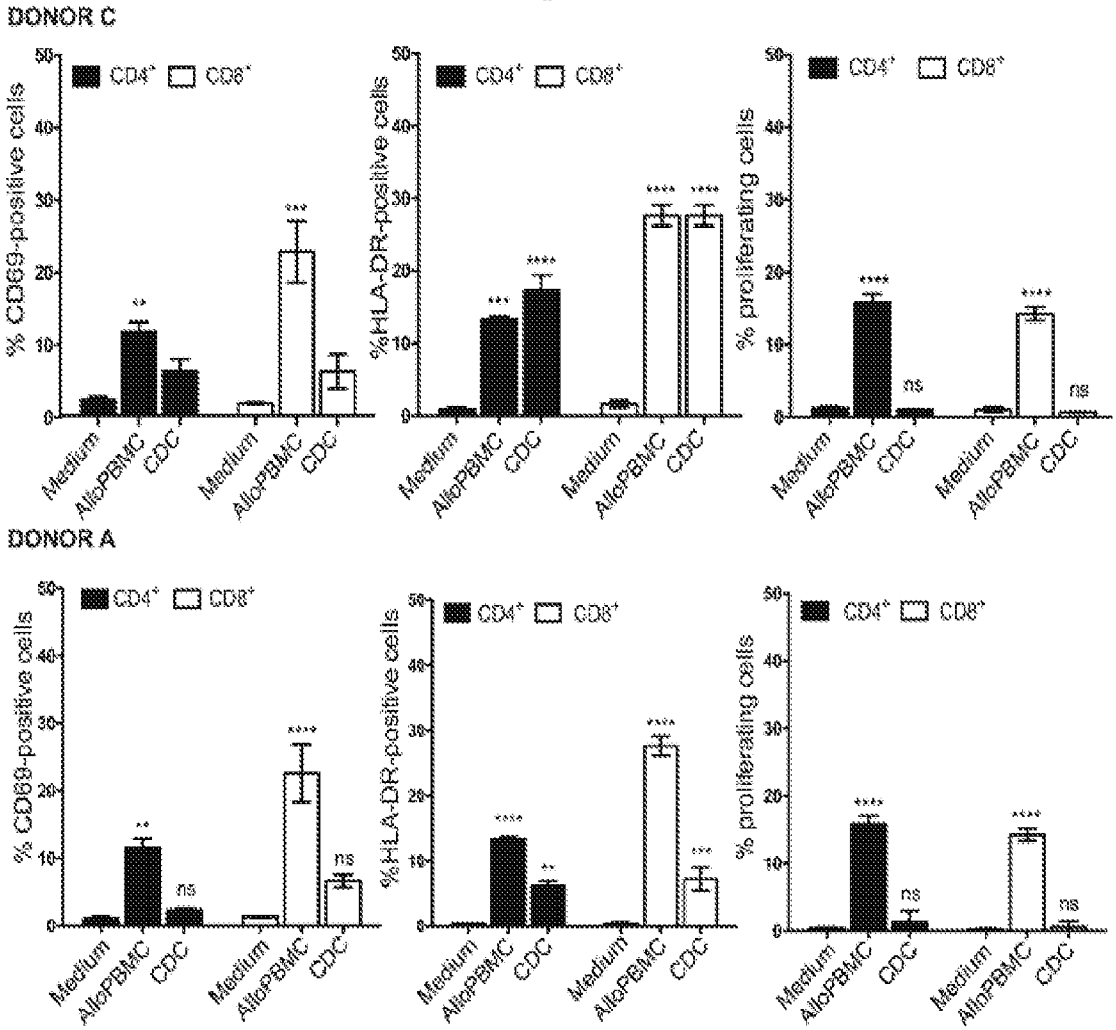

Mean Values ± SEM obtained from Donor C and Donor A

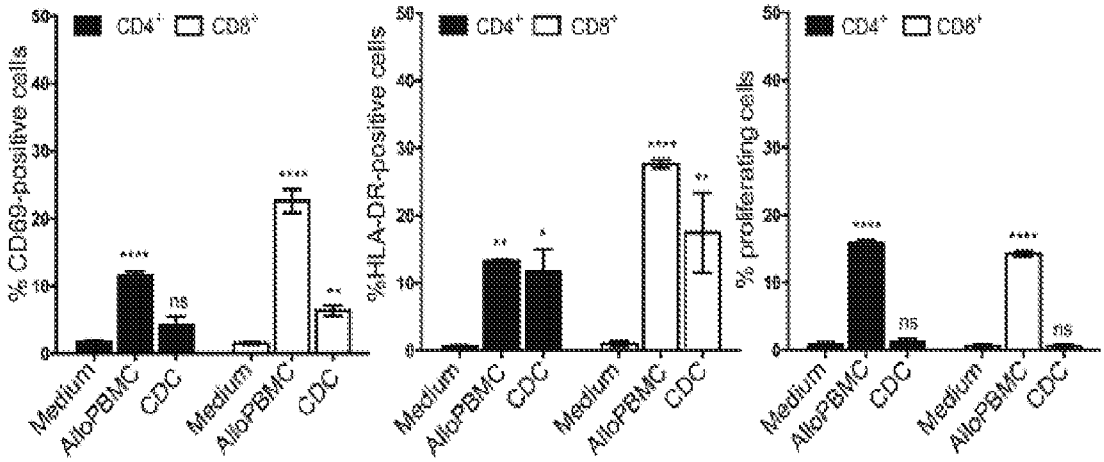

Fig. 69

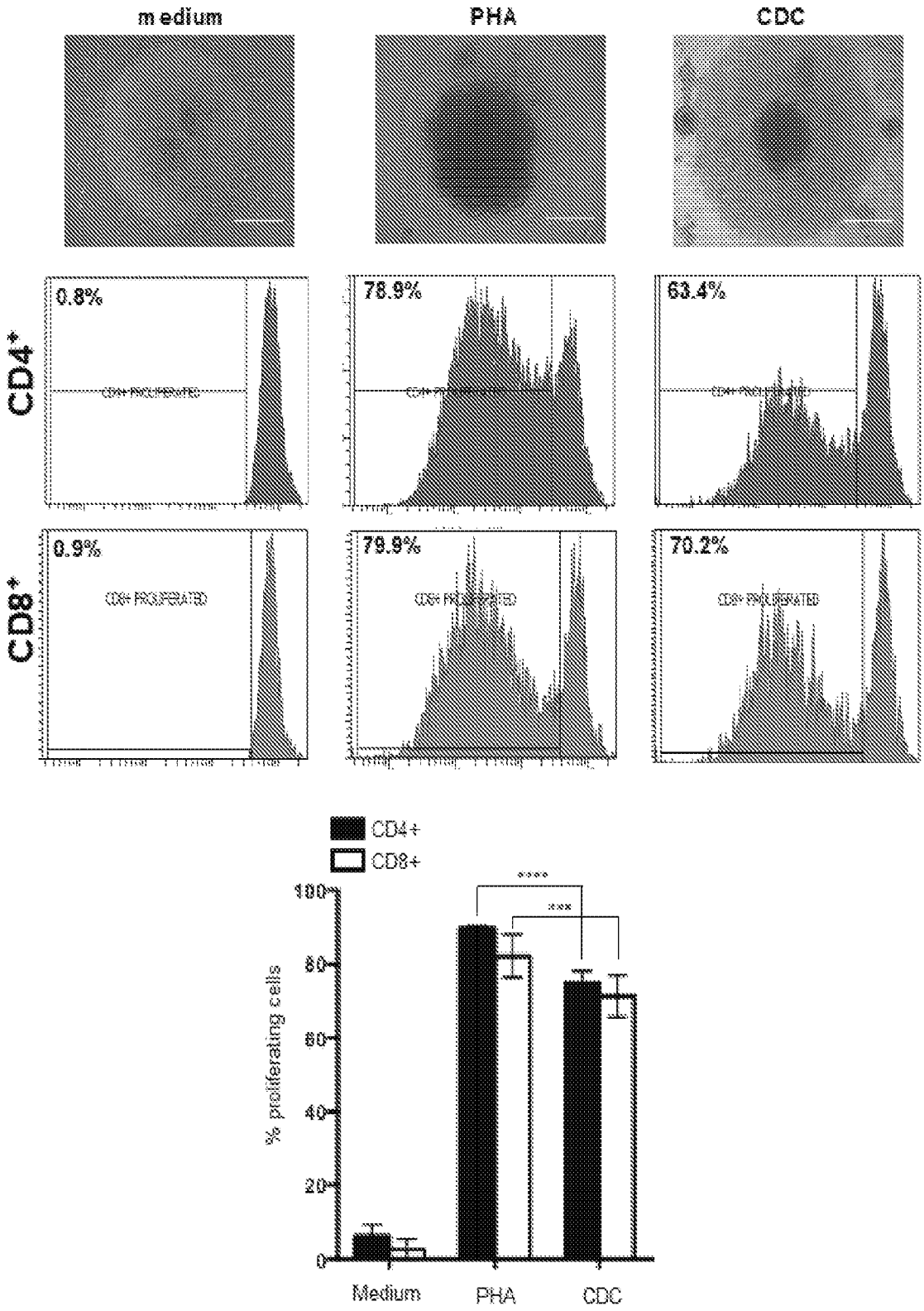
medium
PHA
CDC
CD4+
CD8+
0.8%
78.9%
63.4%
0.9%
79.9%
70.2%
CD4+
CD8+
% proliferating cells
100
80
60
40
20
0
****
***
Medium
PHA
CDC

Fig. 70

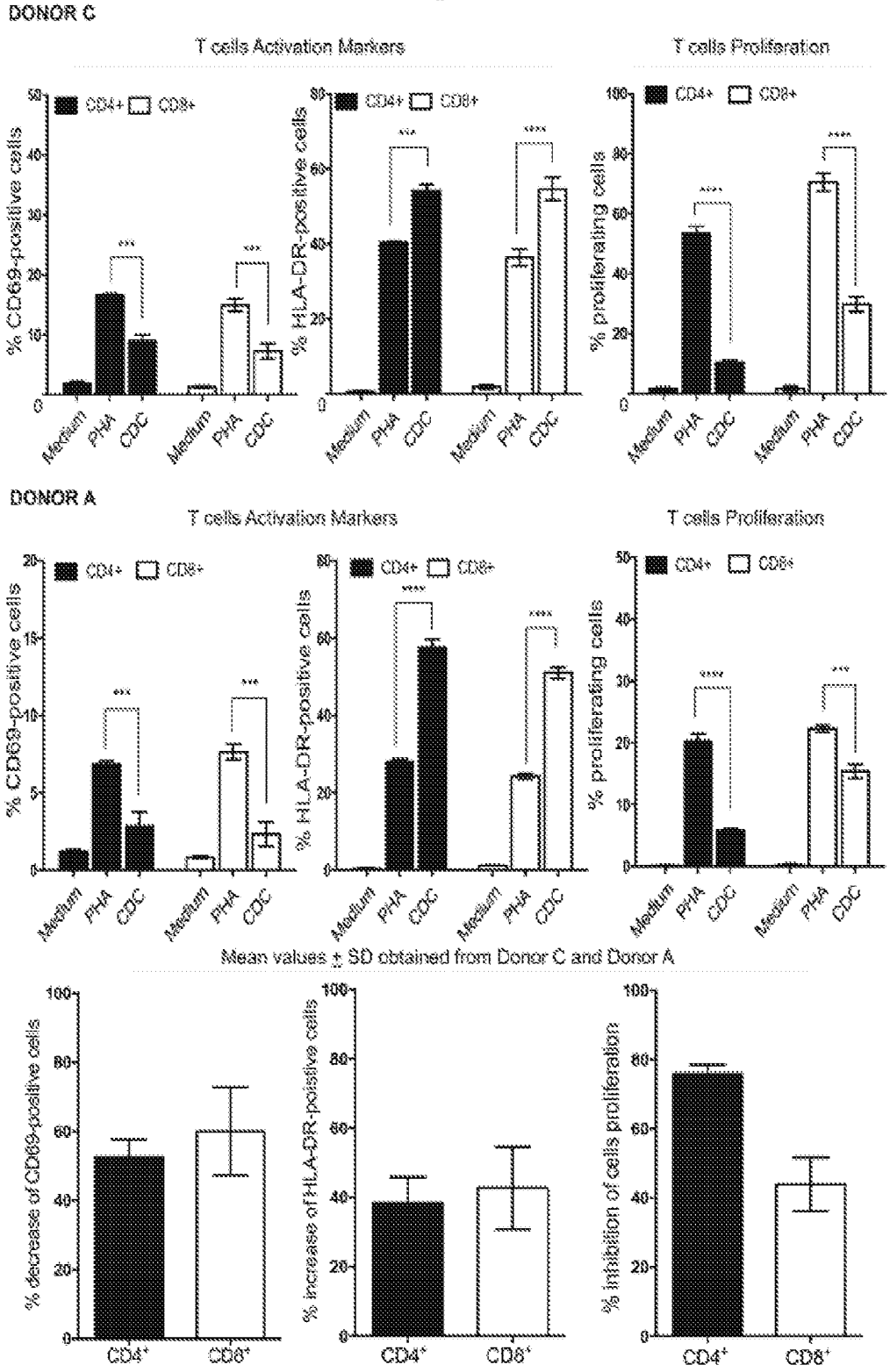
DONOR C
T cells Activation Markers
T cells Proliferation
CD4+ CD8+
% CD69-positive cells
% HLA-DR-positive cells
% proliferating cells
Medium PHA CDC Medium PHA CDC
DONOR A
T cells Activation Markers
T cells Proliferation
Mean values ± SD obtained from Donor C and Donor A
% decrease of CD69-positive cells
% increase of HLA-DR-positive cells
% inhibition of cells proliferation
CD4+ CD8+

Fig. 71

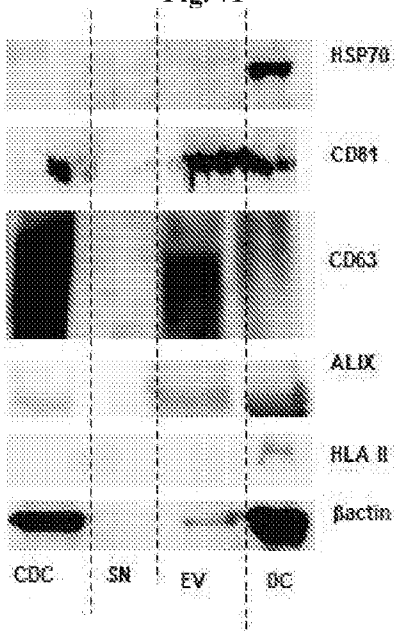
HSP70
CD81
CD63
ALIX
HLA II
βactin
CDC
SN
EV
DC

Fig. 72

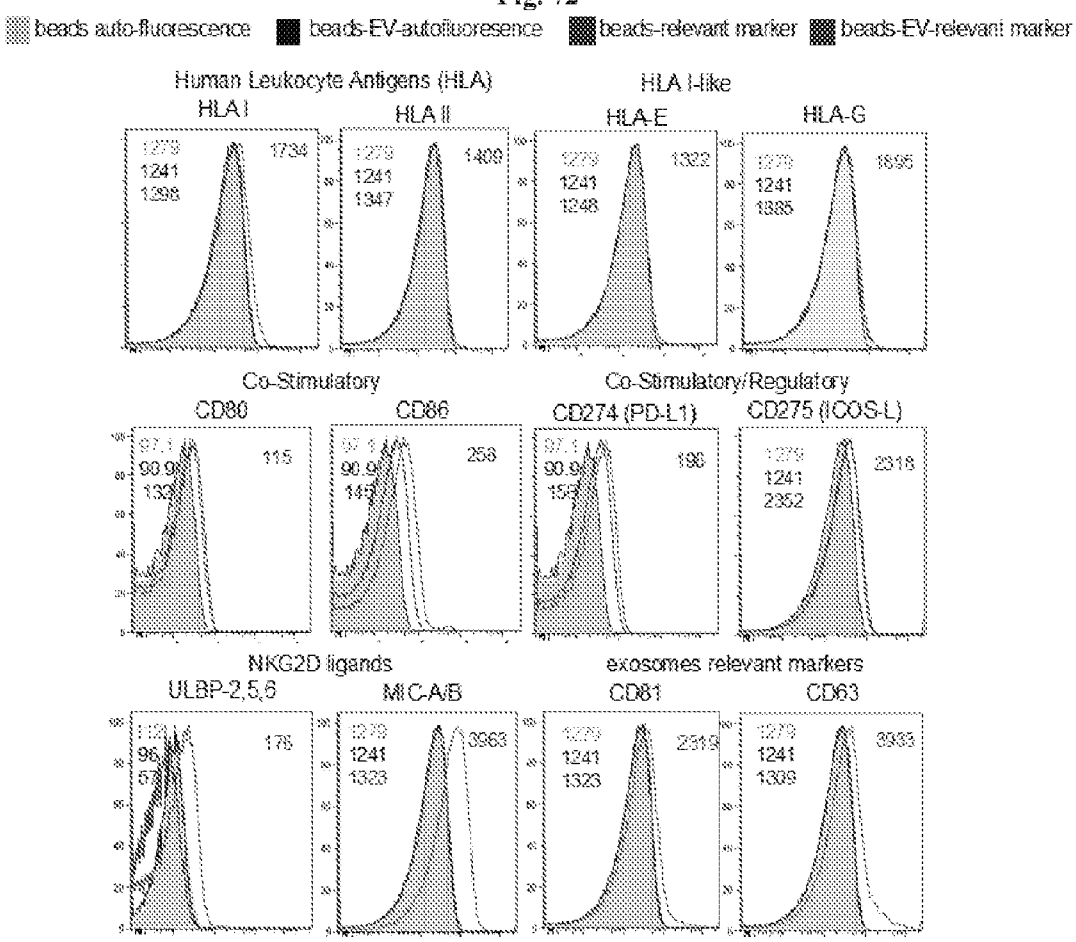
beads auto-fluorescence
beads-EV-autofluoresence
beads-relevant marker
beads-EV-relevant marker
Human Leukocyte Antigens (HLA)
HLA I
HLA II
HLA I-like
HLA-E
HLA-G
Co-Stimulatory
CD80
CD86
Co-Stimulatory/Regulatory
CD274 (PD-L1)
CD275 (ICOS-L)
NKG2D ligands
ULBP-2,5,6
MIC-A/B
exosomes relevant markers
CD81
CD63

Fig. 73A

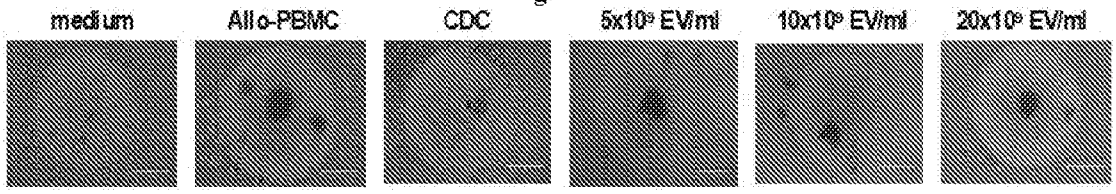

Fig. 73B

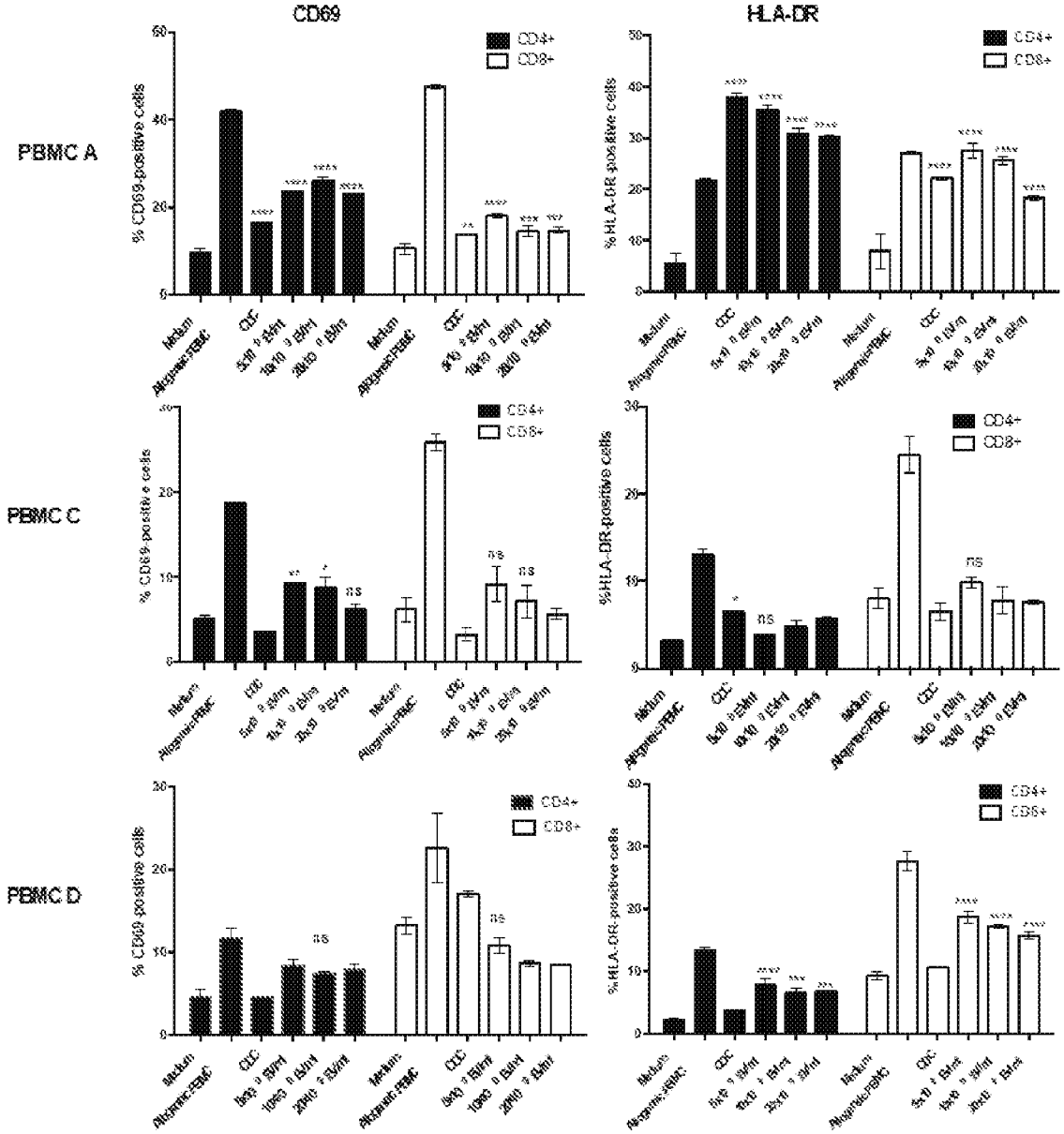

Fig. 74A

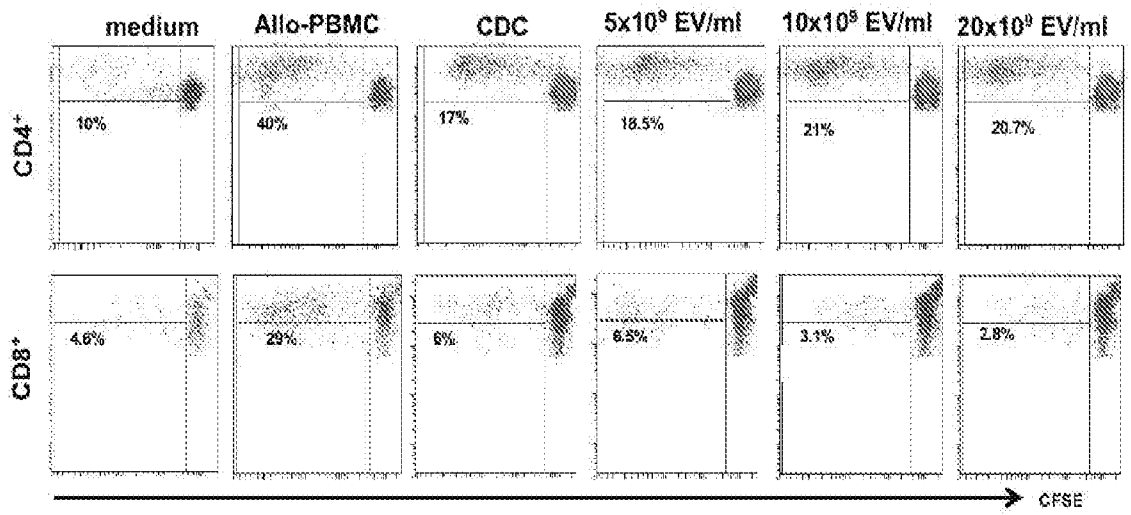

Fig. 74B

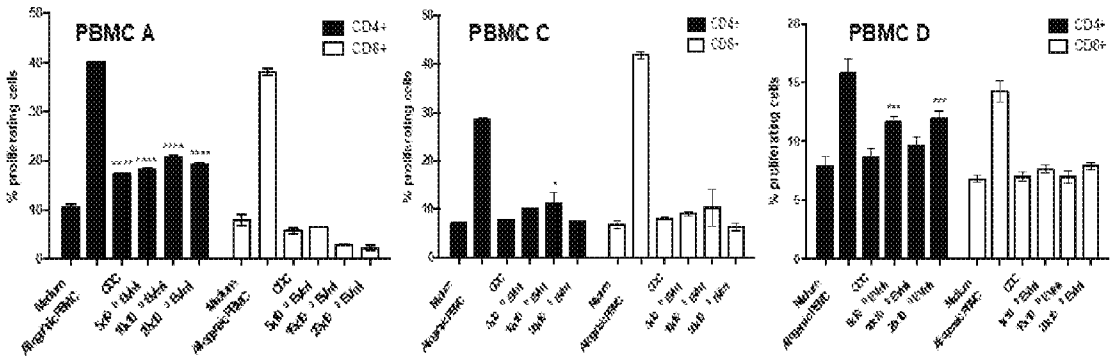

Fig. 75

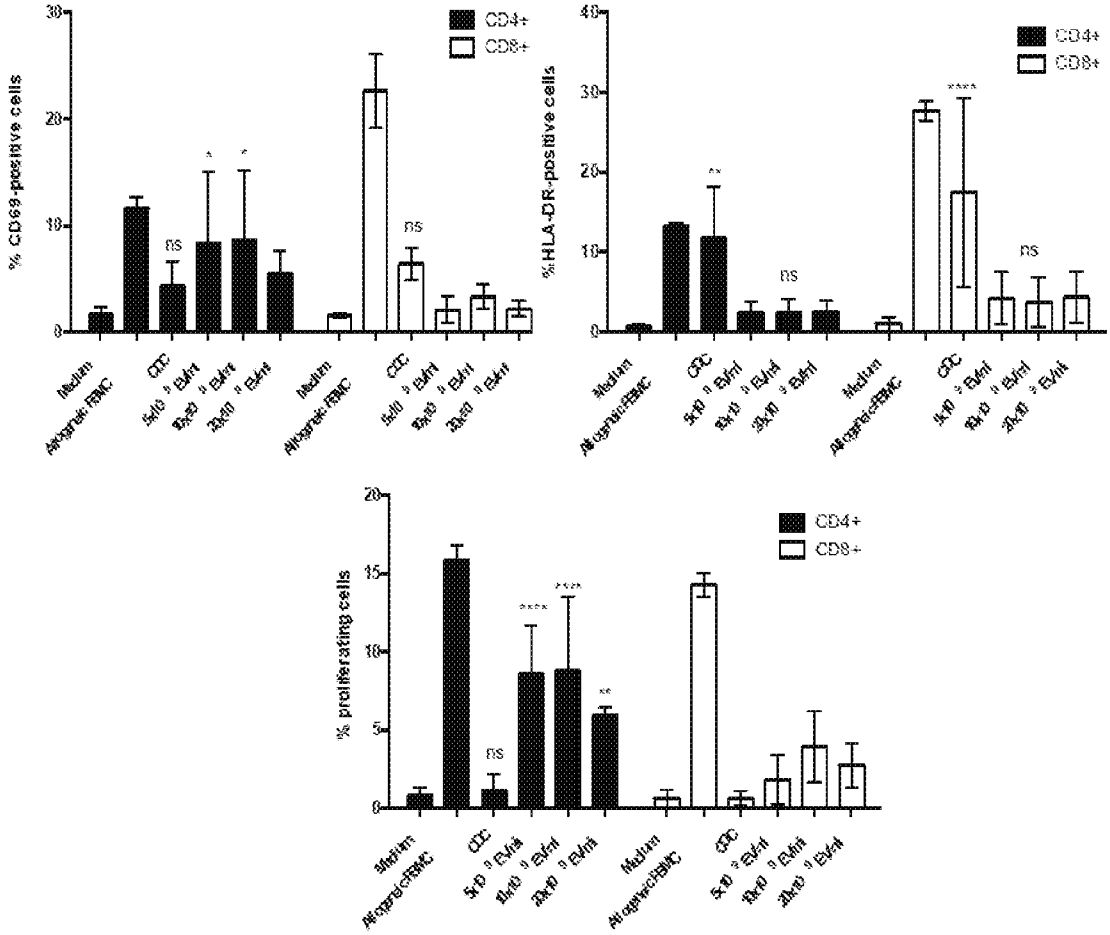
% CD69-positive cells
% HLA-DR-positive cells
% proliferating cells
CD4+
CD8+
ns
Medium
Allogeneic PBMC
cDC
5x10^3 EV/ml
10x10^3 EV/ml
20x10^3 EV/ml

Fig. 76

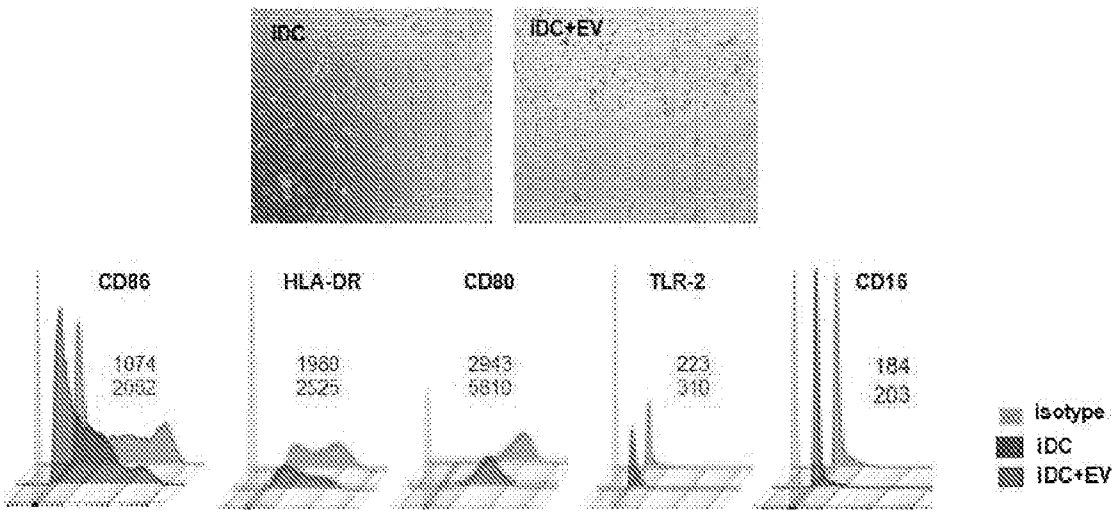
iDC
iDC+EV
CD86
1074
2662
HLA-DR
1980
2525
CD80
2943
5810
TLR-2
223
310
CD16
184
203
isotype
iDC
iDC+EV

Fig. 77

Donor 1

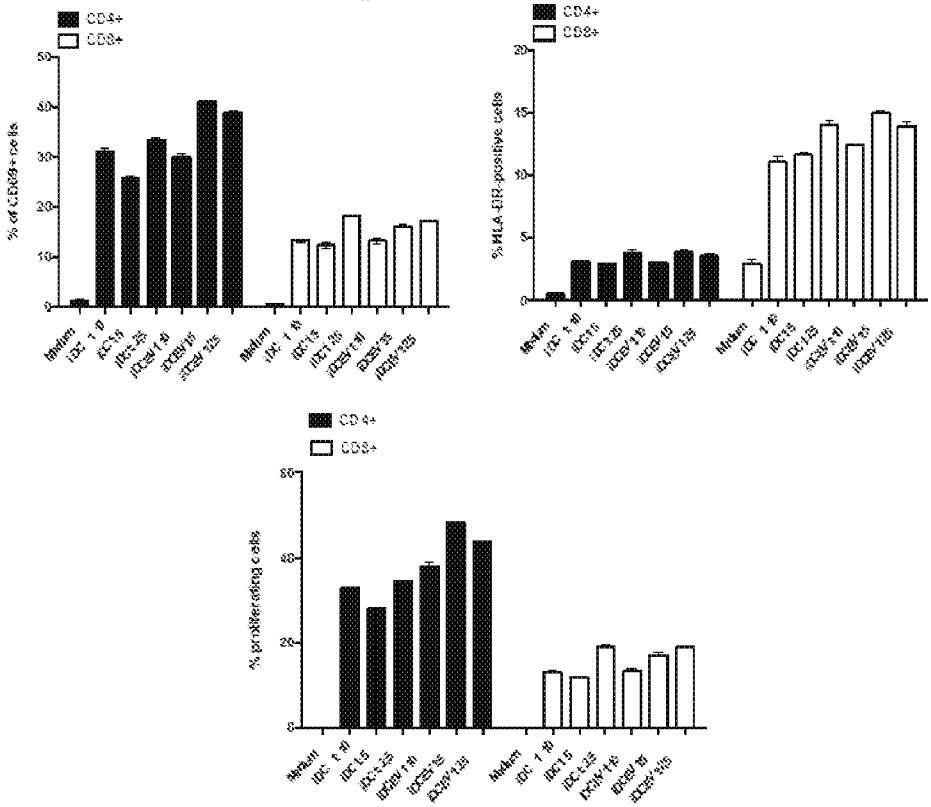

Donor 2

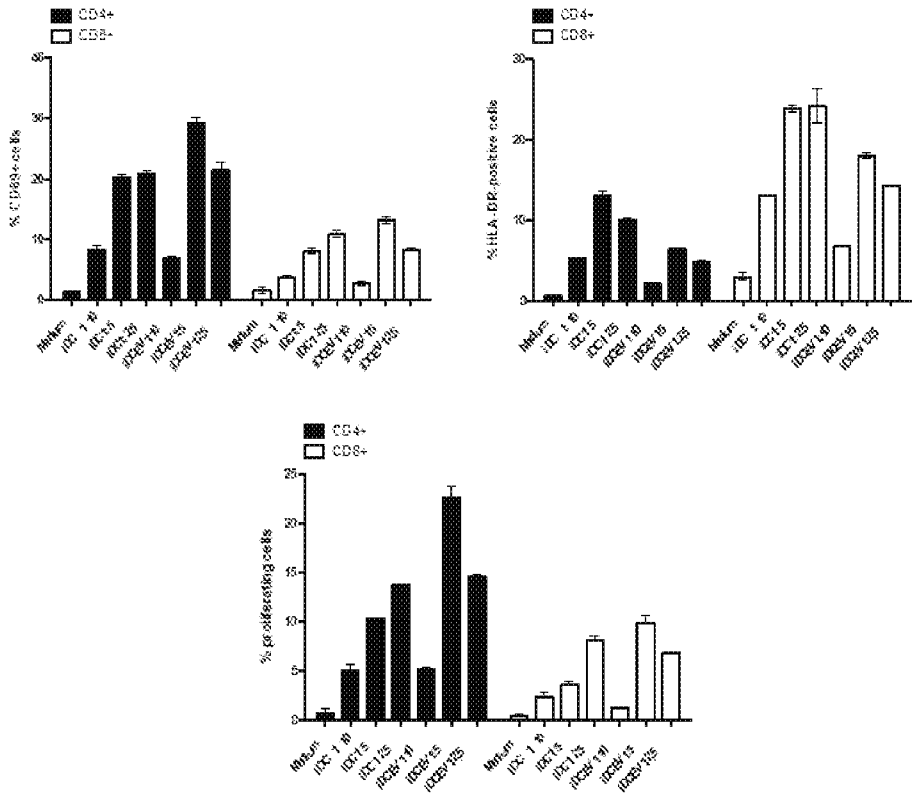

Fig. 78

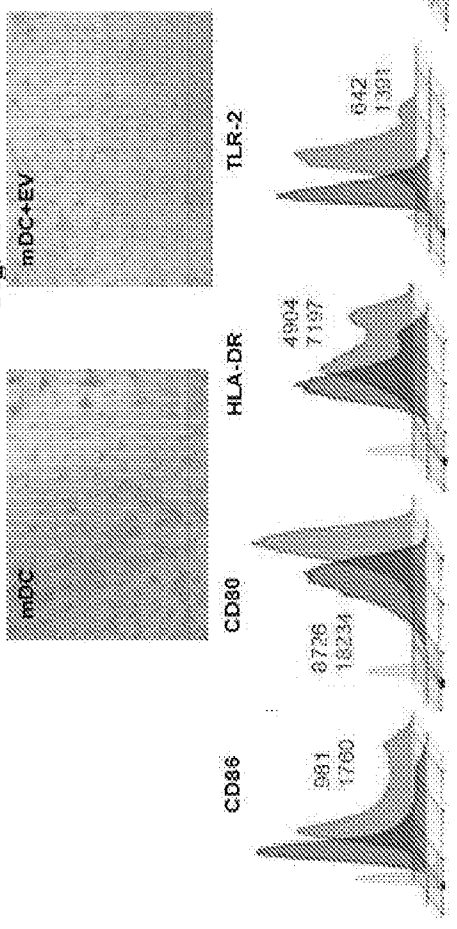
mDC
mDC+EV
CD86
CD80
HLA-DR
TLR-2
CD16
931
1760
6736
18234
4304
7197
642
1331
1357
1229
isotypes
mDC
mDC+EV

Fig. 79

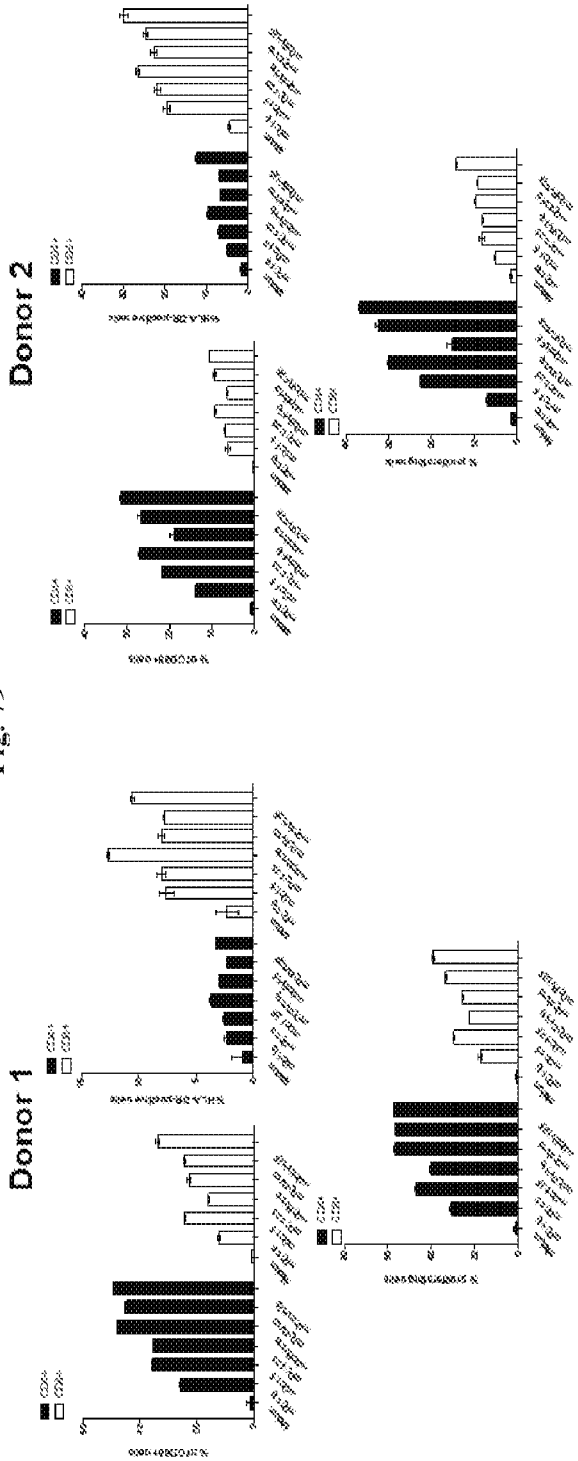
Donor 1
Donor 2

Fig. 80

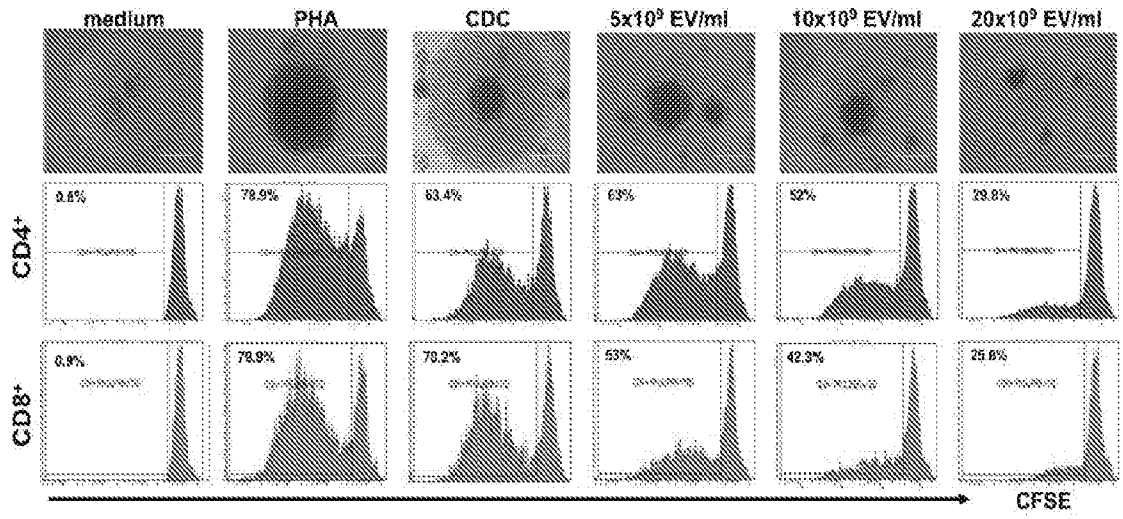
medium
PHA
CDC
5x10⁹ EV/ml
10x10⁹ EV/ml
20x10⁹ EV/ml
CD4+
CD8+
0.6%
78.9%
63.4%
63%
52%
29.8%
0.9%
78.9%
70.2%
53%
42.3%
25.6%
CFSE

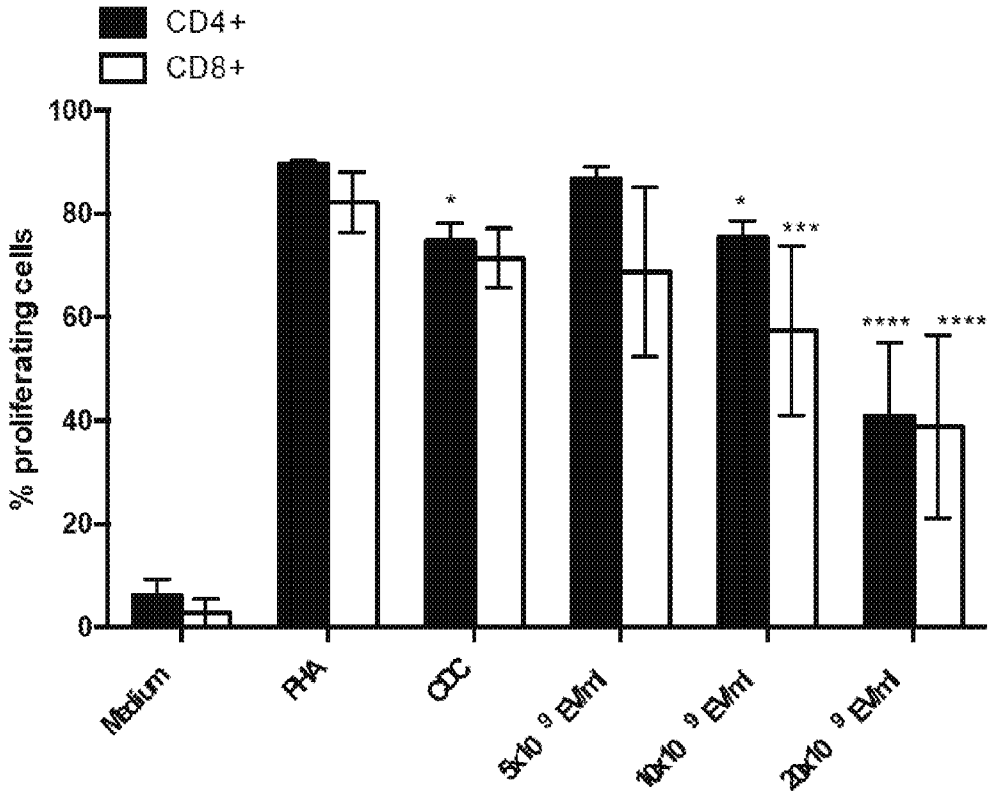
CD4+
CD8+
% proliferating cells
100
80
60
40
20
0
*
*
***
****
****
Medium
PHA
CDC
5x10 9 EV/ml
10x10 9 EV/ml
20x10 9 EV/ml

Fig. 81

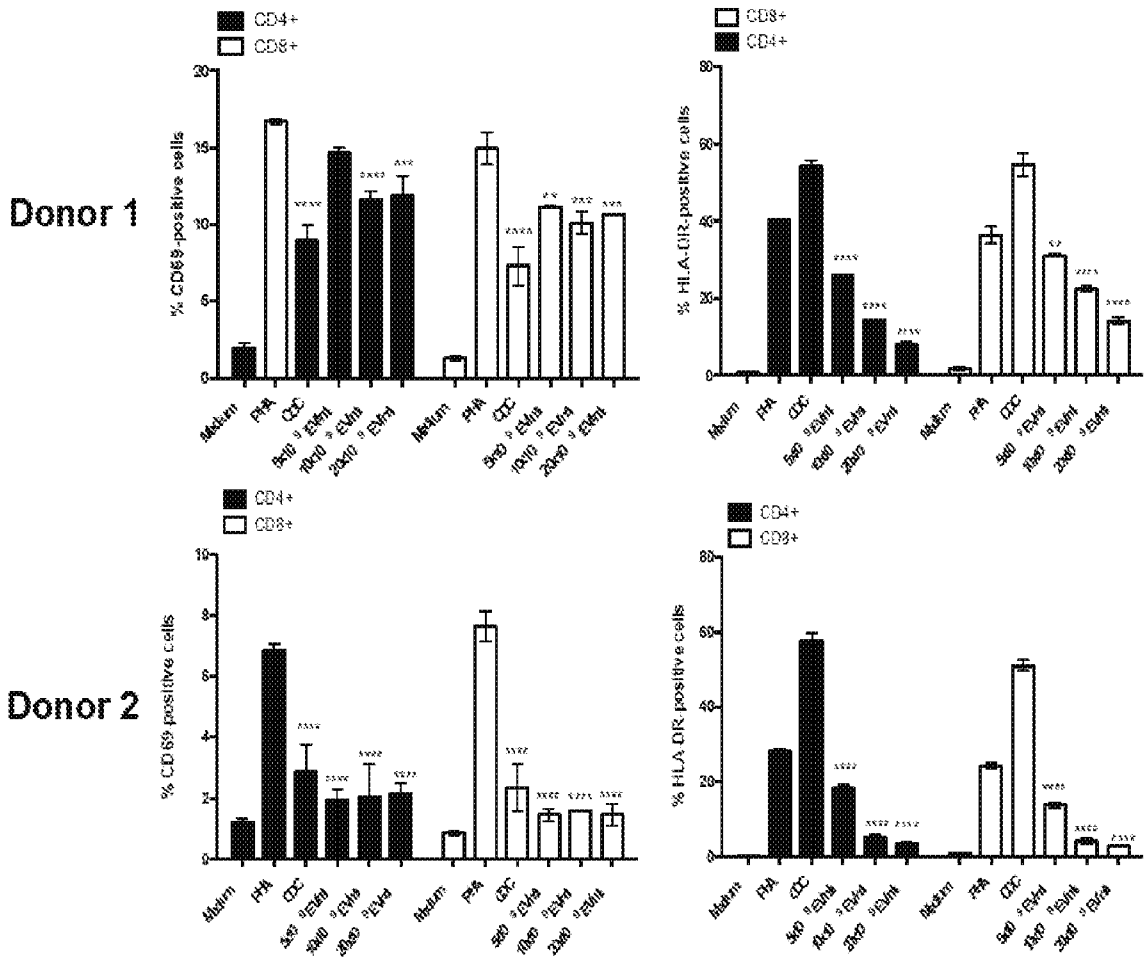
Donor 1
Donor 2
CD4+
CD8+
% CD69-positive cells
% HLA-DR-positive cells
% CD69 positive cells
% HLA DR positive cells
Medium
PHA
CDC
5x10 3 EVs/ml
10x10 3 EVs/ml
20x10 3 EVs/ml
5x0 3 EVs/ml
10x0 3 EVs/ml
20x0 3 EVs/ml

Fig. 82

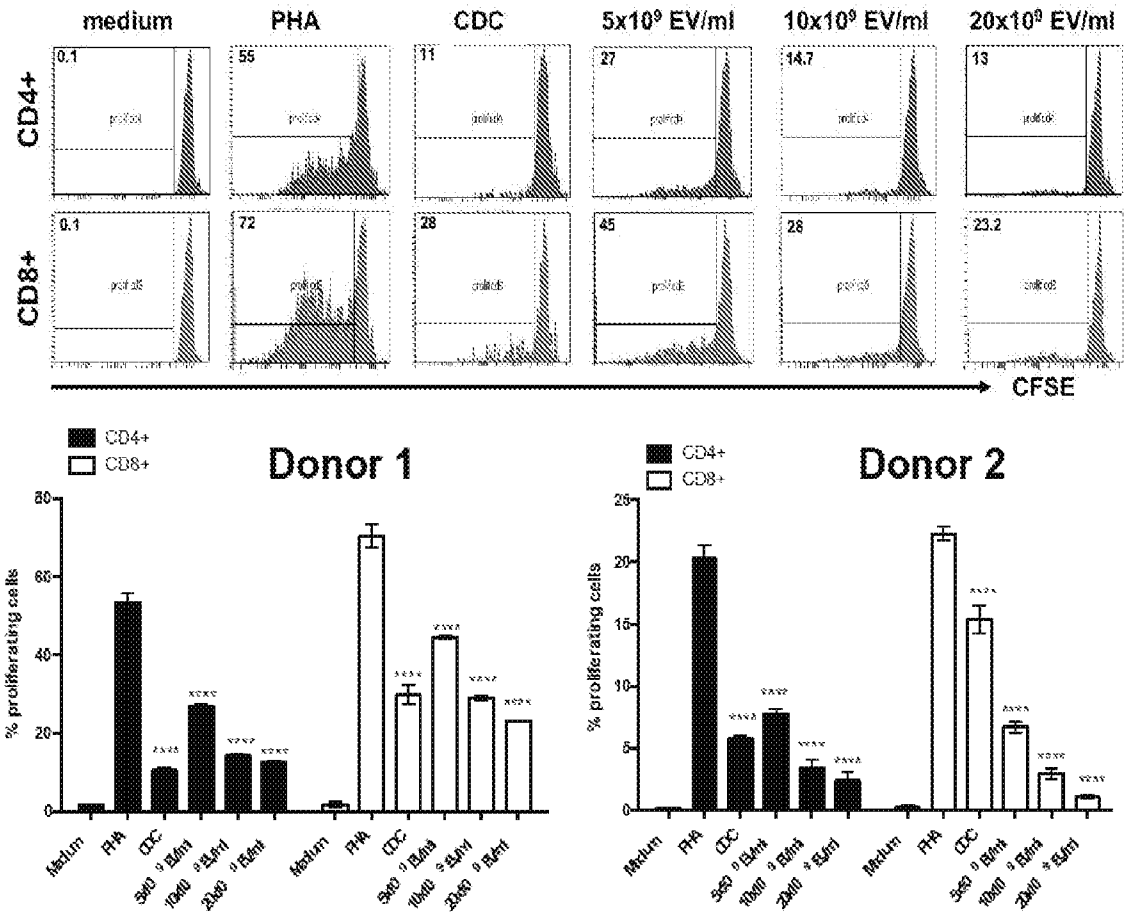
medium
PHA
CDC
5x10⁹ EV/ml
10x10⁹ EV/ml
20x10⁹ EV/ml
CD4+
CD8+
CFSE
Donor 1
Donor 2
% proliferating cells

Fig. 83

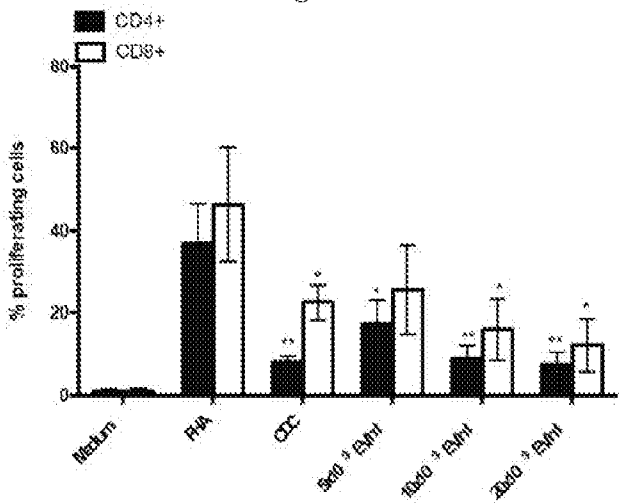
CD4+
CD8+
% proliferating cells
Medium
PHA
CDC

Fig. 84A

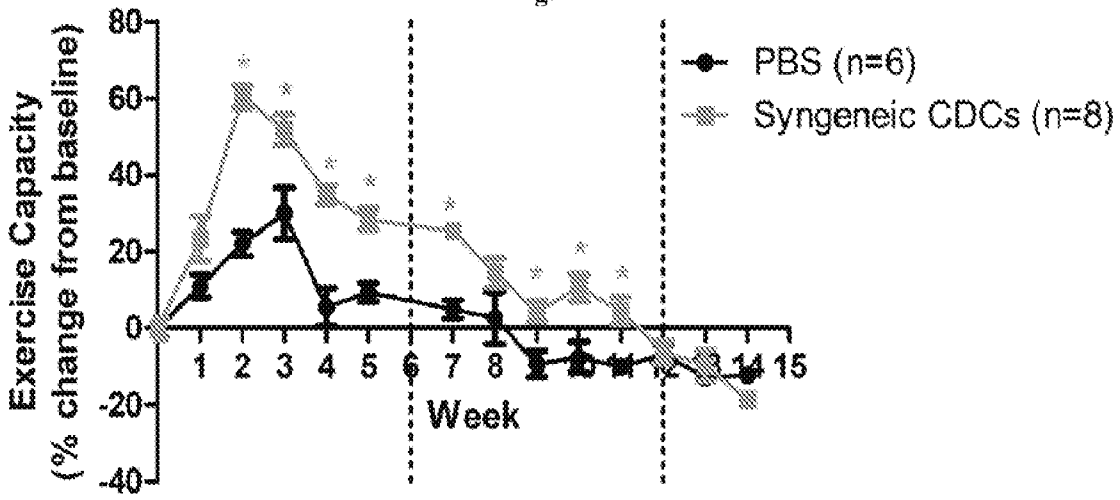

Fig. 84B

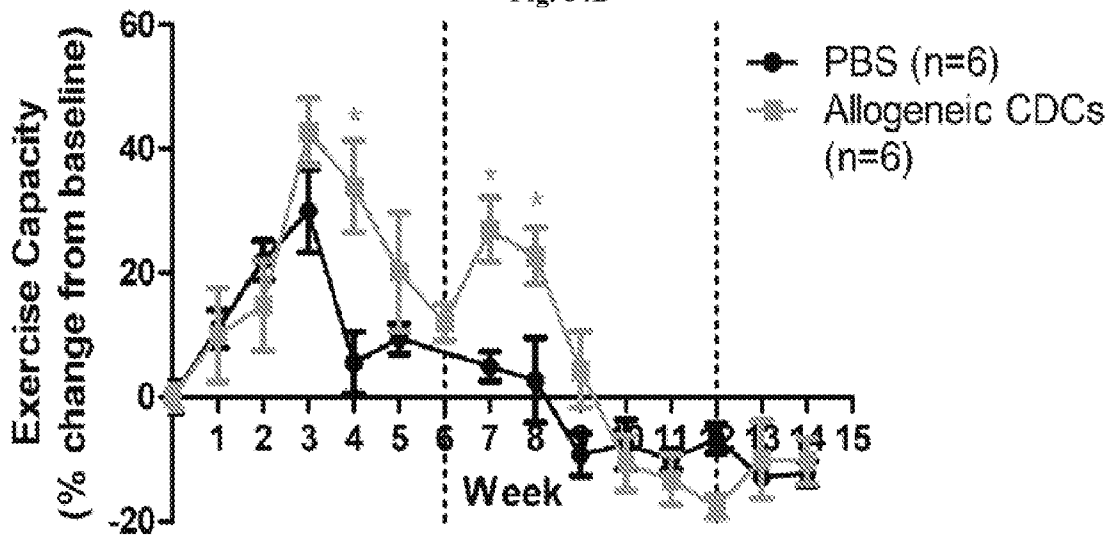

Fig. 84C

Mouse model:	Mdx mice (8-10 months old)
CDCs:	C3H (allogeneic) and syngeneic
Dose:	150K
Injection route:	Jugular
Injection time:	Week 0, 6, 12

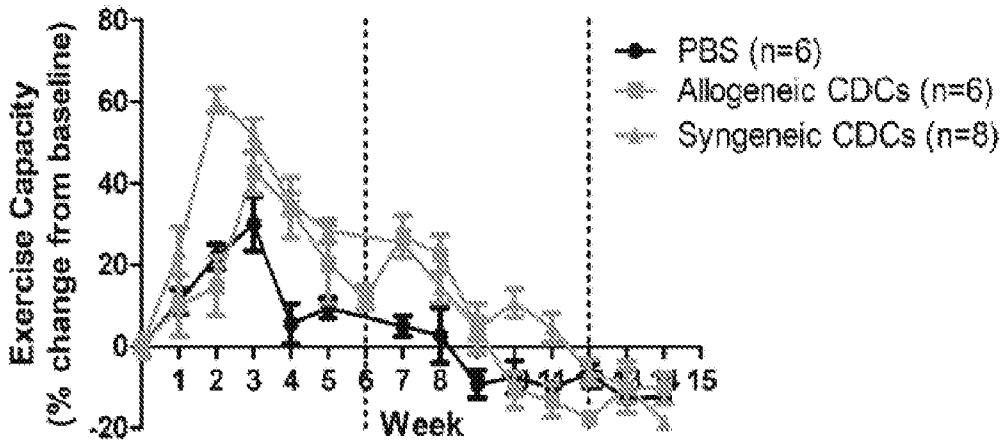

Fig. 85A

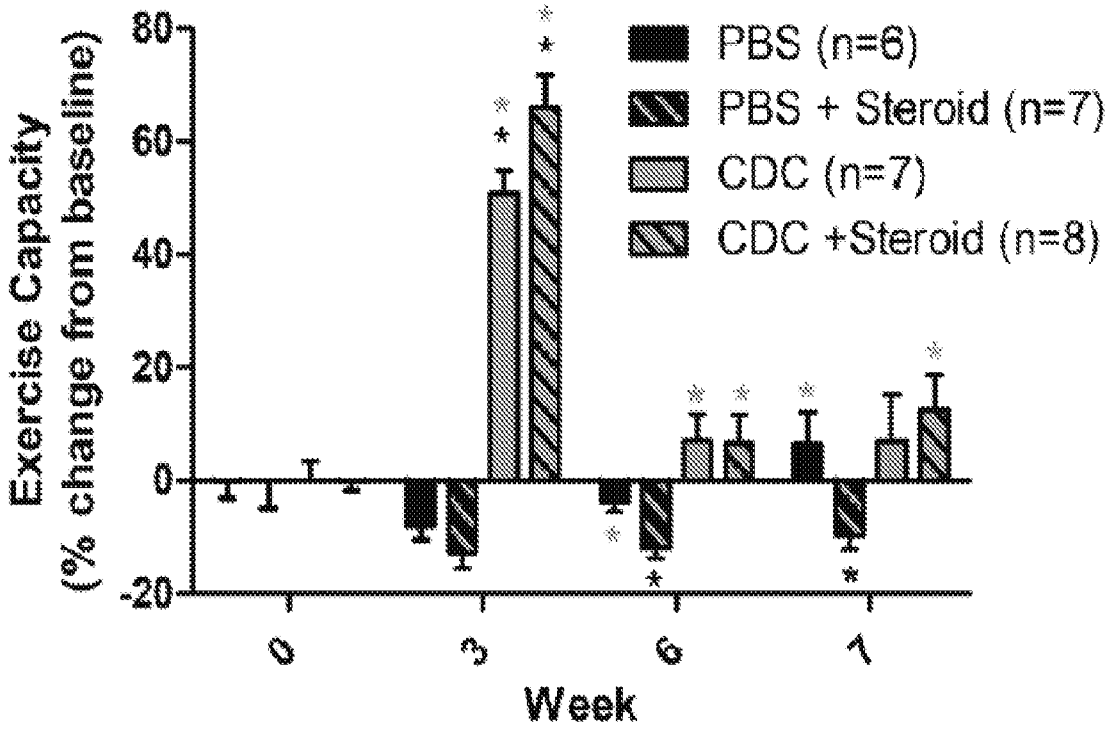
Exercise Capacity
(% change from baseline)
80
60
40
20
0
-20
0
3
6
7
Week
PBS (n=6)
PBS + Steroid (n=7)
CDC (n=7)
CDC +Steroid (n=8)

Fig. 85B

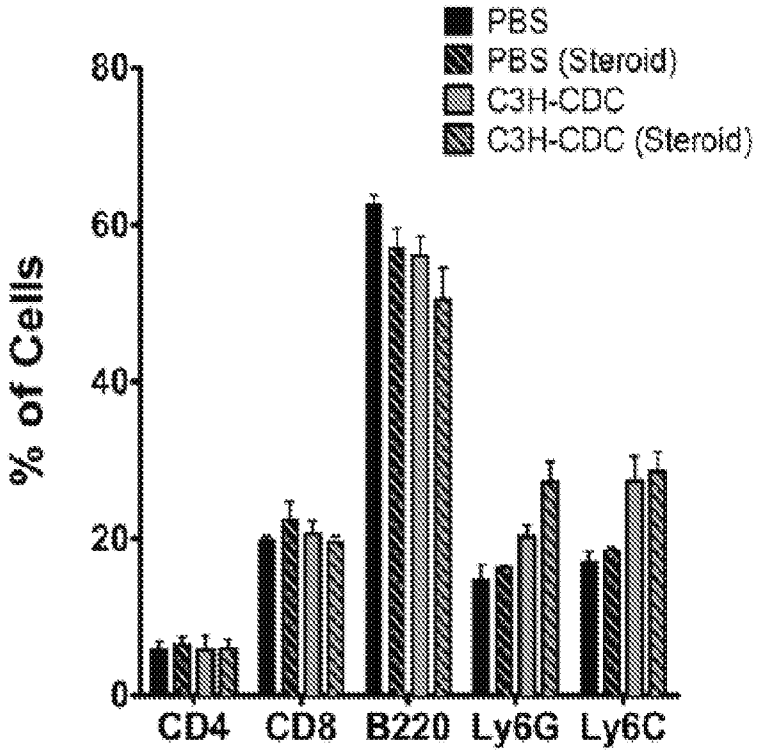
PBS
PBS (Steroid)
C3H-CDC
C3H-CDC (Steroid)
% of Cells
80
60
40
20
0
CD4
CD8
B220
Ly6G
Ly6C

Fig. 85C

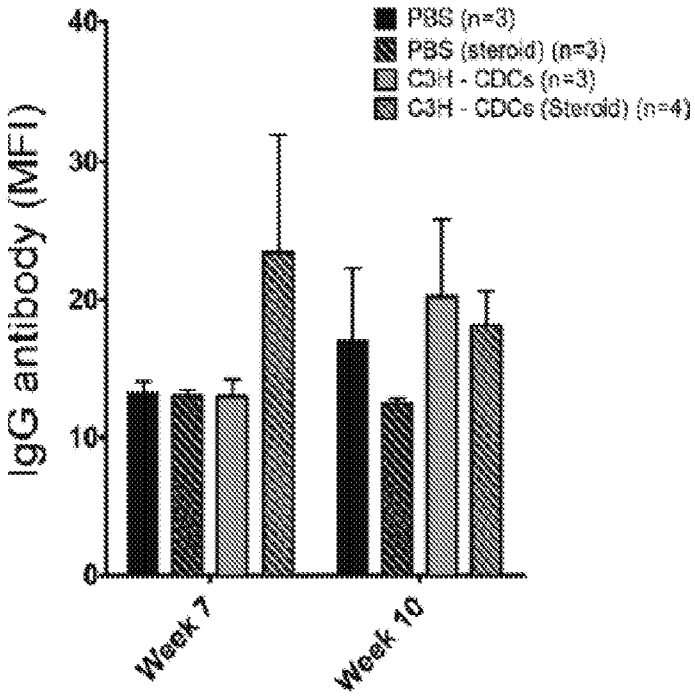
PBS (n=3)
PBS (steroid) (n=3)
C3H - CDCs (n=3)
C3H - CDCs (Steroid) (n=4)
IgG antibody (MFI)
40
30
20
10
0
Week 7
Week 10

Fig. 86

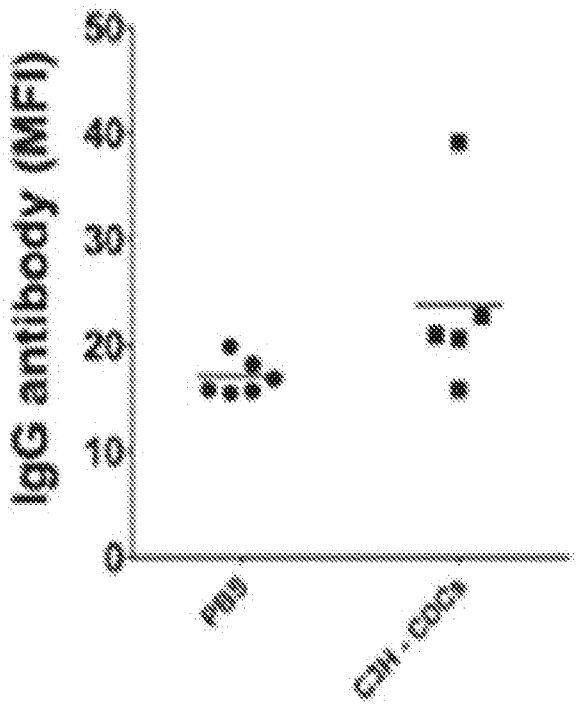

SEQUENCE LISTING

<110> Cedars-Sinai Medical Center
Capricor, Inc.

<120> METHODS AND COMPOSITIONS FOR TREATING SKELETAL MUSCULAR DYSTROPHY

<130> CPRIC.039WO

<150> US 62/487,402
<151> 2017-04-19

<150> US 62/487,393
<151> 2017-04-19

<150> US 62/487,408
<151> 2017-04-19

<150> US 62/35,672
<151> 2017-07-21

<150> US 62/569,440
<151> 2017-10-06

<150> US 62/614,753
<151> 2018-01-08

<160> 6

<170> PatentIn version 3.5

<210> 1
<211> 68
<212> RNA
<213> Homo sapiens

<400> 1
gaggcaaagu ucugagacac uccgacucug aguaugauag aagucagugc acuacagaac 60

uuugucuc 68

<210> 2
<211> 22
<212> RNA
<213> Homo sapiens

<400> 2
aaaguucuga gacacuccga cu 22

<210> 3

<211> 22
<212> RNA
<213> Homo sapiens

<400> 3
ucagugcacu acagaacuuu gu 22

<210> 4
<211> 115
<212> RNA
<213> Homo sapiens

<400> 4
uguacacaga ggcugaucga uucucccuga acagccuauu acggaggcac ugcagaucaa 60

gcccgccugg agagguggag uuucaagagu cccuuccugg uucaccgucu ccuuu 115

<210> 5
<211> 113
<212> RNA
<213> Homo sapiens

<400> 5
uguacacggu ggaguuucaa gagucccuuc cugguucacc gucuccuuua gaggcugauc 60

gauucucccu gaacagccua uuacggaggc acugcagauc aagcccgccu gga 113

<210> 6
<211> 115
<212> RNA
<213> Homo sapiens

<400> 6
uccccacaga ggcugaucga uucucccuga acagccuccu ccggaggcac ugcagaucaa 60

gcccgccugg agagguggag uuucaagagu cccuuccugg uucaccgucu ccuuu 115